The Functional and Clinical Significance of Myoepithelial Cell Galectin-7 in the Progression of Ductal Carcinoma In Situ

Thesis submitted in partial fulfilment of the requirements of the Degree of Doctor of Philosophy

Natalie Allen

Queen Mary University of London
2019

Acknowledgements

I have many people to thank; without their support this thesis would not have been possible

My thanks goes to Professor Louise Jones, my primary supervisor, for affording me the opportunity to undertake this project. Her constant support, enthusiasm and dedication has inspired and driven me from the first day.

I would like to thank Dr Mike Allen for sharing his extensive scientific knowledge, advice, and patience in helping me plan many of the experiments, and teaching me many of the experimental techniques I have used.

Many thanks to Miss Rachel Nelan for all her advice and assistance in my RNA extraction work. Her great friendship has helped me throughout.

Many thanks the cell bank; Dr Jenny Gomm, Dr Linda Haywood, Mr Iain Goulding, and Dr Adrienne Morgan for providing me with a continuous supply of primary cells and experimental help.

Thanks to the tissue bank for the supply of tissue samples, in particular Dr Sally Smith.

I would also like to thank Dr Mary-kate Hayward, Dr Kathryn Hawkesford and Dr Alastair Ironside for all the support and nights out that made this a really fun experience, and all the other members of the breast group.

Thanks to Dr George Elia for cutting my sections and paraffin embedding of organotypic gels.

Thanks to the Royal College of Surgeons England for funding towards my studies.

Thank you to my parents for their continued support.

Finally huge thanks goes to my husband Paul and little boy Alexander for their constant support, patience, and understanding for all the times I wasn't there.

STATEMENT OF ORIGINALITY

I, Natalie Allen, confirm that the research included within this thesis is my own work or that where it has been carried out in collaboration with, or supported by others, that this is duly acknowledged below and my contribution indicated. Previously published material is also acknowledged below.

I attest that I have exercised reasonable care to ensure that the work is original, and does not to the best of my knowledge break any UK law, infringe any third party's copyright or other Intellectual Property Right, or contain any confidential material.

I accept that the College has the right to use plagiarism detection software to check the electronic version of the thesis.

I confirm that this thesis has not been previously submitted for the award of a degree by this or any other university.
The copyright of this thesis rests with the author and no quotation from it or information derived from it may be published without the prior written consent of the author.

Signature:

Date: 20.05.2019

20.05.19

Details of collaborations:

Paraffin embedding of collagen gels and cutting of sections was performed by Dr George Elia, Core Pathology Lab, Barts Cancer Institute, London.

Immunohistochemical staining of β6 by Dr Mary- Kate Hayward, Barts Cancer Institute, London.

Parental myoepithelial cell line (Myo-1089) was obtained from Prof M. O'Hare and Prof P. Jat, Institute of Neurology, University College London, London.

Myoepithelial cell lines; N-1089 and β6-1089 were generated by Dr M. Allen, Barts Cancer Institute, London.

Primary normal breast cells were isolated by magnetic bead isolation by Dr J Gomm, Dr L Haywood and Mr I Goulding, Barts Cancer Institute, London.

Immunohistochemical staining of GPER by Dr M. Allen, Barts Cancer Institute, London.

Bioinformatics analysis was performed by Professor Claude Chelala, Dr E Gadaleta, and Dr A Nagano, Bioinformatics group, Centre for Molecular Oncology and Imaging, Barts Cancer Institute, London, UK

Details of invited oral presentations:

Pathological society oral presentation- Myoepithelial Cell-Associated Galectin-7: Functional and Clinical Relevance in DCIS Progression- January 2018

Details of awards:

Winner of the Rosetrees essay prize -The Royal College of Surgeons England- Defining Molecular Signatures to Personalise Management of Patients with Early Breast Cancer- March 2019

The RCS/Saven Research and Development Programme Grant of £5,500 July 2018

One year surgical research fellowship- Royal College of Surgeons England 2016-2017

Abstract

Background: The epithelial cells in Ductal Carcinoma in-situ (DCIS) are as genetically advanced as those in invasive disease therefore attention has focused on the tumour microenvironment (ME). A key component of the ME in DCIS is the myoepithelial cell (MEC) lying at the interface of the epithelial and stromal compartments. MEC are altered in DCIS with loss of Galectin-7 and upregulation of $\alpha v\beta 6$. Galectin-7 is proposed to play a role in control of apoptosis and adhesion. The hypothesis of this study is that changes in MEC phenotype in DCIS leads to an altered ME that promotes tumour progression.

Methods: Galectin-7 expression was assessed using immunohistochemistry in a series of pure DCIS samples (low risk model) and DCIS with co-existent invasion (high risk model).

An in-vitro model of normal primary myoepithelial cells was used to investigate the functional impact of loss of Galectin-7. The effect of Galectin-7 loss on MEC apoptosis, adhesion and migration was investigated. The global impact of loss of MEC Galectin-7 was explored using RNA sequencing.

Results: There was greater loss of Galectin-7 in DCIS with co-existent invasion compared to the pure DCIS cohort, whilst the inverse was shown for $\alpha v\beta 6$. Functional assays demonstrated knockdown of Galectin-7 sensitised MECs to apoptosis. They were less adhesive and more migratory to laminin and more adhesive and less migratory to Collagen I.

RNA sequencing shows that silencing Galectin-7 increased LOX expression - a key regulator of the collagen matrix of the microenvironment.

Conclusion: This study shows that loss of MEC Galectin-7 is associated with DCIS progression. Loss predisposes MEC to apoptosis and switches adhesion from basement membrane to interstitial matrix, all of which destabilizes this key interface in DCIS. Galectin-7 has the potential to be used in a risk stratification tool for DCIS.

List of Figures

List of Tables

List of Abbreviations

ABC Avidin-biotin complex

ADH Atypical ductal hyperplasia

ANOVA Analysis of variance

BCN Breast Cancer Now

BCI Barts Cancer Institute

BM Basement membrane

BPE Bovine pituitary extract

BSA Bovine serum albumin

CDH1 E Cadherin

CK Cytokeratin

CM Conditioned media

COL Collagen

DAB Diaminobenzidine

DAPI 4',6-diamidino-2-phenylindole

dH$_2$0 distilled water

DCIS Ductal carcinoma in situ

DMSO Dimethyl sulphoxide

DPX Distyene-tricresyl phosphate-xylene

DSC Desmcollin

DSG Demoglein

ECL Enhanced chemiluminescence

ECM Extra-cellular matrix

EDTA Ethylenediaminetetraacetic acid

EGF Epidermal growth factor

EpCAM Epithelial cell adhesion molecular

ER Oestrogen receptor

F-12 Nutrient mixture hams F-12

FACS Fluorescence-activated cell sorting

FBS Foetal bovine serum

FC Fold change

FEA Flat epithelial atypia

FFPE Formalin-fixed paraffin-embedded

FN Fibronectin

GSEA Gene set enrichment analysis

H+E Haematoxylin and Eosin

Her2 Human epidermal growth factor receptor 2

HGF Hepatocyte growth factor

HRP Horse radish peroxidase

HRT Hormone replacement therapy

IgG Immunoglobulin

IHC Immunohistochemistry

KD Knock-down

IKKβ IκB-kinase-β

LDH Lactate dehydrogenase

LOX Lysyl oxidase

LOXL Lysyl oxidase-like

miR Micro RNA

MAPK Mitogen-activated protein kinase

MEC Myoepithelial cell

MMP Matrix metalloproteinase

NBF Neutral buffered formalin

NHSBSP National Health Service Breast Screening Programme

NICE National Institute for Health and Care Excellence

PBS Phosphate buffered saline

PBST Phosphate buffered saline and tween 20

PFA Paraformaldehyde

PDGFRα/β Platelet derived growth factor receptor alpha/beta

PIP3 Phosphatidylinositol (3,4,5)-trisphosphate

PR Progesterone receptor

qRT-PCR Quantitative real-time polymerase chain reaction

RIPA Radioimmunoprecipitation assay

RT Room temperature

SDS Sodium dodecyl sulphate

SDS-PAGE SDS-Polyacrylamide gel electrophoresis

siRNA Small interfering RNA

SMA Alpha smooth muscle actin

SNP Single nucleotide polymorphism

TDLU Terminal duct lobular unit

TEMED Tetramethylethylenediamine

TGF-β Transforming growth factor beta

TIMP Tissue inhibitor of metalloproteinase

TME Tumour microenvironment

TNF Tumour necrosis factor

TN Triple negative

TP53 Tumour protein p53

VEGF Vascular endothelial growth factor

1 Introduction

1.1 Breast anatomy

The physiological function of the female breast is lactation. The human breast comprises a branching network of ducts and lobules embedded in a surrounding stroma, which is encased in a variable amount of adipose tissue. The ducts converge towards the nipple (figure 1.1) The ducts are comprised of two types of epithelial cells; inner luminal epithelial cells and outer myoepithelial cells, surrounded by a protein-rich basement membrane (figure 1.2)

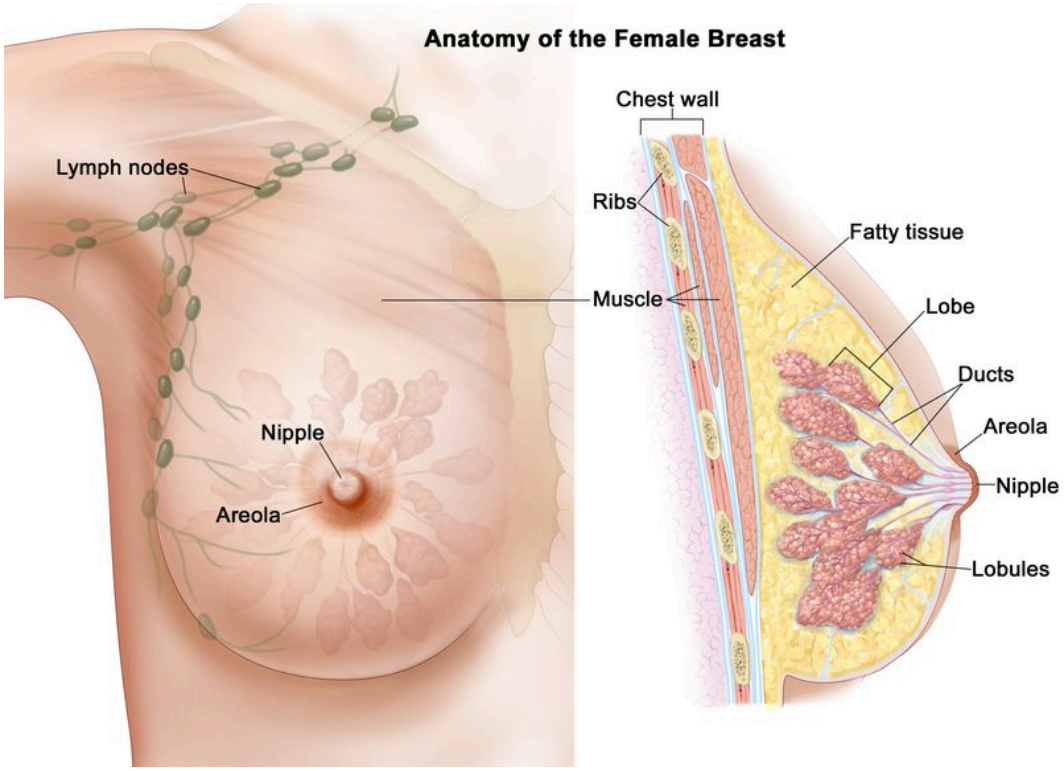

Figure 1-1 Breast anatomy

The diagram shows a branching network of ducts, lobules and surrounding stroma. (From the National Cancer Institute © 2011 Terese Winslow LLC)

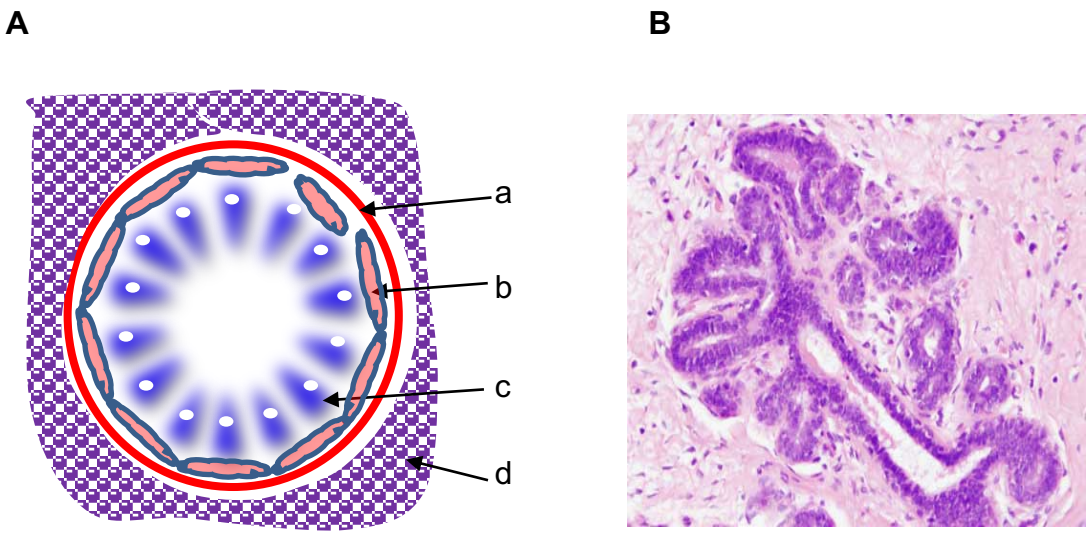

Figure 1-2 Structure of a normal breast duct.

Normal breast duct A) schematic where arrows indicate; a) basement membrane, b) myoepithelial cell, c) luminal epithelial cell and d) stroma. B) Haematoxylin and eosin stained duct.

1.2 Breast cancer risk factors

There are numerous risk factors which can increase the likelihood of developing breast cancer. Some risk factors are genetic and others environmental. Early diagnosis of breast cancer can lead to good prognosis and increased survival rates, and the breast screening program is instrumental in early detection. A key area of current research is breast cancer prevention in modifying risk factors (Figure 1-6) (Kamińska, Ciszewski, Łopacka-Szatan, Miotła, & Starosławska, 2015).

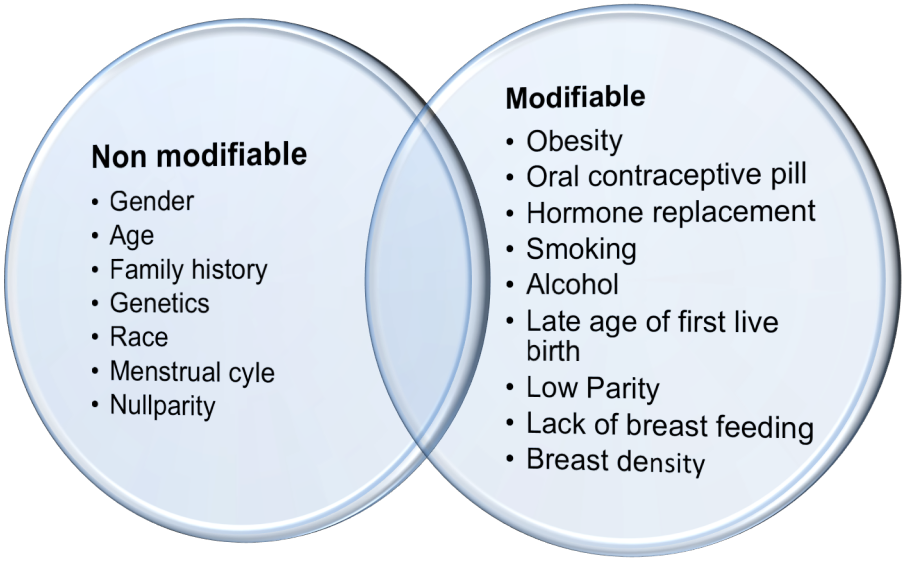

Figure 1-3 Breast cancer risk factors.

An outline of modifiable and non-modifiable breast cancer risk factors.

1.2.1 Age

Ageing is one of the most important risk factors for breast cancer, with the incidence increasing with advancing age as shown in Figure 1-4. In 2016, approximately 99.3% and 71.2% of all breast cancer-associated deaths in America were reported in women over the age of 40 and 60, respectively (Siegel, Miller, & Jemal, 2017).

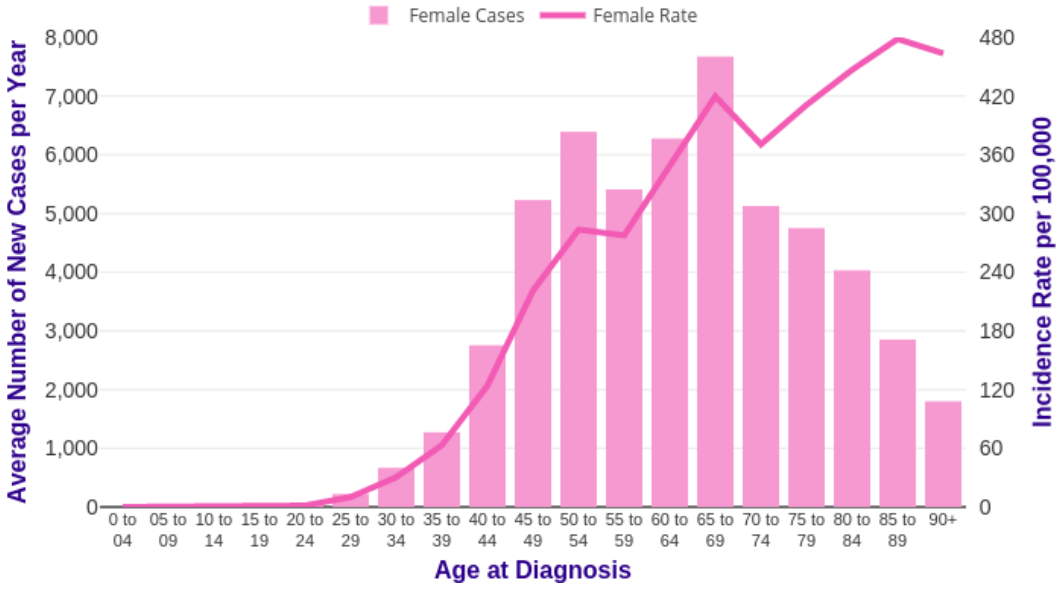

Figure 1-4 Age-specific breast cancer incidence.

Breast cancer average number of new cases per year and age-specific incidence rates per 100,000 population, females, UK, 2013-2015 ("http://www.cancerresearchuk.org/health-professional/cancer-statistics/statistics-by-cancer-type/breast-cancer/incidence-in-situ,")

1.2.2 Family history

Women who have a family history of breast cancer have an increased risk of developing breast cancer. A UK cohort study involving 113,000 women, demonstrated women with one first-degree relative and those with two or more first degree relatives have a 1.75 fold risk and 2.5 fold or higher risk, respectively, of developing breast cancer than those women without any affected relatives (Brewer, Jones, Schoemaker, Ashworth, & Swerdlow, 2017).

1.2.3 Obesity

Obesity is an established risk factor for postmenopausal breast cancer, at least in part due to oestrogen production by adipose tissue. The Genesis Centre in Manchester has been a leader in breast cancer risk prevention, leading studies into the benefits of lifestyle modification. In 2005, Harvie *et al.* collaborated with investigators running the Iowa Women's Health Study in the United States to assess the effect of weight loss on breast cancer risk. This showed that women losing 5% body weight and maintaining this reduced their risk of breast cancer by approximately 25%-40% compared with women who continued to gain weight (Harvie et al., 2005).

1.2.4 Mammographic density

Mammographic density is defined as the proportion of the mammogram image which is occupied by dense fibroglandular tissue. This is defined as a percentage; a higher percentage conferring an increased density. Women with mammographic density in the highest quartile have a risk of developing breast cancer 4-6 times higher than those with mammographic density in the lowest quartile (Boyd et al., 2005). High breast density in the general population is common, therefore the attributable risk is substantial, and it is estimated that approximately one third of breast cancers could be explained by density in more than 50% of the breast (Boyd et al., 2005). The impact of high mammographic density is two-fold – biological and technical. There is a decrease in mammographic sensitivity with increasing tissue density: in two separate reports of film-screen mammography, mammographic sensitivity decreased from a level of 85.7%–88.8% in patients with almost entirely fatty tissue to 62.2%–68.1% in patients with extremely dense breast tissue (Carney et al., 2007). Keely *et al.* used a mouse model of high density which showed increased tumour formation associated with increased collagen density (P. P. Provenzano et al., 2008). The alignment of collagen fibres is also an important factor. Weaver *et al.* used a LOX-overexpressing mouse model to demonstrate that increased lysyl oxidase (LOX), which functions to crosslink

collagen, results in a stiffer mammary fat pad (Levental et al., 2009) and enhanced tumour formation. Collagen crosslinking accompanies tissue fibrosis (van der Slot et al., 2005) and fibrosis increases risk to malignancy (Colpaert et al., 2003). Moreover, LOX is proposed to have a key role in facilitating tumour metastasis (Erler et al., 2006).

Breast density is modifiable to a degree and there are therapeutic options to reduce breast density.

1.2.5 Hormonal factors

Reproductive factors such as early menarche, late menopause, late age at first pregnancy and low parity can increase breast cancer risk (Sun et al., 2017). Each 1-year delay in menopause increases the risk of breast cancer by 3%. Each 1-year delay in menarche or each additional birth decreases the risk of breast cancer by 5% or 10%, respectively (Dall & Britt, 2017).

1.3 Breast cancer incidence

The incidence of breast cancer increases with age. Cancer Research UK have monitored cancer incidence using figures from the Office of National Statistics. Advancements in diagnostics and the screening program have contributed towards earlier detection. In 2003, 2-view mammography was introduced contributing towards an increase in breast cancer incidence in the 65-69 age group, with small breast cancers that were not detected on single view mammography being detected with the introduction of 2-view mammography (Figure 1-5).

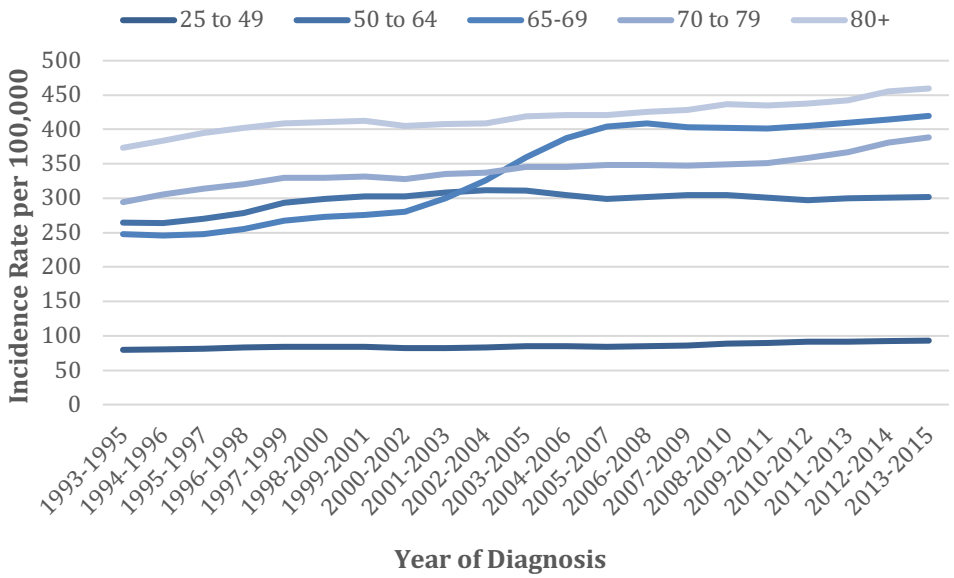

Figure 1-5 Invasive breast cancer age-standardised incidence rates, by age, UK, 1993-2015.

Breast cancer incidence rates have increased overall in all broad adult age groups in females in the UK since the early 1990s. Rates in 25-49s have increased by 17%, in 50-64s have increased by 14%, in 65-69s have increased by 69%, in 70-79s have increased by 32%, and in 80+s have increased by 23%. ("http://www.cancerresearchuk.org/health-professional/cancer-statistics/statistics-by-cancer-type/breast-cancer/incidence-in-situ,")

1.4 Ductal carcinoma *in situ* (DCIS) incidence

The introduction of breast screening led to a significant increase in DCIS incidence. DCIS is often asymptomatic and is detected through breast screening or at symptomatic clinics as an incidental finding. DCIS can less commonly present as a mass or bloody nipple discharge. Age standardised incidence rates are shown in Figure 1-6.

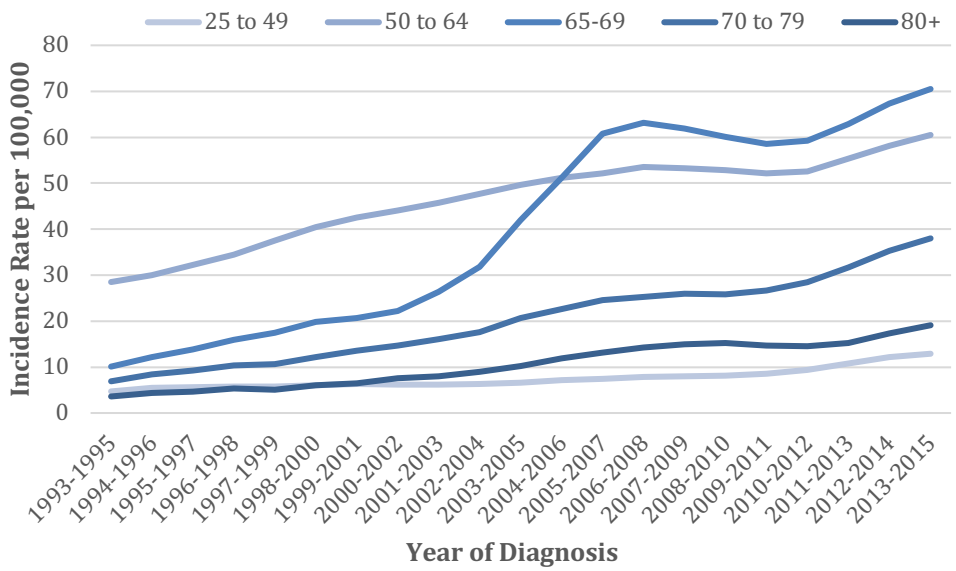

Figure 1-6 *In situ* breast cancer age-standardised incidence rates, By Age, UK, 1993-2015.

Breast carcinoma *in situ* incidence rates have increased overall in all broad adult age groups in females in the UK since the early 1990s.[1-4] Rates in 25-49s have increased by 172%, in 50-64s have increased by 112%, in 65-69s have increased by 600%, in 70-79s have increased by 450%, and in 80+s have increased by 424%.("http://www.cancerresearchuk.org/health-professional/cancer-statistics/statistics-by-cancer-type/breast-cancer/incidence-in-situ,")

The Office of National Statistics have published DCIS rates across different regions (Figure 1-7), the variation over time may be multifactorial. Regions will have switched to digital mammography at different times, which may be a contributing factor to this variation.

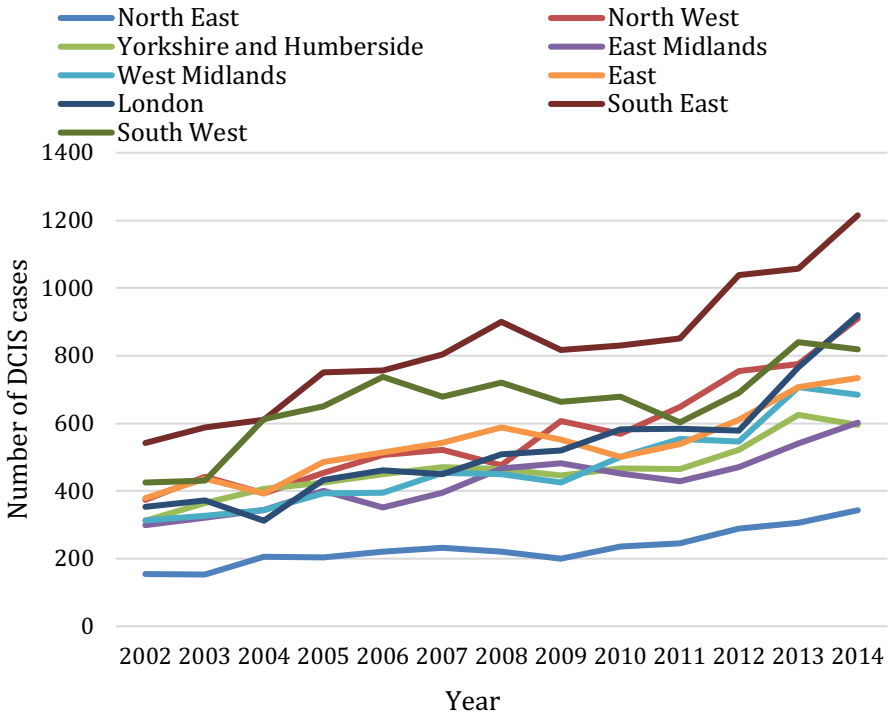

Figure 1-7 *In situ* breast cancer cases in females between 2002 and 2014 across screening regions.

The variation in DCIS across different screening region is evident.

1.5 Breast cancer histological classification

Breast cancer is a heterogeneous disease. The progression to invasion is defined as when the malignant epithelial cells have breached the basement membrane and invaded the surrounding stroma. The two most common histological types of invasive breast cancer are ductal and lobular carcinomas, accounting for approximately 75 and 15% of all cases in the US, respectively (C. I. Li, Anderson, Daling, & Moe, 2003). The histological subtype of cancer is clinically relevant as this can alter the diagnostic work up of the patient and subsequent treatment, however the grade of the tumour is a more relevant prognostic feature. Invasive lobular carcinomas (ILC) are more often multifocal and bilateral and can be mammographically occult when compared to invasive ductal carcinoma (IDC), therefore a bilateral breast MRI is often performed prior to the commencement of treatment. The special type tumours often have a more favourable prognosis and include tubular carcinoma, cribriform carcinoma, mucinous carcinoma, medullary carcinoma, papillary carcinoma and adenoid cystic carcinoma (Berg & Hutter, 1995).

In addition to the classical histological subtypes, Perou described four molecular subtypes: Luminal A, Luminal B, HER-2 overexpressing and basal-like (Perou et al., 2000). These molecular subtypes were defined on gene expression analysis but they can be defined using immunohistochemistry and fluorescent *in situ* hybridisation. Sorlie et al., showed these subgroups had differing prognosis and treatment options as summarised in Table 1-1.

Tumour subtype	Receptor expression	Tumour characteristics	Proportion of breast cancer	10 year survival	Targeted therapies
Luminal A	ER + PR +/- HER-2 -	Low grade	71%	79-84%	Hormonal
Luminal B	ER + PR +/- HER-2 +	Low grade	6%	60-87%	Hormonal Trastuzumab
HER-2	ER - PR - HER-2 +	High grade aggressive	6%	52-55%	Trastuzumab
Basal	ER - PR - HER-2 -	High grade aggressive	10-25%	62-75%	None

Table 1-1 Breast cancer molecular subtypes.

The basal subtype of breast cancer is often referred to as Triple Negative breast cancer, since they lack oestrogen and progesterone receptors and Her2. These are often regarded as equivalent to the basal subtype however, not all triple negative tumours express basal cytokeratins (CKs). Basal-like tumours are more accurately defined using gene expression and this is an important prognostic indicator (Carey et al., 2006), (Rakha et al., 2007).

1.6 Ductal Carcinoma *in situ* (DCIS)

1.6.1 DCIS pathological classification

The pathological classification of DCIS is complex and for many years there have been discrepancies in the way in which this is classified, one challenge includes the heterogeneity of DCIS such that the type of DCIS is often mixed. DCIS has generally been categorised on architectural pattern using five main groups: comedo (layer of neoplastic cells surrounding a central area of necrosis), cribriform (radially oriented neoplastic cells forming glandular lumina), papillary (large papillations with fibrovascular stalks), solid (ductal filling with neoplastic cells), and micropapillary (finger-like papillary projections into dilated ductal spaces) (Leonard & Swain, 2004). An important diagnostic factor and predictor of prognosis is the presence of comedo necrosis (Burstein, Polyak, Wong, Lester, & Kaelin, 2004). The presence of comedo necrosis is included in the Van Nuys score as a poor prognostic feature.

In current clinical practice in the UK, DCIS is classified as low, intermediate and high grade, with high thought to be the most aggressive. However, a challenge of risk stratifying DCIS is that often pathologists do not agree on the grade. The classification is the assessment of the size of the nuclei compared with adjacent normal cells, typically either normal epithelial or red blood cells. High grade DCIS is composed of large, pleomorphic cells with prominent nuclei, with a high mitotic count. The nuclei of high grade DCIS are typically more than 2.5 the size of red blood cells in diameter (Lester et al., 2009). Low grade DCIS is formed of regular cells with monotonous nuclei (Pinder, 2010), with a low mitotic count. Intermediate grade DCIS is used to classify DCIS when the nuclei show pleomorphism, but not to the degree that is seen in high grade DCIS and lack the regularity of cells seen in low grade DCIS. Within the UK National Health Service (NHS) Breast Screening Programme, the poorest agreement amongst clinicians is the categorisation of intermediate grade DCIS (Ellis et al., 2006). There is a shift in practice with some clinicians using high grade versus non-high grade and the thought is this should increase the reproducibility of the reports.

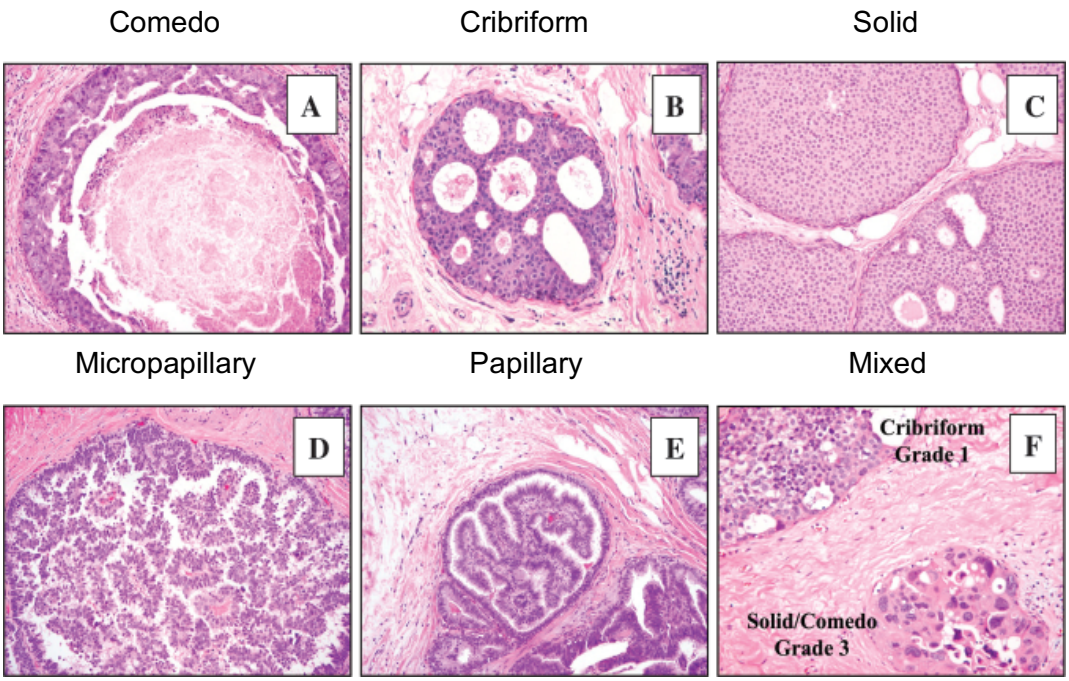

Figure 1-8 Architectural patterns of DCIS.

Comedo (A), cribriform (B), solid (C), micropapillary (D), and papillary (E) subtypes. However, a large proportion of DCIS shows complex mixtures of growth patterns (F), which adds to the complexitiy of catogrising DCIS (Allred, 2010).

1.7 Breast screening program

The NHS has a population-based breast screening program, currently offered to all women aged 50-70. There is currently an age extension trial that includes women in the 47-49 and 71-73 age range in order to assess if the screening age range should be expanded. Healthy individuals are screened to identify those whom have developed a breast lesion which may potentially be malignant. With regards to breast screening, women undergo a 2-view mammogram, these are then dual reported by radiologists. Any woman whose mammogram detects an abnormality is offered further investigations. There can be problems with false positives and false negatives. As a result of breast screening, breast carcinomas are more likely to be detected at the pre-invasive or early stage, increasing the chances of curing the patient. However, concerns regarding over-diagnosis and subsequent over-treatment have been raised.

1.7.1 Breast screening invitations

For screening to be effective it is important to screen the majority of the women invited for screening. The minimum standard is that 70% of those invited for screening should attend. It is only in London that the screening attendance falls below 70%. The breakdown shows that central London has the poorest screening attendance. This is likely to be due to the social demographic mix of these regions. It is important to make screening acceptable to women and this may increase uptake of screening.

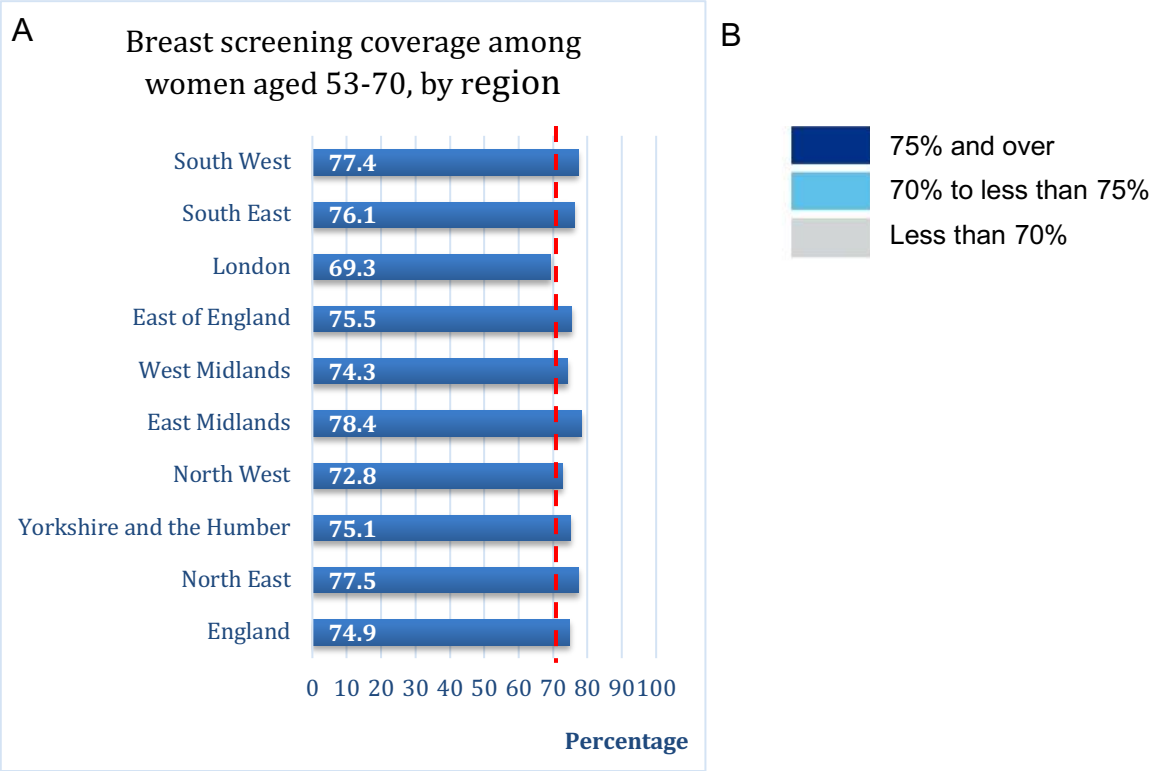

Figure 1-9 Breast screening invitation uptake.

A) Breast screening coverage among women aged 53-70 by region reported in England, March 2018 (Watson & screening and immunisation team, 2019) All regions apart from London reported coverage above the minimum standard of 70%. B) This illustrates the breakdown of screening coverage in London (Watson & screening and immunisation team, 2019).

1.7.2 DCIS progression

For several decades it has been accepted that DCIS constitutes a non-obligate precursor of IDC. In 1973, Wellings and Jensen proposed that DCIS lesions are precursors of invasive breast cancer (IBC) based on the evidence of gradual histological continuity observed in normal and abnormal breast tissues (Wellings & Jensen, 1973). Longitudinal studies of patients with DCIS managed with biopsy alone have revealed that only 20–50% of this population later developed IBC in the same quadrant of the same breast as the original DCIS (Page, Dupont, Rogers, & Landenberger, 1982) (Page, Dupont, Rogers, Jensen, & Schuyler, 1995),(Sanders, Schuyler, Dupont, & Page, 2005). Ozanne and colleagues created a simulation model to assess DCIS progression: this estimates that a lesion of a >1 cm, high grade DCIS in women under 45 years old would have a 60% rate of progression to IBC and those women more than 45 years of age with a <2.5cm, low or intermediate grade lesion to have a rate of progression to IBC of 10% (Ozanne et al., 2011).

There is difficulty in establishing the rate of DCIS progression as most patients have definitive treatment at the time of diagnosis so halting the natural history. Leonard reviewed studies of patients with IBC who had previously had a benign biopsy. On re-evaluation of these biopsies, evidence of DCIS was identified in 14-73% of cases (Leonard & Swain, 2004). It is likely that the rate of recurrence is an overestimate, however, since the cases of invasive cancer were retrospectively reviewed.

Study	Number of Cases	Follow-up (years)	Histology	Number (%) of cases that developed invasive carcinoma
Kraus(KRAUS & NEUBECKER, 1962)	4	10-12	Papillary	2 (50%)
Farrow(Farrow, 1970) (	25	1-6	NR	5 (20%)
Haagensen (Haagensen, Lane, & Lattes, 1972)	11	10	Papillary	8 (73%0
Millis(Millis & Thynne, 1975)	8	0-19	NR*	2 (25%)
Page (Page et al., 1982) (Page et al., 1995)	28	3-30	Noncomedo	9 (32%)
Eusebi (Eusebi et al., 1994)	80	5-28	Comedo Noncomedo	11 (14%)

Table 1-2 DCIS with invasive recurrence.

**NR Non recorded*

A Dutch based population cohort study assessed all-cause mortality in 9799 women treated for primary DCIS between 1989 and 2004. The standardised mortality rates for breast cancer decreased from 7.5 to 2.8 for women aged <50 and >50 years, respectively. DCIS patients >50 years at diagnosis, had lower all-cause mortality than the general female population. The lower mortality rates in women >50 years may reflect the demographic of women who attend breast screening or changes in lifestyle following DCIS diagnosis (Elshof et al., 2018). The higher risk in younger women may also reflect the greater time period available to develop recurrence.

An Australian autopsy study of 207 women with a mean age of 60 years identified 27 women with carcinoma *in situ*, of which 21 were DCIS, 4 were mixed and 2 were LCIS. 37% of all carcinoma *in situ* identified was multicentric. This study identified 12% of women had occult DCIS (Bhathal, Brown, Lesueur, & Russell, 1985). A review of autopsy data in which women

thought not to have breast cancer at the time of death was performed by Gilbert and Welch in an attempt to establish how many women are dying with undiagnosed DCIS,. There are limitations to this review with pathological examination not being consistent between studies, with some studies examining 5 slides from the breast and one study examining 95 slides per breast. The median prevalence of DCIS was 8.9% within this review, but the rates varied widely (Welch & Black, 1997). In 2017, a further review of autopsy studies was performed which includes some data from the previous review with their estimate for the prevalence pool of incidental *in situ* breast cancer at ~9% (E. T. Thomas et al., 2017).

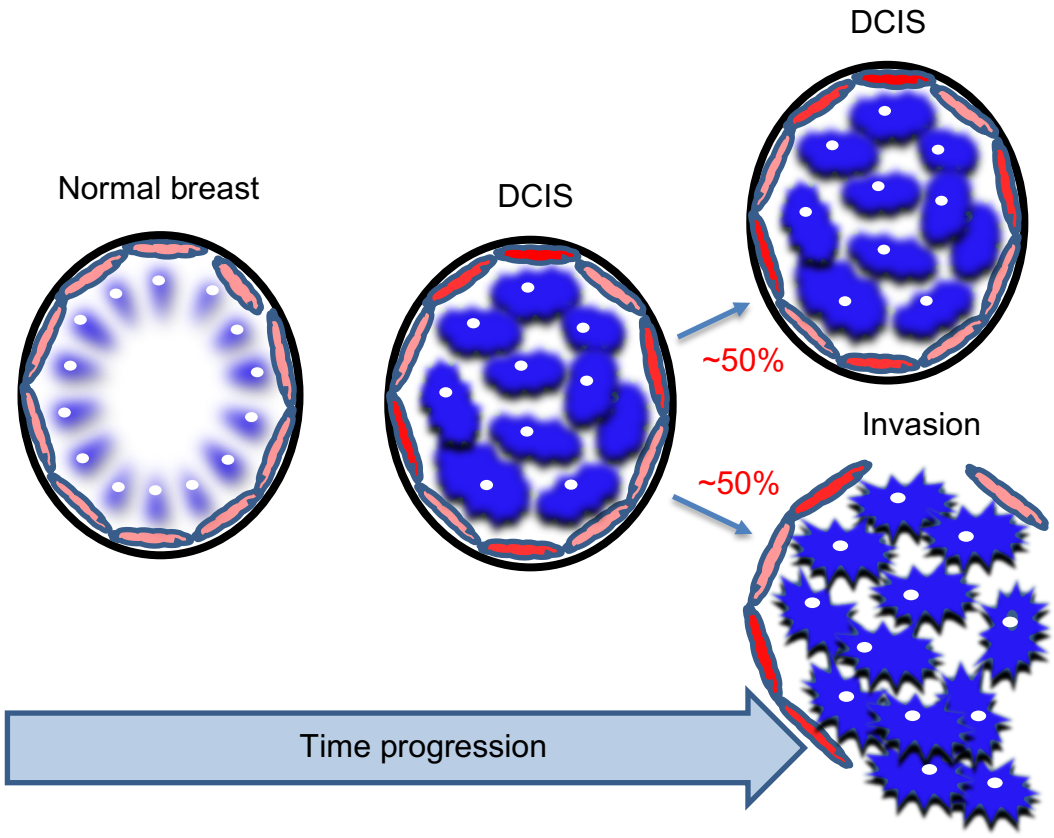

Figure 1-10 Schematic of DCIS progression.

It is predicted that only a subset of DCIS will progress to invasive breast carcinoma with many (estimates vary between 10-80%) never developing into invasive cancer.

1.7.3 Markers of DCIS progression

Many studies have investigated markers that might predict or are associated with progression of DCIS, however to date the most important factors used clinically to predict progression is age, DCIS size, grade and margins.

A DCIS scoring algorithm has been developed to risk stratify DCIS and is outlined in Table 1-4. The scoring system uses age, DCIS size, grade, necrosis and margin width, a score of 4-6 is low risk, 7-9 intermediate risk and 10-12 high risk. This was initially developed to guide treatment decisions.

Score	1	2	3
Age	>60	40-60	<40
DCIS size (mm)	<16	16-40	>40
Histological grade	1-2 No necrosis	1-2 Necrosis	3 Necrosis
Margin width (mm)	≥10	1-9	<1

Table 1-3 Van Nuys prognostic index.

Silverstein and Lagios assessed recurrence in 949 patients treated with breast conservation, 345 with excision and radiation therapy, and 604 with excision alone and assessed recurrence at 12 years. There were 165 local recurrences of which 103 patients underwent excision only (37 invasive carcinoma and 66 DCIS) and 62 patients were treated with excision plus post-operative radiation therapy (34 invasive carcinoma and 28 DCIS). The USC/Van Nuys prognostic index score was analysed to assess its predictive value (Silverstein, 2003).

Score	Number of patients	Treatment	Local recurrence at 12 years
4-6	320	Excision alone	5.4%
		Excision with radiotherapy	2.5%
7	219	Excision alone	30%
		Excision with radiotherapy	13%
10-12	98	Excision with radiotherapy	>40%

Table 1-4 Analysis of recurrence using the USC/Van Nuys prognostic index.

A higher incidence of recurrence is seen in the patients with a USC/Van Nuys score of 10-12 (Silverstein, 2003).

The recurrence rates at 12 years are much higher with the 10-12 Van-Nuys score, an illustration the importance of grade and presence of necrosis.

A range of biological markers has been investigated to assess their utility in predicting DCIS progression. ER negativity has been associated with an increased risk of DCIS recurrence (E. Provenzano et al., 2003). A study assessing 195 cases of low grade DCIS found 100% were ER positive and 85.3% were PR positive (Koh et al., 2019). A study by Roka and colleagues of 132 women diagnosed with DCIS treated with breast conserving surgery (BCS) with or without radiotherapy discovered a significantly lower rate of ipsilateral breast recurrence in patients with ER-positive DCIS compared to patients whose DCIS did not express ER (3.7% vs 12.2%, $p<0.04$).(Roka et al., 2004). HER-2 is a marker used in clinical practice to guide therapy for invasive breast cancer. Holmes and colleagues analysed 141 patients with DCIS who underwent breast conserving surgery, with confirmed disease-free surgical margins. There were 60 recurrences at a median time of 191 months. HER-2 positivity (3+) was found to be significantly associated with reduced

time to tumour recurrence (Holmes et al., 2011). The immune response may have a role in DCIS progression. Immunotherapy is an evolving therapeutic option in many cancers, however to date success has been limited in the breast cancer field. In DCIS the tumour cells are separated from the immune system by the myoepithelial cell layer and an intact basement membrane, when there is progression to invasion the immune cells are intermingled with the tumour cells (Gil Del Alcazar et al., 2017). Polyak *et al*. investigated the immune infiltrate with particular focus on the T cells examining the difference between normal breast tissue, DCIS and IDC (Gil Del Alcazar et al., 2017). They showed that T cells in DCIS are enriched in activated effector CD8+ T cells characterised by the expression of Granzyme B (GZMB) and MKI67, while they were reduced in invasive disease. This was particularly evident in DCIS cases that recurred locally as IDC, implying that decreased immune activity may be necessary for invasive progression (Gil Del Alcazar et al., 2017).

Some theories propose the extracellular matrix (ECM) is a key driver in DCIS progression. Lyons *et al*., showed that mammary gland involution post pregnancy drives tumour progression by remodelling the ECM (Lyons et al., 2011). They used post-partum murine models, demonstrating that involution resulted in large tumours with increased collagen deposition and over-expression of cyclooxygenase-2 (COX-2) (Lyons et al., 2011). Hu *et al.* have shown in a xenograft model with up regulation of COX-2 an increase in VEGF and MMP14 expression, which may contribute to the larger tumour weight and invasive histology. A selective COX-2 inhibitor celecoxib was given and was found to decrease tumour weight and inhibit invasion (Hu et al., 2009). LOX elevation also causes modification of the ECM which in turn causes an increase in invasiveness and subsequent metastasis. Erler *et al.,* assessed LOXL2 expression in patient samples using IHC, and xenograft models to investigate the function. They showed that LOXL2 promotes invasion by regulating the expression and activity of the extracellular proteins TIMP1 and MMP9 (Barker et al., 2011).

Theories of DCIS progression include linear and evolutionary progression. The linear multistep process initiates as flat epithelial atypia (FEA), progresses to atypical ductal hyperplasia (ADH), evolves into DCIS and progresses to IDC (Bombonati & Sgroi, 2011). Historically, it has been proposed there is a low-grade and high-grade pathway of progression, hence low-grade DCIS develops into low-grade IDC and high-grade DCIS develops into high-grade IDC. The low-grade-like pathway is characterised by recurrent chromosomal loss of 16q, gains of 1q, a low-grade-like gene expression signature, with expression of oestrogen and progesterone receptors. The high-grade-like gene expression molecular pathway is characterised by recurrent gain of 11q13, loss of 13q, expression of a high-grade-like gene expression signature, amplification of 17q12, and lack of oestrogen and progesterone receptors expression (Sgroi, 2010). Figure 1-6 illustrates hypothetical models of DCIS progression. In contradiction to this, more than one grade of DCIS is frequently present within a lesion (Chapman et al., 2007), thus this theory is likely to be oversimplified.

An alternative theory of DCIS progression is the evolutionary bottleneck model of progression. In this model a single cell in the duct gives rises to multiple clones, one of these clones passes through the bottleneck and subsequently escapes the basement membrane developing into invasive cancer, as shown in Figure 1-11.

Tumour heterogeneity is one of the key challenges of DCIS management and contributes significantly towards the diagnostic and therapeutic dilemmas. The Navin lab have used a single cell DNA sequencing method, using laser capture microdissection to microdissect thousands of tumor cells from the *in situ* and invasive regions of a lesion for deep-exome sequencing: such an approach has emerged as a powerful tool for resolving intratumor heterogeneity (Navin et al., 2011), (Xu et al., 2012),(Zong, Lu, Chapman, & Xie, 2012). The results from this study support a multi-clonal invasion model, showing that multiple clones transform inside the duct and then one or more clones escape the ducts and migrate into the adjacent tissues to establish the invasive carcinoma. However, this recent study analysed only 10 patient samples of which 8/10

cases were high-grade, so it is likely that as with previous studies there are also alternative models of DICS progression (Casasent et al., 2018). Consistent with Navin's model, a study using flow-sorting and single cell copy number profiling in a single DCIS patient also reported evidence that multiple clones invaded the basement membrane (Martelotto et al., 2017).

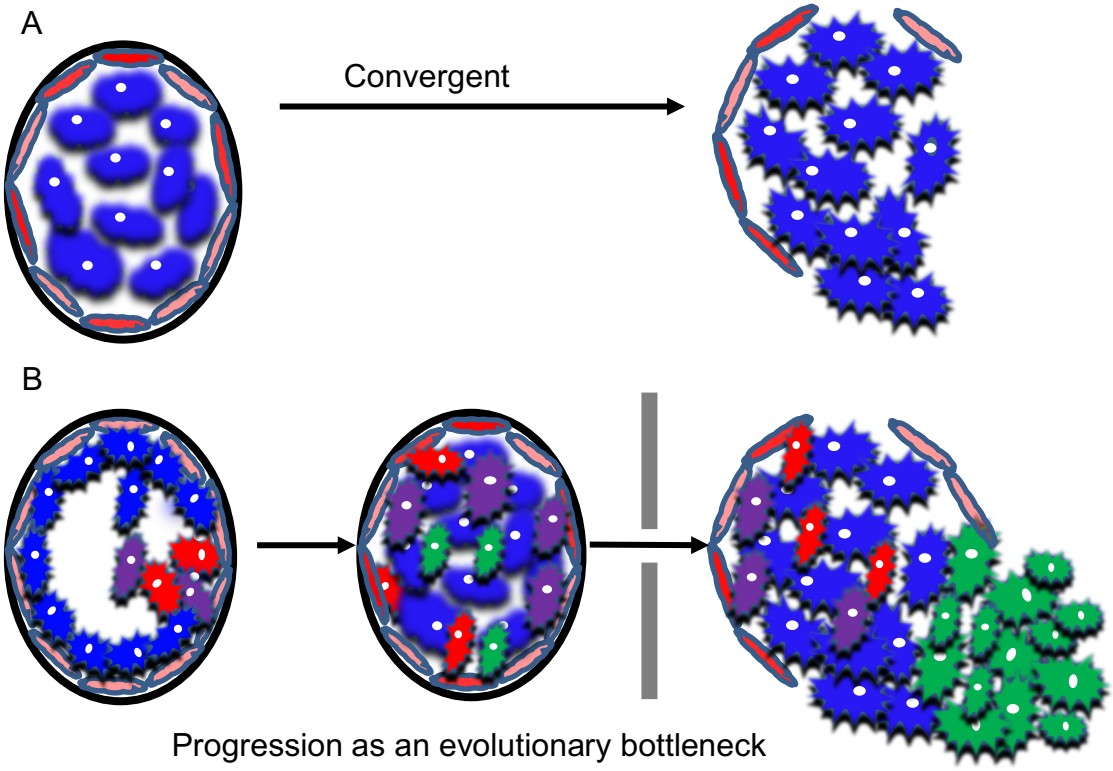

Figure 1-11 Schematic of hypothetical models of DCIS progression

A) Progression from DCIS to invasive breast cancer as a convergent phenotype, where several combinations of somatic genetic and/or epigenetic aberrations result in the acquisition of the biological properties required for cancer cells to progress from *in situ* to invasive disease (i.e. the genetic/epigenetic aberrations selected for are distinct between patients but all result in the progression to invasive disease)

B) Evolutionary bottleneck model when a single cell in the duct gives rise to multiple clones , a single clone and passes through the bottleneck (in the schematic the green cell) escapes the basement membrane to become invasive breast cancer

Adapted from (Lopez-Garcia, Geyer, Lacroix-Triki, Marchió, & Reis-Filho, 2010)

1.7.4 Artificial Intelligence in breast screening

There is a recognised need to improve reliability and accuracy of breast screening. One factor in this improvement process is the accuracy of mammography interpretation. One focus is the use of artificial intelligence (AI) in the analysis of mammograms. Tech company google have developed an interest in breast screening - they have an AI team who have assessed the mammograms of 7500 women. These mammograms are anonymised and stored in a database held by CRUK. The aim is to assess if there are machine learning algorithms that can alert radiologist more accurately than current available techniques ("https://deepmind.com/blog/applying-machine-learning-mammography/," 2017). In addition to improved accuracy, these approaches have the potential to address workforce issues - at present there are challenges with NHS service provision with currently 13% of substantive consultant breast radiologist posts being vacant. Professor Anne Mackie, Director of Programmes for the UK National Screening Committee at Public Health England, commented: “Mammography is a key service for the NHS in the early detection of breast cancer. Exploring innovative new technologies such as machine learning has the potential to increase the efficiency of these services and make better use of the resources available to NHS screening programmes("https://deepmind.com/blog/applying-machine-learning-mammography/," 2017).”

1.7.5 The effect of screening on breast cancer incidence

Breast cancer remains the most commonly diagnosed cancer among women in the UK, accounting for a third of female cancer cases, and the second most common cause of female cancer related deaths ("http://www.cancerresearchuk.org/health-professional/cancer-statistics/statistics-by-cancer-type/breast-cancer/incidence-in-situ,"). The UK National Health Service screening program was implemented in 1988. Duffy and colleagues performed a case control study, assessing the impact of screening in London. Results showed that attendance at breast screening led to a decrease in breast cancer mortality of 35% (Massat et al., 2016). Incidence rates of DCIS increased by 40% between 1979-1981 and 1988-1990, then by almost two-and-a-half times (142% increase) between 1988-1990 and 1997-1999. Rates increased by 87% between 1997-1999 and 2011-2013 ("http://www.cancerresearchuk.org/health-professional/cancer-statistics/statistics-by-cancer-type/breast-cancer/incidence-in-situ,"). These trends in female *in situ* breast carcinoma incidence largely reflect the impact of the UK breast screening programme.

1.7.6 Over-diagnosis and over-treatment

The screening program has evolved over time leading to increased cancer detection rates. A surgical oncologist, who was key in establishing the breast screening program, has called for the program to be stopped, arguing it leads to healthy women being labelled 'cancer victims' and has not reduced the number of invasive tumours. The controversies associated with breast screening led to an independent review in 2012.

This review found that for every 10000 UK women aged 50 who attended screening for 20 years, 43 deaths from breast cancer would be prevented and 129 cases of invasive and non- invasive breast cancers would be over-diagnosed. Over-diagnosis is defined as the detection of a cancer that would not have been clinically apparent in woman’s lifetime if they had not attended

screening. This is a key concern as this can lead to over-treatment which may subsequently mean that in certain cases the harm of breast screening outweighs the benefits. The review found that one breast cancer death is prevented for about every three over-diagnosed cases identified and treated (Screening, 2012). It is also important to differentiate that the figures are different for women who are invited and those who actually attend screening, those women who actually attend are likely to be more engaging with health care. From the independent screening review the estimate was made for every 235 women invited to screening one death from breast cancer would be prevented, however the absolute benefit would be higher for those women that actually attended screening: 180 women would need to be screened to prevent one breast cancer death (Screening, 2012). These figures have been interpreted from previously performed trials and there is some concern with regards to validity of these trials in modern breast screening. Table 1.5 is from the breast screening review and is used to illustrate that differing trials have shown large differences in how beneficial breast screening is.

A further study estimated 52% over-diagnosis of breast cancer in a population offered organized mammographic screening (Torjesen, 2015). The NIH State of Science conference on DCIS, highlighted the need to understand more about the biological and molecular mechanisms underlying the progression of DCIS to invasive disease in order to achieve robust prognostic and therapeutic patient stratification (Allegra et al., 2010). An Independent UK panel on Breast Cancer Screening stated: 'Further research is needed to improve the precision of screening to better distinguish between breast cancers that will or will not cause harm during a woman's lifetime' (Screening, 2012).

	Description	Number of women
Independent screening review(Screening, 2012)	Based on RR reduction of 20% for women aged 55-79 years in the UK	235 women invited 180 women screened
Cochrane review (Gøtzsche & Jørgensen, 2013)	Absolute risk reduction based on the 13-year follow-up in the trials considered adequately randomised	20000 women invited
US task force (Nelson et al., 2009)	Based on 7 years of screening and 13 years of follow-up	1339 women invited aged 50-59 years, and 377 invited aged 60-69 years
Canadian Task Force(Tonelli et al., 2011)	Women aged 50–69 years screened every 2–3 years for about 11 years	720 women screened
Duffy et al, 2010 (Duffy et al., 2010)	Based on 22-year follow-up of women aged 50–69 years in the Swedish Two-County trial, assuming that the absolute risk reduction for the 7 years of screening can be multiplied up to reflect 20 years in the UK screening programmes	113 women screened
Beral et al, 2011 (Beral et al., 2011)	Women aged 50–70 years regularly screened for 10 years, based on summary of published evidence	400 women screened

Table 1-5 Absolute risk reduction, expressed as number of women who need to be invited or screened to prevent one breast cancer death, in the trials of breast cancer screening.

Due to the strength of opinion with regards to the value of breast screening prior to the 2012 screening review, there were divergent opinions in response to the screening review, stating the panel either underestimated or overestimated the problem of over-diagnosis. As a result of the strong response the panel reconvened to respond to these questions. Hanley and colleagues commented that the reduction in breast cancer mortality may be greater if a shorter follow up was used (Hanley, McGregor, Liu, Strumpf, & Dendukuri, 2013). A Danish study of the effects of screening showed the burden of over-diagnosis was less when compared to the Marmot review, among 1,000 women invited to screening from age 50 and followed until 79, 2–3 women would be prevented from dying from breast cancer for every woman over-diagnosed with invasive breast cancer or DCIS (Beau, Lynge, Njor, Vejborg, & Lophaven, 2017). Thus, there is an internationally recognized

need to better understand the biology of DCIS in order to more appropriately tailor therapy to individual patients. This means better biomarkers are needed for DCIS based on biological mechanisms that can help stratify patients into those that are at risk of disease progression and those who are not.

1.7.7 DCIS clinical trials

A number of clinical trials have been developed to evaluate the potential to treat non-high-grade DCIS by surveillance alone. There are currently trials open in the United Kingdom, Netherlands and United States. These trials aim to gain a better understanding of the natural course of certain types of DCIS.

LORIS is a phase III clinical trial of surgery versus active monitoring for Low Risk Ductal Carcinoma in Situ recruiting in the UK. The trial started recruiting in July 2014 and recruitment is due to end March 2020, cases are required to be screen detected or incidental microcalcification, biopsy results confirmed as non-high-grade DCIS, which are then submitted for central review prior to recruitment to the trial. Memorial Sloan Kettering Cancer Centre reviewed their DCIS patients and only 16 percent of their patients with DCIS met the LORIS inclusion criteria, emphasizing that the results of this observation study will apply to only a minority of patients (Pilewskie et al., 2016). The original LORIS recruitment target was 932 this has been readjusted to 188, currently there are 138 patients recruited to the trial. The LORIS Trial has many challenges with patient recruitment due to a combination of factors including the numbers of low-risk DCIS cases and entrenched ideology about how DCIS should be treated (https://www.dcisprecision.org/clinical-trials/loris/)

The LORD (LOw Risk DCIS) trial opened to recruitment in January 2017 in the Netherlands, and there are currently 28 sites open with 33 patients recruited from a target of 1240. The trial compares standard local surgical treatment for DCIS vs active surveillance consisting of annual digital mammography for 10 years. The primary outcome of the trial is Ipsilateral invasive breast cancer-free rate at 10 years (https://www.dcisprecision.org/clinical-trials/lord/)

The Comparison of Operative to Monitoring and Endocrine Therapy (COMET) trial for low risk DCIS is currently recruiting in the United States. The primary outcome is to compare the number of patients that develop ipsilateral invasive cancer that received guidance-concordant care (standard treatment surgery +/- radiotherapy) to the number of ipsilateral invasive cancers in patients that were placed on active surveillance after 2 years of follow-up. The trial recruited the first patient in February 2017, 80 sites are open to recruitment and there are currently 253 patients recruited to the trial. The challenges for recruitment include low numbers of low risk DCIS and this has led to a change in eligibility criteria to accept comedo necrosis ("https://www.dcisprecision.org/clinical-trials/comet/,").

The aim of the trials currently undergoing active recruitment is to gain an in depth understanding of DCIS. However, the clinical and scientific community are also striving to increase the biological understanding of DCIS progression to provide a more robust way of predicting DCIS progression. Table 1.6 shows a summary of current DCIS trials, patients recruited have been updated to reflect current status.

	LORIS	LORD	COMET
Phase	III	III	III
Study	AS	AS	AS+ET (choice)
Screening	MMG	MMG	MMG
Nuclear grade	1 or 2	1	1 or 2
Comedo necrosis	No	No	Eligible
ER	N/S	N/S	Positive
HER-2	N/S	N/S	Negative ***
Size	N/S	Any size	Any size
Patients/Target	138/932	28/1240	253/1200

Table 1-6 Summary of DCIS clinical trials

AS: Active surveillance, ET: Endocrine therapy, N/S: Not stipulated in study protocol, * single arm confirmatory trial, ** breast US and MRI, *** if tested.

The current DCIS trials have common issues with problems to recruit, this is a recurrent problem with surgical de-escalation trials. Along with recruitment difficulties only a small proportion of DCIS seen in the clinic is low risk DCIS and with low risk DCIS there is often a lack of agreement between pathologists as to the grade of DCIS and this had led to many cases being rejected at pathological central review. An international approach has now been applied with the PREvent ductal Carcinoma In situ Invasive Overtreatment Now (PRECISION) (van Seijen et al., 2019) initiative which is a multinational initiative to address current controversies in DCIS management. This will use data from patients recruited into LORIS, LORD and COMET. PRECISION has seven interlinked work packages (WP):

1. WP1 -Retrospective DCIS data and tissue block collection.
2. WP2- Comprehensive genomic characterization of DCIS.
3. WP3- Characterisation of the role of the immune microenvironment as a determinant of DCIS clinical biology.
4. WP4- The role of imaging in DCIS prognosis and outcome.
5. WP5- Functional validation of DCIS drivers.
6. WP6- Building and validation of DCIS risk stratification model.
7. Using ctDNA and multi-OMICS in active surveillance of DCIS using LORIS, LORD and COMET trials.

1.8 Microenvironment

1.8.1 DCIS Microenvironment

It is now well recognised that the tumour microenvironment plays a central role in tumour progression. The DCIS microenvironment is complex, consisting of fibroblasts, immune cells and cells that support the blood vessels. It also includes many secreted proteins produced by all of the cells present in the tumour that support the growth of the cancer cells (Polyak, 2010). A unique component of the DCIS microenvironment is the myoepithelial population. It has been suggested that epigenetic alterations in the stroma may be involved in the progression from in situ to Invasive breast cancer (Hu et al., 2005). The components of the tumour microenvironment and their role in DCIS progression will be discussed in detail further on in this chapter.

Angiogenesis is the formation of new blood vessels, which is required for tumour growth. Teo et al., assessed 355 DCIS cases of which 32 developed recurrence. A CD34 antibody was used to detect microvessel density (MVD). MVD was higher around foci of DCIS than around normal breast lobules ($P=0.001$) and was significantly higher in cases of DCIS that recurred ($P<0.0001$) (Teo et al., 2003). Two distinct vascular patterns have been described; an increase in stromal vascular density with angiogenic factors released by accessory cells and an increase in periductal vessels in which the angiogenic factors are secreted by intraductal tumour cells (Guidi et al., 1997), (Engels, Fox, Whitehouse, Gatter, & Harris, 1997), the latter pattern appears to be more associated with progression.

Whilst there are certain common features in the microenvironment of DCIS and invasive breast cancers, some studies have shown differences. For example, upregulation of *MFAP2, MMP11, MMP2, COL1A2, VIM,* and *PLAU* and downregulation of *CDH1* and *F2RL1* has been demonstrated in invasive disease compared to isolated DCIS (Abba et al., 2015). Ma et al compared gene expression changes in epithelial and stromal cells during DCIS progression (Ma, Dahiya, Richardson, Erlander, & Sgroi, 2009). They demonstrated changes in epithelial and stromal cells in the

transition from normal to DCIS however there were no significant changes in epithelial cells in the transition of DCIS to invasion, though there were differences in the gene expression of the stromal cells. There were 76 upregulated genes and 229 downregulated genes when comparing invasive cancer stroma to DCIS stroma (Ma et al., 2009). Genes increased in invasive cancer stroma included MMP11, MMP2 and MMP14, whilst there was decreased expression of genes involved in vasculature development (EMCN, FLT1. KDR,SEL,MTH11, EDNRB and PODXL).

1.8.2 The role of normal myoepithelial cells

The position of the myoepithelial cell (MEC) between the luminal cells and the stroma places them in the ideal anatomical position in which to influence both compartments and mediate environmental cross-talk. Myoepithelial cells are attached to luminal cells by desmosomes and to the basement membrane by hemidesmosomes (Adriance, Inman, Petersen, & Bissell, 2005). The myoepithelial cells contribute significantly to the formation of basement membrane, comprising collagen IV, fibronectin, laminin, nidogen, glycosaminoglycans, and proteoglycans. It forms a continuous layer separating myoepithelial cells from the stroma. Receptors for basement membrane components, especially integrins, present in MECs, are responsible for interactions with the matrix (Koukoulis et al., 1991).

MECs have a prominent smooth muscle actin cytoskeleton which is responsible for their contractile phenotype (Murrell, 1995), (Bussolati, Cassoni, Ghisolfi, Negro, & Sapino, 1996), in keeping with their physiological function in the ejection of milk.

1.8.3 The role of myoepithelial cells in tumour suppression

There is significant evidence for a regulatory role played by normal myoepithelial cells in the mammary gland, including control of epithelial cell polarity and anti-proliferative, anti-invasive and anti-angiogenic properties, thus providing a broad tumour-suppressor environment (Barsky & Karlin, 2006). Myoepithelial cells, which surround ducts and acini of glandular organs, form a natural border separating proliferating epithelial cells from basement membrane and underlying stroma, thus physically preventing tumour cell invasion (Pandey, Saidou, & Watabe, 2010).

Myoepithelial cells have been shown to down-regulate expression of matrix metalloproteinases (MMPs) in both tumour cells as well as fibroblasts, so promoting an anti-invasive phenotype (Jones, Shaw, Pringle, & Walker, 2003). Maspin is one of the most important tumour suppressor proteins that is secreted by normal myoepithelial cells which acts as an inhibitor of angiogenesis (Hopkins & Whisstock, 1994),(Pemberton et al., 1995). Thus, the myoepithelial cell could be considered as 'guardian of the ductal microenvironment' in the normal breast.

1.8.4 The role of myoepithelial cells in tumour progression

Whilst acting as a tumour suppressor in the normal breast, myoepithelial cells in DCIS are different to normal MECs. They have been described as showing loss of hemidesmosome formation, thereby altering the key interaction with the basement membrane (Bergstraesser, Srinivasan, Jones, Stahl, & Weitzman, 1995). They also show up-regulation of pro-invasive ECM proteins such as Tenascin-C (Adams, Jones, Walker, Pringle, & Bell, 2002). Allinen *et al.,* showed that myoepithelial cells exhibit more dramatic changes than any other cell component between normal and DCIS tissues, suggesting extensive abnormal paracrine interactions in DCIS. Indeed, xenograft studies suggest that dedifferentiation of host myoepithelial cells leads to the transition of *in situ* to invasive disease (Allinen et al., 2004). Man et al (Man & Sang, 2004) hypothesised that myoepithelial cells are lost through cell death in the progression to invasive cancer: this theory is investigated further in chapter 3 of this thesis.

Work in our laboratory has shown that expression of αvβ6 integrin is up-regulated in myoepithelial cells in a subset of DCIS, leading to altered myoepithelial cell function and the establishment of a pro-tumorigenic environment. Myoepithelial cells expressing αvβ6 integrin lead to enhanced tumour invasion through TGFβ -dependent up-regulation of MMP-9 (Allen, Marshall, & Jones, 2014). We also have shown that up-regulation of αvβ6 integrin on DCIS-associated myoepithelial cells is associated with an increased periductal immune infiltrate (unpublished data).

An alternative theory to that proposed by Man *et al* is that myoepithelial cells become more migratory and less adhesive in the progression from DCIS to invasion. Structurally, myoepithelial cells form distinct desmosomes with both luminal cells and other myoepithelial cells, generate gap junctions and cadherin–cadherin interactions with other myoepithelial cells, and adhere to the basement membrane (BM) via integrins in focal adhesions and in hemidesmosomes(Ahmed, 1974), (Koukoulis et al., 1991), (Bergstraesser et

al., 1995), (Pitelka, Hamamoto, Duafala, & Nemanic, 2009). Runswick *et al.,* found that inhibition of the myoepithelial-specific desmosomal cadherins, desmocollin 3 (Dsc 3) and desmoglein 3 (Dsg 3), prevented morphogenesis of the bilayered acinus structure and disrupted the basal positioning of myoepithelial cells (Bissell & Bilder, 2003), (Runswick, O'Hare, Jones, Streuli, & Garrod, 2001), demonstrating the importance of these interactions in maintaining normal duct structure.

Whilst MECs exhibit altered characteristics in DCIS, loss of the myoepithelial cell population is pathognomonic of invasive breast disease. The recognition of myoepithelial cells is crucial in the diagnosis of a number of pathological breast lesions (Joshi, Smith, Perusinghe, & Monoghan, 1986). A number of markers can be used in diagnostic pathology to identify the myoepithelial cells, of which α-Smooth Muscle Actin (αSMA) and the basal cytokeratin CK5/6 are the most commonly used.

1.8.5 Fibroblasts

Fibroblasts are embedded within the stroma surrounding the glandular unit. A key function of fibroblasts is to maintain the stability of the extracellular matrix (ECM) and they are the major source of collagen and fibronectin which provide mechanical and structural support for the epithelial tissue. Fibroblasts also produce proteases, such as MMPs, which degrade the ECM, resulting in stromal reorganization and release of growth factors (Inman, Robertson, Mott, & Bissell, 2015). Fibroblasts are important in collagen deposition and alteration of collagen fiber orientation which are potentially important in DCIS progression. Provenzano et al., demonstrated distinct patterns of collagen signatures at different stages of tumour progression (P.P. Provenzano et al., 2006). Hu et al used a 3D co-culture model in which MDFDCIS cells were co-cultured with fibroblasts in recombinant basement membrane, the presence of fibroblasts led to increased invasive branching in the matrix, which was accompanied by increased levels of MMP-14 and MMP-9 in the co-cultures (Hu et al., 2009). A study assessing DCIS samples with micro

invasion showed myofibroblasts uPA, uPAR and MMP-13 which are linked to invasion (Nielsen, Rank, Illemann, Lund, & Danø, 2007).

1.8.6 Immune cells

The immune infiltrate of the stroma surrounding DCIS ducts is of increasing interest as a potential marker for DCIS progression and as a therapeutic target. Increased inflammation in DCIS is associated with high nuclear grade and HER2 positive lesions (A. H. Lee, Happerfield, Bobrow, & Millis, 1997a; Ramachandra, Machin, Ashley, Monaghan, & Gusterson, 1990). Esserman has also shown CD 68+ macrophages are also associated with high grade DCIS with comedo necrosis (Esserman et al., 2006). These are indications that an increased immune infiltrate within the stroma is likely to be a driver in tumour progression with the cross talk between the malignant epithelial cells and the progression with the cross talk between the malignant epithelial cells and the stroma. The tumour associated macrophages (TAMs) represent a major component of the immune infiltrate within the stroma of many tumours, M2 associated macrophages have pro-tumoral functions, including promotion of angiogenesis and matrix remodeling. There is an increase in periductal immune infiltrate associated with DCIS in particular showing increased numbers of T regulatory (Treg) cells, and this periductal immune infiltrate has been suggested to predict progression of DCIS to invasion (A. H. Lee, Happerfield, Bobrow, & Millis, 1997b). A functional role for inflammatory cells in the transition of DCIS to invasive disease has been hypothesised by Man and his group (Man, 2007), who suggest that factors released by the immune cells can damage myoepithelial cells, ultimately leading to their loss through apoptosis, so breaching the duct wall facilitating tumour invasion. Tumour necrosis factor related apoptosis-induced ligand (TRAIL) is a pro-apoptotic ligand, which is expressed by peripheral T lymphocytes (Salehi et al., 2007) including CD4+ve T cells (Sato et al., 2006). Therefore, an increase in the immune infiltrate in the DCIS microenvironment may lead to DCIS-associated myoepithelial cells being physiologically exposed to TRAIL.

The immune response of the tumour microenvironment is vitally important for both predicting progression and potential therapeutic targets. Tumour progression is likely to be compromised by the infiltration of CD8/Th1 T cells, NK and M1 TAM whereas tumour progression may be aided by $CD4^+$/Th2/T-reg, MDSC and M2 TAM. A study of 27 cases of DCIS, 24 of which were pure DCIS, showed higher numbers of TILs were in ER- DCIS, and a higher CD8/Treg ratio in ER+ DCIS (Thompson et al., 2016). A comparison of high-grade DCIS was found to have higher percentages of macrophages as identified by the macrophage marker CD68, compared with non-high-grade DCIS (Campbell et al., 2017).

Cell	Tumour suppressive	Tumour promoting
Myoepithelial cell	TIMP-1 Stefin A/B Maspin PAI-1 MMP-8 TSP-1	CXCL12 CXCL14 TGFβ αVβ6
Fibroblasts		IL-6 CXCL1 Cathespin B uPAR uPA MMP-13
Myeloid cells		CCL2 CXCR2- binding chemokines
Lymphocytes	CD8 Th1 CD4	Th2 CD4 Treg

Table 1-7 Summary of stromal cells involved in tumour suppression and progression

1.8.7 The microenvironment in invasive breast cancer

The tumour microenvironment plays a vital role in progression of breast cancer. In 1889 Paget discussed the importance of the microenvironment: metastasis is not due to chance events, but rather that some tumour cells (the “seed”) grow preferentially in the microenvironment of select organs (the “soil”) (Paget, 1989). The microenvironment is composed of fibroblasts, immune cells, endothelial cells, infiltrating inflammatory cells, adipocytes as well as signaling molecules and extracellular matrix (ECM), this is often collectively referred to as stroma (Hanahan & Coussens, 2012). The composition of the

stroma contributes towards breast density. The results of the International Breast Cancer Intervention Study (IBIS)-1 trial has suggested a link between the breast microenvironment and development of breast cancer. In those high-risk women receiving prophylactic Tamoxifen, there was a 63% reduction in risk of breast cancer, but this risk reduction was only seen in those women who exhibited at least 10% decrease in breast density. In those women with no reduction in breast density there was no protective effect of Tamoxifen. This links the protective effect of Tamoxifen to a change in the breast microenvironment (Cuzick et al., 2011). Fibroblasts are the most abundant cell type within the breast stroma. Normal fibroblasts can have tumour suppressive functions, but these suppressive functions are lost in tumour progression (Alkasalias, Moyano-Galceran, Arsenian-Henriksson, & Lehti, 2018). The switch of normal fibroblasts to cancer associated fibroblasts (CAFs) is an important factor in tumour progression. Orimo et al., showed that fibroblasts derived from primary human invasive breast carcinomas significantly enhanced tumour growth in xenograft models compared to their normal counterparts (Orimo et al., 2005). The ECM becomes progressively stiffer and more collagen-rich during tumour progression (Paszek et al., 2005). Lysyl oxidase (LOX), primarily secreted by fibroblasts, increases cross-linkage in collagens and elastin, increasing the insoluble matrix and contributing to tensile strength (Kagan & Li, 2003). LOX has been shown to regulate invasion: high levels of LOX in primary breast tumours or systemic delivery of LOX in mouse models leads to osteolytic skeletal lesion formation that was abrogated when LOX was genetically silenced (Cox et al., 2015). The pleiotropic effects of the tumour microenvironment are summarised in figure 1-12. Changes to the normal microenvironment promote tumour invasion. Altered function of carcinoma-associated fibroblasts and induction of an inflammatory infiltrate lead to release of pro-angiogenic factors. Development of a desmoplastic stroma, partly in response to hypoxia, leads to tumour-specific interactions with tumour cell-surface receptors that enhance invasion (M. Allen & Louise Jones, 2011; Paszek et al., 2005). As in DCIS, the immune microenvironment also has been implicated in invasive breast cancer. Finak et al identified three gene clusters from the stroma around invasive breast cancer and showed that the good-outcome cluster overexpress a distinct set of immune-related genes,

including T cell and NK cell markers indicative of a TH1–type immune response (GZMA, CD52, CD247, CD8A) (Finak et al., 2008). Recently, an in-silico analysis across nine datasets identified three distinct immune clusters dependent on both the abundance and composition of the infiltrate (Tekpli et al., 2019). Immune clusters were characterised as Cluster A (immune cold), Cluster B (immune intermediate) and Cluster C (immune hot), where Cluster B was associated with significantly poorer relapse-free and overall survival across all invasive cancer subtypes. Cluster B was associated with an epithelial–mesenchymal transition (EMT) or proliferative phenotype. Whether similar clusters exist in the DCIS microenvironment remains to be established(Tekpli et al., 2019).

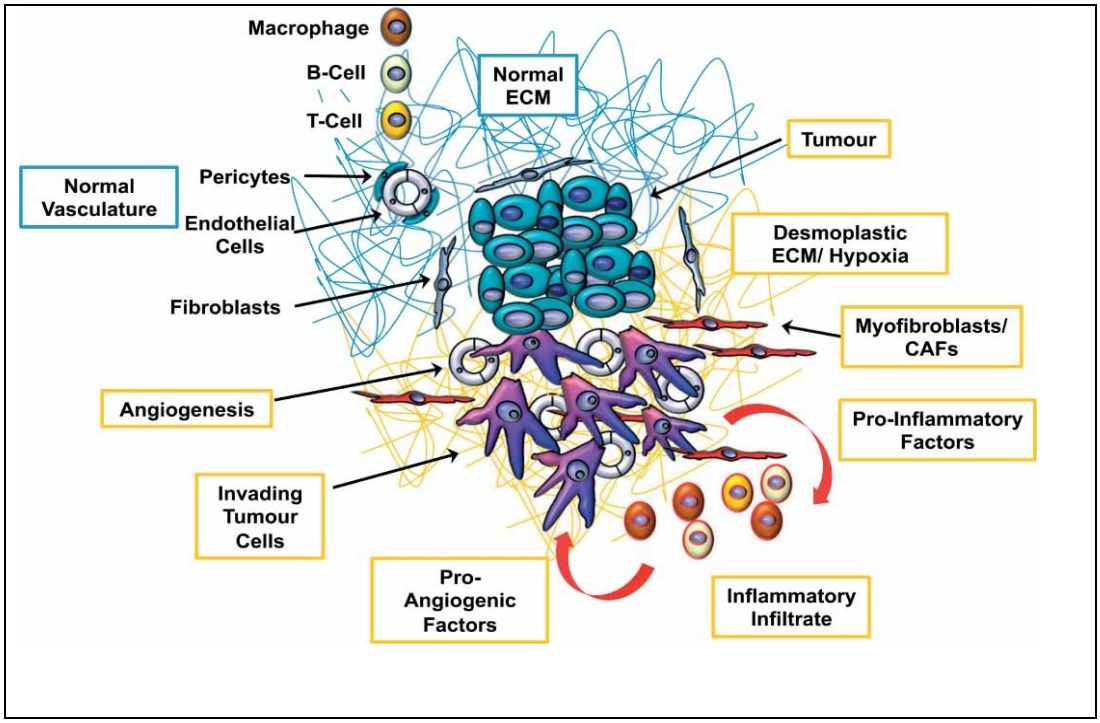

Figure 1-12 Tumour microenvironment schematic

Changes to the normal microenvironment promote tumour invasion. Altered function of carcinoma-associated fibroblasts and induction of an inflammatory infiltrate lead to release of pro-angiogenic factors. Development of a desmoplastic stroma, partly in response to hypoxia, leads to tumour-specific interactions with tumour cell-surface receptors that enhance invasion.(M. Allen & Louise Jones, 2011; Paszek et al., 2005)

1.9 Cell Adhesion

Cell adhesion is the process by which cells interact and attach to neighbouring cells and the extracellular matrix. These interactions are regulated by specialised cell surface molecules and are vitally important for the stability of the normal breast duct. Breakdown in these interactions may contribute to loss of cellular organisation and potentially subsequent progression to invasive disease.

Adherens junctions and tight junctions are present at cell-cell contacts. The adherens junctions' mediate cell-cell adhesion via the actions of nectins and cadherins. The tight junctions regulate passage of ions and small molecules between cells and establish cell polarity (Campbell, Maiers, & DeMali, 2017).

Hemidesmosomes (HDs) are highly specialized integrin-mediated epithelial attachment structures (Walko, Castañón, & Wiche, 2015). They are important in maintaining structural stability of epithelial cells by anchoring them to the basement membrane (Alberts et al.). $\alpha 6\beta 4$ is the key integrin component of hemidesmosomes and shows strong, basal expression in normal myoepithelial cells (Bergstraesser et al., 1995).

Desmosomes are intercellular junctions that tether intermediate filaments to the plasma membrane. Desmogleins and desmocollins, members of the cadherin superfamily, mediate adhesion at desmosomes (Delva, Tucker, & Kowalczyk, 2009). The various adhesion structures in breast epithelial cell populations are summarised in figure 1-13.

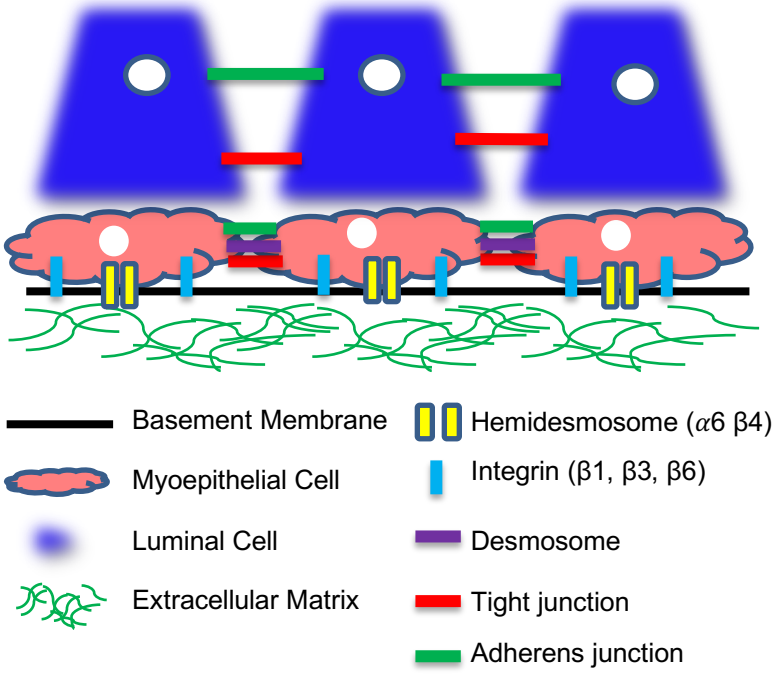

Figure 1-13 Schematic of cell adhesion

A summary of cell-cell junction and cell-matrix junction structures illustrating the interplay between cells and the extracelllar matrix.

1.10 Integrin αvβ6

As a member of the integrin family, integrin αvβ6 is a heterodimer made up of two subunits, αv and β6, and both are necessary for complete functioning (Niu & Li, 2017). Integrin αvβ6 is not expressed in healthy adult epithelia but is upregulated during wound healing and in cancer. αvβ6 has been shown to modulate invasion, inhibit apoptosis, regulate the expression of matrix metalloproteases (MMPs) and activate TGF-β1(Bandyopadhyay & Raghavan, 2009). Integrin αvβ6 appears to promote cell invasion and migration, both of which are involved in metastasis. The expression of αvβ6 is often associated with a poor prognosis (G. J. Thomas, Nyström, & Marshall, 2006).

Allen et al have shown upregulation of integrin αvβ6 by myoepithelial cells in 52% to 69% of non–high-grade and high-grade DCIS, respectively, but it is present in almost 100% of DCIS associated with invasive disease (M. D. Allen, Thomas, et al., 2014). To assess if αvβ6 may be used to predict recurrence, expression was assessed in a cohort of DCIS cases treated with local excision, confirmed margins free of disease and with long-term follow-up as part of the UK/ANZ DCIS trial (Cuzick et al., 2014). This showed a significant correlation between αvβ6 expression in myoepithelial cells and recurrence of breast cancer either as in situ or invasive disease, independent of patient age, disease grade, or extent. Those with αvβ6 positivity developed recurrence more quickly than those lacking αvβ6, with median time to recurrence of 2.3 versus 11.4 years, respectively (M. D. Allen, Thomas, et al., 2014).

1.11 Galectins

Galectins are a family of carbohydrate binding proteins, with a wide range of cellular functions. There are 15 different members which have been named in order of discovery. All Galectins contain a carbohydrate binding recognition domain (CRD). There are 3 groups which have differing structure; proteolytic galectins have one CRD (galectin 1,2,5,7,10,11,13,14,and 15), the tandem repeat galectins contain two homologous CRDs linked by a single polypeptide chain (galectin 4,6,8,9 and 12) and chimeric galectin which has a CRD connected to a non- lectin N terminal is galectin- 3. (R. Y. Yang, Rabinovich, & Liu, 2008)

Galectins have a diverse physiological role with functions in; cell adhesion, cell migration, apoptosis, differentiation. They have both intracellular and extracellular roles and their function can be location dependent. Galectins have been shown to have roles in inflammation, angiogenesis, immune response and cancer(Klyosov & Traber, 2012)

The dysregulation of galectin expression is frequently observed in cancer tissue (Vladoiu, Labrie, & St-Pierre, 2014), frequently in a tissue-specific manner.

1.12 Galectin-7

1.12.1 The Role of Galectin-7 in DCIS

Galectins are a family of evolutionary-conserved carbohydrate binding proteins. Essential functions include regulation of development, differentiation, cell-cell adhesion, cell-matrix interaction, growth and apoptosis. Galectins exhibit a wide range of subcellular localisations, and are found in both intracellular and extracellular compartments, however, Galectin-7 is reported to be predominantly intracellular (Grosset et al., 2014), and in normal breast it is strongly and exclusively expressed by the myoepithelial cells, located predominantly in the nucleus (Demers et al., 2010). Several functions have been described for Galectin-7. It has been shown to suppress TGFβ-mediated gene transcription by promoting nuclear export of SMAD2/3 (Gendronneau et al., 2008), so acting as an antagonist of TGFβ signalling. It has also been identified as a regulator of apoptosis with both pro- or anti-apoptotic effects being described (Demers et al., 2010). Thus, Galectin-7 has the potential to antagonise the pro-tumourigenic TGFβ-mediated signalling generated by myoepithelial-associated β6 integrin, and to modulate response to apoptotic signals generated in the periductal environment that might compromise the myoepithelial barrier. Therefore Galectin-7 may comprise part of the tumour-suppressor armoury of normal myoepithelial cells. Thus, loss of Galectin-7 from DCIS associated myoepithelial cells may be predicted to augment the effects of β6 integrin and destabilise the myoepithelial-basement membrane barrier so predisposing to progression to invasive disease. Establishing the functional relevance of Galectin-7, its interaction with β6 integrin and the myoepithelial response to pro-apoptotic stimuli in the periductal environment, would clarify the role of Galectin-7 and may identify loss of Galectin-7 as an important marker of disease progression.

1.12.2 The role of Galectin-7 in Breast Carcinoma

There have been various studies regarding the role of Galectin-7 in breast carcinoma. In the normal breast duct, myoepithelial cells strongly express Galectin-7, while luminal cells are negative. Demers *et al.,* used mouse models to demonstrate the effect of Galectin-7 in breast cancer. Breast cancer cells expressing high levels of Galectin-7 exhibit an increased ability to metastasise to lungs and bone. Examination of normal and malignant human breast tissue indicated that Galectin-7 is expressed in breast carcinoma with an aggressive phenotype (Demers et al., 2010). High levels of Galectin-7 in breast cancer cells render them more resistant to apoptosis and they metastasise earlier. The resistance of breast cancer cells to apoptosis is suggested to be dependent on the subcellular localisation of Galectin-7. To demonstrate this, the MCF-7 breast carcinoma cell line was transfected with a mutant form of Galectin-7 (R74S) with altered sub-cellular location (Grosset et al., 2014). Normally, intracellular Galectin-7 is found in the cytoplasm, nucleus and mitochondria. The mutation at position 74 affected the translocation of Galectin-7 to mitochondrial and nuclear compartments. Both mutant and wild type Galectin-7 were found to give equal resistance to drug induced cell death, indicating that the anti-apoptotic function of Galectin-7 is independent of subcellular localization (Grosset et al., 2014), however, this study is limited to one cancer cell line and therefore appropriate weighting should be applied. Other studies have shown the importance of subcellular localization of Galectin-7 and indicate that this may vary between different cancers or cell lines. Lu *et al.,* found Galectin-7 is overexpressed in chemically induced mammary carcinoma in rat models. Galectin-7 was restricted to the mammary carcinoma and not found in any normal tissue pointing to a role for Galectin-7 in tumour progression (Lu, Pei, Kaeck, & Thompson, 1997). These studies indicate that the cellular context in which Galectin-7 is expressed may determine its function: thus, in myoepithelial cells Galectin-7 appears to favour tumour-suppression whilst in invasive cancer cells it associates with more aggressive behaviour.

1.12.3 Role of Galectin-7 in other cancers

1.12.3.1 Prostate Carcinoma

Prostate and breast carcinoma have many biological similarities. St-Pierre's group investigated the role of Galectin-7 in prostate carcinoma and found Galectin-7 was expressed in the basal cells of normal prostate tissue – the equivalent of breast myoepithelial cells - and this was down regulated in prostate cancer (Labrie et al., 2015). The prostate cancer cell line DU-145 was transfected with Galectin-7 and demonstrated increased sensitivity to apoptosis following treatment with the pro-apoptotic drug cisplatin, using cleavage of PARP as a marker (Labrie et al., 2015). DU-145 cells transfected with wild -type or mutant Galectin-7 injected into adult male NOD/SCID mice showed a modest but significant reduction in tumour size with overexpression of Galectin-7^{wt}. The mutant Galectin-7 transfectant resulted in a significant increase in tumour size compared with control and Galectin-7^{wt}. The mutant form of Galectin-7 exhibited a change in the carbohydrate recognition domain (Labrie et al., 2015). This study illustrates the complex diverse role of Galectin-7, acting as a tumour suppressor in-vitro and as a pro-tumorigenic protein in-vivo. This suggests the role of galectins in cancer likely involves a delicate balance of pro and anti-tumoural interactions occurring within intra and extracellular compartments with the microenvironment playing an important role (Labrie et al., 2015).

1.12.3.2 Gastric Carcinoma

A study on tissue microarrays of gastric cancers showed low expression levels of Galectin-7 in malignant tissue compared with matched normal tissue (S. J. Kim, Hwang, Ro, Lee, & Chun, 2013). Advanced TNM stage was associated with decreased expression of Galectin-7. In gastric carcinoma Galectin-7 is thought to act as a tumour suppressor, with expression of Galectin-7 suppressing the proliferation, migration, and invasion of gastric cancer cells (S. J. Kim et al., 2013).

1.12.3.3 Colorectal Carcinoma

The human colorectal cancer cell line DLD-1 was used in a study to assess the impact of Galectin-7. The ectopic expression of Galectin-7 in DLD-1 rendered the cells more sensitive to apoptosis (Ueda, Kuwabara, & Liu, 2004). Reduced angiogenesis may also contribute to the tumour-suppressive effect of Galectin-7, histological analysis showed reduction in CD31 expression in Galectin-7 DLD-1 cells compared to control cells (Ueda et al., 2004).

1.12.3.4 Oesophageal Carcinoma

Proteomics analysis revealed that Galectin-7 was highly expressed in oesophageal squamous cell carcinoma tissues when compared to normal oesophageal tissue. The alteration in the expression of Galectin-7 was confirmed on a tissue microarray. These findings suggest that Galectin-7 could be used as a potential biomarker for oesophageal cell carcinoma (X. Zhu et al., 2010). As previously discussed the subcellular localisation may be of importance in the role Galectin-7 plays in cancer progression. In normal tissue Galectin-7 was localised in the nuclei, whereas it was distributed throughout the cytoplasm, nuclei and membranes of oesophageal squamous cell carcinoma cells. These results suggest that tumour progression of oesophageal cell carcinoma may be associated with a translocation of Galectin-7 from the nucleus to the cytoplasm(X. Zhu et al., 2010). Zhu and colleagues also showed well differentiated oesophageal tumours had a stronger expression of Galectin-7 compared to poorly differentiated tumours and suggested up-regulation of Galectin-7 may be a mechanism of organ self-protection, and this early up-regulation could be a potential marker for detection of early treatable oesophageal carcinoma (X. Zhu et al., 2010).

1.12.3.5 Ovarian Carcinoma

In ovarian carcinoma a number of studies have demonstrated that increased levels of Galectin-7 is an indication of poor prognosis**.** Elevated Galectin-7 expression was found to be positively correlated with histological grade of tumour, advanced age, high mortality rate and poor survival outcome (H. J. Kim et al., 2013; Labrie, Vladoiu, Grosset, Gaboury, & St-Pierre, 2014) Immunohistochemical analysis of Galectin-7 expression in tissue microarrays showed that while Galectin-7 was not detected in normal ovarian tissues, positive cytoplasmic staining for Galectin-7 was detected in tumour cells of all epithelial ovarian carcinoma histological subtypes, but was more frequent in high grade tumours and metastatic samples (Labrie et al., 2014).

1.12.3.6 Cervical carcinoma

In cervical squamous cell carcinoma Galectin-7 appears to have a protective effect. Expression of Galectin-7 in cervical carcinoma tissues was shown to be negatively associated with lymph nodes metastasis and expression of Galectin-7 was negatively correlated with MMP-9 expression in the clinical samples (H. Zhu et al., 2013). Lack of Galectin-7 in cervical carcinoma samples identified a cohort of patients with a lower 5 year overall survival rate as compared to those tumours with positive staining, as indicated by Kaplan - Meier survival analysis (H. Zhu et al., 2013). Elevated Galectin-7 expression had been associated with improved outcomes after radiation therapy (Tsai et al., 2013).

1.12.3.7 Lymphoma

Galectin-7 has a similar role in conferring resistance to apoptosis in both lymphoma and breast carcinoma (Demers et al., 2010). Demers and colleagues used a Galectin-7 vector to transfect low metastatic lymphoma cells this increased their metastatic behaviour through inducing MMP-9 in a mouse model (Demers, Magnaldo, & St-Pierre, 2005). In a further study Demers has shown using a mouse model inhibition of Galectin-7 in aggressive lymphoma cells correlated with a decreased invasion of tumour cells in target organs(Demers et al., 2007). Abnormal expression of Galectin-7 is thought to

favour dissemination of lymphoma cells. Galectin-7 was found in a significant proportion of mature human B cell lymphoid neoplasms, but not in normal B lymphocytes (Demers et al., 2007).

1.12.3.8 Melanoma

An analysis of whole transcriptome profiling of human melanoma tissues revealed that Galectin-7 mRNA was detected in in more than 90% of biopsies of patients with nevi, while its expression was rarely found in biopsies collected from patients with malignant melanoma (Biron-Pain, Grosset, Poirier, Gaboury, & St-Pierre, 2013).

The expression patterns and relationship to behaviour in various tumour types is summarised in Table 1-7.

Type	Galectin-7 +ve/ high	Galectin-7 –ve/low	Role/ relevance	Ref
Skin	Galectin-7 is positive throughout all layers of the skin with the strongest being in the basal layer.	Expression rarely found in malignant melanoma	A study showed overexpression of Galectin-7 is insufficient to modulate the growth of primary tumors or the dissemination of B16 melanoma cells to the lung.	(Biron-Pain et al., 2013)
Breast	Normal Myoepithelial Cells Expressed in Basal phenotype of Breast Cancer	Normal Luminal Cells	High levels of Galectin-7 in breast cancer cells render them more resistant to apoptosis and thus this aggressive subtype metastasise earlier.	(Demers et al., 2010)
Cervical	Squamous epithelial cells	Negative staining in cervical carcinoma showed significantly lower 5 year	Elevated Galectin-7 expression is associated with improved outcomes after radiation therapy	(H. Zhu et al., 2013) (Tsai et al., 2013)
Ovarian	Galectin-7 was detected in epithelial cells in all epithelial ovarian carcinoma histological subtypes but was more frequent in high grade tumours and metastatic samples	Normal Ovarian Tissue	A number of studies demonstrate that increased levels of Galectin-7 are an indicator of poor prognosis.	(H. J. Kim et al., 2013; Labrie et al., 2014)
Oesophagus	Galectin-7 was highly expressed in Oesophageal Squamous Cell Carcinoma	Normal Oesophageal tissue	Associated with well-differentiated tumours	(X. Zhu et al., 2010)
Gastric	Normal Gastric tissue	Associated with advanced Gastric Carcinoma	In gastric carcinoma Galectin-7 acts as a tumour suppressor, with expression of Galectin-7 supressing the proliferation, migrations and invasion gastric cancer cells.	(S. J. Kim et al., 2013)
Prostate	Galectin-7 was present in basal cells of normal prostate tissue	Down regulated in prostate cancer	This study illustrates a complex relationship between Galectin-7 and apoptosis, with Galectin-7 acting as a tumour suppressor in-vitro and as a pro tumorigenic protein in-vivo. This study suggests mutation in the CRD drives a phenotypic switch in the prostate carcinoma cells.	(Labrie et al., 2015)
Lymphoma	Galectin-7 is present in normal B and T lymphocytes	Abnormal expression of Galectin-7 is thought to favour dissemination of lymphoma cells	Galectin-7 increases the metastatic behaviour of lymphoma cells and induces expression of MMP-9	(Demers et al., 2005) (Demers et al., 2007)

Table 1-7 Summary of Galectin-7 expression in cancer

1.13 Aims and hypothesis

The hypothesis of this study is that loss of expression of Galectin-7 by myoepithelial cells in DCIS alters myoepithelial cell function and contributes to a transition in myoepithelial cell function from tumour suppressor to tumour promotor. Specifically, the hypothesis is that loss of Galectin-7 combined with gain of avb6 indicates a more advanced stage of DCIS. Furthermore, since galectins have a role in modulating adhesion and apoptosis, the hypothesis is that a loss of Galectin-7 may alter myoepithelial cell adhesion to the basement membrane and promote apoptosis, so leading to loss of integrity of the myoepithelial -basement membrane barrier.

To investigate this further the aims are

1. Establish the expression of Galecin-7 and avb6 in tissue samples of pure DCIS and DCIS with associated invasion using immunohistochemistry.

2. Investigate the functional relevance of changes in the levels of myoepithelial cell Galectin-7 focusing on its role in apoptosis and adhesion.

3. Undertake RNA sequencing to investigate the global effect of altered myoepithelial Galectin -7.

Together, this work will further dissect the role of DCIS-altered myoepithelial cells in DCIS behaviour, and specifically elucidate the impact and potential clinical utility of Galectin-7.

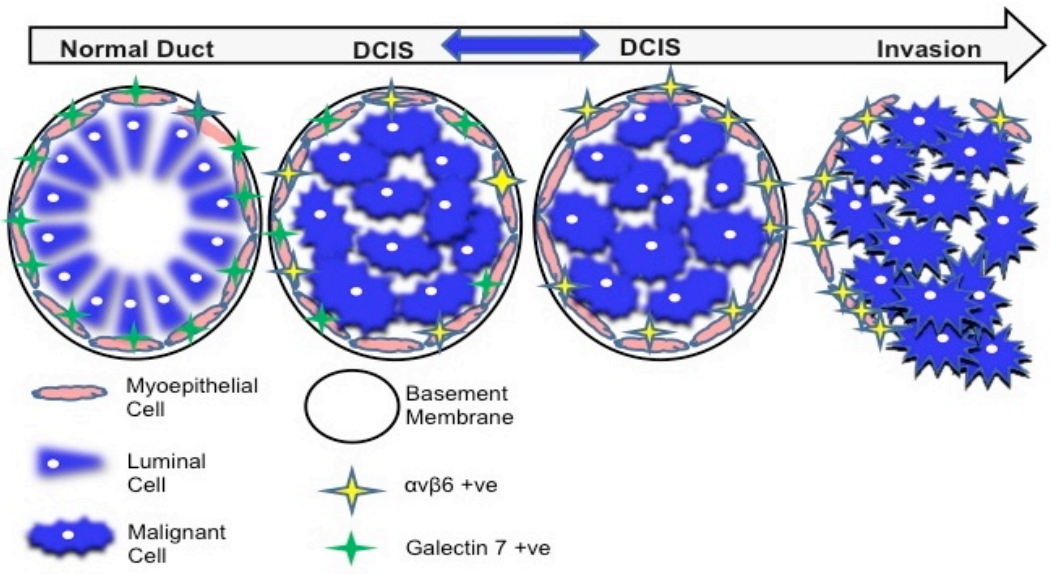

Figure 1-14 Hypothetical progression of DCIS

This schematic illustrates a normal breast duct with luminal cells organised and polarised with myoepithelial cells strongly positive for Galectin-7 and negative for $\alpha v\beta 6$. There is then transition to DCIS with neoplastic proliferation of epithelial cells within the ductal-lobular structures of the breast that does not penetrate the myoepithelial basement membrane interface. The myoepithelial cells have an altered phenotype with loss of Galectin-7 and up-regulation of $\alpha v\beta 6$. In the DCIS ducts that progress to invasive disease there is loss of the myoepithelial basement membrane interface, possibly through TRAIL-induced apoptosis.

2 Myoepithelial cell expression of Galectin-7 has an inverse correlation with poor prognostic marker αvβ6

2.1 Material and methods- Immunohistochemistry

2.1.1 Sample selection

Formalin Fixed Paraffin Embedded (FFPE) sections from a cohort of 45 patients collected between 2000 and 2015 at Barts Health NHS Trust were used for immunohistochemical characterization. All patients had consented to the Barts Cancer Institute tissue bank for their tissue to be used in research (Ethical Approval Reference 10/H0308/49, Cambridgeshire Ethics Committee October 2010). The cohort included 23 patients with pure DCIS (without any associated invasion) and 22 patients with DCIS with associated invasion, representing low-risk and high-risk models respectively (see introduction).

Sections at 4μM were cut onto charged glass slides and heated for 18 hours at room temperature. All antibodies used throughout were optimised with positive and negative controls prior to using on the DCIS tissue sections. Initial optimisation studies included varying the incubation time with the primary antibody, variable concentration of primary antibody and different concentrations of BSA for blocking non-specific staining in order to achieve optimal staining and minimal background. Optimal conditions are described in Table 2-1.

Sections were heated at 60°C for 10 minutes, and incubated serially in xylene (Fisher Scientific, X5-1) for 2 x 5 minutes then in decreasing alcohol dilutions and $_dH_2O$ after which endogenous peroxidase was blocked with a 10-minute incubation in 100% methanol/0.9% hydrogen peroxide. Antigen retrieval was performed using boiling citrate buffer at pH 6.0 for 8 minutes. Sections were blocked with appropriate serum (depending on the secondary antibody used) and BSA/PBS, as outlined in Table 2-1, for 15 minutes, then primary and

secondary antibodies were applied as outlined in Table 2-1. The incubation for all primary antibodies was 4°C overnight as this gave optimal results following the optimisation.

Following incubation, sections were then washed with PBS in triplicate followed by incubation with the secondary antibody at room temperature for 40 minutes. The sections were then washed again in triplicate followed by incubation with an avidin-biotin peroxidase complex (ABC) reagent (Vectastatin ABC Kit, Vecor Laboratories PK Rabbit 6101, Mouse 6102) for 30 minutes at room temperature. Sections were washed again in triplicate with PBS before developing using a DAB kit (Vectastain, Vector Laboratories SK 4100) and then counterstained with Haematoxylin for 2 minutes (Sigma, MHS16). The sections were washed with tap water and dehydrated through graded alcohols and xylene, and mounted with DPX (Sigma, 06522) and glass cover slips.

Antibody	Source/clone	Species	Dilution	Antigen retrieval	Positive control
Galectin-7	Abcam/ Ab108623	Rabbit	1:750 in 5% BSA	Citrate	Skin Normal breast tissue
β6	Calbiochem / 407317	Mouse	1:800 in 5% milk	Pepsin	β6 Positive DCIS
Oestrogen	Abcam / Ab16660	Rabbit	1:500 in 1% BSA	Citrate	ER positive breast cancer
Her 2	Abcam/ Ab134182	Rabbit	1:20 in 1% BSA	Citrate	Her 2 positive DCIS
Progesterone	Novocastra/ NCL-PGR-312	Mouse	1:100 in 1% BSA	Citrate	Normal breast
LOX	Novus Bio/ NB 1002327	Rabbit	1:500 in 1% BSA	Citrate	Colorectal cancer
P-Cadherin	BD Biosciences/ 616228	Mouse	1:25 in 1% BSA	Citrate	Tonsil

Table 2-1 Details of primary antibodies used in immunohistochemistry.

2.1.2 Scoring of Galectin-7 and αvβ6 staining

Sequential sections were used for Galectin-7 and αvβ6 staining. All slides were scanned on the Panoramic 250 slide scanner (3D HISTECH). The computer program 'panoramic viewer' was used for analysis. Each DCIS duct was annotated as shown in Figure 2-1 and a score of either positive, heterogeneous or negative was assigned to each DCIS duct. DCIS ducts with myoepithelial cells homogenously positive for either Galectin-7 or αvβ6 were positive, as detailed in Figure 2-2. DCIS ducts with some positive myoepithelial cells were designated heterogeneous, whilst DCIS ducts where the myoepithelial cells were homogenously negative were defined as negative.

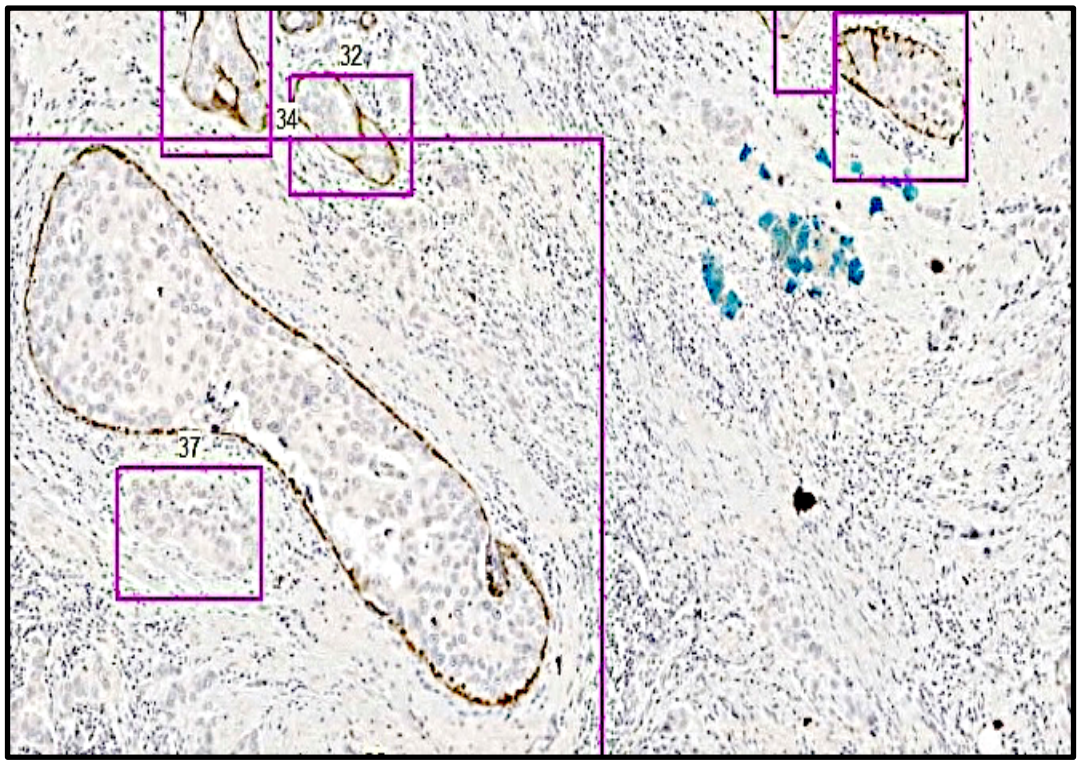

Figure 2-1 Annotation of ducts using panoramic viewer program.

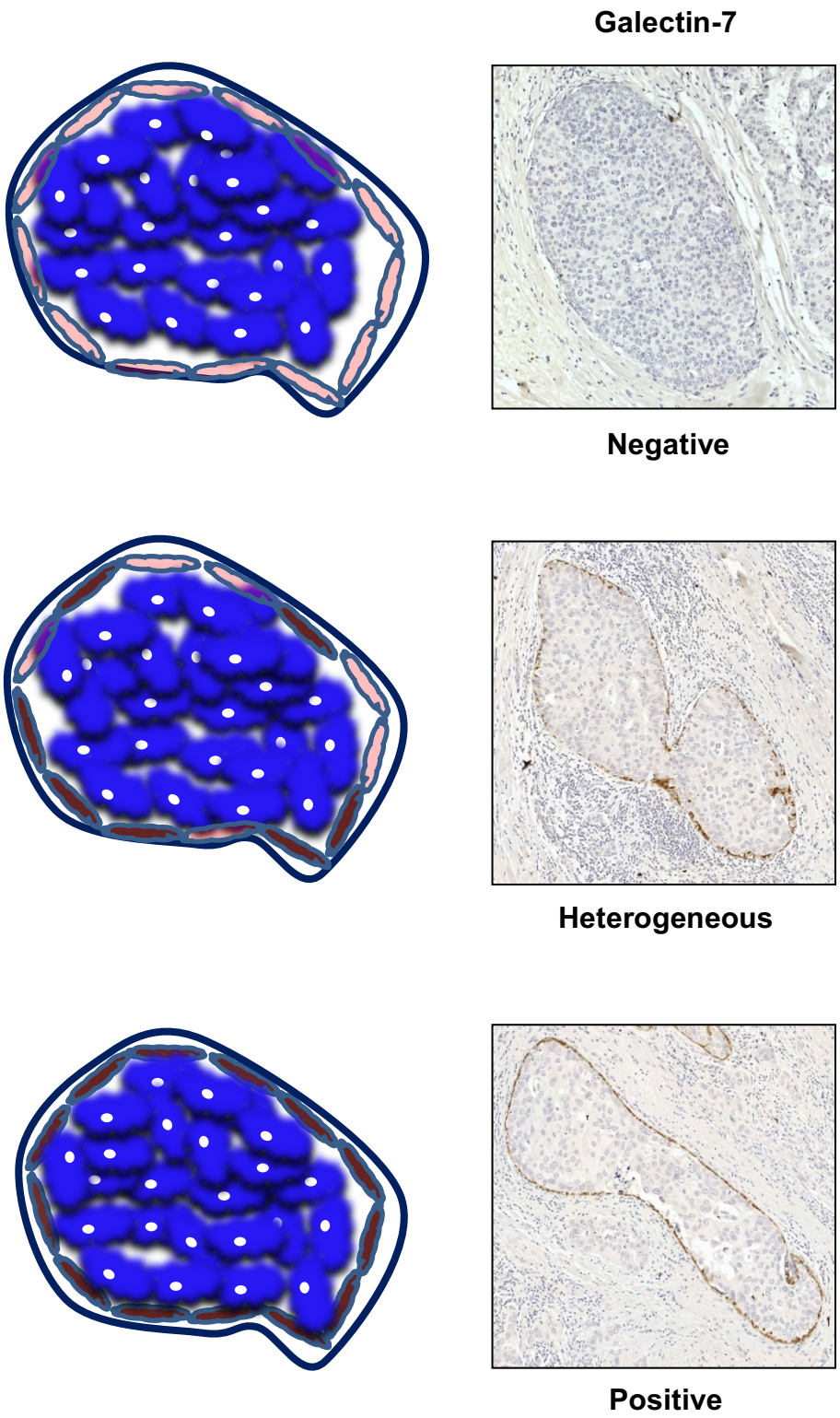

Figure 2-2 Schematic of DCIS duct scoring.

Individual ducts were assessed and scored. The staining of the myoepithelial cells was scored as negative (no staining), heterogeneous (some myoepithelial cells were stained) or positive where all myoepithelial cells in the duct were positive. Galectin-7 and $\alpha v\beta 6$ both were scored using this method. Galectin-7 staining is shown in this figure.

2.2 Results- Immunohistochemistry

2.2.1 Patient Cohort

The cohort of 45 patients included 23 cases of pure DCIS and 22 cases of DCIS with associated invasion, representing low-risk and high-risk models, respectively. Serial sections were used for staining for Galectin-7 and $\alpha v\beta 6$. There is some disparity between the markers in the number of ducts scored as DCIS ducts were not always present in all sections. There was no significant difference in the age of the patients or in the type of surgical intervention between the two groups (p-0.854, Table 2.2).

		Pure DCIS	DCIS with associated invasion	P value
Age (mean)		55.0	55.6	0.587
Size (mm)		31.3 (5-90)	22 (6-43)	
DCIS Grade (Number of patients)	High	15	20	
	Intermediate	6	0	
	Low	2		
	Unknown		2	
Type of DCIS	Comedo Necrosis	7	14	
	Solid	6	3	
	Cribriform	1	0	
	Mixed	2	2	
	Apocrine	1	0	
	Micropapillary	4	0	
	No special type	0	1	
	Unknown	2	2	
Surgery (%)	Mastectomy	64.0	66.7	0.854
	Wide Local excision	36.0	33.3	
Axillary Surgery (%)	None	48.0	9.5	0.0002
	SNS	44.0	38.1	
	ANS	4.0	33.3	
	ANC	4.0	19.0	

Table 2-2 Patient Cohort- summary of age distribution and operative management

2.2.2 Galectin-7 and αvβ6 Immunohistochemistry

Each DCIS duct was initially scored for Galectin-7 and αvβ6 independently, being blinded to the status of the other marker. On completion of scoring, the ducts were identified and the score for each marker combined.

2.2.3 Galectin-7 Immunohistochemistry

A total of 1926 DCIS ducts were scored for Galectin-7 and significant differences were seen between pure DCIS cases and DCIS with associated invasion. Pure DCIS and DCIS with associated invasion had 338 and 144 homogenously positive DCIS ducts, respectively (p=0.0014). Pure DCIS and DCIS with associated invasion had 286 and 413 heterogeneous DCIS ducts respectively (p=0.89), with 99 pure DCIS and 646 DCIS with associated invasion being homogenously negative for Galectin-7 (p=0.0002). Thus, there are significantly more Galectin-7 negative DCIS ducts in the DCIS with associated invasion cohort and significantly more Galectin-7 positive ducts in the pure DCIS group as shown in Figure 2-3.

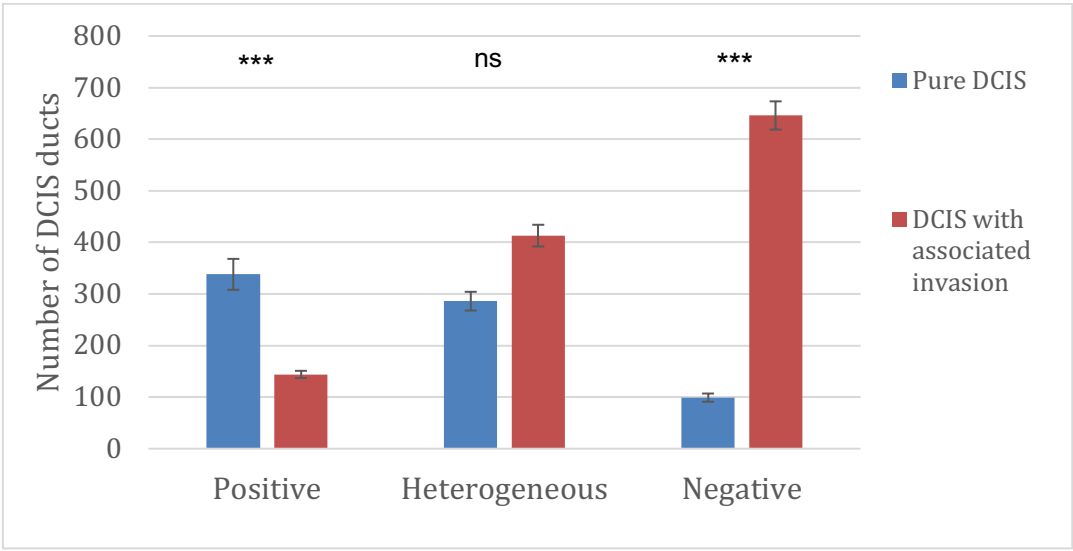

Figure 2-3 Myoepithelial expression of Galectin-7 in DCIS

Comparison between pure DCIS and DCIS with associated invasion patient cohorts for Galectin-7 showing the number of DCIS ducts homogenously positive, heterogeneously positive and homogenously negative.

2.2.4 αvβ6 Immunohistochemistry

A total of 1888 DCIS ducts were stained for αvβ6. Pure DCIS and DCIS with invasion had 102 and 207 homogeneously positive DCIS ducts, respectively (p=0.165). Pure DCIS and DCIS with invasion had 319 and 267 heterogeneously positive ducts, respectively (p=0.716), whilst pure DCIS had 770 negative ducts and DCIS with associated invasion had 223 negative ducts (p=0.02). This indicates that significantly more DCIS ducts are negative for αvβ6 in DCIS with associated invasion compared to the pure DCIS cohort, as shown in Figure 2-4.

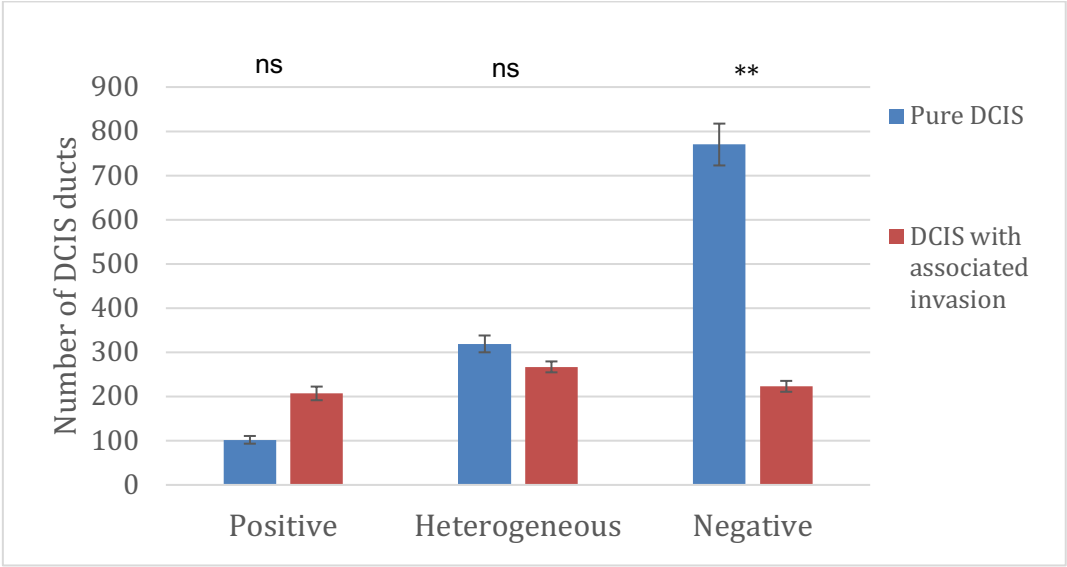

Figure 2-4 Myoepithelial expression of β6 in DCIS

Comparison between pure DCIS and DCIS with associated invasion cohorts for β6 showing the number of DCIS ducts homogenously positive, heterogeneously positive and homogenously negative.

2.2.5 Combined Galectin-7 and αvβ6 score

Following the independent scoring of Galectin-7 and αvβ6, the ducts were identified, and the scores combined. For this analysis, only DCIS ducts that were present in both the Galectin-7 and the αvβ6 sections were included. Each DCIS duct was given a Galectin-7/αvβ6 score. This analysis provides more information for each DCIS duct than assessing the markers in isolation. The potential score combinations are:

1. Galectin-7 positive/αvβ6 negative
2. Galectin-7 positive/ αvβ6 heterogeneous
3. Galectin-7 heterogeneous/αvβ6 negative
4. Galectin-7 negative /αvβ6 positive
5. Galectin-7 heterogeneous /αvβ6 positive
6. Galectin-7 negative /αvβ6 heterogeneous

Of these, scores, combinations 1-3 were identified in significantly higher number of DCIS ducts in the pure DCIS cohort compared to the DCIS with associated invasion cohort. Conversely, the score combinations 4-6 were identified in a significantly higher number of DCIS ducts in the DCIS with associated invasion cohort (Tables 2-3 & 2-4 and Figure 2-5).

Pure DCIS	β6 Positive	β6 Heterogeneous	β6 Negative	Total
	Number of DCIS ducts (% of total DCIS ducts)			
Galectin-7 Positive	38 (5.38)	79 (11.19)	224 (31.73)	341 (48.30)
Galectin-7 Heterogeneous	10 (1.42)	58 (8.22)	205 (29.04)	273 (38.67)
Galectin-7 Negative	5 (0.71)	18 (2.55)	69 (9.77)	92 (13.03)
Total	53 (7.51)	155 (21.95)	498 (70.54)	706 (100.00)

Table 2-3 Pure DCIS cohort combined Galectin-7/ αvβ6 score

The number (percentage) of DCIS ducts assigned to each Galectin-7/ αvβ6 score category.

DCIS with associated invasion	β6 Positive	β6 Heterogeneous	β6 Negative	Total
	Number of DCIS ducts (% of total DCIS ducts)			
Galectin-7 Positive	52 (9.59)	16 (2.95)	48 (8.85)	116 (21.40)
Galectin-7 Heterogeneous	54 (9.94)	59 (10.88)	88 (16.20)	201 (37.08)
Galectin-7 Negative	57 (10.51)	68 (12.55)	100 (18.41)	225 (41.51)
Total	163 (30.07)	143 (26.38)	236 (43.54)	542 (100.00)

Table 2-4 DCIS with associated invasion cohort combined Galectin-7/ αvβ6 score

The number (percentage) of DCIS ducts assigned to each Galectin-7/ αvβ6 score category.

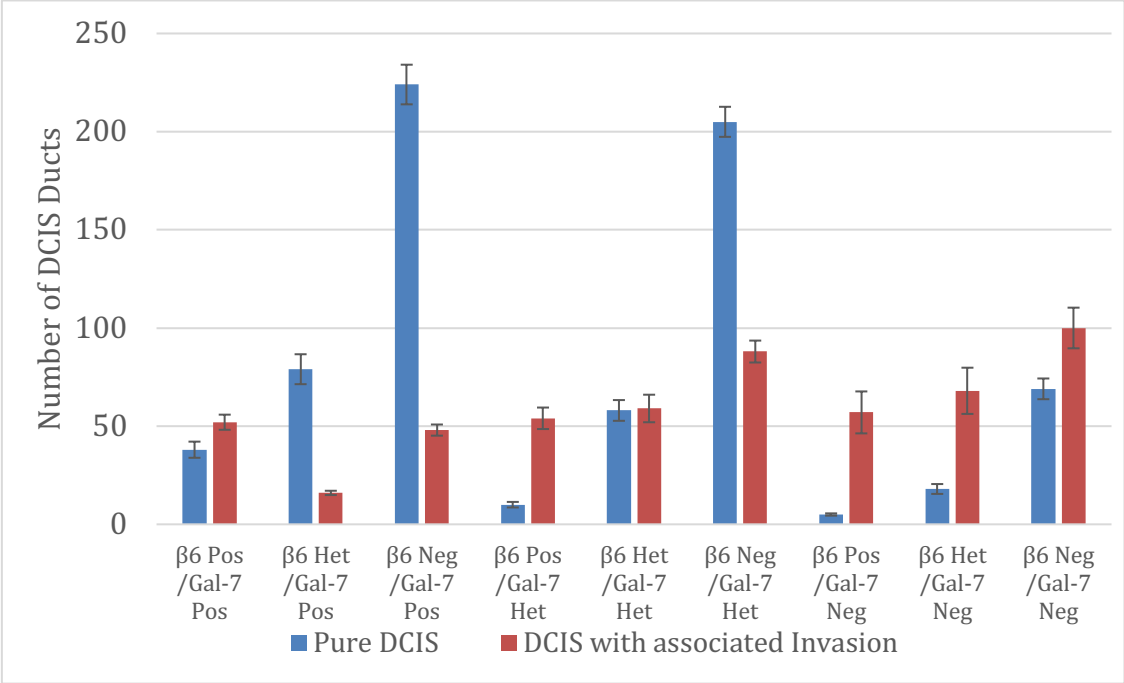

Figure 2-5 Analysis of Galectin-7/αvβ6 combination scores

A comparison between pure DCIS and DCIS with associated invasion cohorts assessing Galectin-7/αvβ6 combination scores. Error bars represent standard deviation.

Only homogeneously positive or homogenously negative Galectin-7 and αvβ6 ducts were included in a further analysis. This shows higher numbers of Galectin-7 positive, αvβ6 negative DCIS ducts in the pure DCIS cohort compared to the DCIS with associated invasion cohort and higher numbers of Galectin-7 negative, αvβ6 positive DCIS ducts in the DCIS with associated invasion cohort compared to the pure DCIS cohort (Figure 2-6).

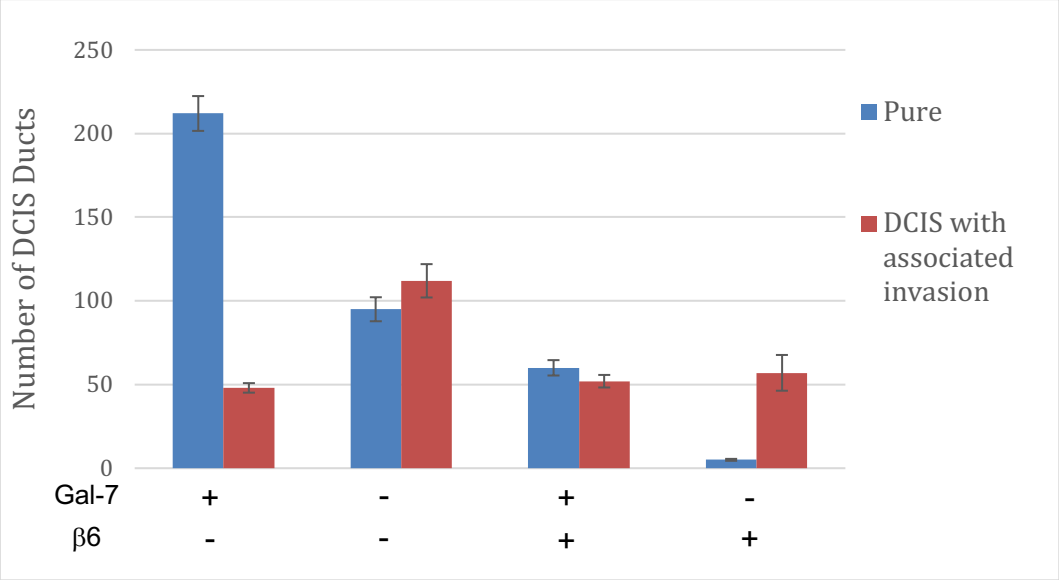

Figure 2-6 Analysis of Galectin-7/αvβ6 combination scores (homogenously positive and negative scores only)

A comparison between pure DCIS and DCIS with associated invasion cohorts assessing Galectin-7 / αvβ6 combination scores assessing homogenously positive and negative scores only. Error bars represent standard deviation.

2.2.6 Chi-squared analysis

Chi-squared is used to assess the relationship between the 2 markers Galectin-7 and αvβ6 in the pure DCIS and DCIS with associated invasion cohort. We have shown both these markers to change in our high risk DCIS model. There is the possibility that these markers are independent of each or that change in one protein may influence a change in the other protein.

A chi-squared calculation has been performed for the pure DCIS and DCIS with associated invasion cohorts. The analysis indicates a significant inverse relationship between Galectin-7 and αvβ6 in both the pure DCIS and DCIS with associated invasion cohorts (p=<0.001 for both cohorts; Tables 2-5 & 2-6). In pure DCIS there is more frequent Galectin-7 positivity and negativity for αvβ6, whilst in DCIS with associated invasion, the reverse is seen.

Pure DCIS	β6 Positive	β6 Heterogeneous	β6 Negative
Galectin 7 Positive	38 (25.6) [6.01]	79 (74.87) [0.23]	224(240.54) [1.14]
Galectin7 Heterogeneous	10 (20.49) [5.37]	58 (59.94) [0.06]	205(192.57) [0.8]
Galectin-7 Negative	5(6.91) [0.53]	68 (59.36) [1.26]	69(64.90 [0.26]

Chi square	14.63
p value	0.005518

Table 2-5 Chi squared calculations for the pure DCIS cohort

DCIS with associated invasion	β6 Positive	β6 Heterogeneous	β6 Negative
Galectin 7 Positive	52 (34.89) [8.40]	16 (30.61) [6.97]	48 (50.51) [0.12]
Galectin7 Heterogeneous	54 (60.45) [0.69]	59 (53.03) [0.67]	88 (87.52) [0.0]
Galectin-7 Negative	57 (67.67) [1.68]	68 (59.36) [1.26]	100 (97.97) [0.04]

Chi square	19.8326
p value	0.000539

Table 2-6 Chi squared calculations for the DCIS with associated invasion

2.3 Galectin-7 analysis to assess variation between patients

As an alternative method of analysis, each patient has been assessed individually, as grouping the ducts from the pure DCIS cohort and DCIS with associated invasion together may mean certain patients with higher numbers of ducts would skew the data.

The cases have been analysed looking at the number of positive, heterogenous or negative ducts per case, percentage of positive, heterogenous or negative ducts per case and also a score has been assigned to each patient and the method for this is discussed later in the chapter.

In the pure DCIS cohort the average number of ducts scored per patient was 41 whilst the average number of ducts scored in the DCIS with associated invasion group was 52. A T Test was performed, and this difference was shown to not be statistically significant with a p value of 0.19.

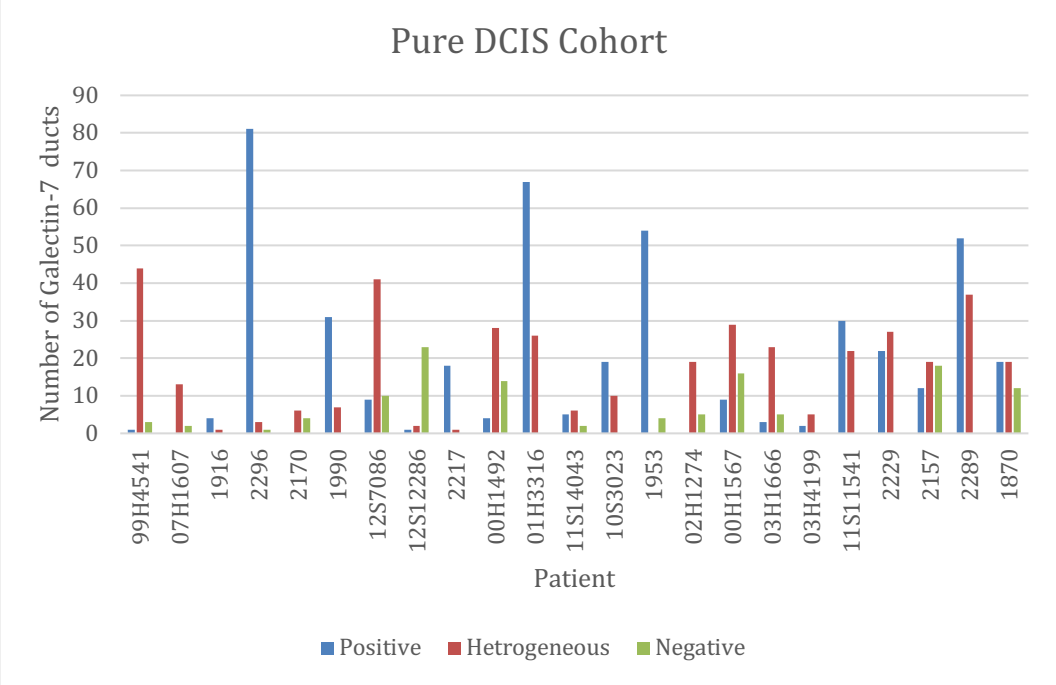

Figure 2-7 Pure DCIS cohort analysis of duct number per patients

Analysis of each patient individually in the pure DCIS cohort to assess the number Galectin-7 positive, heterogeneous and negative ducts.

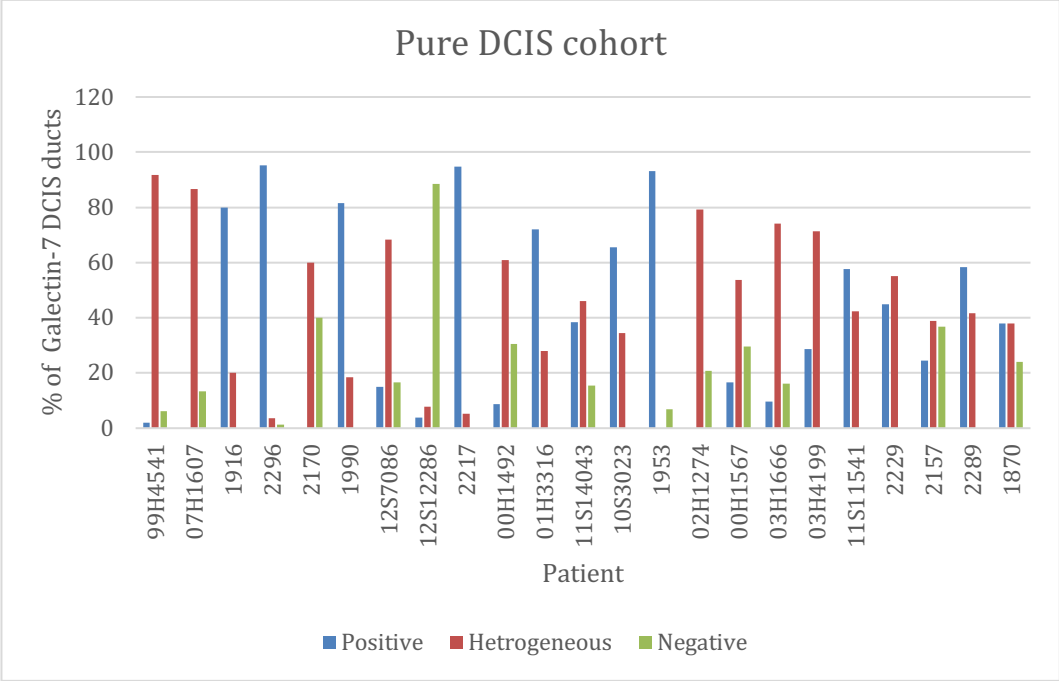

Figure 2-8 Pure DCIS cohort analysis using % of DCIS ducts

Analysis of each patient individually in the pure DCIS cohort to assess the percentage of Galectin-7 positive, heterogeneous and negative ducts.

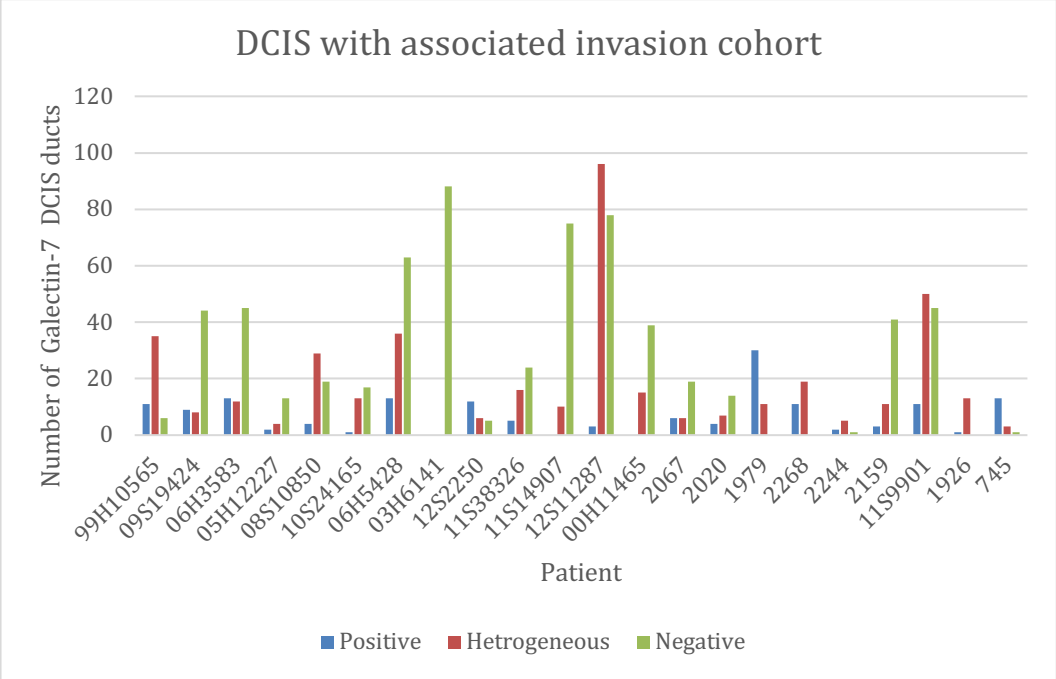

Figure 2-9 DCIS with associated invasion cohort analysis using number of DCIS ducts scored for Galectin-7

Analysis of each patient individually in the DCIS with associated invasion cohort to assess the number of Galectin-7 positive, heterogeneous and negative ducts.

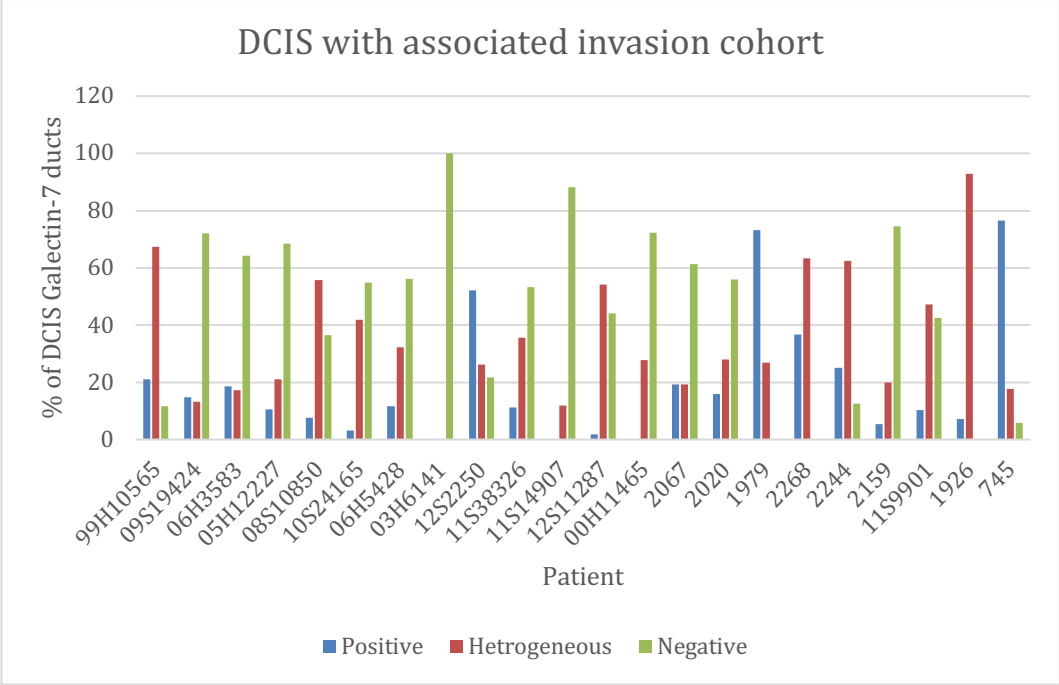

Figure 2-10 DCIS with associated invasion cohort analysing using % of ducts that are scored for Galectin-7

Analysis of each patient individually in the DCIS with associated invasion cohort to assess the percentage of Galectin-7 positive, heterogeneous and negative ducts.

2.4 Galectin-7 score per patient

In order to make comparison between patients and between pure DCIS and DCIS with associated invasion cohort each patient was allocated a score. The score was calculated using a weighting for positive, heterogenous and negative, this was then multiplied by the percentage of ducts that were in each category. The weightings allocated were negative - 0, heterogenous-1 and positive-2.

The distribution of scores for each cohort is shown in Figures 2.11 and 2.12.

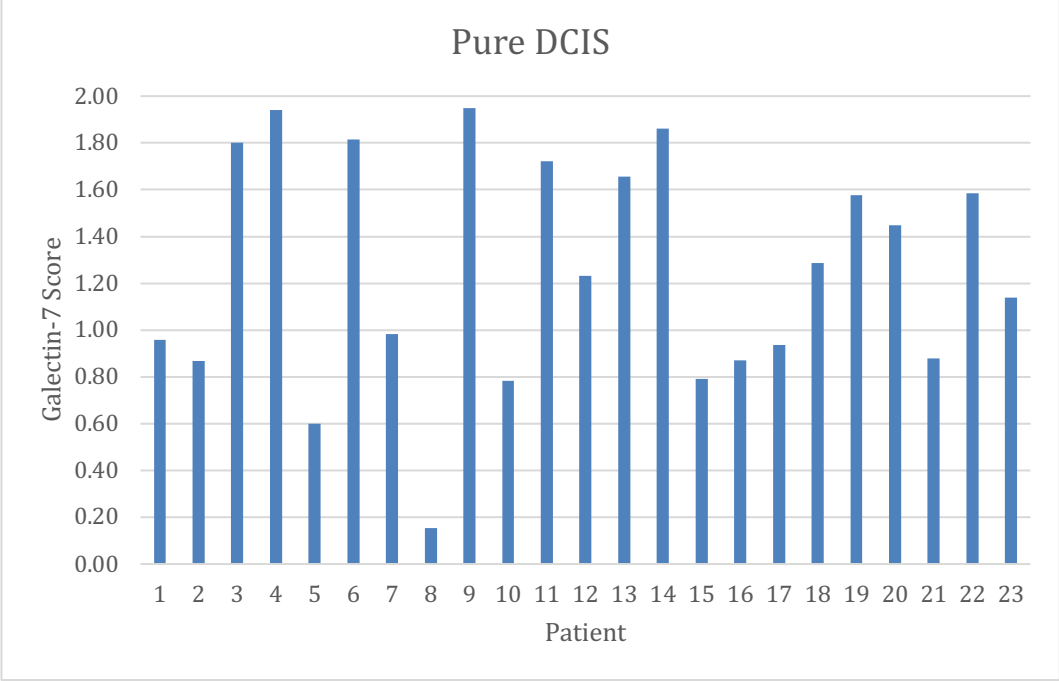

Figure 2-11Pure DCIS Galectin-7 score per patient

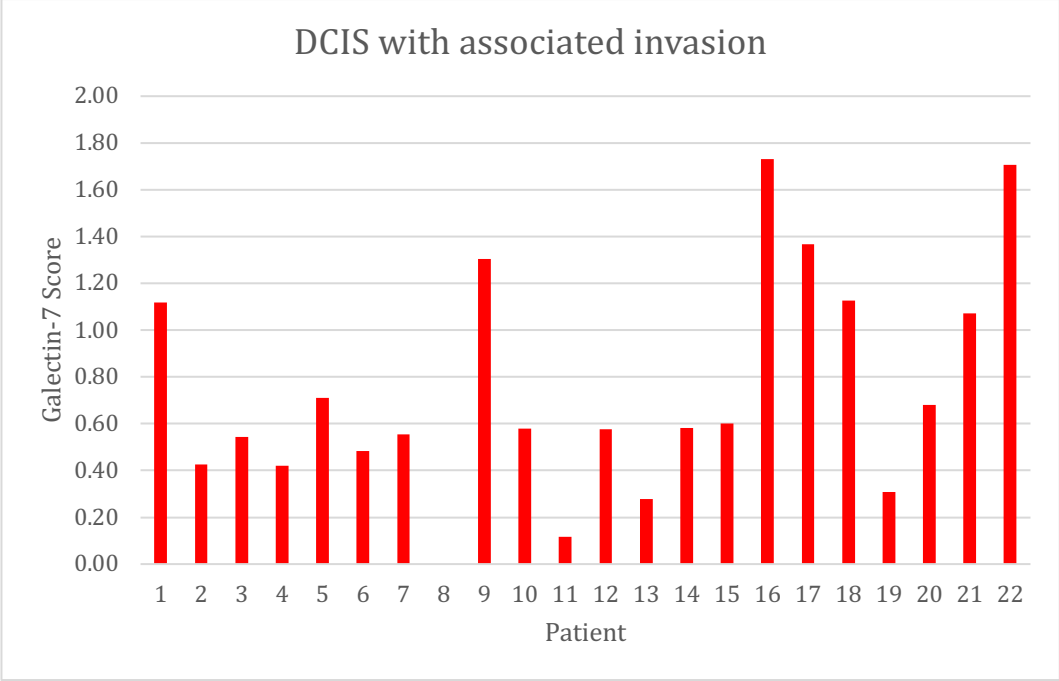

Figure 2-12 DCIS with associated invasion Galectin-7 score per patient

A mean score for each cohort was calculated and a comparison was made between pure DCIS and DCIS with associated invasion cohorts. The mean score in the pure DCIS group is 1.25 and in the DCIS with associated invasion group is 0.74, A Student T Test shows difference is statistically significant (<0.001).

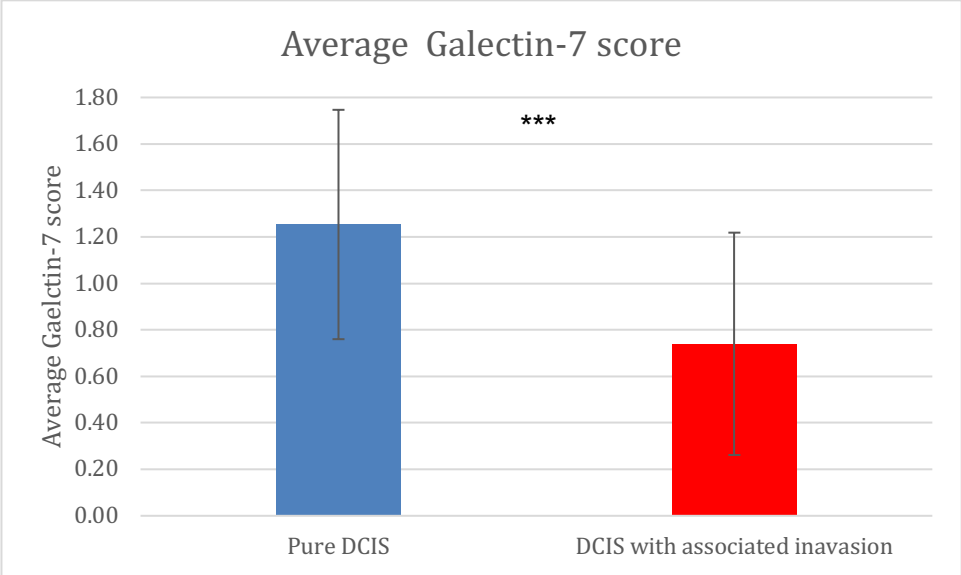

Figure 2-13 Comparison of the average Galectin-7 score between pure DCIS and DCIS with associated invasion cohorts.

The mean score in the pure DCIS group is 1.25 and in the DCIS with associated invasion group is 0.74. Student T Test indicates this difference is statistically significant (<0.001; error bars are standard deviation)

2.5 αvβ6 Scores per patient

A mean score for each cohort was calculated and a comparison was made between pure DCIS and DCIS with associated invasion cohorts. The mean score in the pure DCIS group is 0.27 and in the DCIS with associated invasion group is 0.82. Student T Test indicates this difference is statistically significant (<0.005).

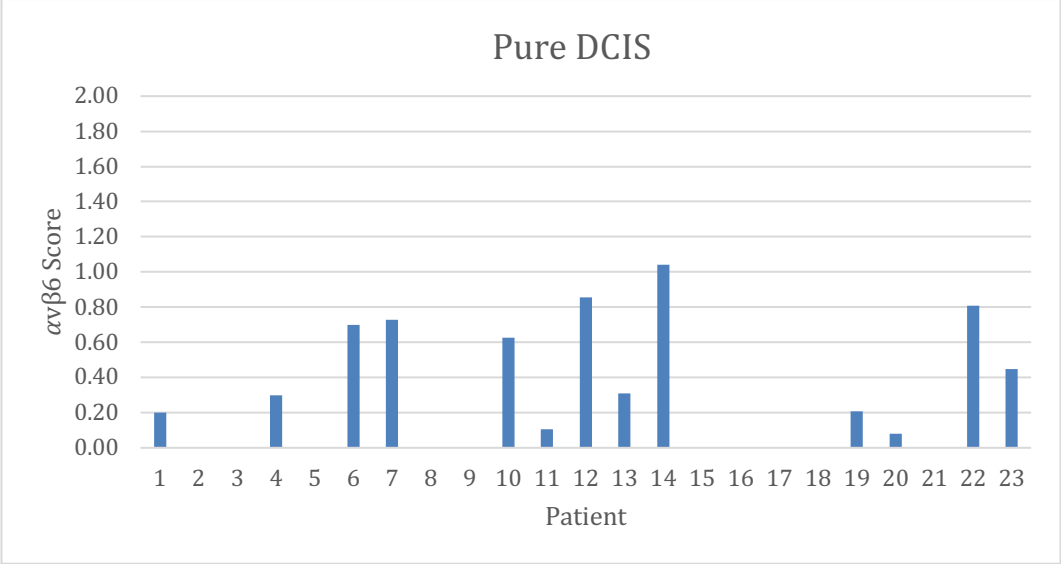

Figure 2-14 Pure DCIS αvβ6 score per patient

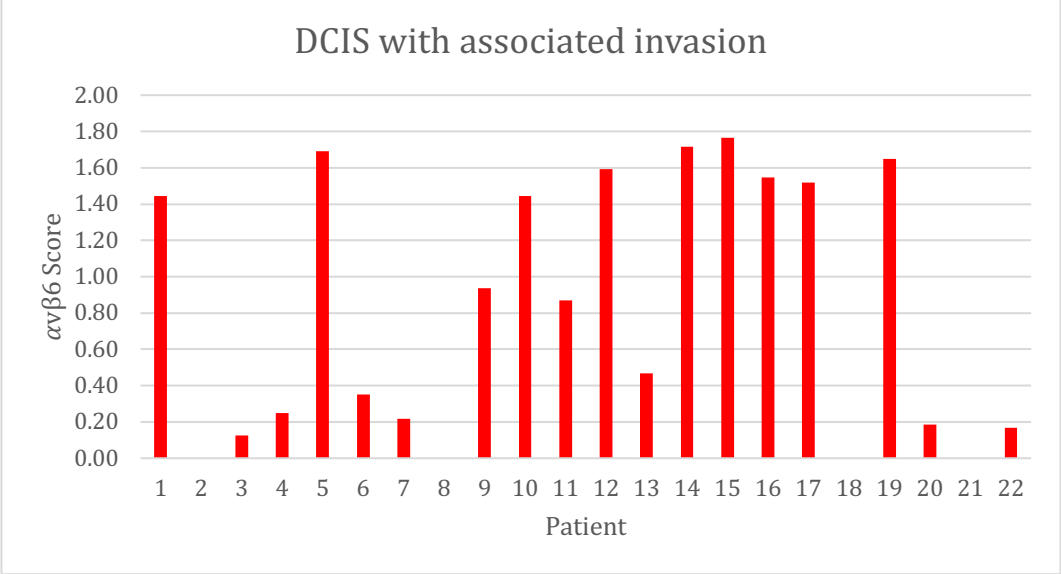

Figure 2-15 DCIS with associated invasion αvβ6 score per patient

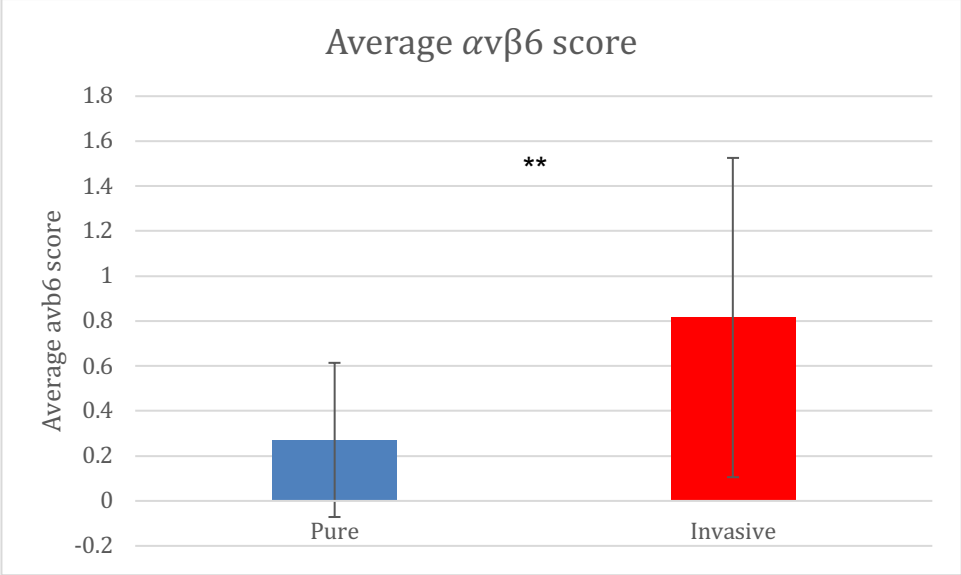

Figure 2-16 Comparison of the average αvβ6 score between pure DCIS and DCIS with associated invasion cohorts.

The mean score in the pure DCIS group is 0.27 and in the DCIS with associated invasion group is 0.82. Student T Test indicates this difference is statistically significant (<0.005).

2.6 A comparison between Galectin-7 and αvβ6 scores

A score for each patient was assigned as described above, a comparison between the Galectin-7 score and αvβ6 was made. The initial hypothesis being that Galectin-7 positivity is a good prognostic sign in DCIS and with this model a high score would be a good prognostic sign therefore higher scores would be expected in the pure DCIS cohort. The analysis supports this hypothesis with a mean score in the pure DCIS group of 1.25 and in the DCIS with associated invasion group of 0.74, which was statistically significant. In support of the hypothesis that αvβ6 positivity is a poor prognostic sign it would be expected that the DCIS with associated invasion would have a higher score. Again, the analysis supports this with the mean score in the pure DCIS group of 0.27 and in the DCIS with associated invasion group of 0.82 which was statistically significant. Then for further analysis, each patient's scores for

Galectin-7 and αvβ6 were plotted together. In devising a risk score for DCIS this would involve a number of markers and different markers would be likely to have more weighting.

2.7 Comparison of Galectin-7 vs αvβ6 score per patient for pure DCIS

A comparison of the scores for Galectin-7 and αvβ6 was made for each patient in the pure DCIS cohort. In all 23 patients the Galectin-7 score was higher than the αvβ6 score.

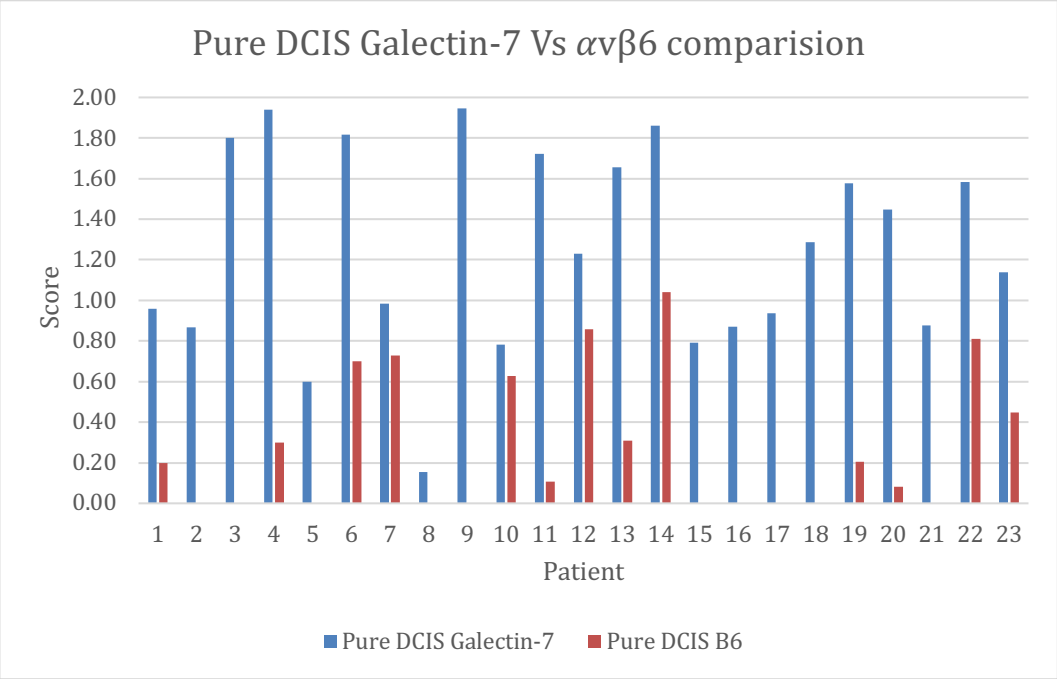

Figure 2-17 A comparison between Galectin-7 and αvβ6 score per patient for the pure DCIS cohort

2.8 Comparison of Galectin-7 vs αvβ6 score per patient for DCIS with associated invasion

A comparison of the scores for Galectin-7 and αvβ6 was made for each patient in the DCIS with associated invasion cohort. The αvβ6 score was higher than Galectin-7 in 10 out of 22 patients, the score was the same in 1 patient and the Galectin-7 score was higher than the αvβ6 score in 11 out of 22 patients.

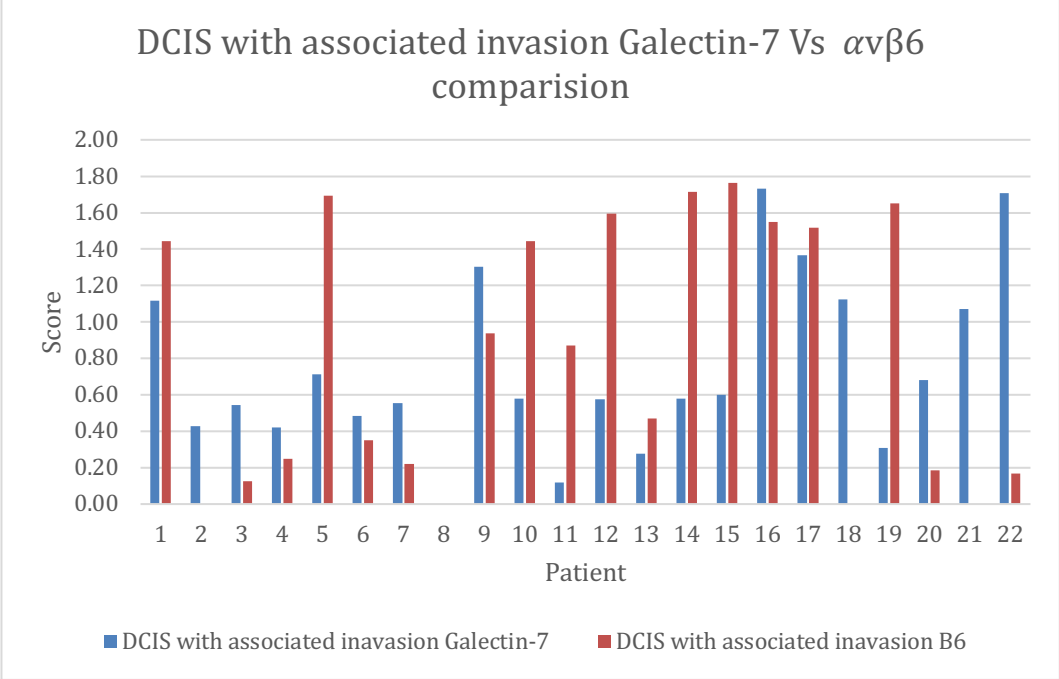

Figure 2-18 A comparison between Galectin-7 and avb6 score per patient for the DCIS with associated invasion cohort

A wilcoxian paired test was performed to assess the score differences between Galectin-7 and αvβ6 in individual patients. A wilcoxian test was used as the data is paired but non-parametric. In the pure DCIS cohort the null hypothesis can be rejected as the test statistic is lower than the critical value, the critical value was 73 and test statistic 0, indicating statistical significance. In the DCIS with associated invasion the critical value was 65 and the test statistic was 129 therefore the null hypothesis cannot be rejected. These were

both for 95% confidence intervals. This is likely to indicate a significant inverse relationship between Galectin-7 and $\alpha v\beta 6$ in pure DCIS, though this is not confirmed in the DCIS with associated invasion. To further test this hypothesis an increased number of patients or different validation set is required however time did not permit this.

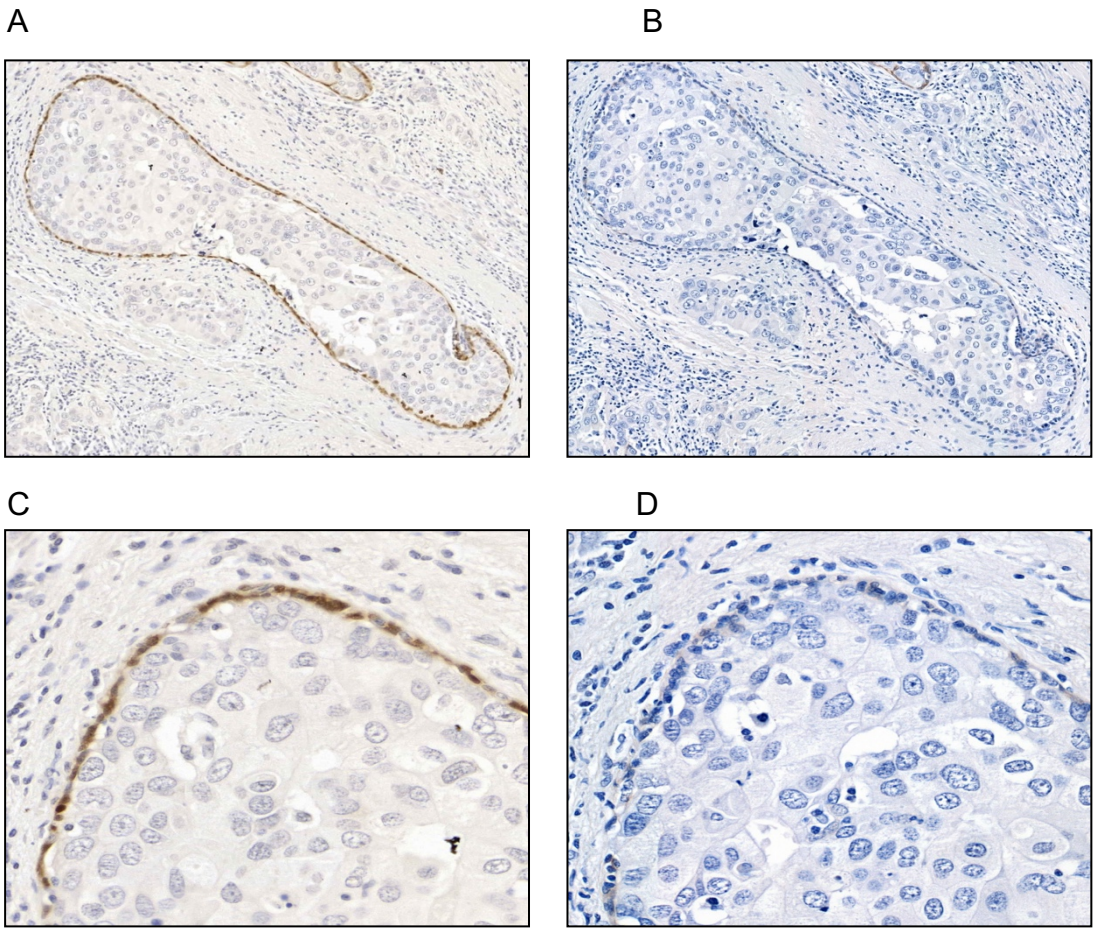

Figure 2-19 Immunohistochemistry images Galectin-7 homogenously positive/αv β6 homogenously negative

Sequential DCIS ducts Galectin-7 homogenously positive x5 magnification (A), β6 homogenously negative x5 magnification (B) Galectin-7 homogenously positive x40 magnification(C), αvβ6 homogenously negative x40 magnification (D).

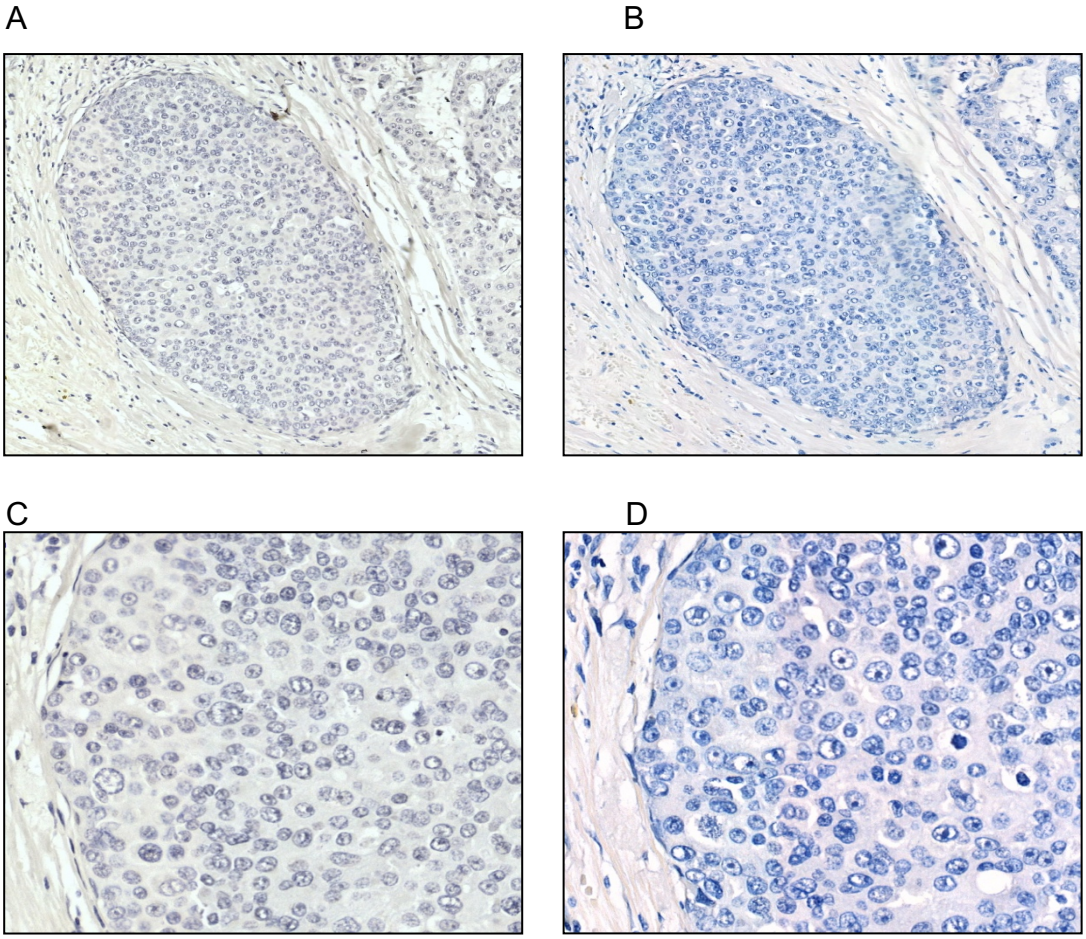

Figure 2-20 Immunohistochemistry images Galectin-7 homogenously negative/αvβ6 homogenously negative

Sequential DCIS ducts Galectin-7 homogenously negative x5 magnification (A), αv β6 homogenously negative x5 magnification (B) Galectin-7 homogenously negative x40 magnification(C), αvβ6 homogenously negative x40 magnification (D).

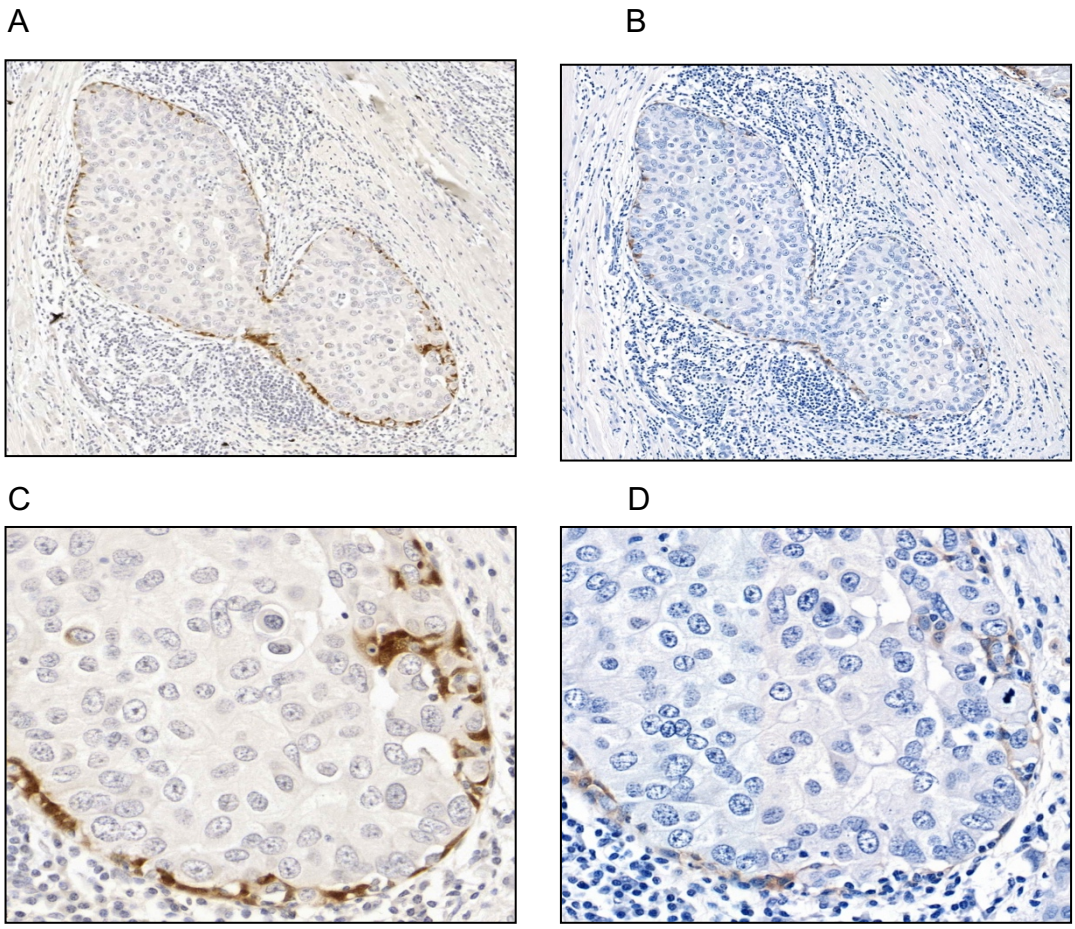

Figure 2-21 Immunohistochemistry images Galectin-7 heterogeneous /αvβ6 heterogeneous

Sequential DCIS ducts Galectin-7 heterogeneous x5 magnification (A), αvβ6 heterogeneous x5 magnification (B) Galectin-7 heterogeneous x40 magnification(C), β6 heterogeneous x40 magnification (D).

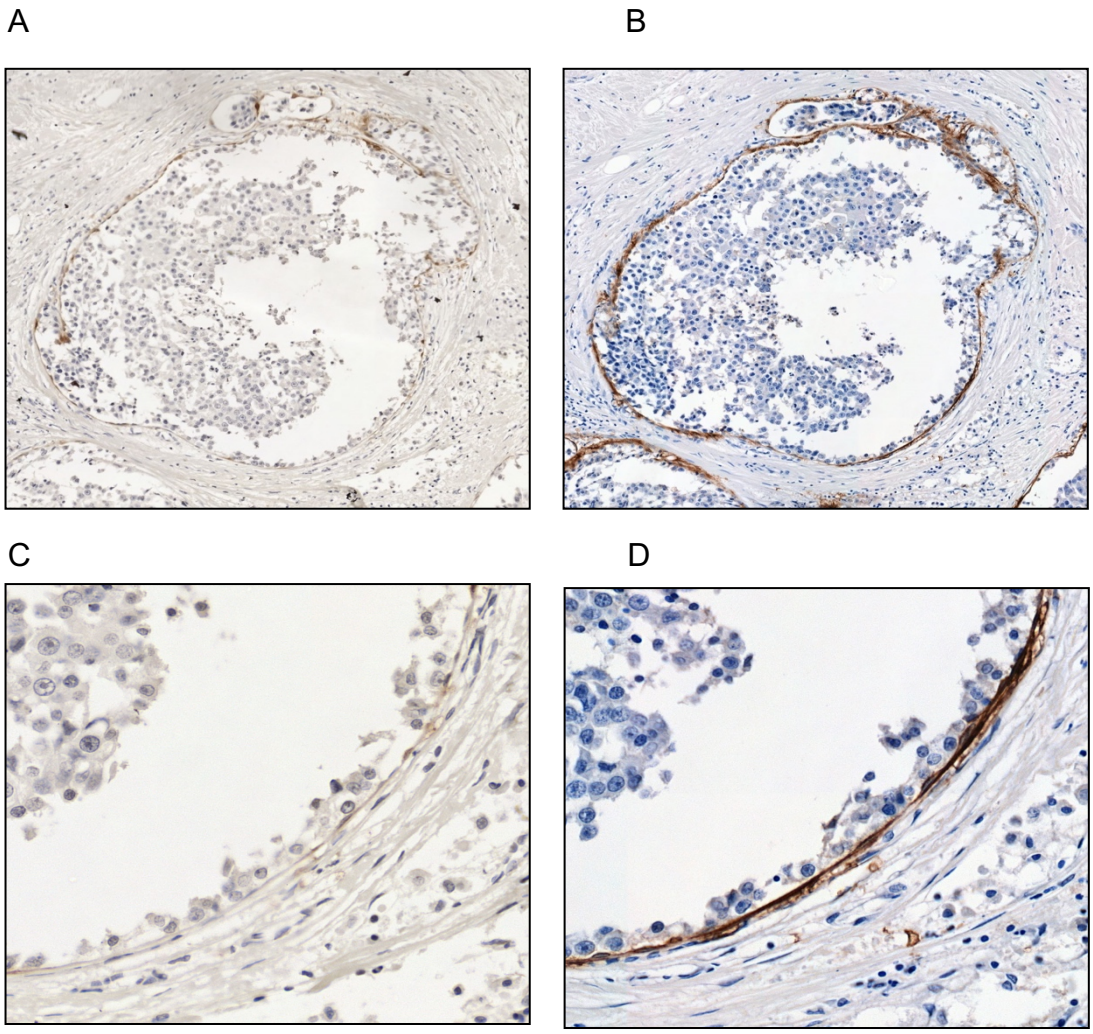

Figure 2-22 Immunohistochemistry images Galectin-7 homogenously negative/αv β6 homogenously positive

Sequential DCIS ducts Galectin-7 homogenously negative x5 magnification (A), αvβ6 homogenously positive x5 magnification (B) Galectin-7 homogenously negative x40 magnification(C), αvβ6 homogenously positive x40 magnification (D).

2.8.1 Oestrogen Immunohistochemistry

Immunohistochemistry for oestrogen receptor (ER), Progesterone receptor (PR) and HER-2 are used routinely in breast diagnostics for invasive carcinoma, though not routinely for DCIS.

For this study, receptor status in DCIS was evaluated. A comparison has been made between the pure DCIS and DCIS with associated invasion cohort on a duct-by-duct basis.

For ER the largest difference between the pure DCIS and DCIS with associated invasion group is a greater number of negative ducts in the pure DCIS group compared to the DCIS with associated invasion group as shown in figure 2.11 C, when assessing the percentage of DCIS ducts the difference between the 2 cohorts is not present. Figure 2.11 A is a representative image of ER positive DCIS ducts and figure 2.11 B is a representative image of an ER negative duct.

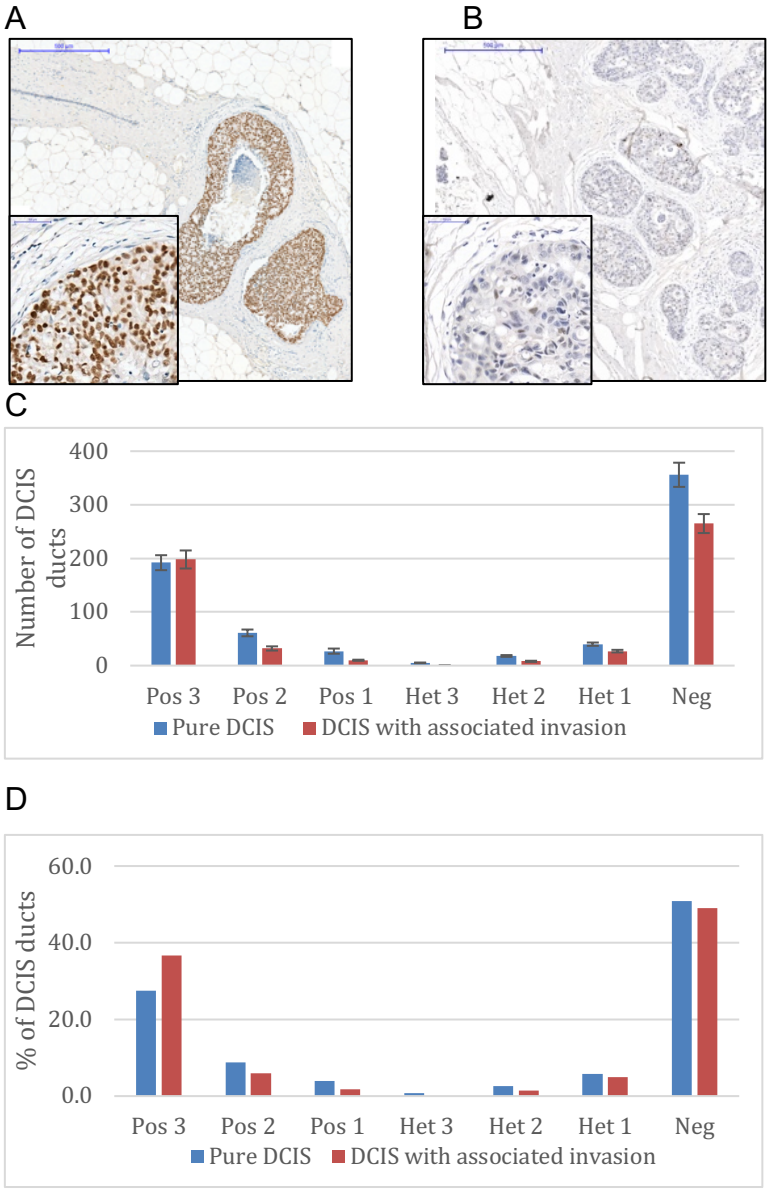

Figure 2-23 ER immunohistochemistry analysis

ER strongly positive DCIS duct (A), ER negative DCIS duct (B), The number of ER DCIS ducts (C) or percentage of ER DCIS ducts(D) in pure DCIS or DCIS with associated invasion cohort across the scoring categories of Positive 3 Positive 2, positive 1, heterogenous 3, heterogenous 2, heterogenous 1, negative. Error bars represent standard deviation.

2.8.2 Progesterone immunohistochemistry

There are a greater number (figure 2.12 C) and percentage (figure 2.12 D) of strongly PR positive DCIS ducts in the DCIS with associated invasion cohort compared to pure DCIS, which contains a greater number and percentage of PR negative DCIS ducts. Figure 2.12 A is a representative image of a PR positive DCIS duct and figure 2.12 B is a representative image of PR negative DCIS duct.

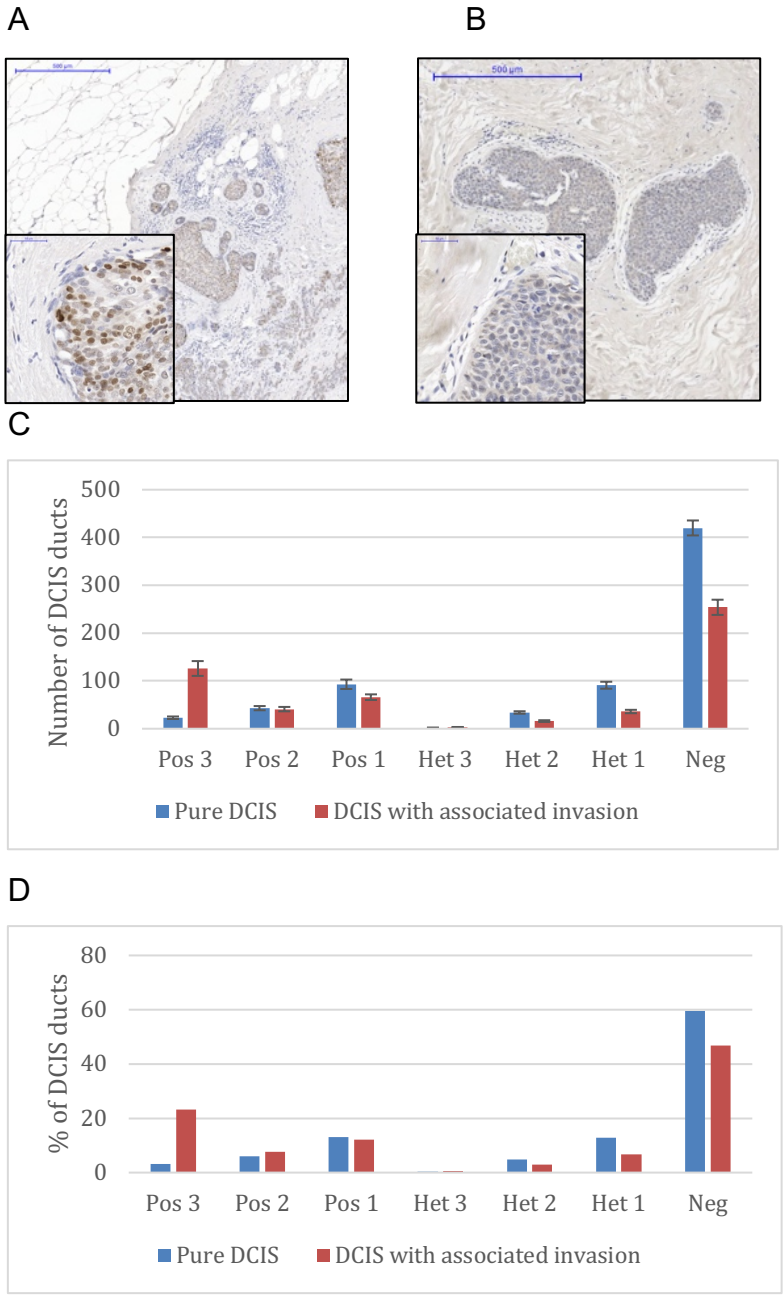

Figure 2-24 PR immunohistochemistry analysis

PR strongly positive DCIS duct (A), PR negative DCIS duct (B), The number of PR DCIS ducts (C) or percentage of PR DCIS ducts (D) in pure DCIS or DCIS with associated invasion cohort across the scoring categories of Positive 3 Positive 2, positive 1, heterogenous 3, heterogenous 2, heterogenous 1, negative. Error bars represent standard deviation.

2.8.3 HER-2 immunohistochemistry

There are a greater number (figure 2.13 C) and percentage (figure 2.13 D) of strongly HER-2 positive DCIS ducts in the pure DCIS compared to DCIS with associated invasion cohort, which contains a greater number and percentage of HER-2 negative DCIS ducts. Figure 2.13 A shows representative images of a HER-2 positive DCIS duct and figure 2.13 B shows a representative image of HER-2 negative DCIS duct.

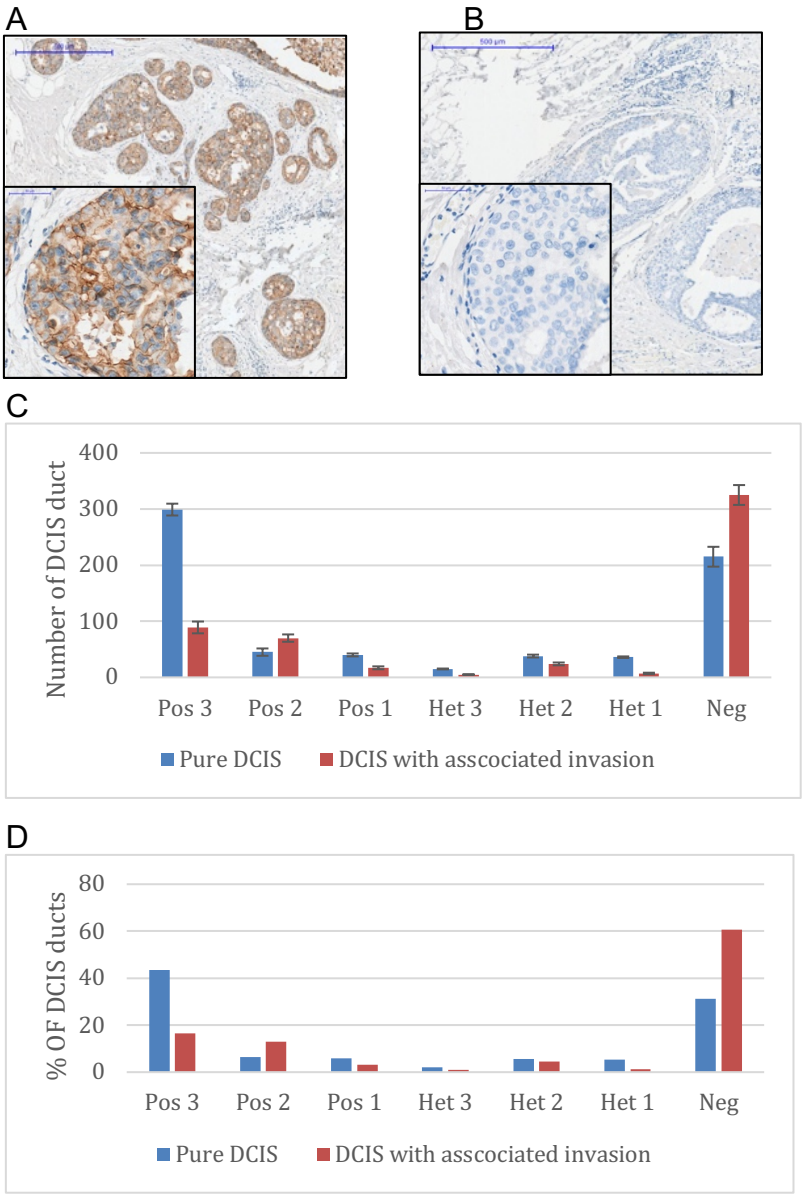

Figure 2-25 HER -2-immunohistochemistry analysis

HER-2 strongly positive DCIS duct (A), HER-2 negative DCIS duct (B), The number of HER-2 DCIS ducts(C) or percentage of HER-2 DCIS ducts(D) in pure DCIS or DCIS with associated invasion cohort across the scoring categories of Positive 3 Positive 2, positive 1, heterogenous 3, heterogenous 2, heterogenous 1, negative. Error bars represent standard deviation.

2.8.4 Molecular subtype of DCIS ducts

The individual markers were collated to define DCIS subtypes comparable to those assigned to invasive breast cancers (Table 2-7 DCIS cohort subtype). Only positive and negative ducts (not heterogeneous) were used in this analysis and only those which could be given a score for all 3 markers were included. Luminal A was defined as ER +ve, PR +ve and Her2 –ve, luminal B was defined as either ER +ve, PR-ve and Her2 –ve or ER+ ve, PR +ve and Her2 +ve or ER +ve, PR-ve and Her2 +ve , Triple negative was defined as ER -ve, PR-ve and Her2 -ve or ER-ve, PR +ve and Her2 -ve and the HER-2 subtype is ER -ve, PR -ve and Her2 +ve or ER -ve, PR +ve and Her2 +ve. The number of DCIS ducts in luminal A category was 36 and 128 for pure DCIS and DCIS with associated invasion respectively, in luminal B was 204 and 86 for pure DCIS and DCIS with associated invasion respectively, and for triple negative was 93 for pure DCIS and 108 for DCIS with invasion. Her-2 +ve ducts which are ER -ve were seen in 231 pure DCIS ducts and 181 DCIS ducts with associated invasion. These results demonstrate, somewhat paradoxically, that the more aggressive molecular phenotype of HER-2 positive DCIS is less associated with invasion, as is the luminal B subtype with luminal A being most associated with invasion.

Subtype	Marker			Number of DCIS ducts			
	ER	PR	HER-2	Pure		Invasive	
Luminal A	+	+	-	36	36	128	128
Luminal B	+	-	-	54	204	21	86
	+	+	+	28		49	
	+	-	+	122		16	
Triple Negative	-	-	-	93	93	68	108
	-	+	-	0		40	
Her-2	-	-	+	129	231	148	181
	-	+	+	102		33	

Table 2-7 DCIS cohort subtype:

The total number of DCIS ducts in each subtype a comparison between pure DCIS and DCIS with associated invasion.

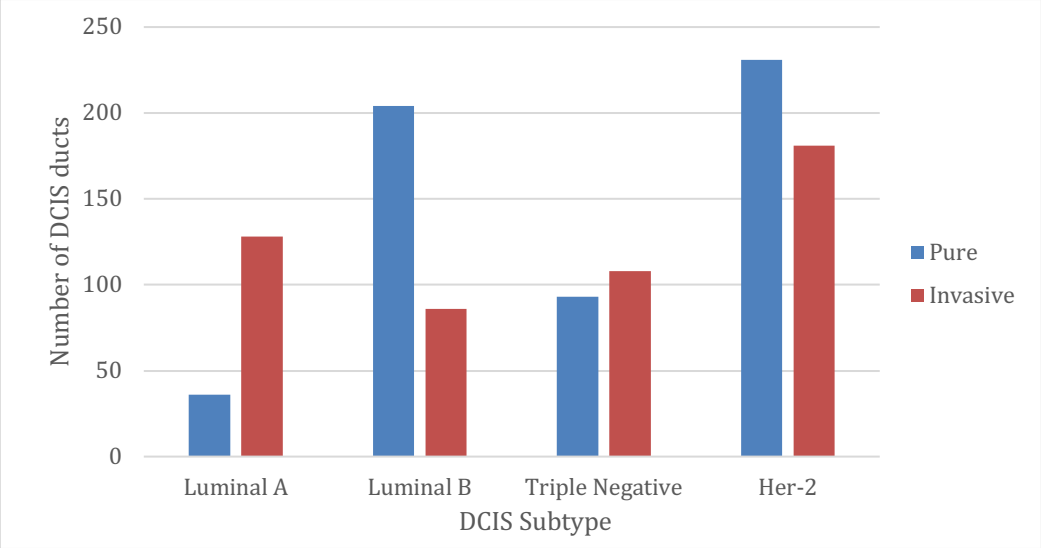

Figure 2-26 The Number of DCIS ducts categorised into DCIS subtypes

This shows a comparison between the pure DCIS and DCIS with associated invasion cohort with a higher number of luminal A ducts in the invasive cohort and a higher number of luminal B ducts in the pure cohort.

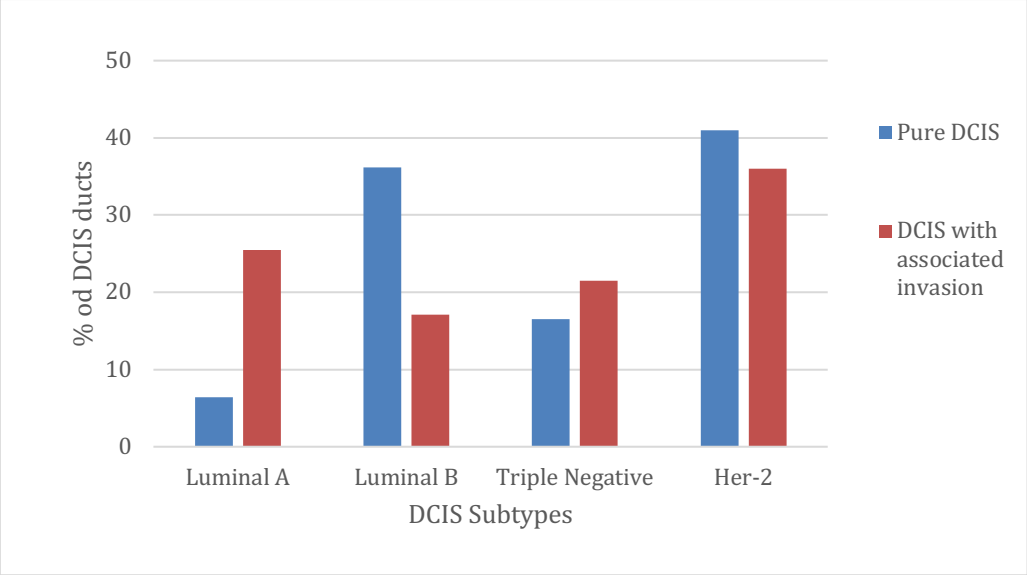

Figure 2-27 The Percentage of DCIS ducts categorised into DCIS subtypes.

This shows a comparison between the pure DCIS and DCIS with associated invasion cohort. With a higher percentage of luminal A ducts in the invasive cohort and a higher percentage of luminal B ducts in the pure cohort.

2.9 Discussion

It is estimated that only half of DCIS cases will progress to invasion within a patient's lifetime, and therefore concerns surround the overdiagnosis and overtreatment of DCIS (Sanders et al., 2005), and is a key criticism of the NHS screening program (Screening, 2012).

In the management of breast cancer, prognostic tools are already available including the Nottingham Prognostic Index, adjuvant online and oncotype Dx. These tools have been developed with an aim to offer more personalised treatment plans. Currently there is no tool in routine clinical practice to aid the risk stratification of DCIS that changes current clinical management. The development of a robust risk stratification tool has the potential to change the management of DCIS and improve the breast screening program. Both conventional histopathological factors and specific biomarkers have been related to DCIS behaviour. High grade DCIS is thought to be more likely to progress than non-high grade DCIS, Ozanne and colleagues created a simulation model to assess DCIS progression: this estimates that a >1 cm, high grade DCIS lesion in women under 45 years old has a 60% rate of progression to IBC and those women more than 45 years of age with a <2.5cm, low or intermediate grade lesion to have a rate of progression to IBC of 10% (Ozanne et al., 2011)

A range of biological markers have been investigated to assess their utility in predicting DCIS progression. ER negativity in DCIS has been associated with an increased risk of DCIS recurrence (E. Provenzano et al., 2003). A study assessing 195 cases of low grade DCIS found 100% were ER positive and 85.3% were PR positive (Koh et al., 2019). A study by Roka and colleagues of 132 women diagnosed with DCIS treated with breast conserving surgery (BCS) with or without radiotherapy discovered a significantly lower rate of ipsilateral breast recurrence in patients with ER-positive DCIS compared to patients whose DCIS did not express ER (3.7% vs 12.2%, $p<0.04$).(Roka et al., 2004).

The Oncotype Dx DCIS Score has been developed and validated to assess risk recurrence in DCIS. It is a 12 gene assay performed on an individual patient's tumour. (Solin et al., 2013) The aim of the oncotype dx DCIS score is to improve the predictions of DCIS recurrence rather than just using standard tumour characteristics alone. Two decision impact studies demonstrated that inclusion of the DCIS score alongside age and tumour size changed treatment recommendations approximately 30% of the time (Manders et al., 2017), (Alvarado et al., 2015).

It is important in the development of a DCIS risk stratification tool that there is an understanding of the biological processes driving DCIS progression. It is now well recognized that the tumour microenvironment plays a central role in tumour progression and this should be encompassed into a tool to predict progression. The myoepithelial cell is a key component of the DCIS microenvironment.

In order to evaluate the association of markers with DCIS progression, two patient cohorts were selected: one with pure DCIS, the other DCIS with associated invasion. These cohorts were chosen as DCIS with associated invasion represents late-stage DCIS and therefore changes critical to DCIS progression should be present in these samples. The pure DCIS samples are likely at different stages of their evolution, but since no more than 50% are ever likely to progress, any change critical to progression should be significantly less frequent.

This study has focused particularly on the myoepithelial cells. Tissue sections from a pure DCIS cohort (low risk model) and DCIS with associated invasion (high risk model) cohort were assessed and scored on a duct-by-duct basis for a number of biological markers. Galectin-7, known to be a myoepithelial marker (Demers et al., 2010), was compared between the 2 cohorts. This shows there are significantly more Galectin-7 negative DCIS ducts in the DCIS with associated invasion cohort and significantly more Galectin-7 positive ducts in the pure DCIS group. This suggests that loss of myoepithelial Galectin-7 is associated with more advanced disease and could be considered

a poor prognostic marker. Work in our lab has previously shown that αvβ6 positivity is a poor prognostic factor in DCIS (M. D. Allen, Marshall, et al., 2014), therefore sequential sections of the two DCIS cohorts were stained for αvβ6. This demonstrated that there were significantly more αvβ6-negative DCIS ducts in the pure DCIS cohort compared to the DCIS with associated invasion, supporting the previous finding that acquisition of αvβ6 by DCIS myoepithelial cells is associated with more advanced disease. Any DCIS risk score will be improved by the integration of multiple markers, thus each duct was assigned a αvβ6- Galectin-7 score. These indicated that scores of Galectin-7 positive/ αvβ6 heterogeneous, Galectin-7 positive/αvβ6 negative, Galectin-7 heterogeneous/ αvβ6 negative were significantly more frequent in DCIS ducts in the pure DCIS cohort compared to the DCIS with associated invasion cohort. Conversely, the combinations of Galectin-7 heterogeneous /αvβ6 positive, Galectin-7 negative /αvβ6 positive and Galectin-7 negative /αvβ6 heterogeneous were seen in a significantly higher number of DCIS ducts in the DCIS with associated invasion cohort. These findings suggest an inverse relationship between Galectin-7 and αvβ6 integrin in DCIS-myoepithelial cells, though it is not clear from immunohistochemistry alone whether the two molecules are functionally related.

The hypothesis is that Galectin-7 positivity is a good prognostic sign in DCIS and αvβ6 is a poor prognostic sign. The same score and weighting has been used for both markers. DCIS with associated invasion has a lower average score for Galectin-7 than the pure DCIS cohort, supporting this hypothesis. For αvβ6, the DCIS with associated invasion had a higher average score than pure DCIS, which would support the hypothesis that αvβ6 positivity is a poor prognostic marker.

The relationship between the expression of oestrogen, progesterone and HER2 receptors with associated invasion has been assessed. All 3 markers reached statistical significance demonstrating a difference between the 2 groups, however the results are clearer for progesterone and HER2. A higher

percentage of ducts strongly positive for progesterone receptor was seen in the DCIS with invasion group compared to the pure DCIS group. In contrast, for Her2, a higher percentage of strongly positive ducts was identified in the pure DCIS group compared to DCIS with invasion. The findings with Her2 are concordant with previous studies by Park et al., and Clark et al., who recognised that there is a higher frequency of Her2-positive DCIS compared with Her2-positive invasive breast cancer though the biological explanation for this is not understood (Park, Han, Kim, Kim, & Shin, 2006), (Clark et al., 2011). In contrast, the higher frequency of ER and PR positive DCIS in DCIS with associated invasion is in contradiction to published studies. Provenzano et al found that PR negativity In DCIS was independently associated with risk of local-regional recurrence (E. Provenzano et al., 2003). These authors compared tissues from patients who subsequently developed ipsilateral recurrence (cases) with those from patients who did not develop a recurrence (controls). Patients who developed a local-regional recurrence were more likely than controls to have PR-negative disease (63% vs. 34%) (E. Provenzano et al., 2003). Furthermore, in the IBIS-I study, ER negative DCIS was associated with higher risk of invasive recurrence (Cuzick et al., 2014). However, interestingly in those cases scored as ER positive, any heterogeneity of staining, that is the presence of any ducts negative for ER, resulted in the same prognosis as those soring ER negative overall. This emphasizes the importance of heterogeneity in DCIS behaviour, and that this needs to be taken into account when considering biomarker expression. A supplementary analysis of the data in the current study confirms this.

The scoring of oestrogen receptor is not wholly consistent across the UK. The method of scoring in this thesis was chosen to both represent how positive a case is and the intensity of the stain, which could be converted into a modified Allred-type scoring system out of 8 as shown in the table below.

	% of cells positive	Staining intensity	Score
Positive 3	100	High	8
Positive 2	100	Moderate	7
Positive 1	100	weak	6
Heterogeneous 3	25-99%	High	5
Heterogeneous 2	25-99%	Moderate	4
Heterogeneous 1	25-99%	weak	3
Negative	0	0	< 2

Table 2-8 Oestrogen and Progesterone staining method

A recognised method is to score the percentage of cells in the case that were positive. Current consensus (ASCO/CAP and Mitch Dowsett, personal communication) is that the recommended cut-off point for positivity versus negativity for ER status is greater than or equal to 1% of tumour cells (Fitzgibbons, Murphy, Hammond, Allred, & Valenstein, 2010; Hammond et al., 2010). However, many laboratories continue to use the Allred score that is comparable to the scoring method th used in this thesis: this assesses the percentage of cells which are positive as well as the intensity. The proportion score (0 to 5) was derived from the percentage of positive cells (0%= 0 ;<1% =1; 1 – 10% =2; 11-33%= 3; 34-66%=4; 67-100%=5).This was combined with visually assessed intensity score (0=negative; 1=weak; 2=moderate; 3=strong) to get the final Allred score (0- 8)(Vijayashree, Aruthra, & Rao, 2015).

There is not a recognised scoring method for oestrogen receptor scoring in DCIS as outlined in the Royal College of Pathologists guidelines. Not all trusts assess hormone receptor status on DCIS samples. Barts Health does not currently routinely assess oestrogen receptor on DCIS specimens. Ductal carcinoma in situ oestrogen receptor status may be assessed in patients with ductal carcinoma in situ for whom endocrine treatment is being considered, but it is not mandatory for all patients. There is no consensus on cut-offs as, unlike for invasive carcinoma, there are no data relating clinical outcome on endocrine treatment to the level of oestrogen receptor expression. At the present time it is recommended that the same scoring method and cut point

for positivity used for invasive carcinoma be used for assessment of DCIS. Hormone receptor status should be recorded on the NHSBSP and dataset forms as positive or negative with the percentage staining as a minimum and the average intensity or the result of the Allred score or H score as for invasive disease (Ellis, 2016)

There is significant evidence for the regulatory role of normal myoepithelial cells in the mammary gland, including control of epithelial cell polarity and anti-proliferative, anti-invasive and anti-angiogenic properties, thus providing a broad tumour-suppressor environment (Barsky & Karlin, 2006). Myoepithelial cells have been shown to down-regulate expression of matrix metalloproteinases (MMPs) in both tumour cells as well as fibroblasts, so promoting an anti-invasive phenotype (Jones et al., 2003). Maspin is one of the most important tumour suppressor proteins that is secreted by normal myoepithelial cells which acts as an inhibitor of angiogenesis (Hopkins & Whisstock, 1994),(Pemberton et al., 1995). Thus, the myoepithelial cell could be considered as 'guardian of the ductal microenvironment' in the normal breast.

Given the consistent change in Galectin-7 and its potential to influence many pathways, this project aims to focus on Galectin-7 and investigate the functional significance of this in myoepithelial cells in order to establish whether it could be causally related to the DCIS-invasive transition.

3 Functional analysis of Myoepithelial Galectin-7

3.1 Materials and methods

3.1.1 Generation of myoepithelial cell (MEC) lines

A breast myoepithelial cell line **N-1089**, derived from human cosmetic reduction breast tissue was a gift from Prof M. O' Hare. This was immortalised with h-TERT/SV40 LgT as described by O'Hare et al (O'Hare et al., 2001) and designated 'Myo 1089' cell line. This cell line originally was a mixed population composed of MECs express differing levels of α6β4. These cells were sorted by their α6β4 expression using β4 antibody (Millipore, MAB 1964) coated magnetic beads (Dynal Invitrogen, 110.31). The cell line generated by this selection was called N- 1089 and fully characterised by Dr M Allen to demonstrate MEC features including expression of vimentin, SMA and p63.

In order to investigate the functional significance of αvβ6 Dr M Allen engineered a β6 overexpressing Myo 1089 cell line. To do this, AM12 packaging cell line was transfected with either empty pBABE-puro vector, or vector containing β6 integrin insert (Addgene plasmid:1734). β4-1089 cells were cultured with the medium containing virus from control or β6 carrying AM12 cells and selected for puromycin (Sigma, P8833, 1μg/ml) resistance. Control and αvβ6 over-expressing cell lines were designated **N-1089** (Myo-puro) and **β6-1089** (Myo-β6) respectively. These cell lines were shown to switch their phenotype over time in culture; most notably they show gradual down-regulation of α6β4 integrin. In order to maintain α6β4 expression, cells are enriched by positive selection on β4 antibody-coated anti-mouse magnetic beads every 10-13 weeks. Along with this enrichment **β6-1089** cells are re-sorted by positive selection on αvβ6 coated beads, whereas N- 1089 cells are negatively selected. These cells were cultured in the presence of hydrocortisone (1μg/ml), Epidermal Growth Factor (EGF, Sigma, 9644, 10ng/ml), insulin (1μg/ml).

The breast cancer cell line **MDA-MB-231** was obtained from ATCC HTB-26 and represent ER negative highly invasive breast cancer cells. The

immortalised fibroblast cell line **MRC-5** was obtained from ATCC. The cell line culture conditions are summarised in Table 3-1.

3.1.2 Isolation of primary myoepithelial cells

Human breast tissue was obtained from samples donated to the Breast Cancer Now Breast (BCN)/ Barts Cancer Institute (BCI) tissue bank (Ethical Approval Reference 10/H0308/49, Cambridgeshire Ethics Committee October 2010).

Normal myoepithelial cells were isolated from reduction mammoplasty tissue. The cell isolation protocol was performed by Dr J Gomm.(Gomm et al., 1995). Reduction mammoplasty tissue was collected and used to prepare breast organoids. The tissue was chopped and then digested overnight at 37˚C with collagenase (1 mg/ml, Sigma, C2674) and hyaluronidase (Sigma, H3506) on a roller. After digestion, the fat layer was separated by decanting and organoids and single cells were washed three times with RPMI (PAA, E15-840), followed by 3 sedimentation steps at room temperature (RT) to isolate the fibroblast-containing stromal compartment. Organoids were digested to a single-cell suspension through digestion with 0.05%/0.02% (w/v) trypsin/EDTA solution (Hyclone, SV30031.01) containing 0.4mg/mL DNase (10104159001, Roche Life Science) for 15 minutes at 37^{o}C, digestion was halted with RPMI containing 10% FBS and the cell suspension was filtered through gauze (pore size: 56µm2, Henry Simon, Stockport). Cells were counted and incubated in a 1:1 ratio sequentially with magnetic beads coated with CD10 antibody (AbD serotech, MCA1556) to isolate MECs, followed by magnetic beads coated with EpCAM (Ber-EP4) antibody (Invitrogen, 161.02) to isolate LECs, at 4˚C for 15 minutes on a roller. Further incubations with magnetic beads were employed until depletion of each cell type was achieved (summarised in Figure 3-1).

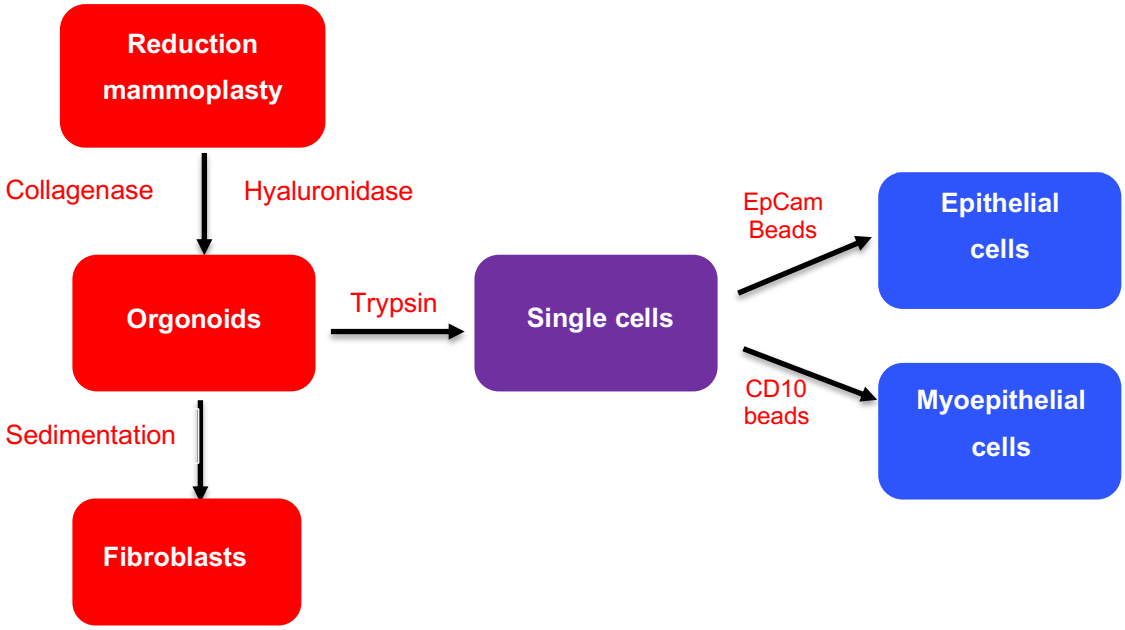

Figure 3-1 Isolation of normal primary breast cells

Diagram showing isolation of normal primary cells from reduction mammoplasty tissue. Adapted from Gomm et al (Gomm et al., 1995)

3.1.3 Cell culture conditions

Cell Type	Source	Media	Passage
N-1089	Gift from M O'Hare	HAM F-12 (Sigma N6658) 10% FBS 1µg/mL Hydrocortisone 5µg/mL Insulin 10ng/mL Epidermal Growth Factor	Maintained in T75 flask Passaged 1:10 37°C in 5% CO_2
β6-1089	Engineered by Dr M Allen	HAM F-12 (Sigma N6658) 10% FBS 1µg/mL Hydrocortisone 5µg/mL Insulin 10ng/mL Epidermal Growth Factor	Maintained in T75 flask Passaged 1:10 37°C in 5% CO_2
MDA-MB-231	ATCC	Dulbecco's Modified Eagles's Medium (DMEM, Sigma, D6429) with 10% FBS	Maintained in T175 flask Passaged 1:10 37°C in 5% CO_2
MRC-5	ATCC	Dulbecco's Modified Eagles's Medium (DMEM, Sigma, D6429) with 10% FBS	Maintained in T75 flask Passaged 1:10 37°C in 5% CO_2

Table 3-1 Cell culture conditions and media

3.1.4 Passage of cells

Cells were grown in 5% CO_2 at 37°C until ~80% confluent then media was aspirated and discarded. Cells were detached using 3ml-5ml of 10x Trypsin/Ethylenediaminetetraacetic acid (EDTA) solution (Sigma 594186) added to T75 and T175 flasks, respectively. The flask was placed at 37°C for 5-10 minutes until cells started to detach. The time taken for cells to detach varied amongst the cell lines with the myoepithelial cell lines taking longer to detach. The trypsin was neutralised with appropriate media and the cells were centrifuged at 1200 rpm for 3 minutes. The supernatant was discarded and cell pellet re-suspended in the appropriate media as outlined in Table 3.1. Cells were then transferred to fresh flasks and plated at a ratio of 1 ml of cell suspension to 9ml of media.

3.1.5 Primary myoepithelial cell culture conditions

Following the isolation of primary myoepithelial cells as outlined in Figure 3-1 cells were frozen and stored at -80°C until needed. Myoepithelial cells were defrosted by hand and re-suspended in myoepithelial cell media. The cells were mixed 1:1 with trypan blue and counted with a glass haemocytometer. The trypan blue was used to ensure only viable cells were plated. 10 μl of cell suspension and 10 μl of trypan blue was mixed and then 11μl of this mixture was pipetted into the haemocytometer. The cells were viewed under inverted phase contrast microscopy. The number of viable cells in each 4x4 grid was counted. The cell count per ml was the average across the 4 grids multiplied by 2 (to account for trypan blue) multiplied by 10000. Myoepithelial cells were seeded at a density of 4-5x10^5 on collagen-coated 6 well plates and incubated in 5% CO_2 at 37°C. Myoepithelial cells were cultured in HuMEC medium (Thermo Fisher Scientific) supplemented with 0.5 μg/ml hydrocortisone, 5 μg/ml insulin, 10 ng/ml EGF and 50 μg/ml bovine pituitary extract (Thermo Fisher Scientific), 0.5 μg/ml fungizone (Invitrogen, 15290-026) and 10 μg/ml gentamicin (Sigma, G1397) which was changed every 48 hours.

3.1.6 Detection of Galectin-7 in Myoepithelial cells by Western blotting

Cell lysis

Cells were harvested for protein analysis. The culture medium was removed from plates and the cells washed with PBS. Radioimmunoprecipitation assay (RIPA buffer) (50mM Tris-hydrochloride (TrisHCl, Sigma, T3253) pH 7.4, 150mM sodium chloride (NaCl, Fisher, 358-1), 1% IGEPAL CA-630 (Calbiochem, 490216), 0.1% sodium deoxycholate (Na-DOC, Sigma, D6750), 1mM EDTA (Fisher, BP 118-500), supplemented with 1:100 protease inhibitor cocktail set (Calbiochem, 539131), was added to the plates. The plate was scraped and the suspension transferred to an eppendorf. The eppendorf was centrifuged at 10000 rpm at 4^{o}C, to pellet the insoluble cell remnants and the supernatant was placed in a fresh eppendorf and stored at -20 ^{o}C.

Protein quantification

Protein concentrations were quantified using the Bio-Rad DC Protein Assay Kit (Bio-Rad Laboratories, Reagent A 500-0113, Reagent B -114, Reagent S -115), according to the manufacturer's instructions. Protein was quantified to ensure equal quantities of samples were loaded onto the gel. BSA (bovine serum albumin, Sigma, A9418) standards were used to create a standard curve and this was used to estimate the sample protein concentration. Cell lysates and BSA standards (diluted in distilled water) were added at 5µl volumes to a 96 well plate in triplicate, before adding 25µl of solution A/S (1000µl reagent A and 20µl reagent S) per well followed by 200µl of reagent B per well. The plate reader was used to read the 96 well plate at 595nm. The protein concentration of the samples was determined using a BSA standard curve and calculated on Microsoft excel using a linear regression equation.

SDS Gel

SDS-polyacrylamide gel electrophoresis (SDS-PAGE) was used to separate the proteins. The gel percentage was adjusted to resolve the relevant protein by altering volumes of dH_2O and 30% acrylamide mix (National Diagnostics, EC

890). The gel was placed into either a 1mm or 1.5mm cassette, which varied according to volume of sample which required loading into the gel. The 8% resolving gel solution comprised of 4.6ml distilled water (dH_2O), 2.7ml 30% acrylamide mix (National Diagnostics, EC 890), 2.5ml 1.5M Tris (pH 8.8), 100µl 10% SDS (Fisher BioReagents 7732-18-5), 100µL 10% ammonium persulphate (APS, Acros organics 7727-54-0) and 6µl TEMED (Flowgen, H17459). Once the gel was placed in the cassette dH_2O was pipetted on top of the gel. When the gel was set the overlaying dH_2O was discarded. Stacking gel (2.7ml dH20, 670µl 30% acrylamide, 500µl 1M Tris (pH6.8), 40µl 10% SDS, 40µl 10% APS and 4µl TEMED) was added to the cassette and a suitable comb was inserted. Once the gel had set the tape was removed from the cassette and placed into the gel tank. Running buffer (100ml tris-glycine/SDS Severn Biotech 20-6400-50 in 900ml dH_20) was added to the tank and then the comb was removed.

Sample preparation

30µg of protein was combined with 4X sample loading buffer (5% SDS, 20% buffer (0.5M tris, 0.2M NaH_2PO_4, pH 7.8), 5% β- mercaptoethanol (Sigma, M7522), 50% glycerol (Fisher, G/0600/17), 0.01% bromophenol blue (Sigma, B8026) and 20% dH_20). Samples were boiled for 5 minutes at 100^oC, centrifuged at 10000rpm for 1 minute and the loaded onto the gel, 10µl of Pageruler (Thermo Scientific 26619) was also loaded onto the gel, this is a prestained protein ladder used as a standard for comparing size of proteins of interest.

Running of the gel

The gel was run at room temperature at 150v between 80 and 90 minutes depending on the protein of interest. On completion of the run, the cassette was opened and gel removed. PVDF membrane was briefly pre-soaked in 100 % methanol prior to being soaked in transfer buffer (100ml tris glycine Severn Biotech, 20-6400-10, 700ml dH20 and 200ml 100% methanol) together with the sponges. A sandwich was made using 2 pre-soaked sponges, 2 pieces of filter paper, gel, membrane, 2 pieces of filter paper and 2 sponges, taking care to

remove any air bubbles. This was placed in the gel tank and the central chamber topped with transfer buffer. The outer chamber was filled with dH_2O and the tank was placed on ice. The transfer was performed at 30v for 90 minutes.

Following the transfer, the membrane was blocked for 30 minutes in 5% skimmed milk (Sigma, 70166)/ PBST (0.1% Tween 20 (Applichem, A4974) in PBS) with gentle rocking at room temperature.

The membrane was then incubated overnight at 4^{o}C with the primary antibody diluted with 5ml of 5% skimmed milk and Tween. Details of the primary antibodies are outlined in Table 3-2.

Membranes were washed 3 x 5 minutes with PBST, prior to being incubated with secondary antibodies (anti-mouse HRP Dako, P0260 or anti-rabbit IgG HRP Dako, P0488,) 1/2000 dilution in 5% skimmed milk 0.1% Tween for 60 minutes at room temperature. It is important to ensure the appropriate membranes are used, the experiment for cleaved caspase-3 was repeated a number of times with different membranes, prior to achieving an interpretable result.

Antibody	Dilution	Manufacture	Species	Membrane
Galectin-7	1/1000	Ab-cam (ab108623)	Rabbit	0.2µm PVDF novex life technologies LC2002
Total-PARP	1/1000	Cell Signalling (9542L)	Rabbit	0.45µm nitrocellulose No.10600002
Cleaved-PARP	1/1000	Cell Signalling (D214)	Rabbit	0.45µm nitrocellulose
Cleaved Caspase -3	1/1000	Cell signalling (D175)	Rabbit	0.2µm Nitrocellulose
P-Cadherin	1/1000	BD Biosciences (610228)	Mouse	0.45µm nitrocellulose
HSC70	1/10000	Santa Cruz (sc-7298)	Mouse monoclonal	0.45µm nitrocellulose

Table 3-2 Antibodies used in Western blotting

3.1.7 Knockdown of Galectin-7 in primary myoepithelial cells

Primary myoepithelial cells endogenously express high levels of Galectin-7. To achieve knockdown of Galectin-7, primary myoepithelial cells were transfected with Galectin-7 siRNA (siGENOME SMART pool LGALS7, Thermoscientific Dharmacon M-011719-01) and compared to a non-targeting control (siGENOME Dharmacon D-001206-14-20).

Myoepithelial cells were seeded at a density of 4-5x10^5 in collagen-coated 6 well plates. siRNA transfection was performed when cells were at 60% confluency.

The quantities were worked out per 1 well in a 6 well plate and scaled up as required. 200µl of cell media was transferred to an eppendorf and combined with 1.1µl of siRNA. 4µl Interferin (polyplus 409-50) was added, vortexed and incubated for 10 minutes. 2ml of fresh media was added to each well and 200µl of the siRNA mixture was then added. The extent of knockdown achieved was

evaluated by western blotting at different time-points and the time-point showing optimal knockdown was used for all future experiments.

3.1.8 Overexpression of Galectin-7 in myoepithelial cells

N-1089 and β6-1089 cell lines were seeded at 6 x 10^5 onto 10 cm plates and incubated in Hams-F12 media with 10% FBS, 2mM glutamine, Hydrocortisone (1µg/ml) EGF (10ng/ml) and Insulin (5µg/ml). At 24 hours cells were transfected with 1µg Galectin-7 pc DNA 3.1 (engineered by Dr M Allen) or empty vector pc DNA 3.1, or GFP to confirm transfection. Transfections were performed using standard Jetprime protocol (polyplus). Briefly, DNA was diluted in 200µl Jetprime buffer, votexed for 10 seconds and then 4 µl jetprime reagent added with further vortexing for 10 seconds followed by incubation at room temperature for 10 minutes. The transfection mixture was then added to 2 ml of myoepithelial cell media and added to the cells. The media was changed at 24 hours.

3.1.9 Treatment with TRAIL pro-apoptotic ligand

Human TRAIL Apo II ligand (peprotech;310-04), was used as a pro-apoptotic ligand to stimulate the extrinsic apoptosis pathway. TRAIL may be produced physiologically by Treg cells in the inflammatory DCIS microenvironment, so was considered an appropriate stimulus. The optimal dose of TRAIL was established using the Alamar blue assay to assess cell viability. The dose of TRAIL used in both cell lines and primary myoepithelial cells was 250ng/ml and 500ng/ml, respectively. The cells were treated with TRAIL at different time-points and the extent of apoptosis assessed by Western blot for the apoptotic markers cleaved PARP and Caspase-3.

3.1.10 LDH cytotoxicity assay

The myoepithelial cell lines were plated on a 24 well plate seeded at a density of 2.5 x 10^4 per well and incubated for 48 hours. The cell lines were transfected with Galectin-7 plasmid or control plasmid. The primary myoepithelial cells were transfected with Galectin-7 siRNA or non-targeting control siRNA. 48 hours post transfection the cells were treated with TRAIL. At 48 and 72 hours post-TRAIL treatment, cytotoxicity was analysed using CytoTox96® non-radioactive cytotoxicity assay (Promega, G1780).

Lysed cells release LDH and the LDH in the conditioned media was used as marker of cell death. The colour change gives an indication of the extent of cell death.

Conditioned media from each well was transferred into separate eppendorfs and stored on ice. For maximal lysis controls, 100 µl of lysis solution (9 % Triton X-100) was added to each control well and left for 45 minutes. Conditioned media was transferred to eppendorfs.

50µl of each conditioned media was transferred to a 96 well plate in quintuplicate and 50µl of reagent was added to each well. This was left to incubate in the dark for 10 minutes after which 50µl of stop solution was added per well. The plates were then analysed at 490nm on a plate reader. The absorbance values obtained in the remaining experimental wells were normalised as a percentage of the maximal lysis value as shown in the equation below.

$$\%\, Cytotox = \left(\frac{\text{Experimental release LDH}}{\text{Max LDH}}\right) x100$$

3.1.11 Apoptosis proteome profile

Sample preparation

Assessment of expression of apoptosis related proteins in primary myoepithelial cells was performed using the Human Apoptosis Array Kit (R&D Systems ARY009) This assesses 35 human apoptosis related proteins from a single sample.

Primary myoepithelial cells were seeded onto collagen-coated 6 well plates at a density of $4x10^4$ cells per well. Galectin-7 siRNA knockdown in primary myoepithelial cells was performed as previously described 3.1.7. Four different conditions were set up:

siRNA non-targeting control
siRNA Galectin-7
siRNA non-targeting control with TRAIL treatment
siRNA Galectin-7 with TRAIL treatment.

The cells were treated with 250ng/ml of TRAIL and harvested at 4 hours post treatment.

Cell Lysis

The plates were placed on ice and cells were lysed using lysis buffer 17 (R&D Systems ARY009) with protease cocktail inhibitor. Protein was quantified using Bio-Rad assay. The Galectin-7 knockdown was confirmed using western blotting prior to protein being assessed on the human apoptosis array. Samples were stored at -80^{o}C until required then thawed on ice.

300μg of protein was used and the maximum volume of lysate was 250μl. 1.25 ml of array buffer 1 was added to each sample. All samples were adjusted to the final volume of 1.5ml by adding lysis buffer 17 as required. Array buffer 1 was aspirated from the dish and samples added to each well and incubated overnight at 4^{o}C on a rocking platform.

Array procedure

All reagents were brought to room temperature prior to use. 2ml of the blocking buffer Array buffer 1 was added to the 4 well multi dish and then each array was placed into the multi dish and was incubated with gentle rocking for 1 hour at room temperature. Following incubation of samples overnight on the nitrocellulose membranes, arrays were washed for 3 x 10 minutes to remove unbound protein with wash buffer.

Detection

Each array was then incubated with a 1.5ml cocktail of biotinylated detection antibodies. 15μl of reconstituted detection antibody cocktail was diluted with 1.5ml 1x Array buffer 2/3 and incubated for 1 hour at room temperature on a rocking platform, Followed by 3 x 10 minute washes. Arrays were then incubated with 2.0ml of diluted streptavidin-HRP reagent for 30 minutes on the rocking platform at room temperature followed by wash steps. Results were detected by adding 1ml of chemi-reagent to each membrane. The chemi-doc system was used to read the protein intensity.

Analysis

The Image-J program was used to assess pixel density and comparison was made between conditions. For each protein there were duplicate spots. The average pixel density for each spot was used. Table 3.3 shows the coordinates and corresponding apoptotic protein for the array shows the coordinates and corresponding apoptotic protein.

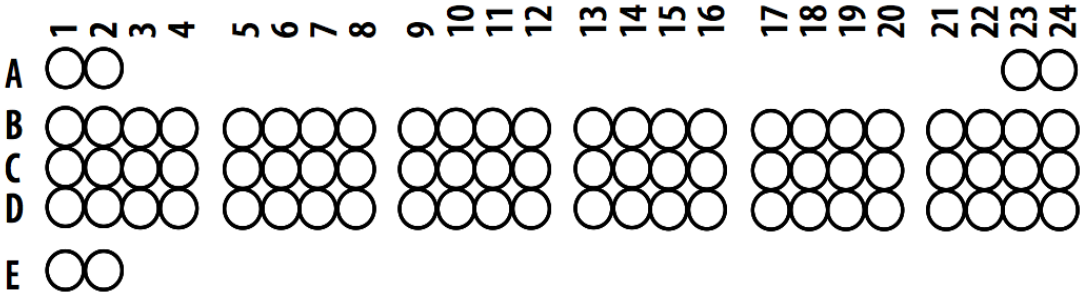

Coordinate	Target	Coordinate	Target	Coordinate	Target
A1, A2, A23, A24	Reference	**C1, C2**	TRAIL R1/ DR4	**D1, D2**	PON 2
B1, B2	Bad	**C3, C4**	TRAIL R2/DR5	**D3, D4**	p21/ CIP1/CDKN1A
B3, B4	Bax	**C5, C6**	FADD	**D5, D6**	P27/ Kip1
B5, B6	Bcl-2	**C7, C8**	Fas/ TNFRSF6/CD95	**D7, D8**	Phospho-p53 (s15)
B7, B8	Bcl-x	**C9, C10**	HIF-1α	**D9, D10**	Phospho-p53 (s46)
B9, B10	Pro Caspase-3	**C11, C12**	H0-1/HM0X1/HSP32	**D11, D12**	Phospho-p53 (s392)
B11, B12	Cleaved Caspase-3	**C13, C14**	H0-2/HM0X2	**D13, D14**	Phospho-Rad17 (s635)
B13, B14	Catalase	**C15, C16**	HSP27	**D15, D16**	SMAC, Diablo
B15, B16	cIAP-1	**C17, C18**	HSP60	**D17, D18**	survivin
B17, B18	cIAP-2	**C19, C20**	HSP70	**D19, D20**	TNF-R1/TNFRSF1A
B19, B20	Claspin	**C21, C22**	HTRA2/0mi	**D21, D22**	XIAP
B21, B22	Clusterin	**C23, C24**	Livin	**D23, D24**	PBS (neg control)
B23, B24	Cytochrome c			**E1, E2**	Reference

Table 3-3 Apoptotic markers represented on the proteome profiler

3.1.12 Adhesion assay

Plate preparation

A non-tissue culture treated 96 well plate was coated with extracellular matrix proteins diluted in PBS. The follow conditions were assessed:

Collagen I 0.5 µg/ml (Corning collagen type I 354236)

Fibronectin 1µg/ml (sigma F1141)

Laminin 10µg/ml (Sigma L6274)

100 µl of ECM was added to each well and 1% BSA was used as base line control. This was incubated for 1 hour at 37^{o}C and then washed with PBS twice to remove excess ECM.

Primary cells

Primary cells from patient 1989 were used to establish if altered Galectin-7 expression influences adhesion to extracellular matrix proteins. Passage 2 myoepithelial cells were used for the adhesion assays. The plating and knockdown was performed as previously described in 3.1.5. At 48 hours post-siRNA treatment for Galectin-7 knockdown and non-targeting control, cells were trypsinised and counted and added to prepared plates.

N-1089 and β6-1089

N-1089 and β6-1089 cells were plated in 6 well plates at a density 5x10^4 cells per well. After 48 hours transfection with Galectin-7 or control vector was carried out as previously described 3.1.8. The cells were washed 3 times with EDTA (0.02%, pH 7.6), cells were then incubated for 10 minutes with 500ul EDTA and trypsin (5ml of EDTA and 100 ul of trypsin). The trypsin was neutralised and the cells spun down and re-suspended in serum free media F12 Hams media. Cells were counted and 2x10^4 cells in 50ul of media were pipetted into each well of the coated 96 well plate.

Adhesion assay

The plate was incubated at 37°C for 40 minutes. The plate was shaken manually once to remove unattached cells. Cells were fixed in 100% methanol for 10 minutes, then the plate was shaken to remove methanol. The plate was then stained with 0.1% Crystal Violet in 30% methanol for 60 minutes at room temperature. The plate was shaken to remove excess crystal violet and then washed 3 times with dH_2O. The cells were solubilised with 30% glacial acetic acid for 10 minutes whilst on the rocking platform. The plate was then read at a wavelength of 595nm. This assay was performed in biological triplicate for both primary cells and cell lines.

Data analysis

Microsoft Excel was used to analyse the data. The average read for adhesion to BSA was subtracted from adhesion to each extracellular matrix protein for the corresponding cells. The absorbance figures were then averaged and standard deviations calculated. The cells where the Galectin-7 levels had been manipulated were compared to the control cells to assess if the percentage adhesion to each extracellular matrix increased or decreased.

3.1.13 Immunofluorescence

Glass coverslips (13mm) were placed in a 24 well plate. The coverslips were pre coated with 10µg/cm_2 COL1 and seeded with 2 x 10^5 primary myoepithelial cells from 3 different patients. The cells were plated and when approximately 60% confluent incubated with siRNA to Galectin-7 or non-targeting control for 48 hours described in more detail in 3.1.7. Media was aspirated prior to cells being fixed with formal saline for 10 minutes. Following three washes with filtered PBS cells were permeabilised with 0.1% Triton 100X (Alfa Aesar, A16046) for 5 minutes. Cells were blocked in 0.1% BSA/PBS for 10 minutes at room temperature. Primary antibody, as outlined in Table 3-4, was added at an appropriate concentration and incubated at 4^oC overnight. Coverslips were washed three times with filtered PBS and incubated with the appropriate secondary antibody diluted in 0.1% BSA/PBS at 1:200, at room temperature for 1 hour in the dark. Coverslips were washed three times with filtered PBS and once with dH_2O. Coverslips were removed from the 24 well plate and mounted onto glass slides using DAPI (Invitrogen P36391). Slides were left overnight at room temperature then viewed on the Zeiss LSM 510 confocal microscope.

Antibody	Source	Clone	Species	Dilution	Secondary
Galectin-7	Abcam	Ab108623	Rabbit	1:750 in 5% BSA	1:200 goat anti-rabbit (Alexa fluro 488 Invitrogen A11008)
P-Cadherin	Novus biologicals	104805	Mouse	1:50 in 1%BSA	1:200 goat anti mouse (Alexa fluro 546 Invitrogen A11008) 1:200 goat anti-mouse (Alexa fluro 488 Invitrogen A11001)
Desmoglein-3	Serotec	AHP319	Rabbit	1:100 in 1% BSA	1:200 goat anti-rabbit (Alexa fluro 488 Invitrogen A11008)

Table 3-4 Antibodies used for Immunofluorescence

3.1.14 Migration assay

The underside of 8µm transwell inserts (Corning 3422) was coated with 100µl of different extracellular matrix proteins. Four transwells were coated per ECM condition. Membranes were coated with either fibronectin (10µg/ml; Sigma sigma F1141), Collagen I 0.5 µg/ml (Corning collagen type I 354236), or 1% BSA as control (Sigma, A8022). These were left to incubate at room temperature for 1 hour, following which any excess extracellular matrix was removed and the inserts rinsed with filtered PBS. 500µl of serum free F12 Hams media was added to each well prior to inserting the transwell.

N-1089 cells transfected with either control or Galectin-7 vector, were counted and re-suspended in serum free media. 3 x10^4 cells in 200µl of media were added to the upper chamber of each transwell. These were incubated for 6 hours at 37^{o}C.

The media was removed from both the upper and lower chambers. 500µl of trypsin was added to each chamber and incubated for 1 hour at 37^{o}C. The trypsin solution was rinsed over the membrane from both upper and lower chambers prior to removal and then transferred to separate tubes of 9.5ml filtered isoton. The number of cells in each tube was counted using the Casy cell counter. The percentage of cells that had migrated to the lower chamber was calculated. This was performed in biological triplicate for the cell lines however this was performed only once with the primary cells. Passage 2 primary myoepithelial cells were used which are a finite resource and therefore it was not possible to perform all experiments in triplicate.

3.1.15 Scratch Assay

Primary Passage 2 myoepithelial cells from patient 1989 were seeded at a density of $4x10^4$ on collagen-coated 6 well plates. After 3 days cells were treated with Galectin-7 siRNA (siGENOME SMART pool LGALS7, Thermoscientific Dharmacon M-011719-01) or a non-targeting control. (Thermoscientific Dharmacon siGENOME D-001206-14-20). 48 hours post siRNA treatment, 2 scratches were made in each well with a 200μL pipette tip to make a central cross. Cells were washed three times with PBS to remove any unattached cells and primary fresh myoepithelial cell media was added to each well. This was performed in duplicate and the experiment was repeated three times. Images were taken at 0,10,12,14 and 16 hours. ImageJ was used to assess the area of the scratch and the rate of closure between Galectin-7 and non-targeting control siRNA treated cells was compared.

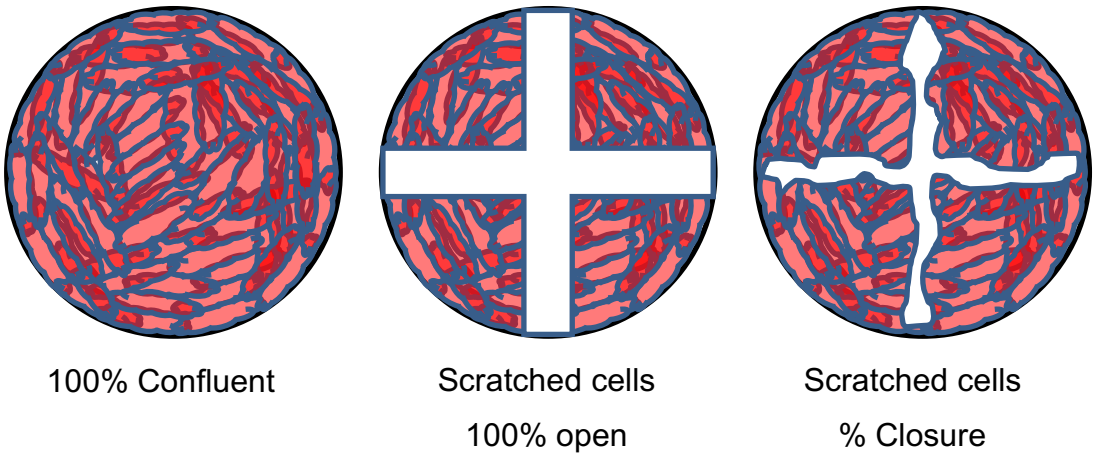

Figure 3-2 Scratch assay method and analysis

3.1.16 Invasion assay

8μm transwell inserts were placed into a 24 well plate. Matrigel (BD biosciences, 354 234) was diluted with ice-cold serum free media (SFM) at a 1:3 matrigel: SFM ratio. 70μl of matrigel:SFM mixture was pipetted into each transwell and incubated at 37^{o}C for 40 mins. MDA MB 231 cells were counted and 3x10^{4} cells in 200μl of SFM were added to each transwell. 500μl of conditioned media was placed in the lower chamber of the transwell. The plates were incubated at 37^{o}C for 24 hours. The media was removed from the lower transwell chamber, 500μl of trypsin was added to each well and incubated for 1hr at 37^{o}C. The trypsin solution was rinsed over the bottom of the membrane removed and transferred to tubes of 9.5ml filtered isoton. The number of cells in each tube was counted using the Casy cell counter. The total number of cells that had invaded through the Matrigel was calculated. The cells that had invaded were calculated as a percentage of total cells. A comparison was made between conditioned media from non-targeting control primary myoepithelial cells and Galectin-7 knockdown myoepithelial cells.

3.1.17 Protease array sample preparation

Primary myoepithelial cells were seeded onto collagen-coated 6 well plate at a density of $4x10^4$ cells per well. Galectin-7 siRNA knockdown and non-targeting control siRNA in primary myoepithelial cells was performed as previously described. Conditioned media was harvested from 4 different patients, centrifuged at 1200 RPM for 3 minutes to remove any dead cells, this was then transferred to -20°C freezer. Prior to incubation on the proteome profiler (R&D Systems - ARY021B) the conditioned media was concentrated through spin columns (Millipore-Amicon Ultra UFC 800324) at x4000g for 25 minutes until a volume of 1ml of concentrated conditioned media remained. 500μL of conditioned media was mixed with 1ml of Array buffer 6 and 15μL of protease detection antibody cocktail, this was incubated at room temperature whilst the nitrocellulose membrane was blocking.

Array procedure

All reagents were brought to room temperature prior to use. 2ml of Array buffer 1 was added to the 4 well multi dish and then each array was placed into the multi dish and was incubated with gentle rocking for 1 hour at room temperature. Following incubation of samples overnight on the nitrocellulose membranes, arrays were washed for 3x 10 minutes to remove unbound protein with wash buffer.

Detection

Each array was then incubated with a 1.5ml cocktail of biotinylated detection antibodies. 15μl of reconstituted detection antibody cocktail was diluted with 1.5ml 1x Array buffer 2/3 and incubate for 1 hour at room temperature on a rocking platform. Washes were repeated as previously described.

Arrays were then incubated with 2.0ml of diluted streptavidin-HRP reagent for 30 minutes on the rocking platform at room temperature followed by washing. Results were detected by adding 1ml of chemi-reagent to each membrane. The chemi-doc system was used to read the protein intensity.

Analysis

The Image-J program was used to assess pixel density and comparison was made between conditions. For each protein there were duplicate spots. The average pixel density for each spot was used. Table 3.5 shows the coordinates and corresponding protease protein.

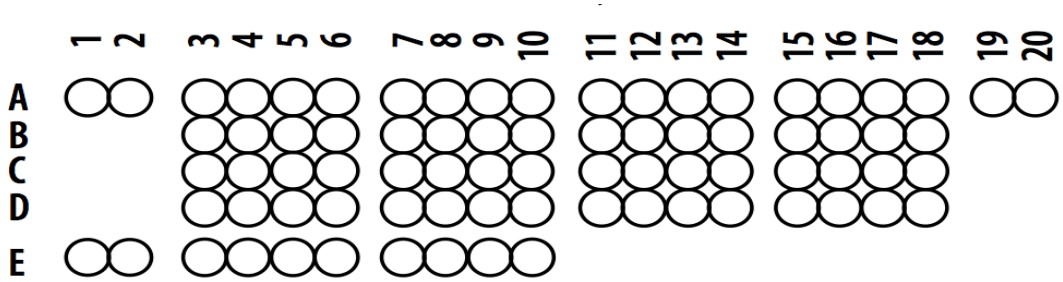

Coordinate	Analyte/Control	Coordinate	Analyte/Control
A1, A2	Reference Spots	C7, C8	Kallikrein 10
A3, A4	ADAM8	C9, C10	Kallikrein 11
A5, A6	ADAM9	C11, C12	Kallikrein 13
A7, A8	ADAMTS1	C13, C14	MMP-1
A9, A10	ADAMTS13	C15, C16	MMP-2
A11, A12	Cathepsin A	C17, C18	MMP-3
A13, A14	Cathepsin B	D3, D4	MMP-7
A15, A16	Cathepsin C	D5, D6	MMP-8
A17, A18	Cathepsin D	D7, D8	MMP-9
A19, A20	Reference Spots	D9, D10	MMP-10
B3, B4	Cathepsin E	D11, D12	MMP-12
B5, B6	Cathepsin L	D13, D14	MMP-13
B7, B8	Cathepsin S	D15, D16	Neprilysin/CD10
B9, B10	Cathepsin V	D17, D18	Presenilin
B11, B12	Cathepsin X/Z/P	E1, E2	Reference Spots
B13, B14	DPPIV/CD26	E3, E4	Proprotein Convertase 9
B15, B16	Kallikrein 3/PSA	E5, E6	Proteinase 3
B17, B18	Kallikrein 5	E7, E8	uPA/Urokinase
C3, C4	Kallikrein 6	E9, E10	Negative Control
C5, C6	Kallikrein 7		

Table 3-5 Protease proteins

Protease protein table and schematic to show how each spot corresponds to each protease marker

3.1.18 Organotypic cultures

Organotypic gels were prepared on ice. The gel comprised of 4.9 ml of rat tail collagen type-I (Corning 354236), 2.1 ml of matrigel (Corning 354234), 1ml 10X DMEM (Sigma D2429) and 1 ml of fetal bovine serum (Sigma F9665). 200μl of 1M NaOH was added slowly until the gel turned pink. 5 x 10^6 MRC-5 fibroblasts were re-suspended in 1ml of DMEM media (Sigma D6429) with 10% FBS and re-suspended into the gel. Eight gels were prepared by adding 1 ml of the mixture to each well of a 24 well plate. The gels were incubated at 37°C for 1 hour. 1 ml of DMEM with 10% FBS media was then added to each well and incubated overnight at 37 °C. N-1089 myoepithelial cell lines were transfected with control or Galectin-7 plasmid as described in 3.1.8. 1 X 10^6 myoepithelial cells were re-suspended in 2 ml of Ham's F12 and 500μl added to each gel each in quadruplicate. After 4 hours at 37°C, 2.5 X 10^5 MDA MB 231 cells were was re-suspended in 500μl DMEM media and added to the surface of each gel. The media was changed every 48 hours. After 8 days the gels were removed from the plate and fixed in 10% neutral buffered formalin (Cell Path BAF-0010-037) for 24 hours prior to being transferred to 70% ethanol for 24 hours. Gels were embedded in paraffin and sectioned.

3.2 Results

3.2.1 Characterisation of MEC lines and primary MEC

Primary myoepithelial cells and the myoepithelial cell lines were characterised using immunocytochemistry. Galectin-7 was strongly expressed in primary myoepithelial cells, however both N-1089 and β6-1089 myoepithelial cell lines lack Galectin-7, therefore the cell lines were transfected with Galectin-7 vector or control vector in order to investigate the impact of Galectin-7.

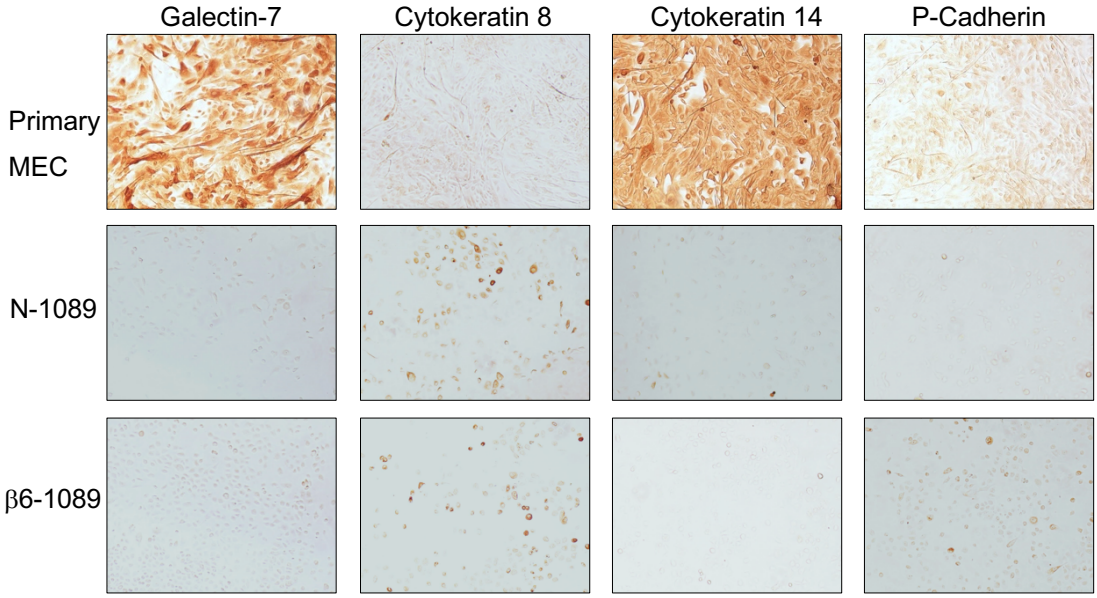

Figure 3-3 Characterisation of MEC cell line and primary MEC

Immunocytochemistry was used to characterise primary myoepithelial cells, N-1089 and β6-1089. Markers assessed were Galectin-7, cytokeratin 8, cytokeratin 14 and P- Cadherin. This was undertaken by Mary-Kate Hayward, PhD student in the lab. This demonstrated that the primary myoepithelial cells show strong expression of Galectin-7 and the myoepithelial-associated cytokeratin 14, retaining the basal P-Cadherin expression but with minimal expression of the luminal-associated cytokeratin 8. In contrast, the myoepithelial cell lines lack Galectin-7 and show mixed expression of cytokeratin 8 and cytokeratin 14, with minimal expression of P-Cadherin.

3.2.2 Expression of Galectin-7 in myoepithelial cells

Baseline expression of Galectin-7 in primary myoepithelial cells and the myoepithelial cell lines N-1089 and β6-1089 was assessed by Western blotting. This demonstrated expression in primary myoepithelial cells but no Galectin-7 protein was detected in N-1089 or β6-1089 cell lines. To generate appropriate models for further experiments, both N-1089 and β6-1089 cells were transfected with Galectin-7 vector or control vector. This achieved successful overexpression with the Galectin-7 vector (Figure 3-4).

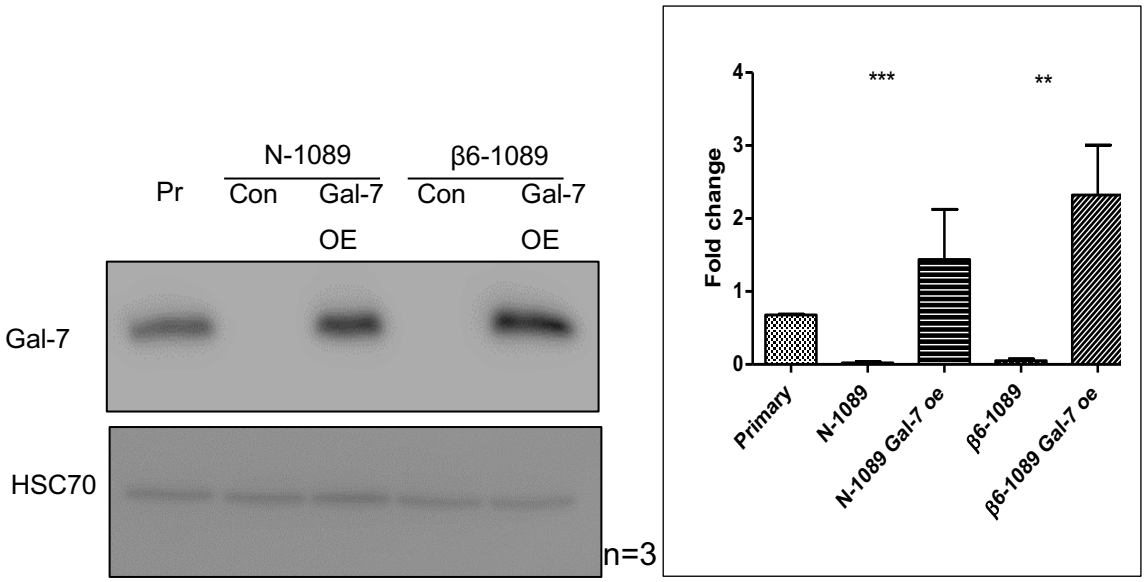

Figure 3-4 Protein expression of Galectin-7 after transfection in N-1089

N-1089 and β6-1089 were transfected with Galectin-7 plasmid or control plasmid. Western blotting shows successful overexpression of Galectin-7 with no expression in cells transfected with control vector. Primary myoepithelial cells (Pr) were used as a positive control.

3.2.3 Knockdown of Galectin-7 in Primary myoepithelial cells

Normal primary myoepithelial cells were treated with Galectin-7 siRNA or non-targeting control siRNA. Substantial knockdown was achieved with the Galectin-7 siRNA at both 48 and 72 hours post treatment. (Figure 3-5.) For further experiments siRNA treatment for 48 hours was used since successful knockdown was achieved and the reduced incubation time increased the chance of subsequent treatments being more successful both due to cell viability and cells not being over confluent.

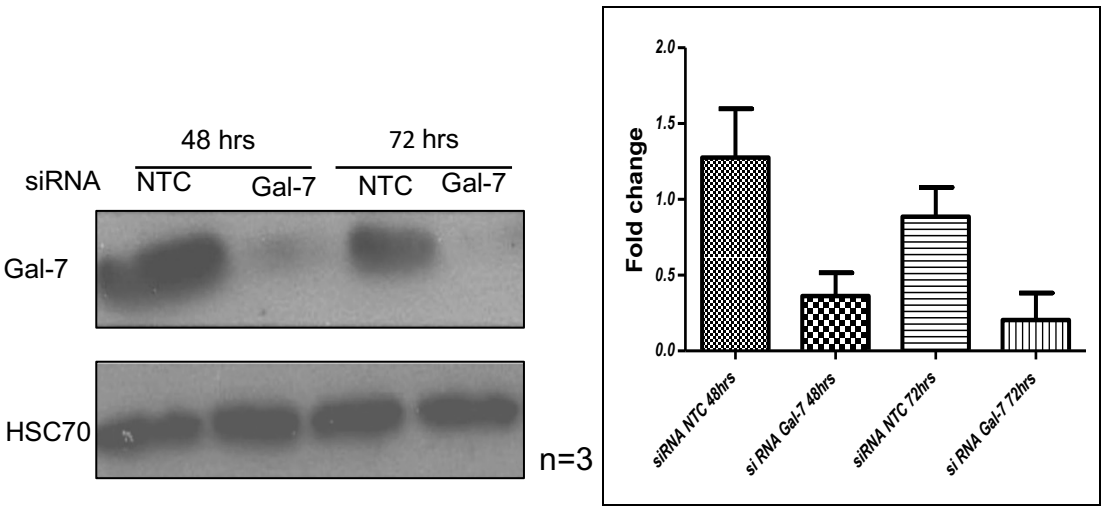

Figure 3-5 Galectin-7 knockdown in primary myoepithelial cells.

Western blot shows loss of Galectin-7 at 48 and 72 hours post Galectin-7 siRNA. No knockdown was seen with a pooled non targeting control siRNA. The loading control is HSC70.

3.2.4 Assessment of apoptosis in Primary myoepithelial cells

Galectin-7 has been implicated in modulation of apoptosis, therefore the effect of knockdown of Galectin-7 on the apoptosis of primary myoepithelial cells was assessed. Control siRNA or Galectin-7 siRNA primary MECs were exposed to TRAIL and expression of cleaved caspase-3, total caspase-3 and cleaved PARP was measured using Western blotting. The images are representative of western blots performed from 2 experiments passage 3 primary myoepithelial cells were used in these experiments. There is an increase in cleaved caspase-3 (figure 3.6) and cleaved PARP (figure 3.8) in all TRAIL treated cells. In non TRAIL treated cells there are higher levels of total caspase across all 3 patients. There are much higher levels of cleaved caspase-3 in the TRAIL treated Galectin-7 knockdown cells across all three patients, indicating that in this model, Galectin-7 has an anti-apoptotic effect. A similar but less marked effect is seen for cleaved PARP. Galectin- 7 levels did not have an effect on total caspase levels.

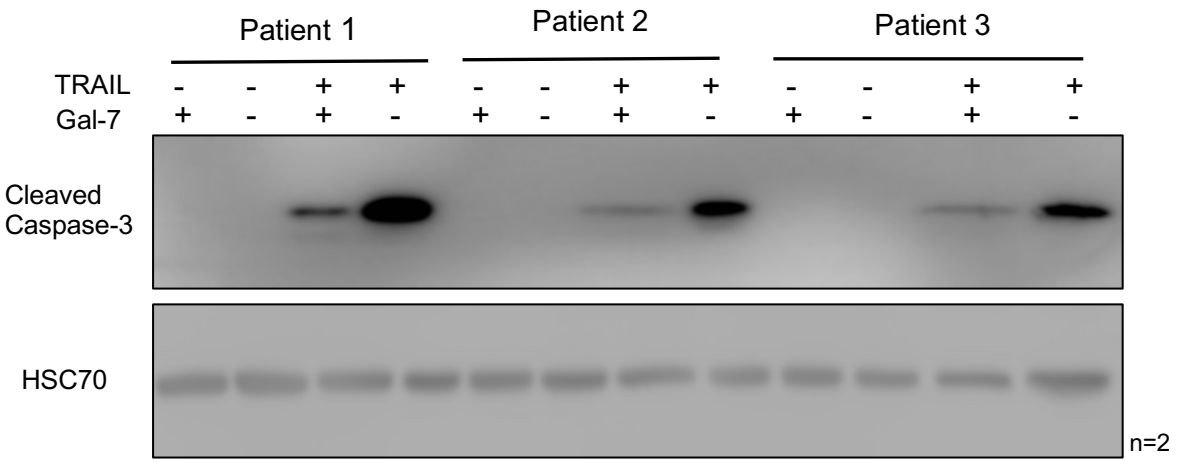

Figure 3-6 Effect of TRAIL treatment of Galectin-7 knockdown primary myoepithelial cells on Cleaved Caspase-3.

In Galectin-7 knockdown cells, there is an increase in cleaved caspase-3 (marker of apoptosis) following TRAIL treatment, HSC70 was used as a loading control. Gal-7 +ve indicates cells were treated with non-targeting control siRNA and Gal-7 –ve indicates cells were treated with siRNA to Gal-7.

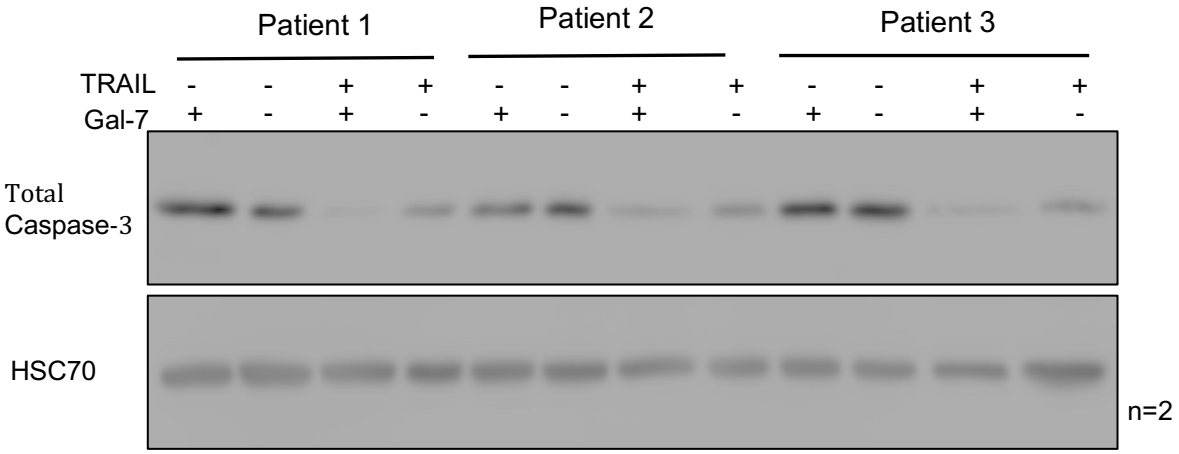

Figure 3-7 Effect on protein expression of Total Caspase-3 following Galectin-7 knockdown in primary myoepithelial cells treated with TRAIL.

There is increased total caspase 3 in the non-TRAIL treated cells. There is slightly increased total caspase 3 in TRAIL treated Galectin-7 knockdown cells. HSC70 was used as a loading control.

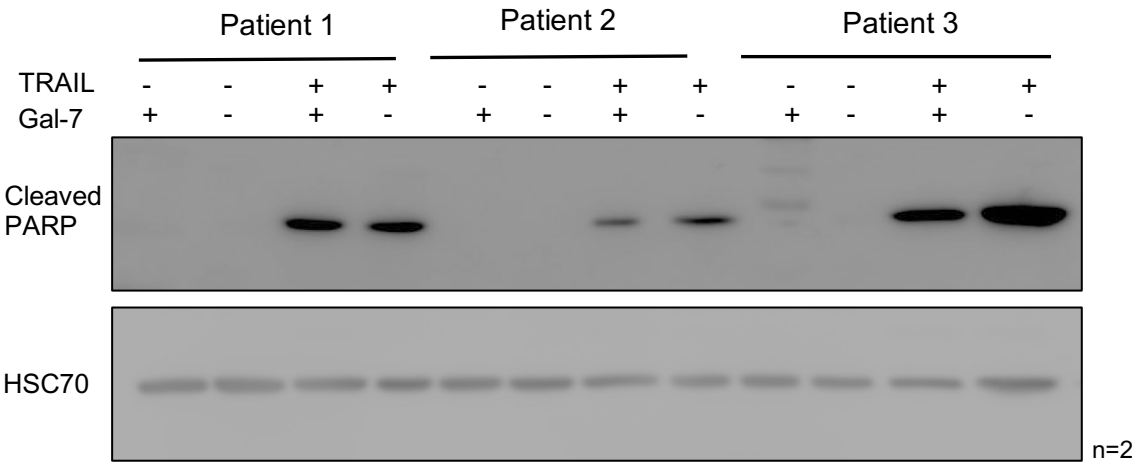

Figure 3-8 Effect on protein expression of cleaved PARP following Galectin-7 knockdown in primary myoepithelial cells treated with TRAIL.

Cleaved PARP (marker of apoptosis) increases with TRAIL treatment. There is slightly increased levels of cleaved PARP in the Galectin-7 knockdown cells versus control cells following TRAIL treatment. HSC70 was used as a loading control.

3.2.5 Galectin-7 overexpression increases apoptosis in N-1089 and β6-1089

Both N-1089 and β6-1089 myoepithelial cell lines lack Galectin-7, therefore the cell lines were transfected with Galectin-7 vector or control vector and these cells exposed to TRAIL for 4 hours In the established myoepithelial cell lines, TRAIL treatment increased cleaved PARP expression in Galectin-7 overexpressing cells compared to control vector(figure 3.9 and 3.10), indicating that in these cell line models, Galectin-7 is pro-apoptotic. For cleaved PARP this was performed in triplicate. Due technical difficulty with the choice of membrane the blots for cleaved caspase -3 did not work.

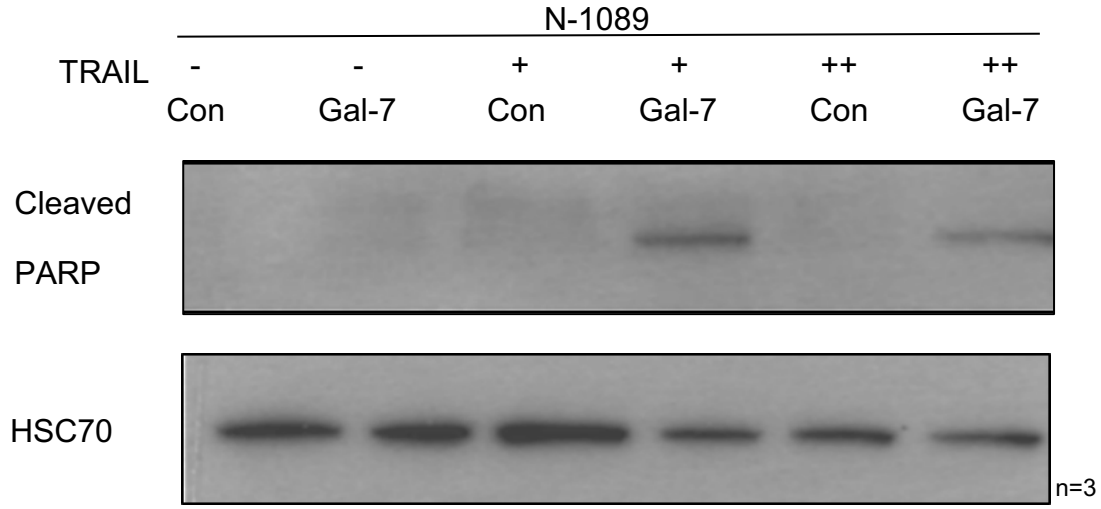

Figure 3-9 Effect of protein expression of cleaved PARP in Galectin-7 overexpressed N-1089 cells following TRAIL treatment

Western blot shows increased cleaved PARP in N-1089 Galectin-7 overexpressed cells treated with TRAIL. (TRAIL + 250ng/ml TRAIL ++ 500ng/ml), indicating overexpressing Galectin-7 increases apoptosis in this model.

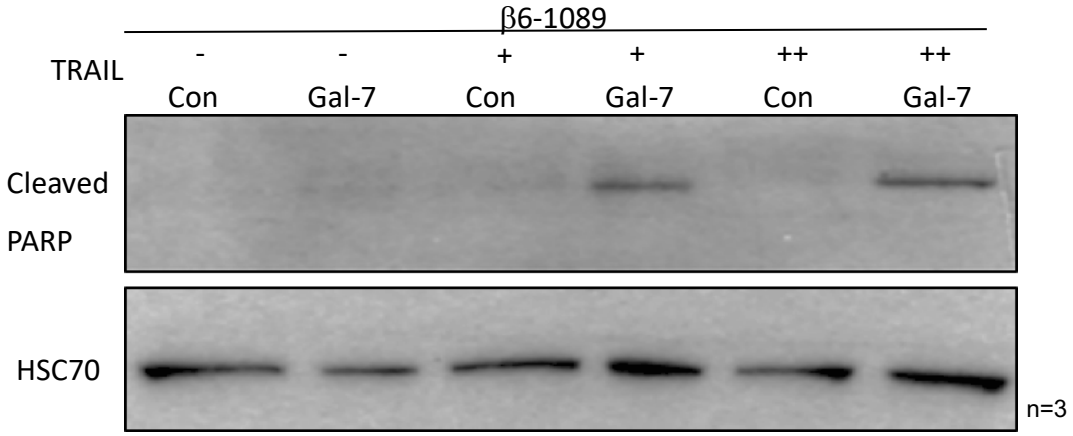

Figure 3-10 Effect of protein expression of cleaved PARP in Galectin-7 overexpressed β6-1089 cells following TRAIL treatment

Western blot shows increased cleaved PARP in β6-1089 Galectin-7 overexpressed cells treated with TRAIL. (TRAIL + 250ng/ml TRAIL ++ 500ng/ml), indicating overexpressing Galectin-7 increases apoptosis in this model.

3.2.6 LDH cytotoxicity assay

An LDH cytotoxicity assay was performed to determine the toxicity of TRAIL on N-1089, β6-1089 and primary myoepithelial cells. The impact of Galectin-7 on toxicity was also analysed, with Galectin-7 overexpressed in N-1089 and β6-1089 and knocked down in primary MECs. A 'maximal lysis' well was performed for each cell type and conditions were all normalised to this with maximal lysis being set as 100% cell death. In this assay, the immortalised cell line model exhibits increased cell death following TRAIL treatment in cells that have higher levels of Galectin-7(Table 3.6 and figure 3.11). In the primary myoepithelial cells there also is increased cell death in the cells which have higher levels of Galectin-7 (Table 3.7 and figure 3.12).

3.2.6.1 LDH cytotoxicity N-1089 and β6-1089

	N-1089 Con	N-1089 Gal-7	p value	β6-1089 Con	β6--1089 Gal-7	p value
0	24%	14%	2.34E-07	20%	11%	1.72E-07
Trail 250ng/ml	29%	38%	0.045625	26%	32%	0.000887
Trail 500ng/ml	25%	44%	2.91E-05	25%	37%	0.214413

Table 3-6 LDH cytotoxicity in N-1089 and β6-1089 overexpressed with control or Galectin-7 vector following TRAIL treatment.

Comparison of LDH cytotoxicity in N-1089 and β6-1089 overexpressed with control or Galectin-7 vector. In both N-1089 and β6-1089 Galectin-7 overexpressed cells there in an increase in cell death following treatment with TRAIL at 250 ng/ml and TRAIL at 500 ng/ml. Experimental results are from 3 pooled experiments.

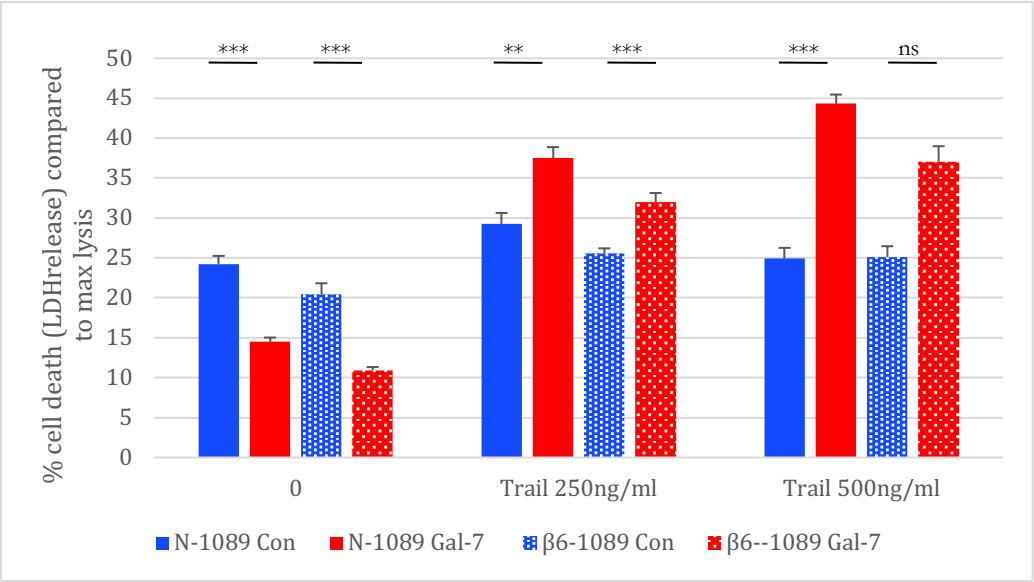

n=3

Figure 3-11 LDH cytotoxicity In N-1089 and β6-1089 overexpressed with control or Galectin-7 vector following TRAIL treatment.

In N-1089 and β6-1089 there is increased cell death in Galectin-7 overexpressed cells following TRAIL treatment. Error bars represent standard deviation. A t-test was performed to assess significance (***<0.001, **<0.01, *<0.05)

3.2.6.2 LDH cytotoxicity in primary myoepithelial cells

	siRNA NTC	siRNA Gal-7	p value
0	11.2%	6.9%	9.9115E-05
Trail 250 ng/ml	31.7%	16.2%	1.04869E-07
Trail 500 ng/ml	42.0%	36.9%	0.524206538

Table 3-7 Effect of Galectin-7 knockdown on cytotoxicity measured by LDH assay in primary myoepithelial cells following TRAIL treatment

In primary myoepithelial cells with Galectin-7 knockdown, there was decreased cytotoxicity on treatment with TRAIL compared to non-targeting knockdown, though this was not significant with a TRAIL dose of 500 ng/ml. Experimental results are from 2 pooled experiments demonstrated in table 3.7 and figure 3.12.

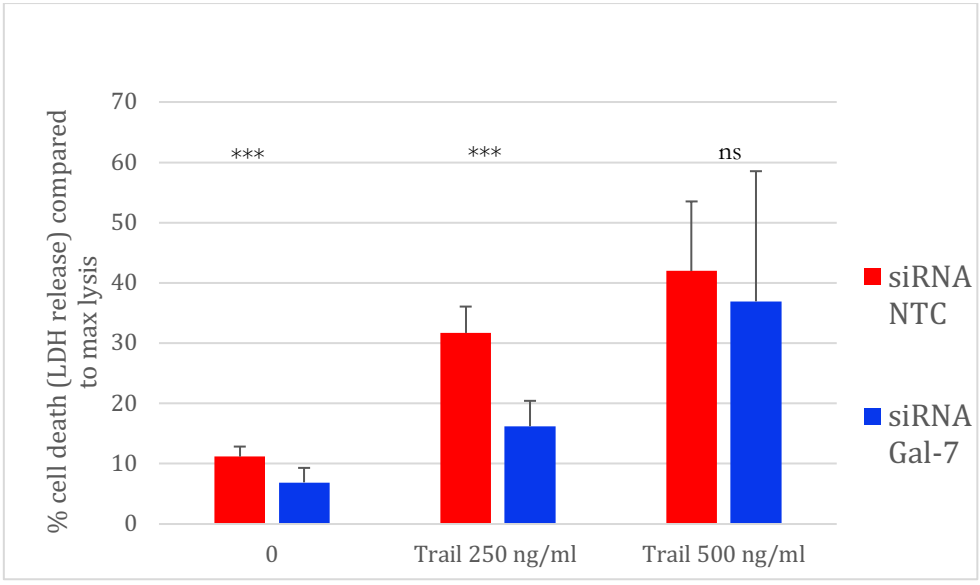

n=2

Figure 3-12 Effect of Galectin-7 knockdown on cytotoxicity measured by LDH assay in primary myoepithelial cells following TRAIL treatment

There is decreased cell death in Galectin-7 Galectin-7 knockdown cells following TRAIL treatment. Error bars represent standard deviation. A T test was performed to assess significance (***<0.001)

3.2.7 Human apoptosis array

A human apoptosis proteome array was used to analyse the impact of knockdown of Galectin-7 on a wider range of apoptosis-related proteins. The difference in pixel density was assessed between non-targeting control and Galectin-7 knockdown treated cells, and TRAIL treated versus vehicle control treated primary myoepithelial cells. Passage 3 myoepithelial cells were used. This experiment was performed in duplicate, however the knockdown of Galectin-7 was checked following the array analysis and sufficient knockdown was not achieved on one occasion. The data from the population of cells in which the knockdown was not achieved was not further analysed. The knockdown was confirmed with western blot as shown in Figure 3-13.

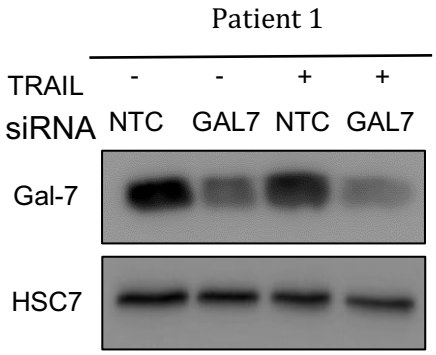

Figure 3-13 Western blot confirming successful Galectin-7 knockdown in the primary myoepithelial cell samples used in the human apoptosis array.

3.2.7.1 Analysis of human apoptosis array

To analyse the apoptosis array, the Image-J program was used to assess pixel density and comparison was made between conditions. For each protein there were duplicate spots. The average pixel density for each spot was used. Table 3-3 shows the coordinates and corresponding apoptotic protein on the array.
Figure 3.14 illustrates each membrane from the human apoptosis array. The average pixel density was then normalised to the siRNA non-targeting control exposed to vehicle only treatment. Figure 3.15 shows all apoptotic markers on the array on one graph these are then split into smaller graphs and described below.

Figure 3.15 illustrates a graph which represents all the apoptotic markers on the array, particular apoptotic markers are shown in further detail in the graphs that follow. Figure 3.16 shows pro caspase 3 (an inactive form of caspase) is not changed by TRAIL treatment, however following TRAIL treatment there Is an increase in cleaved caspase-3. There appears to be minimal effect of Galectin-7 level on apoptotic proteins however this experiment was only performed with on one set of primary cells. There is a large increase in catalase in the Galectin-7 knockdown TRAIL treated cells. Catalase is a key antioxidant enzyme which defends against oxidative stress.

Figure 3.17 shows changes in p53 levels, where all 3 p53 subunits decrease when cells are treated with TRAIL. There is a larger decrease in the Galectin-7 knockdown TRAIL treated cells.

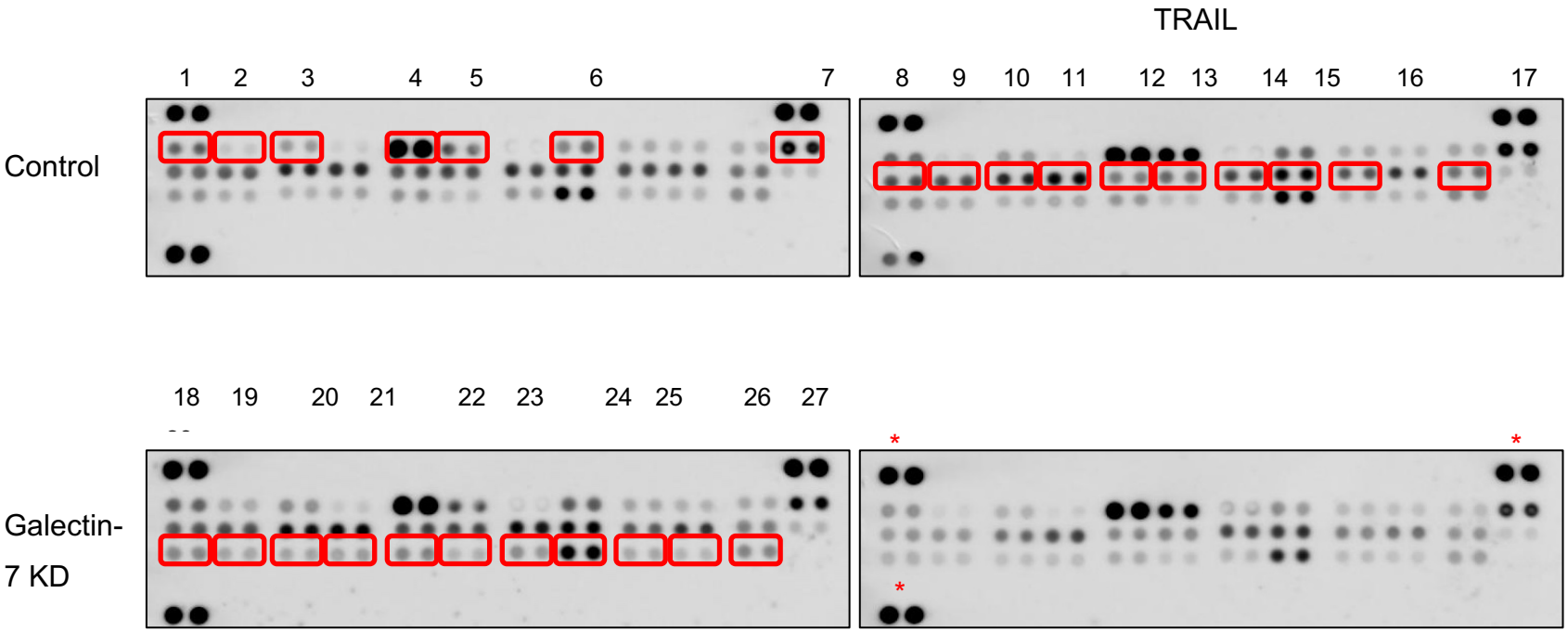

Figure 3-14 Apoptosis Array

1	Bad	11	Fas/ TNFRSF6/CD95	21	Phospho-p53 (s15)
2	Bax	12	HIF-1α	22	Phospho-p53 (s46)
3	Bcl-2	13	H0-1/HM0X1/HSP32	23	Phospho-p53 (s392)
4	Pro Caspase-3	14	H0-2/HM0X2	24	Phospho-Rad17 (s635)
5	Cleaved Caspase-3	15	HSP27	25	SMAC, Diablo
6	cIAP-1	16	HSP60	26	survivin
7	Cytochrome c	17	HTRA2/0mi	27	TNF-R1/TNFRSF1A
8	TRAIL R1/ DR4	18	PON 2	28	XIAP
9	TRAIL R2/DR5	19	p21/ CIP1/CDKN1A	*	Reference spots
10	FADD	20	P27/ Kip1		

The table shows key proteins. Number 5 cleaved caspase 3 shows the largest difference between control and TRAIL treated cells this is also shown in the western blot in figure 3.13.

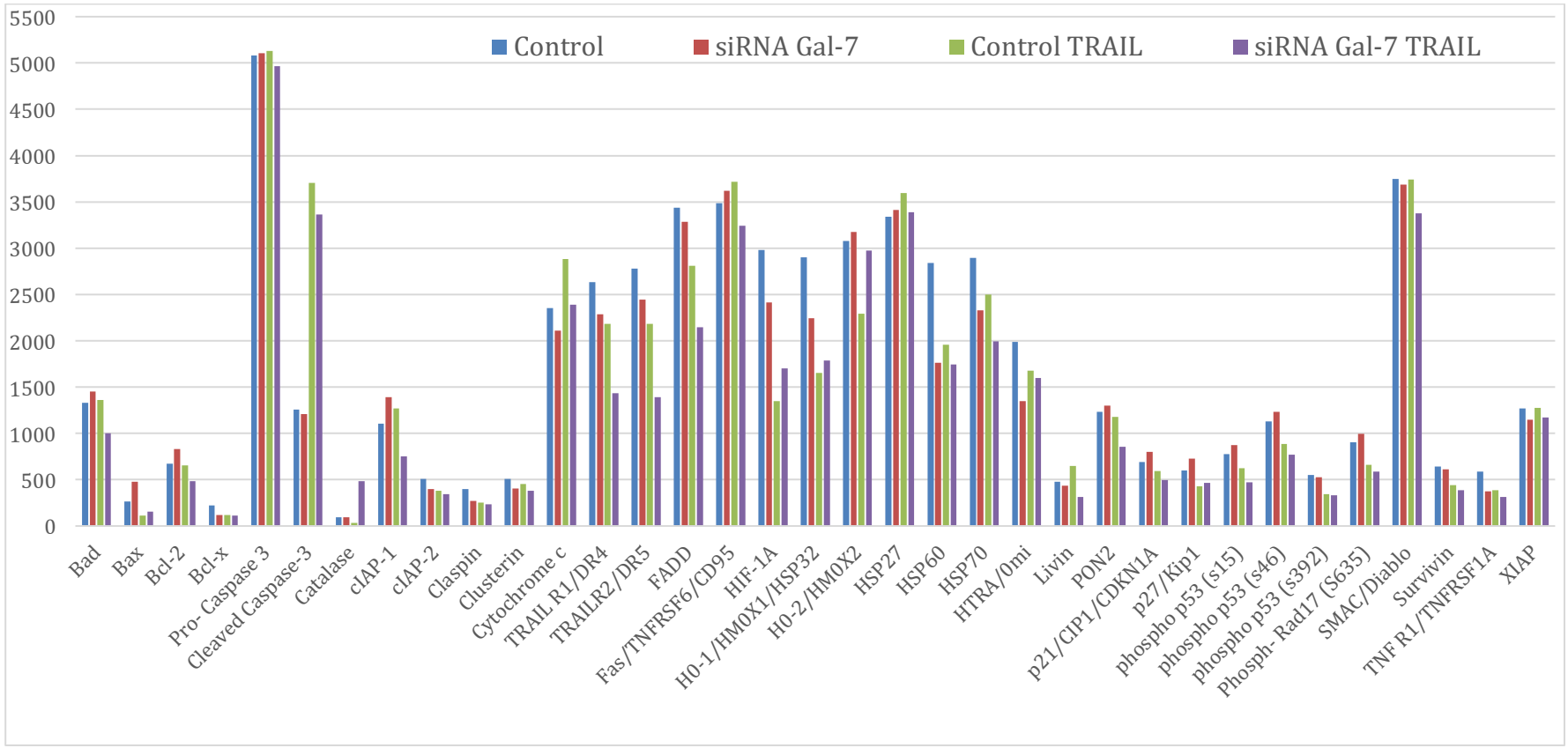

Figure 3-15 Apoptosis array graph

All apoptosis markers on proteome profiler

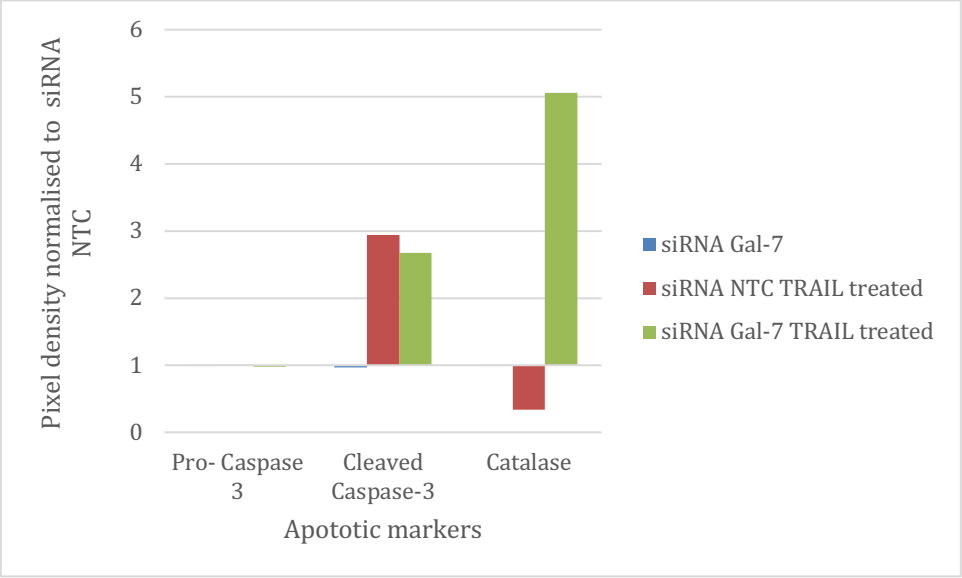

Figure 3-16 Human apoptosis array showing changes in caspase 3 and catalase

Human apoptosis array normalised to si RNA non targeting control shows no change in Pro caspase 3 following TRAIL treatement, an increase in cleaved caspase 3 following TRAIL treatment and there is minimal effect from Galectin-7 knockdownThere is a large increase in catalalse expression compared to control cells in Galectin-7 knockdown TRAIL treated cells.

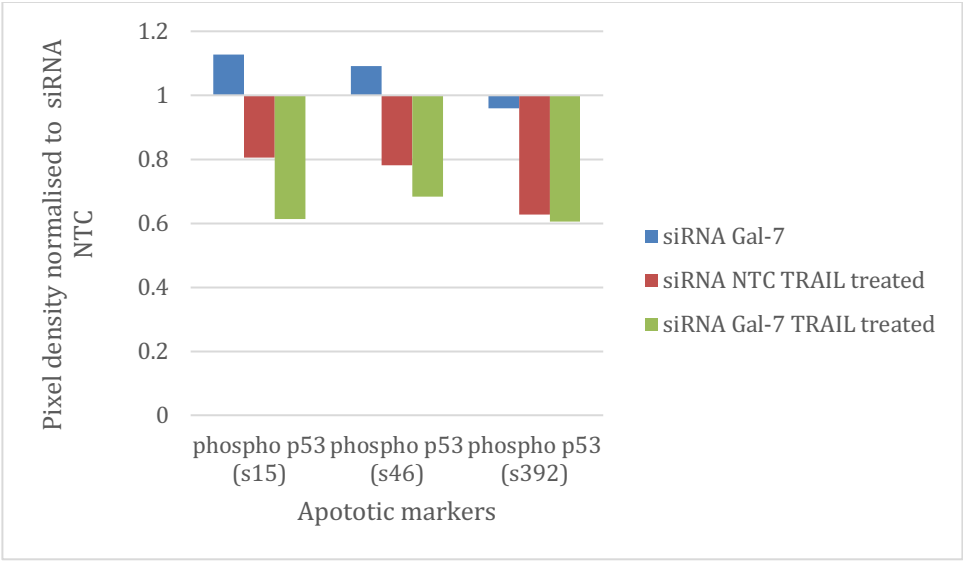

Figure 3-17 Human Apoptosis array showing changes in p53

Human apoptosis array normalised to siRNA non targeting control shows changes in p53 levels: all 3 p53 subunits decrease when cells are treated with TRAIL, there is a greater decrease in the Galectin-7 knockdown TRAIL treated cells.

3.2.8 Adhesion assays- Cell Lines

To establish whether Galectin-7 has an effect on adhesion of myoepithelial cells to the extracellular matrix two different models were used; cell lines were transfected with Galectin-7 while normal primary myoepithelial cells were treated with Galectin-7 siRNA versus non-targeting control, and adhesion to extracellular matrix proteins measured. Results were all normalised to BSA controls.

N-1089 and β6-1089 cell adhesion

In both N-1089 and β6-1089 cells transfected with Galectin-7 vector, the myoepithelial cells showed significantly increased adhesion to Collagen and to Fibronectin compared to control vector (Figure 3.18). A decision was made tp used laminin was used in the primary cell model however this was performed after the cell line experiment and a decision was made to not repeat the cell line experiments.

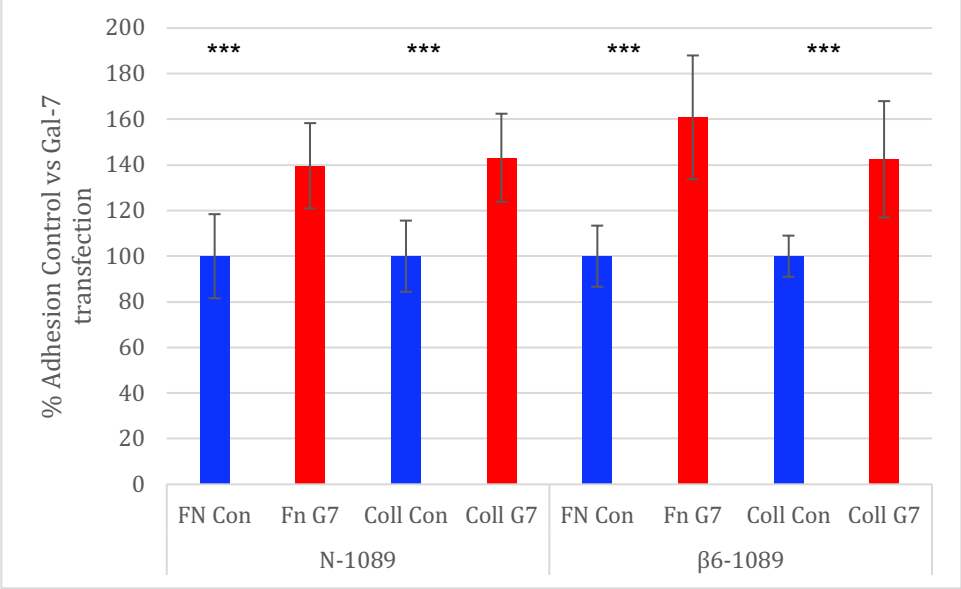

n=3

Figure 3-18 Adhesion assays with N-1089 and β6-1089 cells

N-1089 Galectin-7 transfected cells showed 40% and 43% increased adhesion to Fibronectin and Collagen respectively compared to the control cells. β6-1089 Galectin-7 transfected cells showed 61% and 42% increased adhesion to Fibronectin and Collagen respectively compared to the control cells. There is a significant increase in adhesion in Galectin-7 transfected cells. The results are from pooled data from 3 experiments, error bars represent the standard deviation. (p= T Test ***<0.001)

n=3

3.2.9 Adhesion assays - primary myoepithelial cells

In Galectin-7 knockdown primary myoepithelial cells, the cells showed significantly decreased adhesion to both Fibronectin and Laminin, with significantly greater adhesion to Collagen (figure 3.19). Passage 2 primary myoepithelial cells were used.

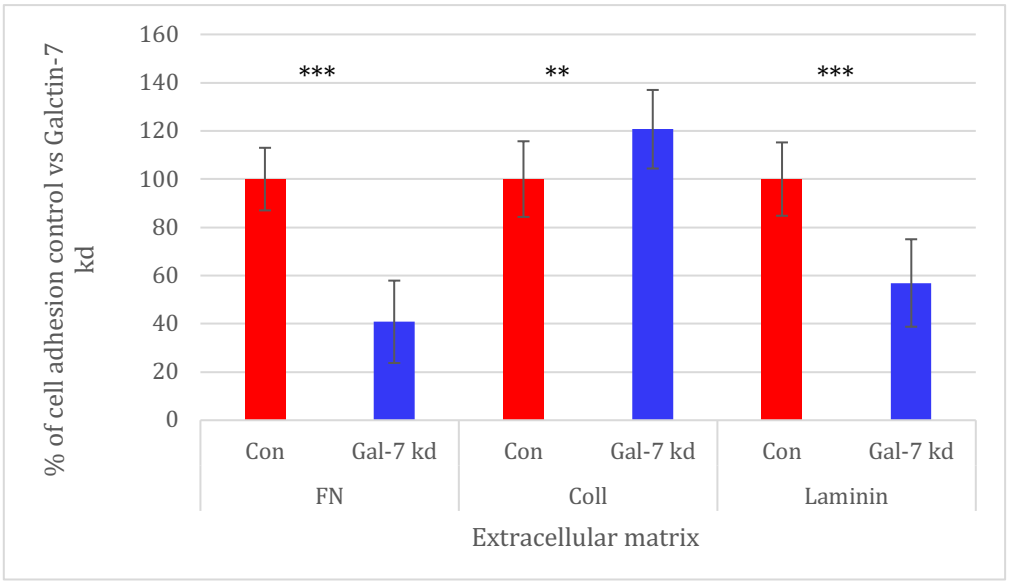

n=3

Figure 3-19 Adhesion assays with primary myoepithelial cells

There is a 59% decrease in adhesion to Fibronectin in the Galectin-7 knockdown cells versus the control cells. Galectin-7 knockdown cells had a 21% increased adhesion to collagen compared to the control. In the Galectin-7 knockdown cells there is a 43% decrease in adhesion to Laminin compared to the control. The results were from pooled data from 3 experiments, error bars represent the standard deviation. (p= T Test ***<0.001, ** <0.01)

3.2.10 Immunofluorescence for P-Cadherin

The effect of knocking down Galectin-7 in primary myoepithelial cells on P-Cadherin expression or localisation at the cell-cell junction was investigated using immunofluorescence. Myoepithelial cells from three different patients were used and experiments were repeated in biological triplicate. Two images were taken from each cover slip on the Zeiss LSM 510 confocal microscope.

Each image was individually assessed, and all P-Cadherin stained junctions were counted and divided by the number of nuclei. All the data from the 3 different patients and 3 different experiments were pooled into non-targeting control and Galectin-7 knockdown. This demonstrated that in myoepithelial cells with Galectin-7 knockdown there were significantly fewer P-Cadherin-positive junctions compared to myoepithelial cells treated with non-targeting control siRNA (Figure 3-20 and 3-21). The standard deviations are large, likely related to the use of primary patient samples with their inherent variation but results still remain highly significant.

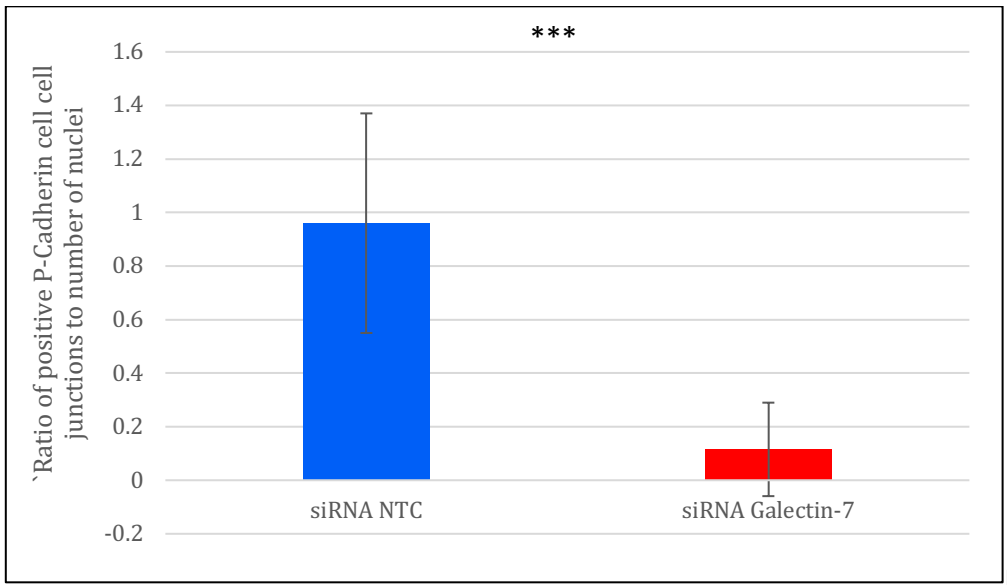

Figure 3-20 Immunofluorescence analysis of P-Cadherin

The ratio of positive P-Cadherin junctions to number of nuclei was assessed. Primary myoepithelial cells treated with non-targeting siRNA had a ratio of 0.96 whilst primary myoepithelial cells treated with Galectin-7 siRNA had a ratio of 0.12 (p value of 0.0003). Data is pooled from 3 experiments. Error bars represent standard deviation.

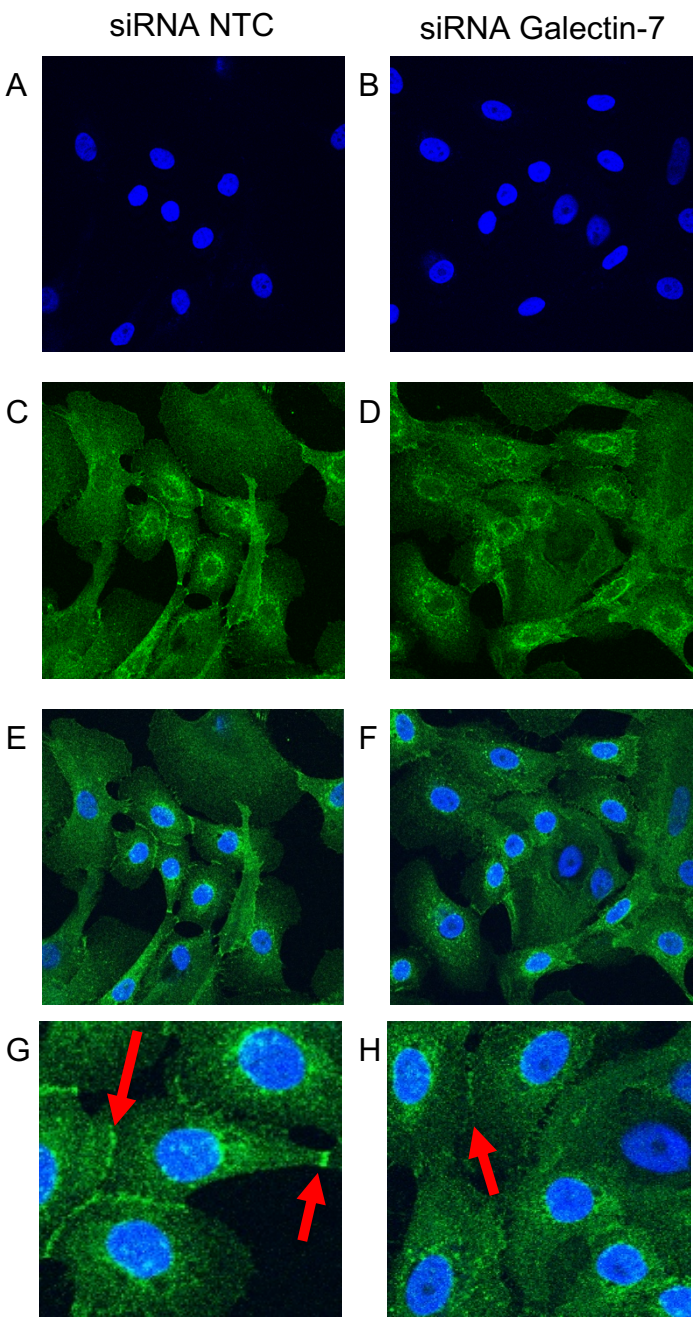

Figure 3-21 P-Cadherin immunofluorescence images

Immunofluorescence for P-Cadherin in primary myoepithelial cells treated either with non-targeting control siRNA (A,C,E,G) or with Galectin-7 siRNA (B,D,F,H). Images A&B represent DAPI stain, C-D indicate staining for P-Cadherin, E&F are merged images, and G&H are high power images. Cells treated with Galectin-7 siRNA show less P-Cadherin positive cell-cell junctions compared to non-targeting control siRNA cells.

3.2.11 P-cadherin Immunohistochemistry

Myoepithelial-associated P-Cadherin expression was assessed in a series of DCIS tissue samples, including pure DCIS or DCIS with admixed invasion. In normal breast ducts, the myoepithelial cells show strong staining for P-Cadherin Figure 3-22. This pattern of staining was maintained in some DCIS ducts but in others there was loss of P-Cadherin. Each case was given a global score of percentage of DCIS ducts positive for P-Cadherin. This showed that DCIS with associated invasion exhibited a greater number of ducts with loss of P-Cadherin staining Figure 3.23.

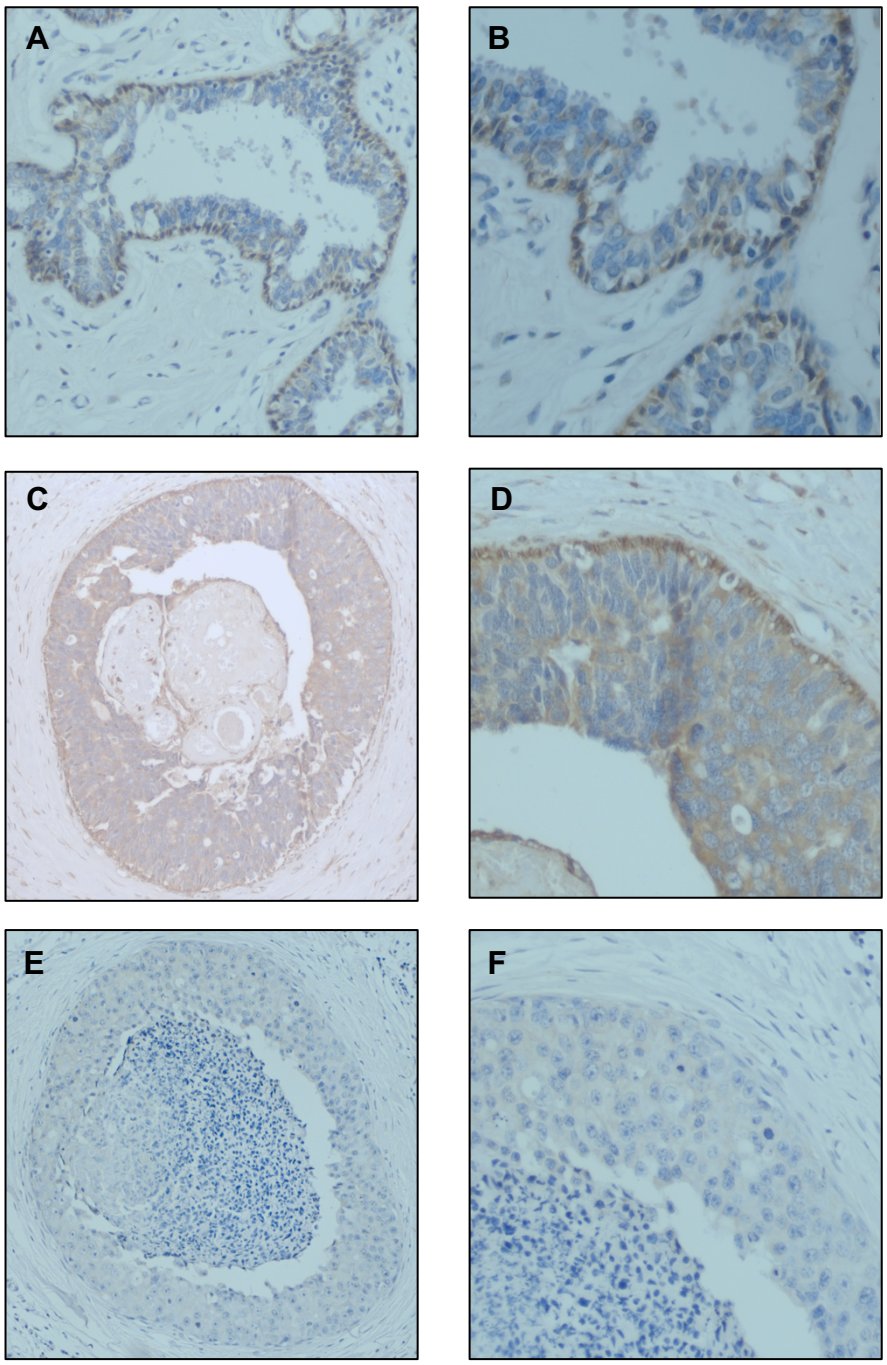

Figure 3-22 P-Cadherin Immunohistochemistry

P-Cadherin staining. Normal breast duct P-Cadherin positive X10 magnification (A), Normal breast duct P-CAD positive X 20 magnification (B), DCIS duct P-Cadherin positive X10 magnification (C), DCIS duct P-Cadherin positive X20 magnification (D), DCIS duct P-Cadherin negative X10 magnification (E), DCIS duct P-Cadherin negative X20 magnification (F).

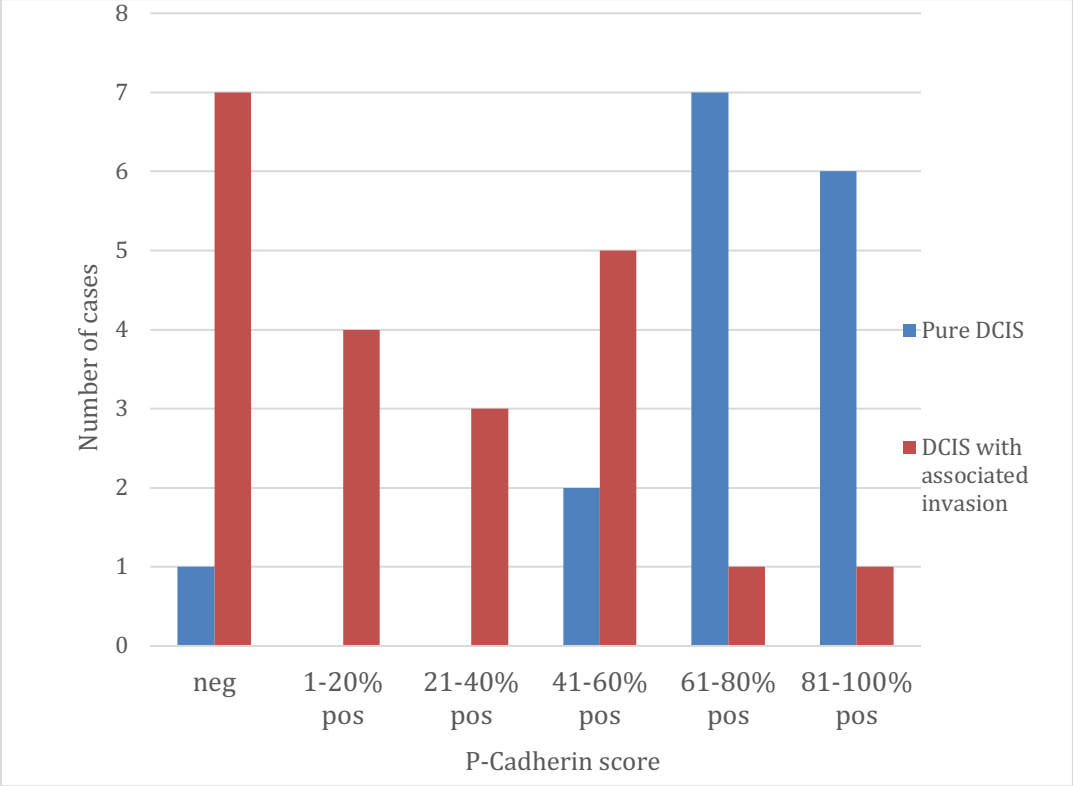

Figure 3-23 P- Cadherin Immunohistochemistry analysis

There is greater loss of P-Cadherin staining in myoepithelial cells in cases where DCIS was associated with an invasive component the difference between the pure DCIS and DCIS with associated invasion is not significant.

3.2.12 Dual staining immunofluorescence- P-Cadherin with desmoglein-3

As shown previously, normal primary myoepithelial cells treated with Galectin-7 siRNA demonstrate a reduction in P-Cadherin localisation at cell-cell junctions (figure 3.21). Immunofluorescence dual staining has been utilised to analyse cell-cell junctions further and the effect of Galectin-7 on these cell-cell interactions. P-Cadherin has been dual stained with ZO-1 and separately with desmoglein-3. Image J was used to quantify P-Cadherin, ZO-1 and desmoglein-3 expression.

Myoepithelial cells from three different patients were used with 3 images analysed from each patient. This was quantified using image J assessing the intensity of P-Cadherin (green) and desmoglein-3 (red). There is a reduction in desmoglein-3 expression in all 3 patients when Galectin-7 is knocked down as shown in Figure 3-24 and Figure 3.25. There is a reduction in ZO-1 in 2 out of 3 patients in the Galectin-7 knock down cells (appendix 6.1), however this staining appears non-specific and the antibody requires further optimisation.

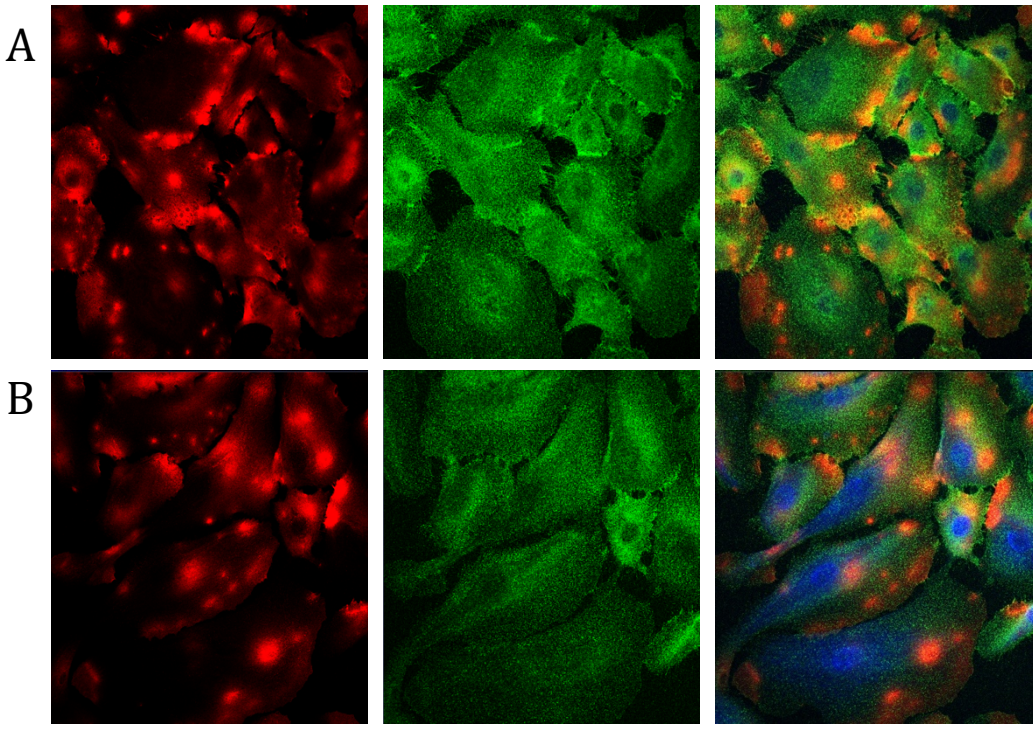

Figure 3-24 Immunofluorescence dual staining for P-Cadherin and desmoglein-3 images.

Immunofluorescence dual staining for P-Cadherin (green) and desmoglein-3 (red). These are representative images from 1 patient. A) Non targeting control myoepithelial cells and B) Galectin-7 knockdown myoepithelial cells

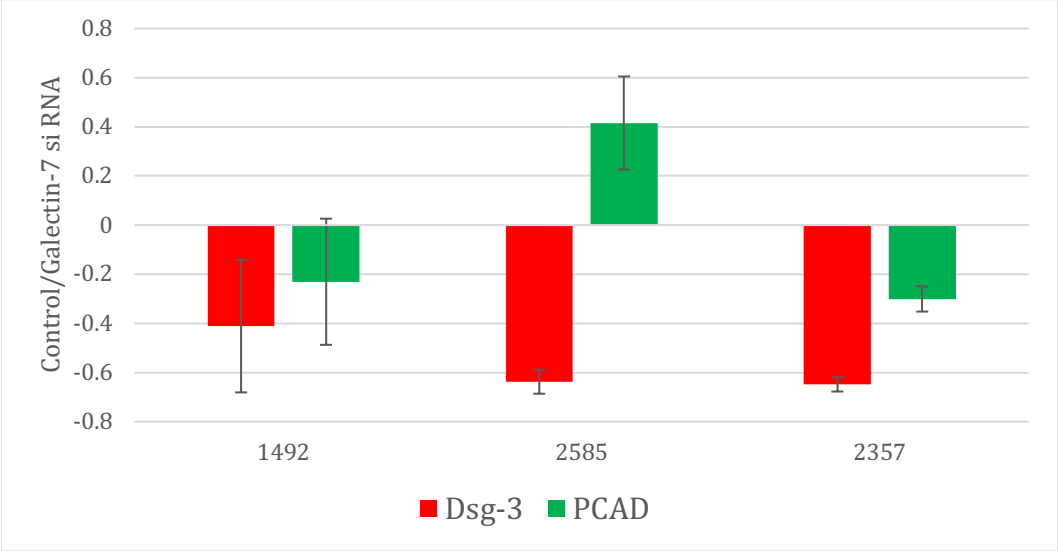

Figure 3-25 Dual immunofluorescence analysis P-Cadherin and desmoglein-3

Ratio of expression of desmoglein-3 and P-Cadherin non-targeting control versus Galectin-7 knockdown myoepithelial cells. This shows that in all 3 patients there is a reduction in in DSG-3 expression. In 1492 and 2357 patients there is a reduction in P-Cadherin in the Galectin-7 knockdown cells. However, in patient 2585 there is an increase in P-Cadherin expression in the Galectin-7 knockdown group.

3.2.13 Migration assays

To assess if Galectin-7 has an effect on myoepithelial cell migration, the N-1089 cell line was transfected with Galectin-7 and normal primary myoepithelial were transfected with Galectin-7 siRNA with appropriate controls as described previously. Subsequently transwell migration assays were performed in triplicate.

After 6 hours incubation the number of migrating cells was determined using the Casy counter and this demonstrated a difference in migration of the N-1089 cells transfected with Galectin-7 to Collagen and Fibronectin compared to vector control, with a mean migration to Collagen of 33.3% and 43.9% for vector control cells and Galectin-7 respectively ($p=0.0021$; Figure 3.26). Similarly, control vector cells and Galectin-7 cells had a mean migration of 35.7% and 46.5% to fibronectin, respectively ($p=0.027$; Figure 3-26).

Experiments knocking down Galectin-7 in primary myoepithelial cells indicate that Galectin-7 had a similar effect on primary cell migration as it does in the cell lines. Non-targeting control siRNA cells and Galectin-7 knockdown cells had a mean migration of 38.2% and 27.7% to Collagen respectively. Non-targeting control cells and Galectin-7 knockdown cells had a mean migration of 60.4% and 48.2% to Fibronectin respectively, and a mean migration of 40.3% and 58.1% to Laminin respectively (figure 3.27). Experiments were performed in technical triplicates, however biological repeats were not performed due to the high cell number required and the finite resource of passage 2 primary myoepithelial cells. While these results were not significant (due to the low number of repeats) the observed trend is the Galectin-7 knockdown cells are less migratory to Collagen and Fibronectin and more migratory to Laminin. This would need to be repeated to assess if the results are significant.

Cell lines

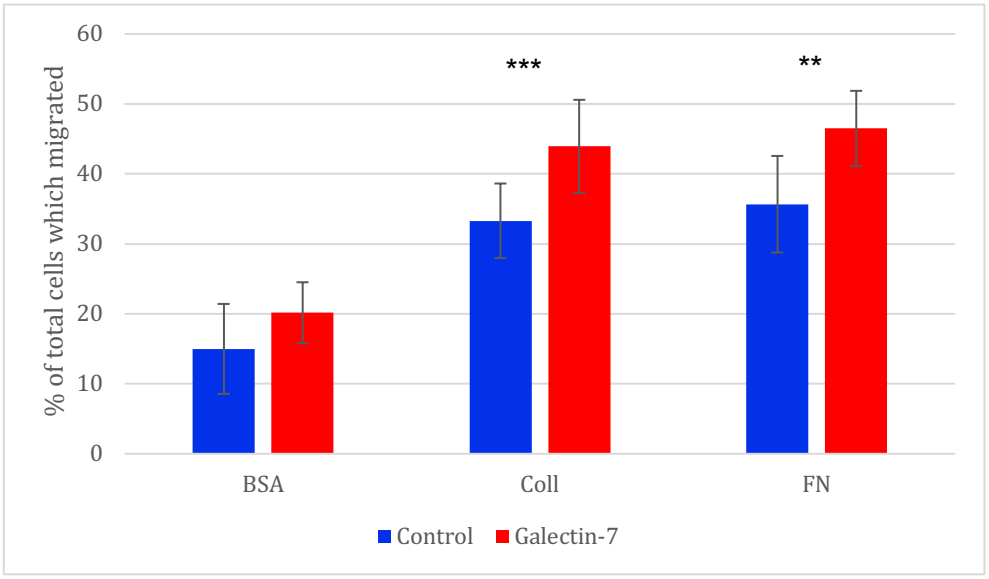

n=3

Figure 3-26 Migration assay with N-1089 cells

Transwell migrations assays. The graphs show the mean migration expressed as percentage of total cells migrated over a 6 hour time period. N-1089 cells transfected with non-targeting control and Galectin-7 vectors. The migration to collagen increased by 10.6% in the Galectin-7 transfected cells vs control cells. The migration to fibronectin increased by 10.8% in the Galectin-7 transfected cells vs control cells. The data was pooled from 3 experiments, error bars show standard deviation.

Primary cells

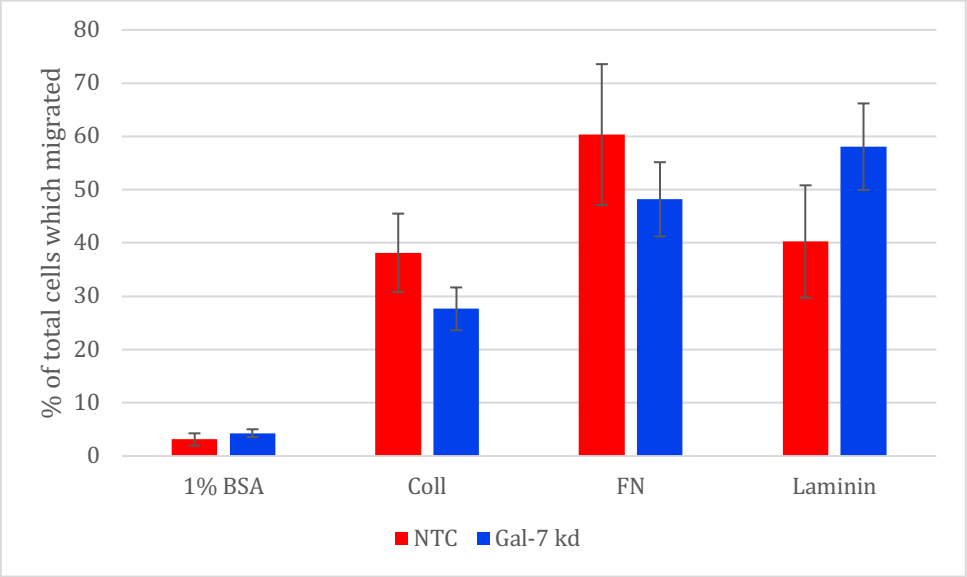

n=1

Figure 3-27 Migration assay with primary myoepithelial cells

Transwell migrations assays. Passage 2 primary myoepithelial cells with Galectin-7 knockdown had an 11% reduction in migration to collagen compared to non-targeting control and 12% reduction in migration to fibronectin Galectin-7 knockdown cells had an 18% increased migration to laminin compared to non-targeting control cells. Difference were not statistically significant; error bars indicate standard deviation.

3.2.14 Effect of Galectin-7 siRNA on myoepithelial cell migration

Scratch assays were used to assess the effect of knocking down Galectin-7 in primary myoepithelial cells on cell migration. Passage 2 primary myoepithelial cells were used from patient 1989. Pictures were taken at 0,10,12,and 14 hours, Image J was used to compare the closure between primary myoepithelial cells treated with non-targeting control siRNA or Galectin-7 siRNA. Galectin-7 siRNA decreased the rate of myoepithelial cell migration compared to non-targeting control siRNA at 16 hours with the percentage closure 46.3% versus 20.7% for siRNA non-targeting control and siRNA to Galectin-7 respectively (p=0.03; Figure 3-28). Closure at 10 and 12 hours showed no significant difference.

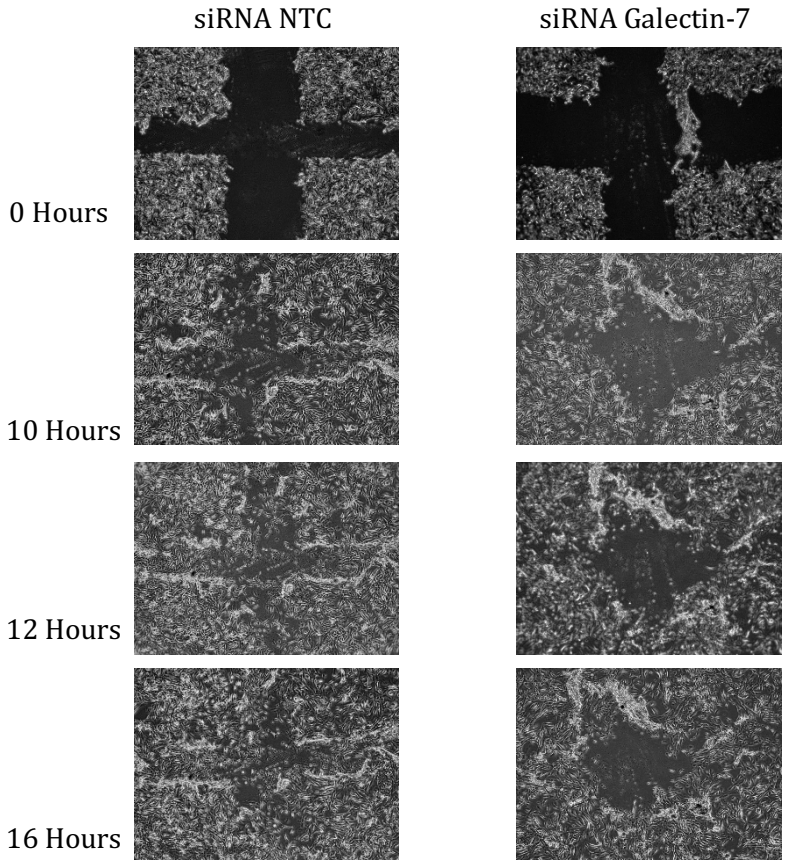

Figure 3-28 Scratch Assay images

Representative images of Scratch assay

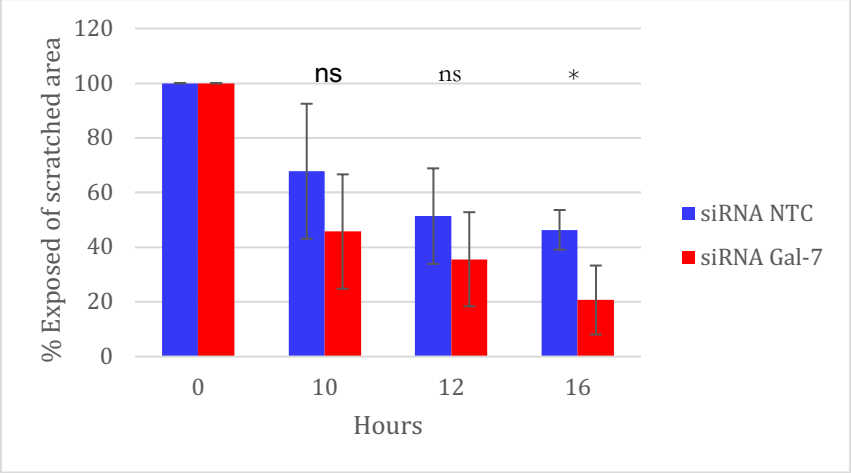

Figure 3-29 Scratch assay analysis

Images at 10 and 12 hours showed a decrease in myoepithelial cell migration in the Galectin-7 knockdown cells however this did not reach statistical significance (p=0.27 and p=0.29 respectively). At 16 hours the difference did reach significance (p=0.03). Representative results are from 3 combined experiments (n=3). T Test was used to calculate p values, error bars represent standard deviation.

3.2.15 Invasion assays

To assess if myoepithelial Galectin-7 has an effect on breast cancer cell invasion, conditioned media (CM) from the primary myoepithelial cells transfected with non-targeting control or Galectin-7 siRNA was added to MDA-MB-231 cells in transwell invasion assays. The MDA-MB-231 cells incubated with CM from Galectin-7 knockdown cells showed 54% less invasion compared to MDA-MB-231 cells treated with CM from non-targeting control cells (figure 3.30). The results were pooled from 3 experiments.

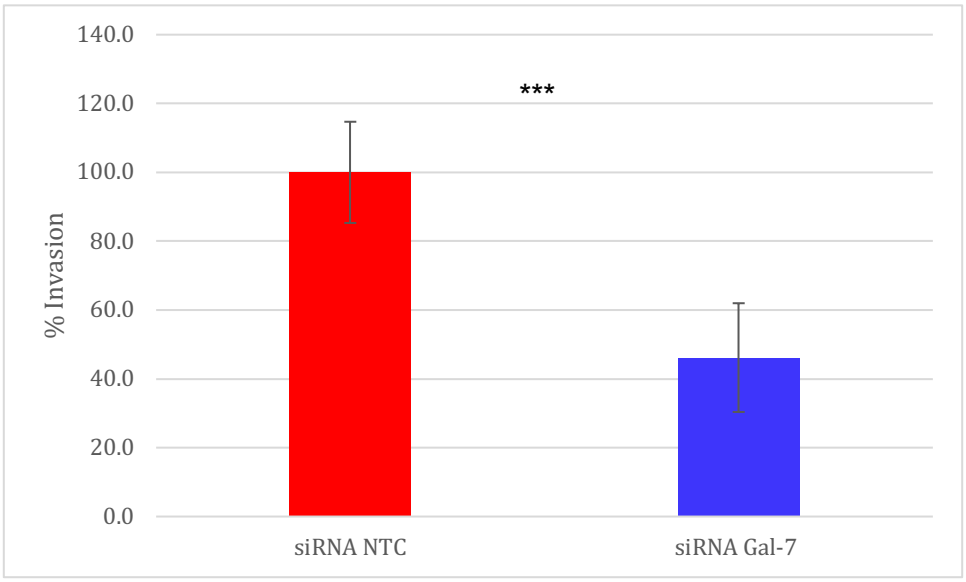

Figure 3-30 Invasion assay analysis with primary myoepithelial cells.

Invasion assay shows 54% reduction in invasion of MDA-MB-231 incubated with conditioned media from Galectin-7 knockdown primary myoepithelial cells compared to MDA-MB-231 incubated with conditioned media from non-targeting control primary myoepithelial cells . T Test was used to calculate p values (<0/001), error bars represent standard deviation

3.2.16 Protease array

The protease array as described in 3.1.17 was used to assess the effect of myoepithelial cell Galectin-7 on expression of a range of proteases. Conditioned media was collected from primary myoepithelial cells treated either with Galectin-7 siRNA or non-targeting control siRNA from 4 different patients. The conditioned media was concentrated as described previously and applied to the protease array membrane. The pixel density of each of the protease array spots was calculated with Image J. The difference in pixel density was calculated by subtracting mean pixel density of Galectin-7 siRNA conditioned media from the mean pixel density with the non-targeting control conditioned media. This was done for each individual primary myoepithelial cell sample, therefore each patient sample (1492,1989,2357 and 2585) are represented by an individual bar

Figure 3-33 represents the changes in concentration of MMP expression on the protease array. A positive result indicates higher levels of MMP in the non-targeting control conditioned media and a negative result indicates higher level of MMP in the Galectin-7 knockdown conditioned media. The non-targeting control conditioned media had a higher concentration of MMP-1, MMP-3, MMP-9, MMP-10, MMP-12 AND MMP-13 compared to the Galectin-7 knockdown conditioned media across all 4 patients. MMP-7 showed the largest difference of all the MMPs in 3 out of the 4 patient samples with higher levels in the non-targeting control conditioned media. Indicating in this model when cells have higher levels of Galectin-7 there is an increase in MMP-7 in the conditioned media.

Figure 3-34 shows higher levels in Kallikreins in control conditioned media: Kallikrein 5 and Kallikrein 10 showed the largest difference with increased concentration in control conditioned media versus Galectin-7 knockdown conditioned media across all 4 patient samples.

Figure 3-35 shows higher levels of Cathespins in the non-targeting control conditioned media compared to Galectin-7 knockdown conditioned media across

all 4 patients, with the highest level in cathepsin B, D, V and X/Z/P. Cathespin B is involved in matrix degradation and cell invasion, high levels of cathepsin D in tumour cells is associated with increased invasion it cleaves fibronectin and laminin. Cathespin V has a role in fibronectin degradation.

Figure 3-36 shows levels of uPA/urokinase in control versus Galectin-7 knockdown cells. In 3 out of 4 patients samples there are higher levels of uPa /urokinase in control conditioned media versus the Galectin-7 knockdown conditioned media. Urokinase is present in the extracellular matrix, this is a plasminogen activator and can subsequently lead to degradation of extracellular matrix and tumour cell migration.

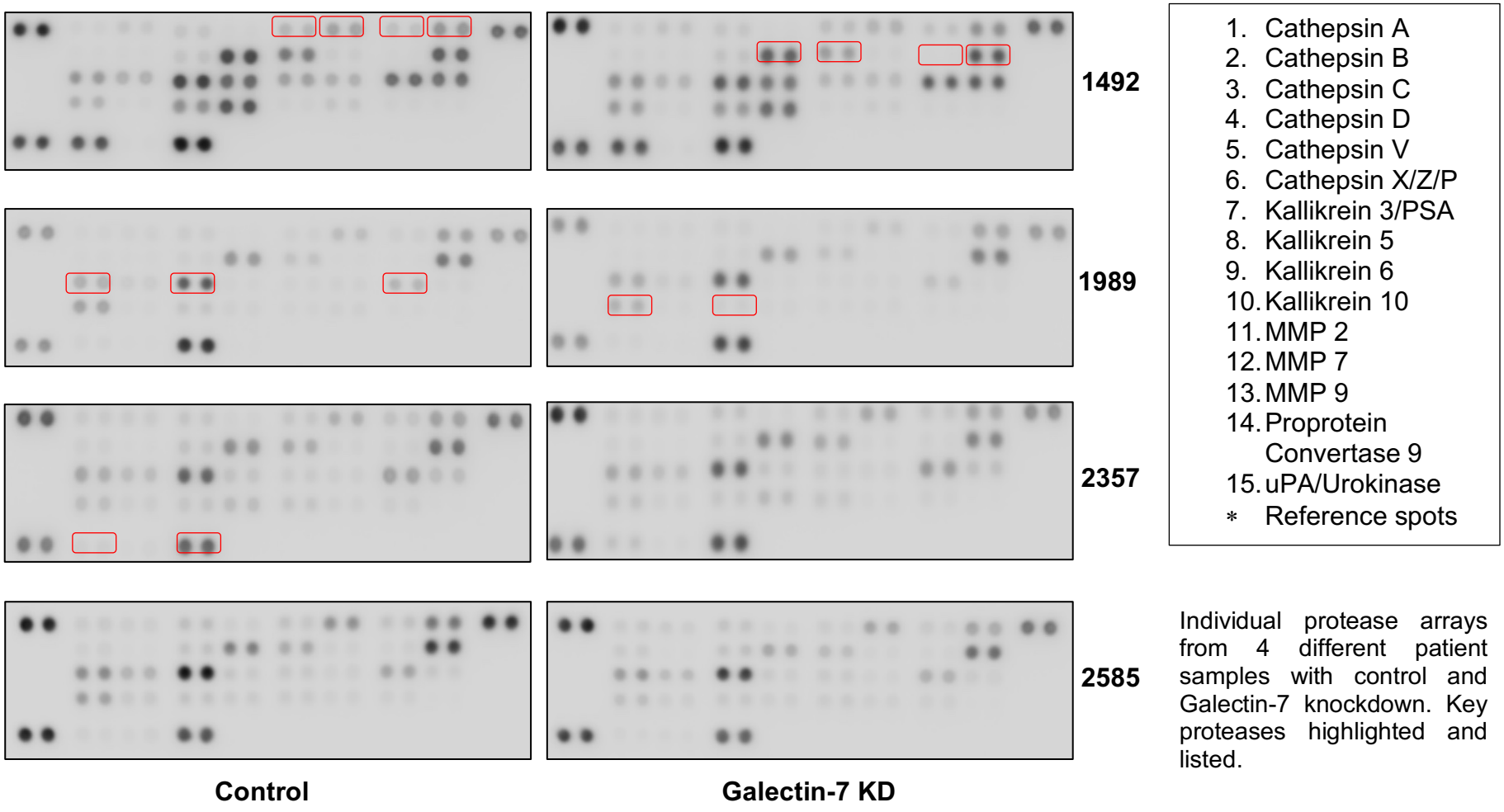

Figure 3-31 Protease Array picture

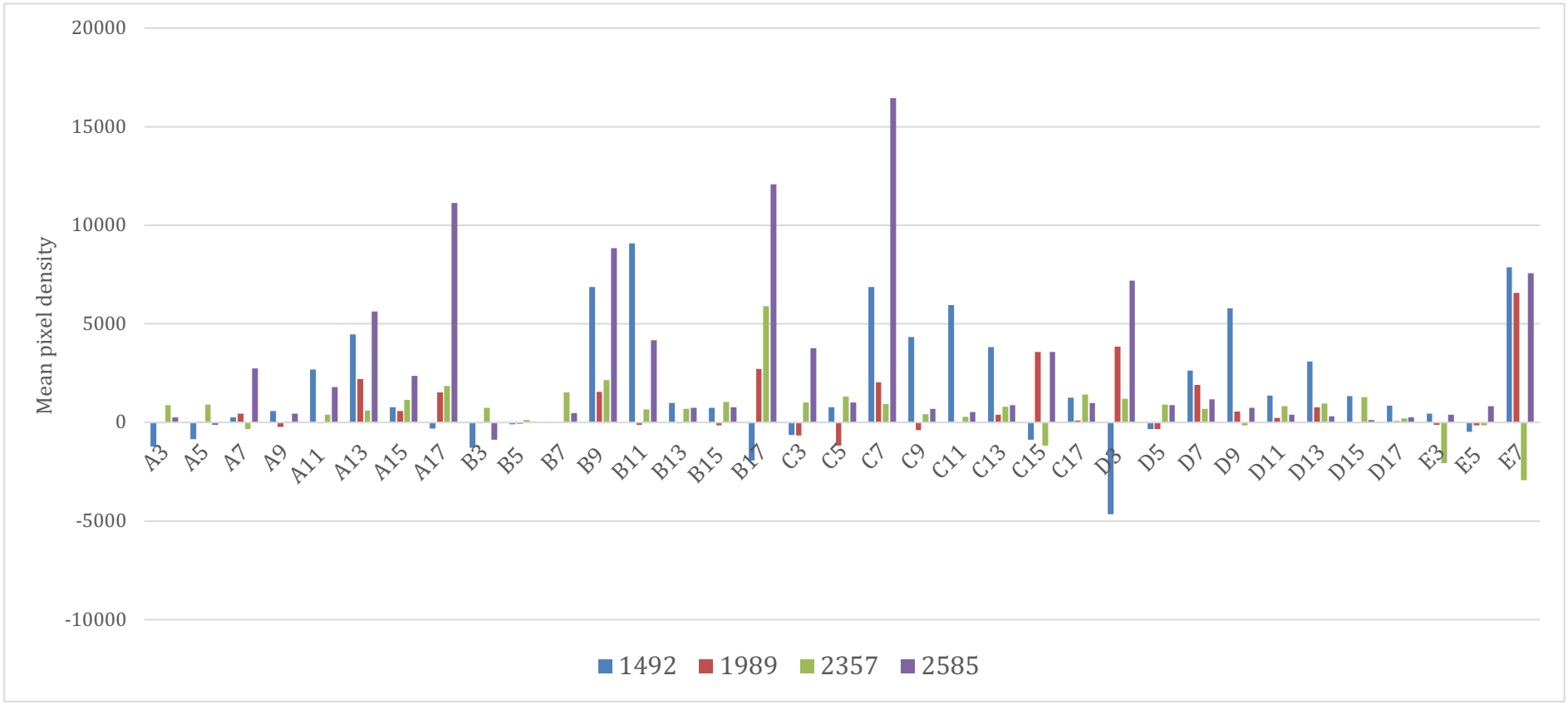

Figure 3-32 Protease array graph of all markers

A graph to show all proteases, each patient is represented by an individual colour, Bars represent mean pixel density of the control conditioned media (CM) minus the mean pixel density of Galectin-7 knockdown conditioned media.

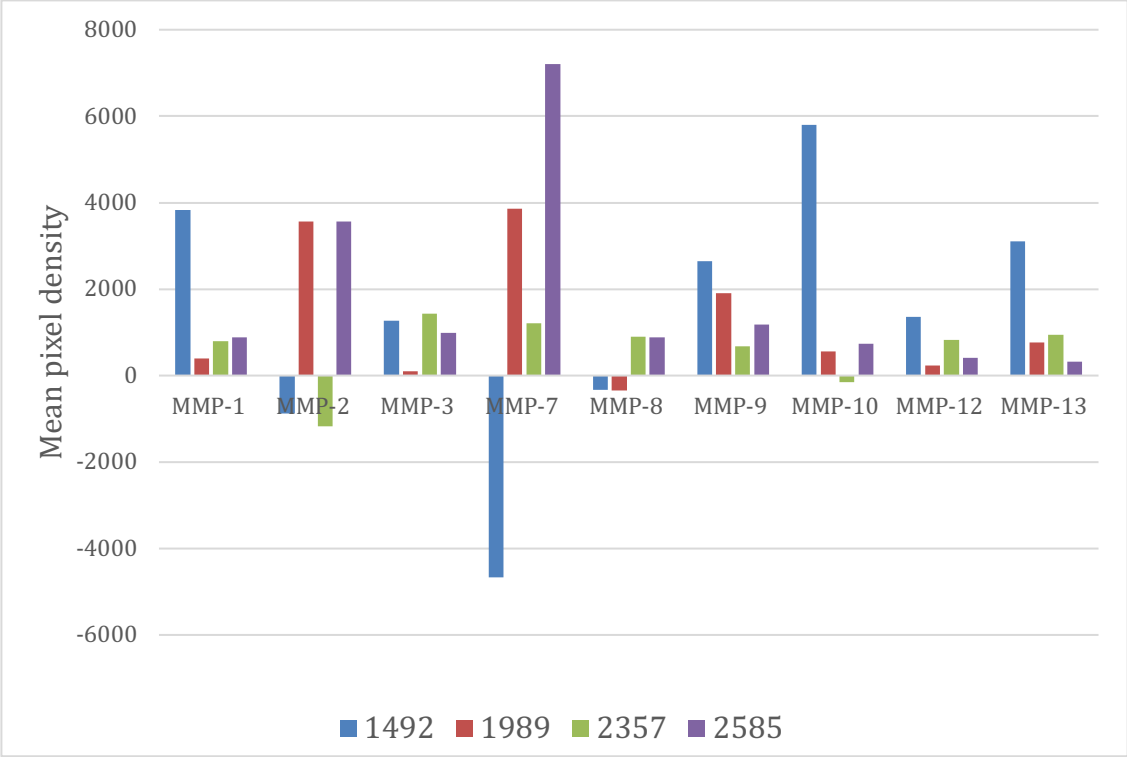

Figure 3-33 Protease array: MMP levels.

Bars represent mean pixel density of the control conditioned media (CM) minus the mean pixel density of Galectin-7 knockdown conditioned media. This, a positive bar represents higher levels in the control CM with a negative bar indicating higher levels in the Galectin-7 knockdown CM. The control conditioned media had higher levels of MMP-1, MMP-3, MMP-9, MMP-10, MMP-12 and MMP-13 compared to the Galectin-7 knockdown conditioned media. MMP-7 showed the largest difference of all the MMPs in 3 out of the 4 patient samples with higher levels in the control conditioned media.

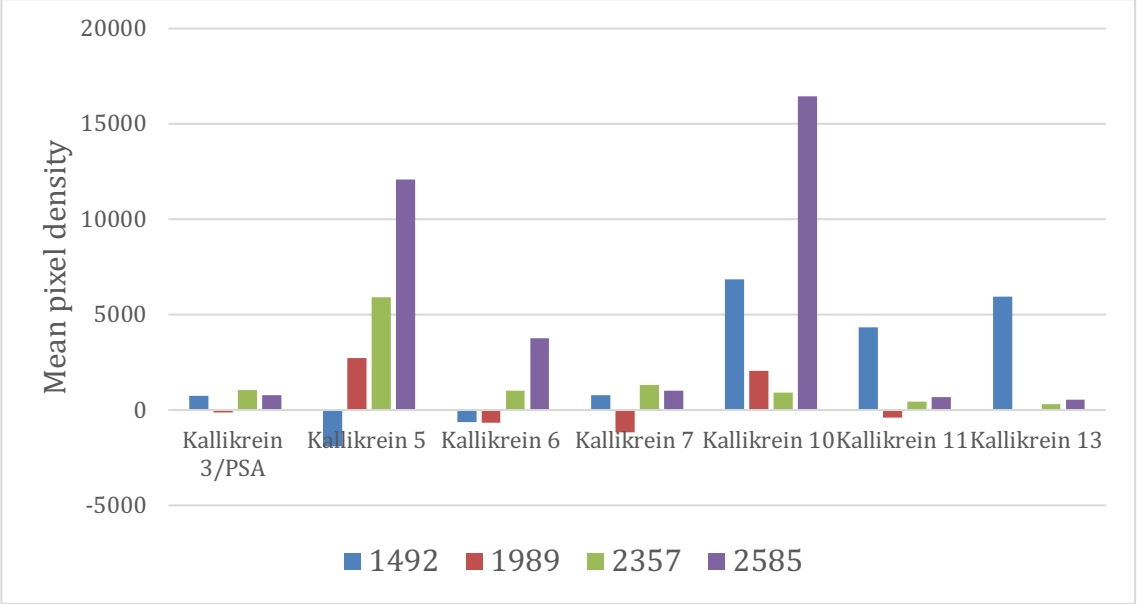

Figure 3-34 Protease array: Kallikreins levels.

Kallikrein 5 and Kallikrein 10 showed the largest difference with increased levels in control conditioned media versus Galectin-7 knockdown conditioned media across all 4 patient samples.

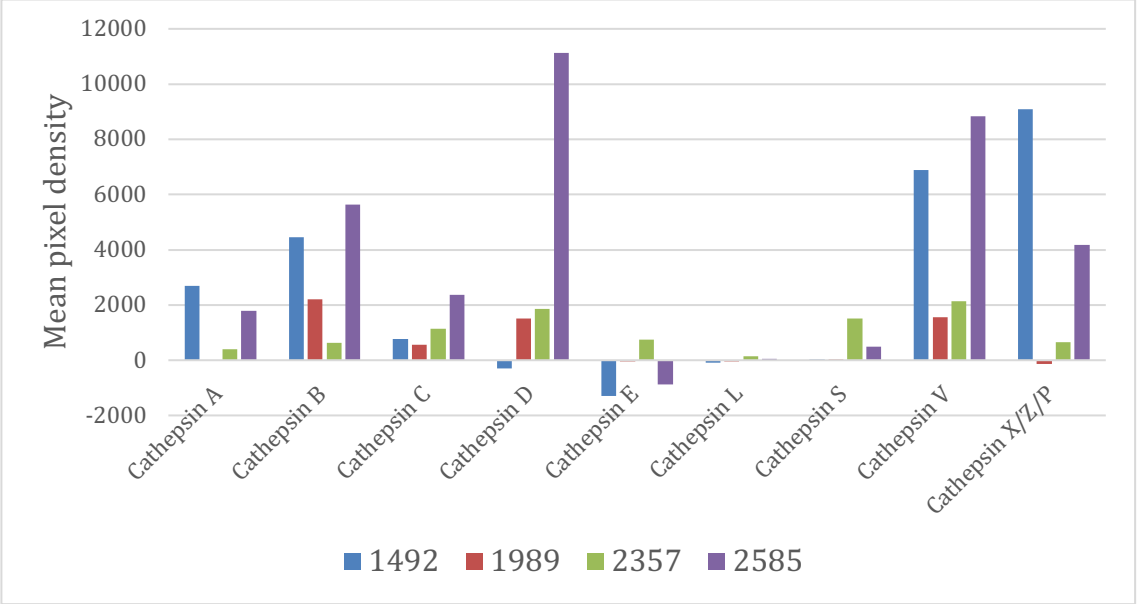

Figure 3-35 Protease array: Cathepsin levels.

The largest differences were increased levels in the control conditioned media in cathepsin B, D, V and X/Z/P compared to Galectin-7 knockdown CM.

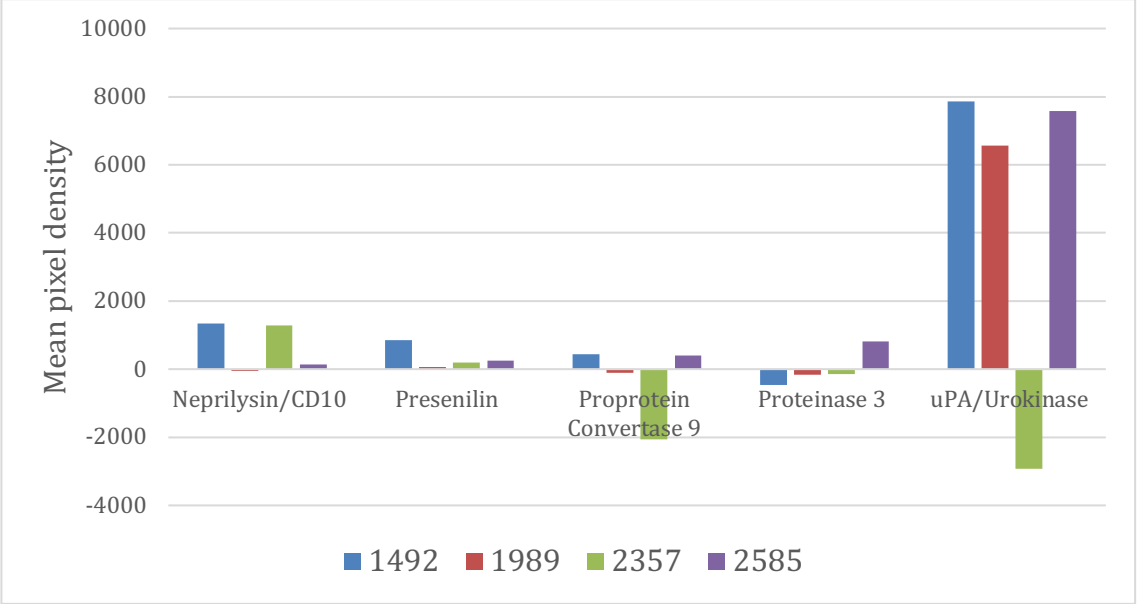

Figure 3-36 Protease array: uPa /urokinase levels.

uPa /urokinase showed a large difference across 3 patient samples with higher levels in control conditioned media versus the Galectin-7 knockdown condition media.

3.2.17 Organotypic Co-Culture Assays

3.2.17.1 Organotypic cultures with primary myoepithelial cells

Organotypic co-culture assays were performed to assess the role of Galectin-7 further using a 3D model rather than 2D. This was performed with both the primary myoepithelial cells and the N-1089 myoepithelial cell line. Immunofluorescence was utilised to assess P-Cadherin in these models as an important cell junction marker. Primary myoepithelial cells are particularly sensitive to changes in conditions and this assay was performed many times in an attempt to optimise the experiment. Figure 3-37 shows representative images of the primary myoepithelial cell organotypic cultures treated either with Galectin-7 siRNA or non-targeting control. The cultures containing non-targeting control myoepithelial cells had more surviving cells indicated by DAPI and this also showed higher levels of P-Cadherin although this may be due to the higher cell number (Figure 3-37). Figure 3-38 is an image of positive control for P-Cadherin using tonsil tissue.

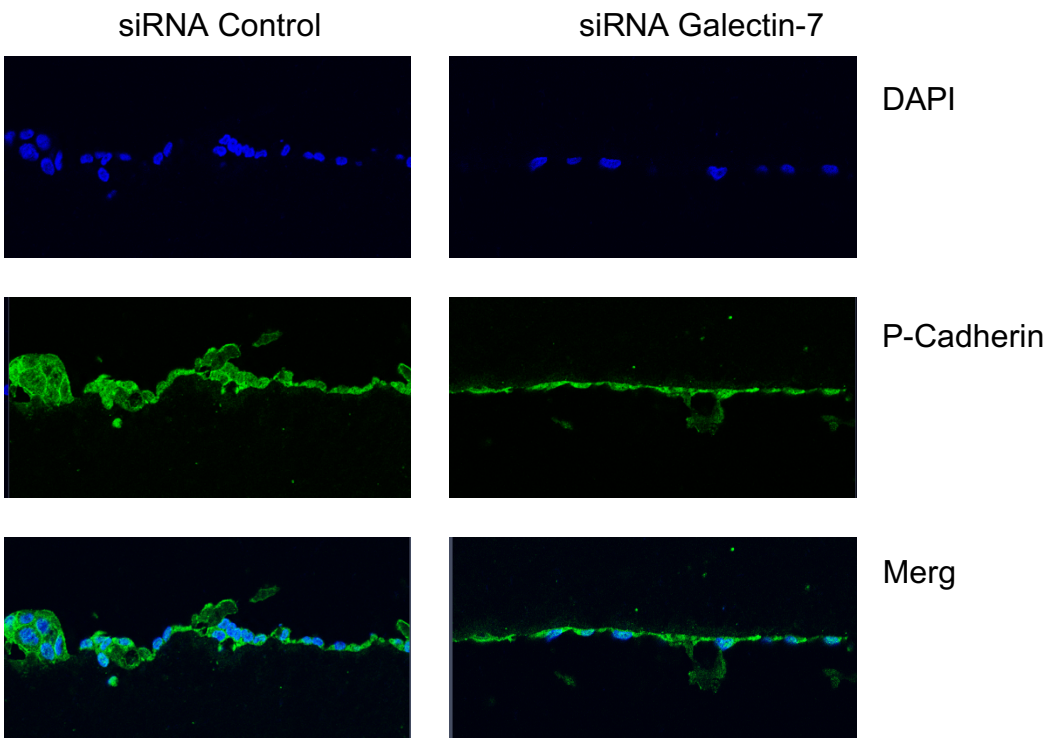

Figure 3-37 Primary Cell Organotypic Cultures.

Organotypic cultures with primary myoepithelial cells treated with either non-targeting control siRNA or Galectin-7 siRNA and stained with P-Cadherin. This shows increased P-Cadherin and number of cells in the control siRNA model. MDA MB 231 breast cancer cells were seeded on day 1.

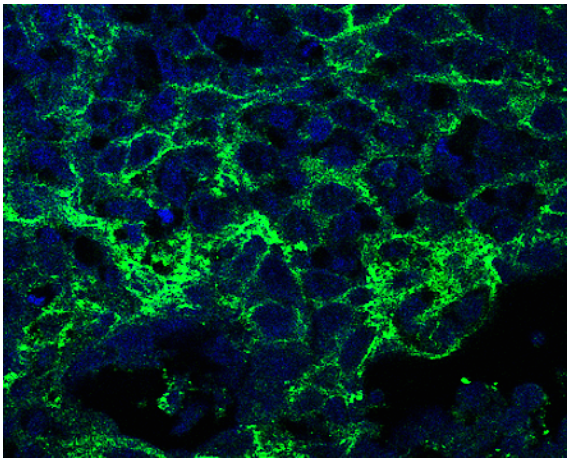

Figure 3-38 Positive control for P-Cadherin immunofluorescence

Tonsil tissue was used as positive control for P-Cadherin

3.2.17.2 Organotypic cultures with N 1089 myoepithelial cell line

The myoepithelial cell line N-1089 was transfected with Galectin-7 vector or control vector and co-cultured with MDA MB 231 cells. In this model the cultures with vector control myoepithelial cells (with lower levels of Galectin-7) exhibit less P-Cadherin staining (Figure 3-39).

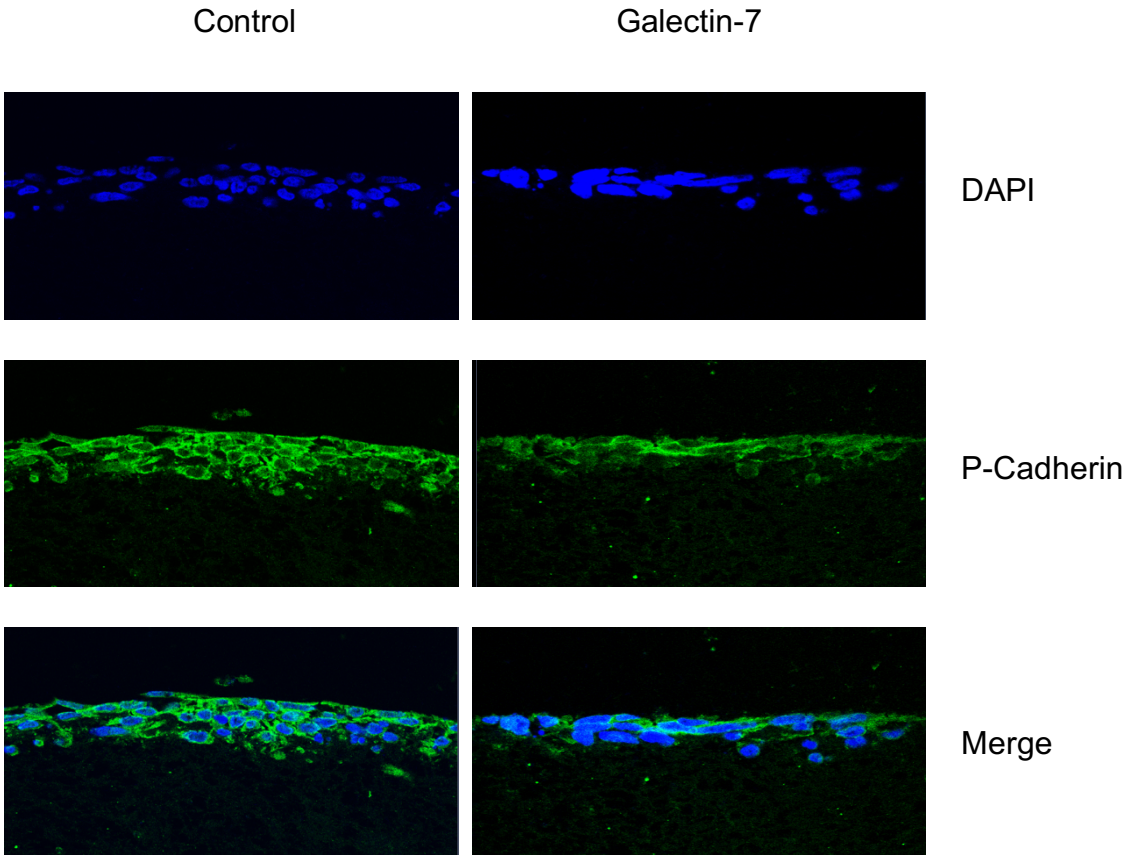

Figure 3-39 Organotypic culture assays with N 1089 myoepithelial cells.

Organotypics with the N-1089 cell transfected with either control plasmid or Galectin-7 plasmid. Sections were stained with P-Cadherin as an assessment of cell-cell adhesion. MDA MB 231 breast cancer cells were seeded on day 1. There appears to be more P-Cadherin in the control vector cultures that those over-expressing Galectin-7.

There is no evidence of invasion of the MDA-MB-231 cells in either the primary myoepithelial cell model or the N-1089 model.

3.3 Discussion

3.3.1 Myoepithelial cell models

In tissues, normal myoepithelial cells express high levels of Galectin-7 with variable loss in DCIS-associated myoepithelial cells. In our laboratory, we have generated cell lines that represent normal (N-1089) and DCIS-altered (β6-1089) myoepithelial cells. These cell lines, together with primary normal myoepithelial cells were used in a series of experiments to explore the functional impact of loss of Galectin-7 in DCIS.

It is essential to characterise any cell population that is being used for in-vitro experiments. Both the myoepithelial cell lines and the primary myoepithelial cells were characterised for expression of a series of myoepithelial and luminal-associated markers. This demonstrated that primary myoepithelial cells had phenotypes consistent with normal myoepithelial cells, however, the cell lines show a drift in phenotype with loss of some myoepithelial cell markers.

Established cell lines are either transformed or immortalised, allowing them to be grown for prolonged periods in vitro. A major advantage is that cell lines can be readily expanded providing ample cells for experiments ,and experimental results are more reproducible, since they employ a homogeneous cell population. However, this is not necessarily representative of the heterogeneity that is evident in patient samples and in clinical practice. It is extremely important to consider these factors when interpreting data from experiments both with primary cells and cell lines. Cell lines are prone to genotypic and phenotypic drift during their continual culture (Burdall, Hanby, Lansdown, & Speirs, 2003). This was highlighted by Osborne and colleagues (Osborne, Hobbs, & Trent, 1987), who demonstrated many discrepancies in the most commonly used breast cancer cell line, namely MCF-7, obtained from different laboratories. Many commonly used breast cancer cell lines are derived from metastasis for example pleural effusion in MCF-7 rather than breast tumour its self (Burdall et al., 2003).

Primary cells are a finite resource and a limited number of passages are possible prior to the cells losing their phenotype. The primary myoepithelial cells used in this project were often grown up to passage 3. Some experiments were performed with passage 2 myoepithelial cells, which are an even more finite recourse. Despite these limitations, the primary cells are considered a strength since they more accurately reflect the in-vivo situation.

Neither of the myoepithelial cell lines was found to express Galectin-7. However, the primary myoepithelial cells retained strong expression. To gain an understanding of the biological role of myoepithelial cell Galectin-7, Galectin-7 was knocked down in the primary cells and was overexpressed in the cell line model.

3.3.2 Galectin-7 in apoptosis

Galectin-7 has previously been reported to play a role in apoptosis (Demers et al., 2010), therefore the effect of altered expression in myoepithelial cells on apoptosis was investigated. Tumour necrosis factor related apoptosis-induced ligand (TRAIL) is a pro-apoptotic ligand, which is expressed by peripheral T lymphocytes (Salehi et al., 2007) including CD4+ve T cells (Sato et al., 2006). DCIS is frequently associated with a periductal immune infiltrate including CD4+ve T cells (M. J. Campbell et al., 2017), therefore, it is plausible that DCIS-associated myoepithelial cells could be physiologically exposed to TRAIL, so TRAIL was used as the pro-apoptotic stimulus in this study. The knockdown of Galectin-7 in primary myoepithelial cells led to enhanced apoptosis on exposure to TRAIL, suggesting that Galectin-7 has an anti-apoptotic role in normal primary myoepithelial cells. However, overexpressing Galectin-7 in both N-1089 and β6-1089 cells led to an increase in apoptosis, as measured by cleaved PARP and cleaved caspase 3. These results appear to directly contradict the findings in the primary cell model and may reflect limitations of the immortalisation process. In

the immortalisation of N-1089 and β6-1089, SV40 large T antigen was used to inactivate the tumour suppressor proteins p53 and Rb, both of which must be inactivated in order for human cells to circumvent cell cycle arrest/apoptosis (Shay, Braester, & Cohen, 1991). Since Galectin-7 is a p53 induced gene, this may be why the N-1089 cells do not endogenously express Galectin-7. Therefore, the immortalised myoepithelial cell lines, which are available to us, are not an ideal model in which to investigate Galectin-7 function. Using cell lines to determine the role of Galectin-7 would not be representative of what is happening in vivo. The cell lines show increased apoptosis with increased Galectin-7 levels, in keeping with Labrie et al, who found overexpression of Galectin-7 sensitised DU-145 prostate cancer cells to apoptosis induced by cisplatin (Labrie et al., 2014). To date, work relating to Galectin-7 in the breast has mainly focused on invasive breast carcinoma. Breast cancer cells expressing high levels of Galectin-7 in the epithelial cells, have an increased ability to metastasise to lungs and bone. Examination of normal and malignant human breast tissue indicated Galectin-7 is expressed in an aggressive breast carcinoma subtype. High levels of Galectin-7 in breast cancer cells render them more resistant to apoptosis, and they metastasise earlier (Demers et al., 2010). It is very possible that Galectin-7 will behave differently in non-malignant cells and given previous discussion it is likely that the primary myoepithelial cells used in these experiments are more representative of the in-vivo situation and should be a gold standard for future work investigating the role of apoptosis in myoepithelial cell loss.

These results suggest that primary myoepithelial cells that have higher levels of Galectin-7 are more resistant to apoptosis. Man et al., have hypothesised that in DCIS progression myoepithelial cells are lost through apoptosis (Man et al, 2007). This data supports the theory that Galectin-7 positivity is a good prognostic sign in DCIS, potentially retaining the myoepithelial cells by preventing their loss through apoptosis.

To assess more global effects of Galectin-7, an apoptosis marker proteome profiler was used to analyse myoepithelial cells with and without TRAIL treatment.

Primary myoepithelial cells from 1 patient were treated either non targeting control siRNA or Galectin-7 siRNA and treated with TRAIL or vehicle only after 48 hours. While using a single sample this might be acceptable with a cell line, given the heterogeneity of primary cells, performing this with samples of more than one patient would have been beneficial, however a decision had already been made to investigate other areas of Galectin-7 function and myoepithelial cells were limited. There was an increase in cleaved caspase-3 in myoepithelial cells following TRAIL treatment, though the effect of change in Galcetin-7 expression was minimal with both control and knockdown myoepithelial cells exhibiting similar effects. However, there was a large increase in catalase levels in the Galectin-7 knockdown TRAIL treated cells.

Catalase is a key antioxidant enzyme which defends against oxidative stress. When cells are exposed to hypoxia there is an increase in reactive oxidative species (ROS). Superoxide dismutases (SODs) are important antioxidant enzymes against reactive oxidant species. The extracellular superoxide dismutase (EC-SOD) is present in the extracellular matrix. Lee et all investigated the role of EC-SOD in the skin using mouse models assessing proteins that were differentially expressed between EC-SOD transgenic mouse and an EC-SOD wild type mouse; Galectin-7 was one of these proteins (J. S. Lee et al., 2012). This study showed the EC-SOD transgenic mouse model had a thinner epidermis than the wild type mouse model. This was due to increased apoptosis in the transgenic model; the transgenic model had higher levels of Galectin-7 (J. S. Lee et al., 2012). Increases in catalase in the TRAIL treated Galectin-7 knockdown cells could potentially indicate that the loss of Galectin-7 increases oxidative stress, resulting in an increase in catalase.

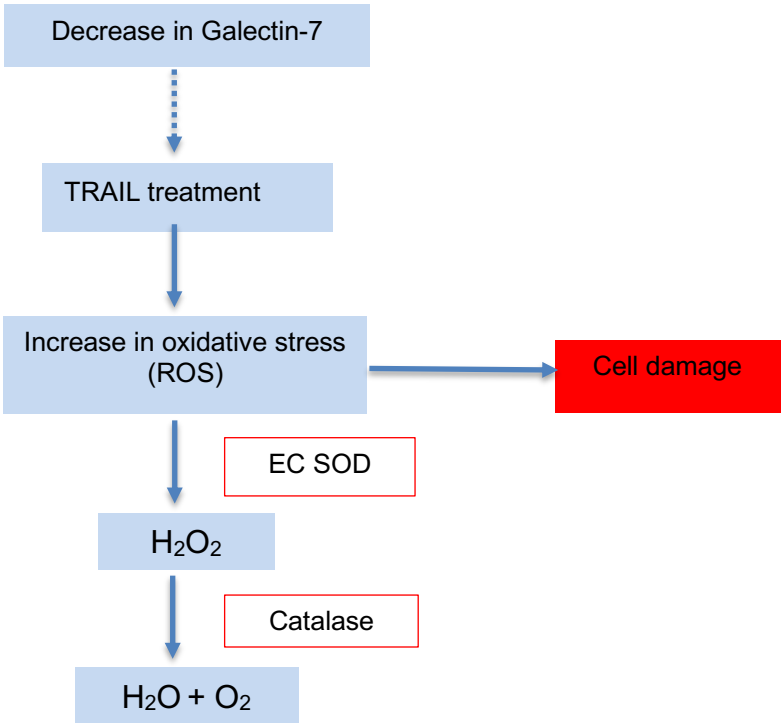

Figure 3-40 Schematic diagram showing the actions and mechanisms of catalase and EC SOD.

This diagram hypothesises from the findings of apoptosis array, in myoepithelial cells that have Galectin-7 knocked down there is an increase in oxidative stress and production of reactive oxidative species (ROS)following TRAIL treatment as a result of this there may either be cell damage or extracellular superoxide dismutase (EC SOD) acts as an important antioxidant defence mechanism with free oxygen radicals being transformed into hydrogen peroxide which in itself can be damaging to cells. Catalase is a second antioxidant enzyme that is recruited to convert hydrogen peroxide to water and oxygen.

To further investigate the role of myoepithelial Galectin-7 in apoptosis, utilising a 3D primary cell model system would be beneficial, to include other components of the microenvironment such as fibroblasts and extracellular matrix.

3.3.3 Adhesion and migration

A major role of myoepithelial cell function is to form the interface with the stromal compartment, where they form stable adhesion with each other and with the basement membrane. It is hypothesised that destabilisation of the myoepithelial-basement membrane interface would involve changes in the adhesive and migratory capacity of myoepithelial cells, and these changes may influence tumour cell invasion. In N-1089 and β6-1089 cell lines, overexpression of Galectin-7 resulted in increased adhesion to fibronectin and collagen I. In primary myoepithelial cells, knockdown of Galectin-7 resulted in decreased adhesion to fibronectin and laminin but increased adhesion to collagen I. Again, the results between the cell lines and primary cells are contradictory, but the primary cells are likely to be more representative. The basement membrane is rich in laminin, whilst collagen I is the major component of the interstitial matrix. The change in adhesion exhibited by Galectin-7 knockdown cells could indicate that Galectin-7 negative myoepithelial cells have preferential binding to the interstitial matrix. Not only would this destabilise the myoepithelial-basement membrane junction, it could also suggest that myoepithelial cells form a leading invasive 'channel' for tumour cells to invade the surrounding stroma. In keeping with this hypothesis, Erik Sahai et al., have shown the importance of the role that stromal cells play in invasion. Cancer associated fibroblasts support cancer invasion creating tracks through which cancer cells migrate (Labernadie et al., 2017). Real time imaging has been used with co-cultures of carcinoma cells and stromal fibroblasts, demonstrating fibroblasts are always the leading cells of invasion in this model. Carcinoma cells move within tracks in the extracellular matrix behind the fibroblasts. Real time imaging would be useful in a DCIS model to investigate the interaction between the myoepithelial cells and fibroblasts (Gaggioli et al., 2007). These adhesion assays suggest that Galectin-7 promotes a more stable to basement membrane related proteins, and thus contributes to the integrity of the myoepithelial- basement membrane barrier.

The immunohistochemical assessment of P-Cadherin in the DCIS tissue samples supports this theory; for DCIS with associated invasion there is associated loss of myoepithelial cell P-Cadherin, in association with loss of Galectin-7. Furthermore, knockdown of Galectin-7 in primary myoepithelial cells leads to reduced cell-cell localisation of P-Cadherin, supporting a relationship between Galectin-7 and cell-cell adhesion, and the integrity of the myoepithelial interface. Paredes et al., showed that P Cadherin was associated with high nuclear grade and ER negativity (Paredes, Milanezi, Viegas, Amendoeira, & Schmitt, 2002). The loss of P-Cadherin in DCIS progression has not previously been published.

Scratch assays were undertaken to assess the effect of Galectin-7 on primary myoepithelial cell migration. Cancer cell migration shows many similarities to the migration seen in wound healing. The role of Galectin-7 in wound healing has been investigated using mouse models. Coa et al., demonstrated upregulation of Galectin-7 in response to corneal injury (Cao et al., 2003). Another study by Gendronneau et al. using Galectin-7 +/+ and -/- mouse models, investigated healing from superficial scratches made on the tails. They showed that wound healing was less efficient in the Galectin-7 -/- mouse (Gendronneau et al., 2008). In the current study, the migration assays show that primary myoepithelial cells with Galectin-7 knockdown migrate less on collagen and fibronectin but show increased migration on laminin. This is consistent with the adhesion assay results. Myoepithelial cells normally exhibit strong adhesion to laminin through $\alpha 6\beta 4$ in hemidesmosomes. However, in would healing models using keratinocytes, it has been shown that $\alpha 6\beta 4$ translocates from hemidesmosomes to focal contacts and mediates migration on laminin (Ozawa et al., 2010). Loss of hemidesmosomes has previously been reported in DCIS (Bergerstrasser et al). Further studies are warranted to establish whether hemidesmosome integrity is modulated by Galectin-7.

3.3.4 Protease arrays

One of the ways in which myoepithelial cells can modulate its microenvironment is through the release of proteolytic enzymes. Up-regulation of αvβ6 in myoepithelial cells leads to TGF-β-dependent up-regulation of MMP-9. To determine whether Galectin-7 influences the proteolytic activity of myoepithelial cells, conditioned media from primary myoepithelial cells with or without knockdown of Galectin-7 was placed onto protease arrays. This demonstrates that knockdown of Galectin-7 in primary myoepithelial cells appears to lead to down-regulation of a series of proteolytic enzymes, including key MMPs, uPa, and cathepsins. This would appear to suggest that Galectin-7 negative myoepithelial cells exhibit an anti-proteolytic phenotype, which seems counterintuitive for a phenotype associated with more progression to invasion. Validation of these results using different approaches, for example qPCR or zymographgy would be important.

Previous work in the lab has indicated that DCIS-associated myoepithelial cells both in-vitro and in tissue studies exhibit elevated levels of MMP-9, and this is critical to their pro-tumourigenic properties. The myoepithelial cells in the studies performed in this thesis were αvβ6-negative. It may be that both acquisition of αvβ6 and loss of Galectin-7 are required for the full pro-tumorigenic phenotype. This would support the notion that the development of a risk stratification DCIS tool would involve a number of markers.

3.3.5 Organotypic co-culture assays

Organotypic cultures represent an alternative method of investigating the role of myoepithelial Galectin-7 and has the advantage of including other important components of the tumour microenvironment. In the primary cell organotypic culture there are less cells in the Galectin-7 knockdown group compared to the non-targeting control, and also lower levels of P-Cadherin expression, though this

was not formally quantified. There may be less cells as myoepithelial cells with lower levels of Galectin-7 are less adherent and could therefore be lost in the assay, however this is speculative and further work is needed to assess if this is significant. Primary myoepithelial cells are extremely sensitive to culture conditions, therefore less cells survive than in the cell line model. For this reason, due to the 14 days required to culture the model, this may have affected the primary myoepithelial cell survival. Invasion of MDA-MB-231 cells was not seen which is unusual in this model system and suggests that the cultures were not fully optimised. Unfortunately, lack of time precluded any further work on these systems. For future work, the use of primary fibroblasts should be considered, particularly from the same patient as the primary myoepithelial cell population, as appropriate cross-talk between the cells may be required to achieve tumour cell invasion.

In conclusion, this series of functional studies has indicated that primary myoepithelial cells are a more physiologically relevant model than the myoepithelial cell lines. These show enhanced apoptosis, increased catalase expression and reduced adhesion to laminin with increased adhesion to collagen I when Galectin-7 is knocked down. In Galectin-7 positive DCIS the myoepithelial cells may be protected from loss by the anti-apoptotic role of Galectin-7 and the increased adhesion to laminin.

4 Global Analysis of Effect of Galectin-7 on Myoepithelial Cells using RNA sequencing

4.1 Materials and methods

4.1.1 Patient Selection

Normal primary myoepithelial cells isolated from reduction mammoplasty were used from four different patients. The sample IDs were 127, 1492, 2858, and 2357. The cells were seeded on collagen-coated 6 well plates in HuMec Medium (see section 3.1.5). When they reached 60% confluency, siRNA treatments for non-targeting control and Galectin-7 was added as per method 3.1.7. After 48 hours cells were typsinised and centrifuged at 1200rpm for 3 minutes.

4.1.2 RNA extraction

RNA was extracted from the cell pellets using the RNeasy Plus Mini kit (QIAGEN, 74136) using a slight modification of the manufacturer's protocol. The pelleted cells were re-suspended and lysed using 600 µl buffer RLT Plus plus 10 µl β-mercaptoethanol per 1ml buffer, followed by vigorous vortexing. The lysate was transferred to a gDNA Eliminator spin column, placed in a 2ml collection tube, and centrifuged for 60 seconds at 10,000 rpm (8000g). 1 volume (600 µl) of 70 % ETOH was added to the column eluate, mixed thoroughly by pipetting and transferred to an RNeasy spin column, placed in a 2 ml collection tube and centrifuged for 15 seconds at 10,000 rpm. The column was transferred to a new 2ml collection tube and 700 µl Buffer RW1 was added to the RNeasy column (which was gently inverted a couple of times to ensure thorough mixing) and centrifuged as above to wash the column. This procedure was repeated using 500 µl buffer RPE, the column was placed in a fresh 2ml collection tube and centrifuged at 10000 rpm. The spin column was transferred to a new 2 ml collection tube and, with the lid open, centrifuged at full speed for 2 minutes. The spin column was placed in a new 1.5 ml collection tube. 35µl of warmed RNase - free water was then added directly to the centre of the silica gel membrane in the

spin column. The samples were left to sit at room temperature for 5 minutes and then centrifuged at 10000 rpm for 60 seconds to recover the RNA. Eluted RNA was placed immediately on wet ice to allow for aliquots to be taken for QC. Stock RNA was then stored at -80C. RNA concentration was quantified using the Qubit ® Fluorometer in conjunction with the Qubit ® RNA HS (High Sensitivity) Assay Kit. Sample purity was measured by A260 spectrophotometry using the Nanodrop. RNA integrity was ascertained using the Agilent 2100 Bioanalyser (Agilent Technologies) in coordination with RNA 6000 Pico Kit (Agilent Technologies)

4.1.3 Bioinformatics Analysis

Bioinformatics analysis was performed by Dr E Gadaleta, Dr A Nagano and Professor C Chelala, Bioinformatics Group, Centre for Molecular Oncology, Barts Cancer Institute, London, UK. Raw data reads were aligned uniquely on the hg38 gene feature. The percentage of reads used for gene quantification was ~60%. The samples were sent in 2 separate batches and common differential gene expression was analysed across both batches.

4.1.4 Validation of RNA sequencing

In order to validate the results from the RNA sequencing data a combination of immunohistochemistry and qPCR was performed. The most relevant genes and those having the most translational promise with regards to the role of the myoepithelial cells in DCIS progression were selected.

The immunohistochemistry analysis of LOX was undertaken on the DCIS patient cohort. The LOX antibody was optimised and then used in patient samples, each patient sample was stained twice with the same antibody. This is not discussed in the main body of the thesis as the results have wide variance in the same case therefore it was decided these data could not be reliably interpreted . LOX is an important protein to investigate further and this work will be continued.

The technique of qPCR was used to validate 3 genes that were upregulated and 3 genes that were downregulated in Galectin-7 knockdown myoepithelial cells. The same 4 patients were used.

4.1.5 qPCR-Isolation of RNA

Residual RNA from the same samples that were submitted for RNA sequencing were used for validation and extracted as previously described (4.2).

4.1.6 qPCR- Synthesis of cDNA

cDNA was obtained by reverse transcription (RT). To initiate RT, 1µL of 50ng/µL hexanucleotide primers (Sigma, H0268) and 1µL of 10 mM deoxynucleotide (dNTPs, Sigma, GE28-4065-57) are added to 1µL of 50ng mRNA with 7µL of nuclease-free dH2O (HyClone, SH30538.02) to give a total volume of 10µL per reaction. The reaction was performed with the following conditions: 70^{o}C for 10 minutes, followed by 4^{o}C for 5 minutes in a Mastercycler Polymerase Chain Reaction (PCR) system (Eppendorf). To synthesise cDNA from the RNA-DNA hybrid by polymerisation, 1µL of Moloney-murine leukaemia virus (M-MLV) reverse transcriptase enzyme and 2µL of M-MLV buffer (Sigma, M1302) was added to the initial reaction mix with 7µL of nuclease-free deionized water to give a final volume of 20µL per reaction. The reaction was performed with the following conditions: 22^{o}C for 10 minutes, 37^{o}C for 50 minutes and 90^{o}C for 10 min. cDNA was kept at 4^{o}C until required.

4.1.7 qPCR

Taqman primers were used for 6 genes to validate the RNA sequencing work. The primers used were from Thermo Fisher and the selected genes were: NT5E (ref Hs00159686_m1), CDH11 (ref Hs00901473_g1), LOX (ref Hs00942480_m1), GPER1 (ref Hs01922715_s1), PDGFD (refHs00228671_m1),

MAP3K12 (ref Hs00951240_m1). For housekeeping 18S Primers were used (ref Hs03003631_g1). A typical reaction was as follows; 10 ul of TaqMan Master Mix 20x (4331182), 1ul Taqman Primer/Probe (FAM), 1ul Housekeeping Primer/Probe (VIC), 7ul dH2O, 1ul cDNA. Each reaction was performed in triplicate. The mixture with the relevant taqman probe and cDNA for control and Galectin -7 knockdown from 4 different patients were added to a 96 well plate. A 'no template' control was also set up to check for contamination.

The change in gene expression was then calculated by the change in cycle threshold (dCT), determined by subtracting the average CT for the reference gene (18S) from the average CT of the target gene. The change in dCT of control samples was then subtracted from the change in dCT of the Galectin-7 knockdown samples (ddCT), this value was then introduced to the formula 2^{-ddCt} to give the relative expression, where a value of 1 is no change, higher than 1 is up-regulation and less than 1 is down-regulation of a gene.

4.1.8 Immunohistochemistry validation of GPER and NT5E

For validation of the RNA sequencing results immunohistochemistry was also used, with tonsil tissue used for optimisation. The method used was the same as the method described in section 2.1. Sections were heated at 60°C for 10 minutes, and incubated serially in xylene (Fisher Scientific, X5-1) for 2 x 5 minutes then in decreasing alcohol dilutions and $_dH_2O$ after which endogenous peroxidase was blocked with a 10-minute incubation in 100% methanol/0.9% hydrogen peroxide. Antigen retrieval was performed using boiling citrate buffer at pH 6.0 for 8 minutes. Sections were blocked with appropriate serum (depending on the secondary antibody used) and 3% BSA/PBS, for 15 minutes, then GPER (Cambridge bioscience HPA027052) or NT5E (Cambridge bioscience HPA02705217357) primary antibodies were applied. The incubation for all primary antibodies was 4°C overnight as this gave optimal results.

Following incubation, sections were then washed with PBS in triplicate followed by incubation with the rabbit secondary antibody at room temperature for 40 minutes. The sections were then washed again in triplicate followed by incubation with an avidin-biotin peroxidase complex (ABC) reagent (Vectastatin ABC Kit, Vecor Laboratories PK Rabbit 6101,) for 30 minutes at room temperature. Sections were washed again in triplicate with PBS before developing using a DAB kit (Vectastain, Vector Laboratories SK 4100) and then counterstained with Haematoxylin for 2 minutes (Sigma, MHS16). The sections were washed with tap water and dehydrated through graded alcohols and xylene, and mounted with DPX (Sigma, 06522) and glass cover slips.

4.2 Results

4.2.1 Analysis of gene expression

14401 genes were filtered to show differential expression analysis. A principle component analysis (PCA) plot was constructed to visualise the difference in gene expression between patients, and between control and knockdown of Galectin-7.

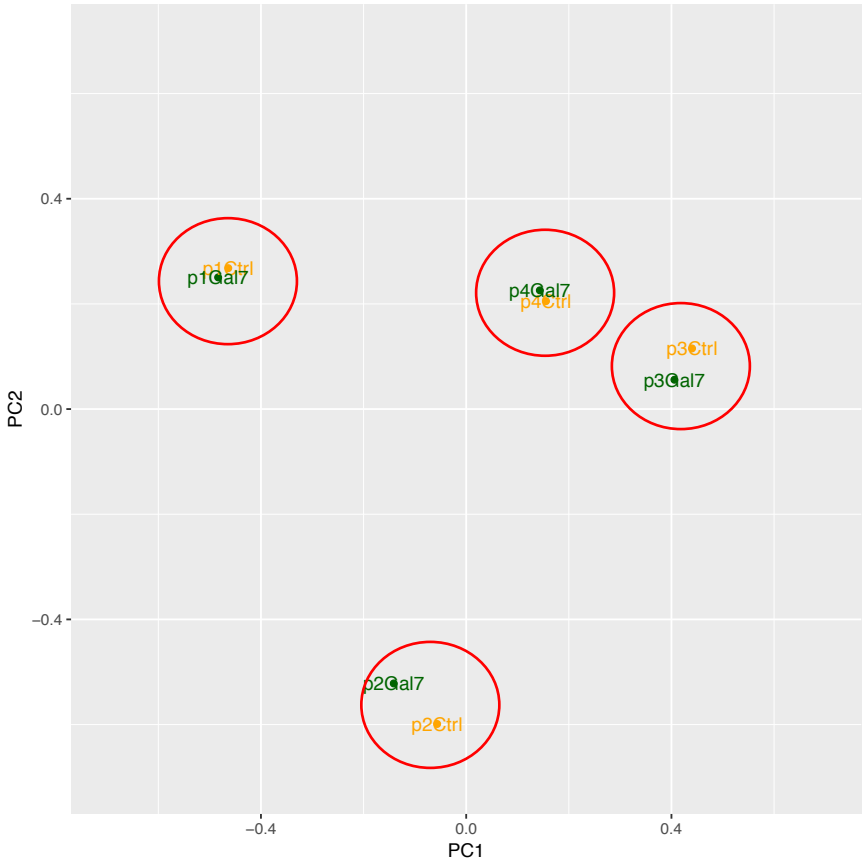

Figure 4-1 PCA plot

PCA plot shows the overall gene expression of the four patient samples with control (orange) and Galectin-7 knock down (green) treatment. The plot shows heterogeneity in baseline gene expression between patients. Each circle contains samples from individual patients.

The RNA sequencing was sent in 2 batches therefore 2 heat maps were constructed (figure 4.2 and 4.3) The left 2 columns (orange) represent non-targeting control and the right 2 columns (blue) represent Galectin-7 knockdown (blue).

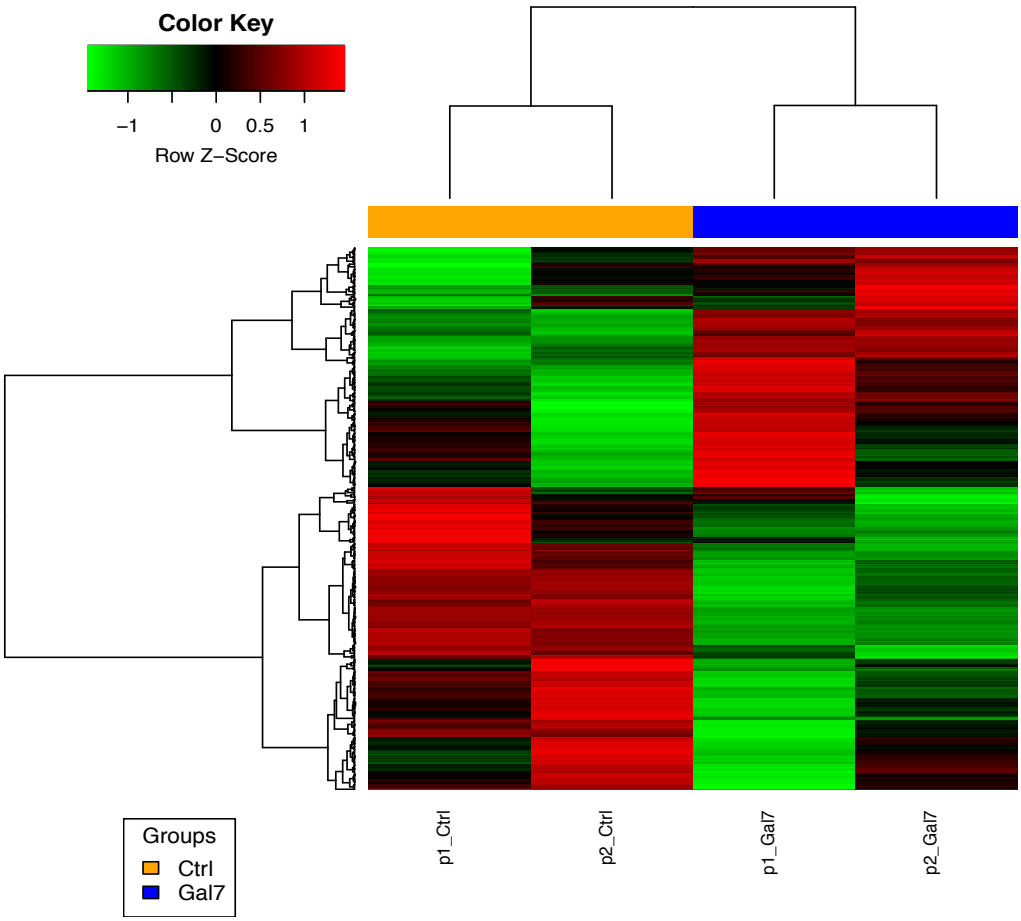

Figure 4-2 Batch 1 heat map

Batch 1 heat map showing differential expression in 417 genes, 184 genes were upregulated in Gal7 knockdown cells; 233 genes were upregulated in Ctrl cell. LGALS7 (Galactin-7) is confirmed as down-regulated in Gal7 samples. Orange represents non-targeting control and blue represents Galectin-7 knockdown.

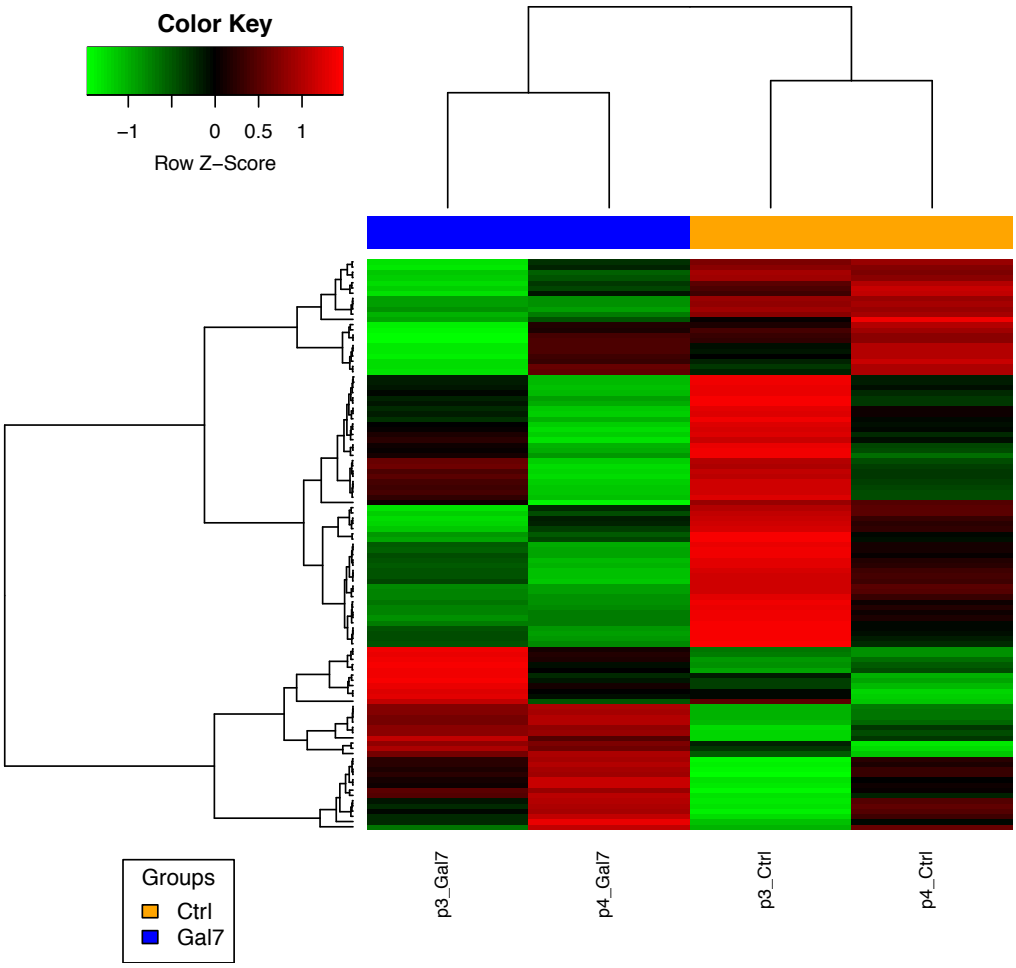

Figure 4-3 Batch 2 heat map

Batch 2 heat map showing differential expression in 109 genes, 35 genes were upregulated in Gal7 knockdown cells; 74 genes were upregulated in Ctrl cells. LGALS7 (Galactin-7) is confirmed as down-regulated in Gal7 samples. Orange represents non-targeting control and blue represents Galectin-7 knockdown.

A Venn diagram (figure 4.4) was used to demonstrate the cross-over between patients of the top 500 differentially expressed genes seen with knockdown of Galectin-7. Each patient P1, P2, P3 and P4 is identifiable by a colour. There ware 16 genes that show consistent changes in all 4 patients. Given the intrinsic variation between patients when using primary cells it is important to acknowledge that there may also be relevant changes in fewer than all patients that still merit further investigation.

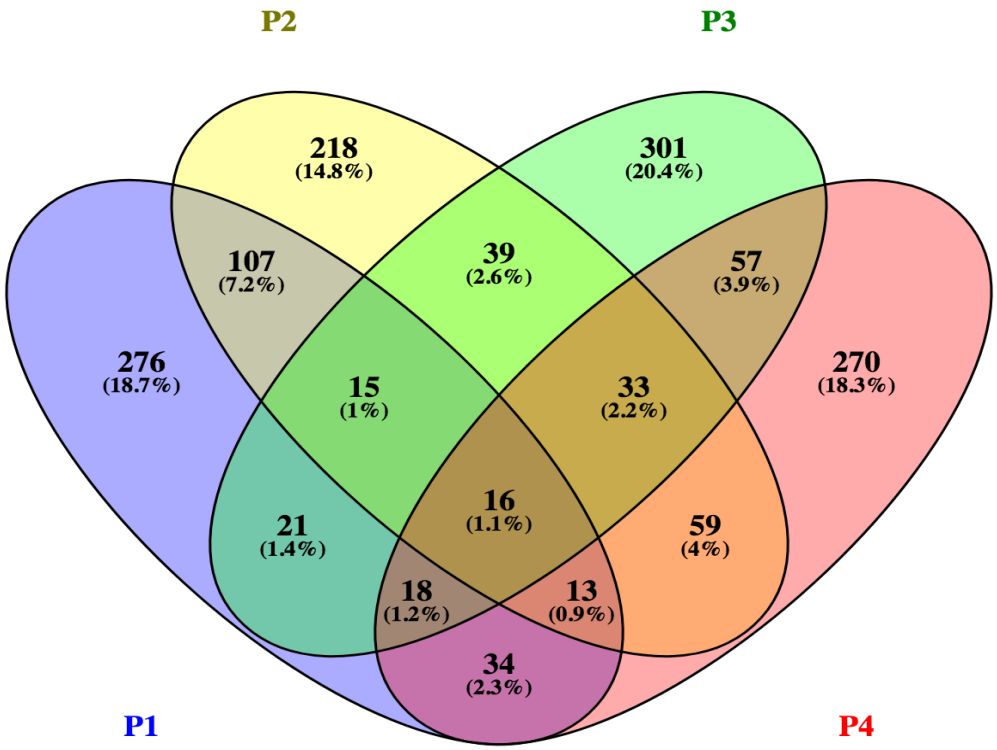

Figure 4-4 Venn chart show the overlap of the top 500 genes

Venn chart illustrates the number and percentage of genes which have an overlap of differential gene expression between patients. There 16 genes which have a common differential gene expression across all 4 patient samples when comparing control to Galectin-7 knockdown.

A multidimensional scaling plot is used to visualise the common genes that are most upregulated and down regulated in the Galectin-7 knockdown samples versus the control samples across all 4 patients.

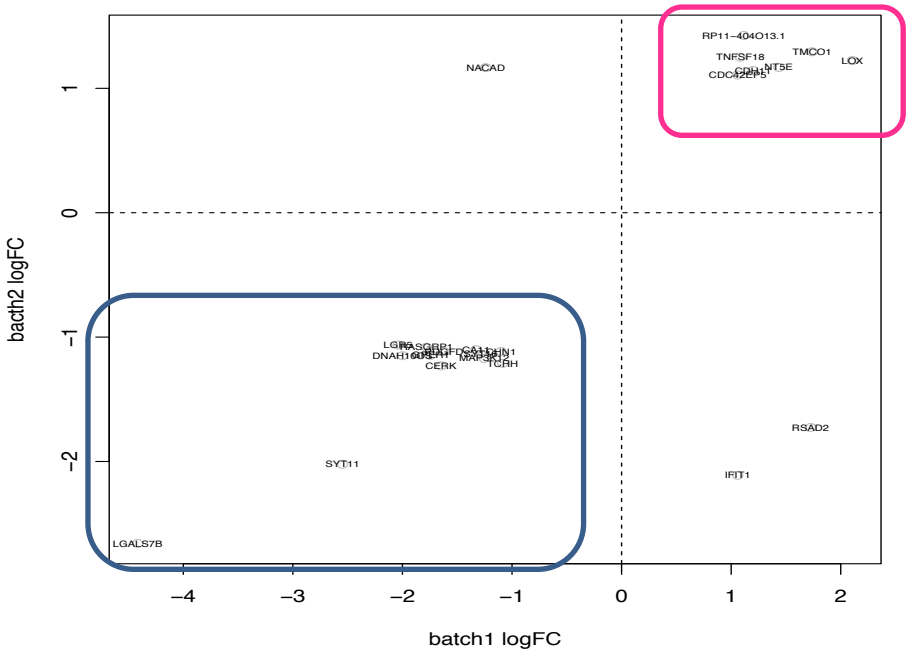

Down-regulated in siRNA Gal7

LGALS7B
SYT11
LGR5
DNAH10OS
RASGRP1
GPER1
CERK
PDGFD
CA11
SYT16
MAP3K12
CHN1
TCHH

Up-regulated in siRNA Gal7

CDC42EP5
TNFSF18
RP11-404O13.1
CDH11
NT5E
TMCO1
LOX

Figure 4-5 Multidimensional scaling plot of global gene expression

This plot shows the most down regulated and upregulated genes which were common across all 4 patients.

4.2.2 qPCR

A heat map was used to demonstrate the qPCR data. The Galectin-7 knockdown cells were compared to non-targeting control cells to assess if there was an increase or decrease in the genes selected as a validation set. Each of the 4 patients has been represented in the table separately. Across the experiment the patient sample 2585 showed large variation in results, possibly due to degradation of RNA quality, as this variation was also seen in the 18S (housekeeping gene). The table is colour coded, with green representing a decrease, red an increase, and grey where there were not enough data points for robust interpretation (Table 4.1). The qPCR data has shown in 2 of 4 patients that CDH11 was upregulated in the Galectin-7 knockdown samples compared to the control samples, 1 of 4 was down regulated, and 1 was not interpretable. In 2 of 4 patients LOX was upregulated in the Galectin-7 knockdown samples and 2 of 4 was down regulated. In 3 of 4 patients NT5E was upregulated in the Galectin-7 knockdown samples and 1 of 4 was down regulated. In 2 of 4 patients GPER was upregulated in the Galectin-7 knockdown samples and 2 of 4 was down regulated. In 3 of 4 patients PDGFD was downregulated in the Galectin-7 knockdown samples and 1 out of 4 was upregulated. In 2 of 4 patients MAP3K12 was downregulated in the Galectin-7 knockdown samples and 1 of 4 was upregulated, and 1 was not interpretable.

RNA sequencing results	UP	UP	UP	Down	Down	Down
Gene	CDH11	LOX	NT5E	GPER1	PDGFD	MAP3K12
Patient						
127	1.160692	0.087635	2.126501	10.88208	0.038022	31.25364
1492	0.104127	0.025317	6.483296	0.57805	0.11715	0.602531
2357	2.4069	2.745192	4.264556	1207.52	59.99287	0.505454
2585	0.160909	239.7238	0.310618	0.004079	0.231797	-

Table 4-1 qPCR results

Demonstrates qPCR validation of RNA sequencing. The red represents an up-regulation in Galectin-7 knockdown RNA compared to the non-targeting control RNA and green represents down-regulation in Galectin-7 knockdown RNA compared to the non-targeting control RNA. Each patient sample is analysed individually, in technical triplicate and the experiment was performed twice.

4.2.3 Immunohistochemistry validation of GPER and NT5E

For immunohistochemical validation of the RNA sequencing tonsil tissue was used to optimise the antibodies as shown in figure 4.6. Sections were chosen from the DCIS cohort dependent on their Galectin-7 status. Table 4.2 shows patients from the DCIS cohort, which were either Galectin-7 positive or Galectin-7 negative.

Despite optimisation, the staining for the NT5E was not interpretable on the DCIS sections and time limitations meant this could not be repeated.

Interpretation of GPER staining also was not straightforward and as analysed there does not appear to be a correlation between Galectin-7 positivity and GPER status. Some sections did not show DCIS as these were from deeper within the block and had evidently 'cut through'.

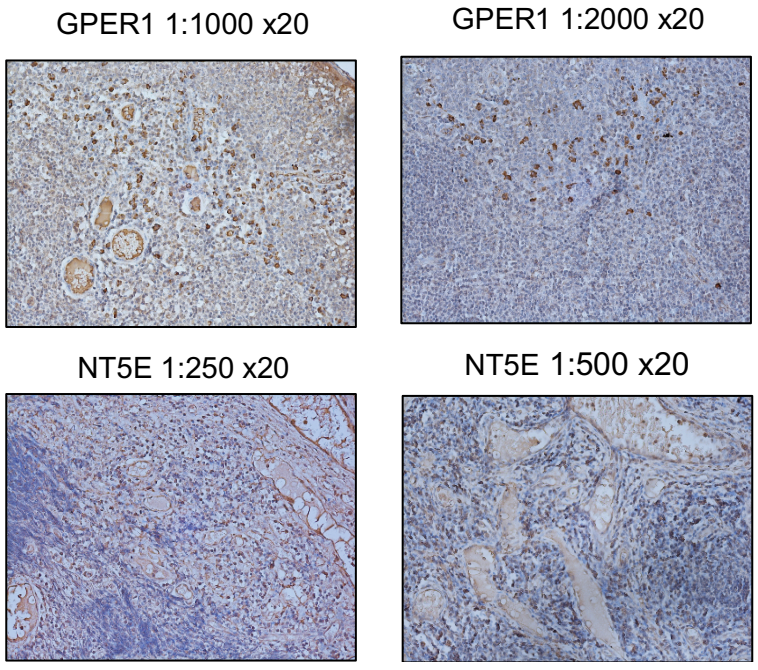

Figure 4-6 GPER and NT5E immunohistochemistry images

Tonsil staining using GPER1 at 1:1000 and 1:2000 and NT5E at 1:250 and 1:500, images were taken at magnification x20.

Patient	Galectin-7 score	GPER1 score	Patient	Galectin-7 score	GPER1
1990	100% Pos	DCIS Neg	**250**	90% Neg 10% Het	100% Pos
1916	100% Pos	DCIS Neg	**93**	80% Neg 20% Het	DCIS Neg
862	100% Pos	HET Pos MECs	**1062**	95% Neg 5% Het	DCIS Neg
1098	100% Pos	DCIS Neg	**1156**	100% Neg	MECs Neg
1115	95% Pos	DCIS Neg	**1161**	80% neg	No DCIS
229	100% Pos	DCIS Neg	**2296**	100% Neg	No DCIS

Table 4-2 GPER1 immunohistochemistry scoring

This table demonstrates the GPER scoring selected patients from the DCIS cohort. In this small set of patents there does not appear to be a correlation between Galectin-7 status and GPER status.

4.3 Down regulated genes in Galectin-7 knockdown cells

A short synopsis of selected genes showing differential expression on knockdown of Galectin-7 is given below, with particular focus on those where previous studies suggest a role in breast biology.

4.3.1 GPER1 (G-protein-coupled estrogen receptor-1)

This gene encodes a multi-pass membrane protein that localises to the endoplasmic reticulum and is a member of the G-protein coupled receptor 1 family. This receptor binds to oestrogen and activates multiple downstream signalling pathways, leading to stimulation of adenylate cyclase and an increase in cyclic AMP levels, while also promoting intracellular calcium mobilisation and synthesis of phosphatidylinositol 3,4,5-trisphosphate in the nucleus. This protein therefore plays a role in the rapid nongenomic signalling events widely observed following stimulation of cells and tissues with oestrogen ("https://www.ncbi.nlm.nih.gov/gene/2852,").

GPER signalling can activate tyrosine kinase Src, inducing the release of heparin-bound epidermal growth factor (HB-EGF) and subsequent transactivation of the epidermal growth factor receptor (EGFR), activating downstream signalling pathways such as PI3K/Akt and ERK/MAPK. With regards to previous investigations in to the role of Galectin-7 in apoptosis, GPER1 triggers mitochondrial apoptosis during pachytene spermatocyte differentiation, stimulates uterine epithelial cell proliferation, contributes to thymic atrophy by inducing apoptosis. GPER-1 is also involved in regulation of cancer progression as it stimulates proliferation of cancer-associated fibroblast (CAF) by a rapid genomic response through the EGFR/ERK transduction pathway. This is associated with EGFR and may act as a transcription factor activating growth regulatory genes (c-fos, cyclin D1), which promotes integrin alpha-5/beta-1 and fibronectin (FN) matrix assembly in breast cancer cells.

Recently, GPER has been evaluated as a candidate biomarker for growth regulation of triple negative breast cancers (TNBC). In particular, the knockdown of GPER expression was shown to prevent the proliferation of TNBC cells as well as the EGFR activation and *c-fos* expression induced by E2 (Girgert, Emons, & Gründker, 2012). A potential role elicited by GPER in TNBCs was suggested by a retrospective analysis demonstrating that GPER is prevalent in TNBCs, associated with young age and possible malignant recurrence (Steiman, Peralta, Louis, & Kamel, 2013). Taken together, this data suggests that the inhibition of GPER might be an appropriate targeted therapy in TNBC. GPER also plays a role in breast cancer progression and tamoxifen resistance (Lappano, Pisano, & Maggiolini, 2014).

4.3.2 MAP3K12 (Mitogen-Activated Protein Kinase Kinase Kinase 12)

MAP3K12 (Mitogen-Activated Protein Kinase Kinase Kinase 12), the mitogen-activated protein kinase (MAPK) pathways respond to diverse extracellular stimuli to regulate cellular processes including proliferation, differentiation, migration, survival and apoptosis(Johnson & Lapadat, 2002).

Mixed-lineage kinase 3 (MLK3) is recognised as a player in oncogenic signalling. MLK3 is a mitogen-activated protein kinase kinase kinase (MAP3K) that mediates signals from several cell surface receptors including receptor tyrosine kinases (RTKs), chemokine receptors, and cytokine receptors. Once activated, MLK3 transduces signals to multiple downstream pathways, primarily to c-Jun terminal kinase (JNK) MAPK, as well as to extracellular-signal-regulated kinase (ERK) MAPK, P38 MAPK, and NF-κB, resulting in both transcriptional and post-translational regulation of multiple effector proteins. In several types of cancer, MLK3 signalling is implicated in promoting cell proliferation, as well as driving cell migration, invasion and metastasis (Rattanasinchai & Gallo, 2016).

Chen et al., used a 3D DCIS model and induced the expression of active MLK3. Multiple features of DCIS were observed, including bypass of growth arrest and re-initiation of luminal filling. The increase in the proliferation marker Ki-67 and suppression of the proapoptotic BimEL upon MLK3 induction reveals both proliferative and novel antiapoptotic roles for MLK3 in the context of breast cancer (Chen, Miller, & Gallo, 2010).

4.3.3 PDGFD (platelet-derived growth factor D)

The protein encoded by this gene is a member of the platelet-derived growth factor family This is a growth factor that plays an essential role in the regulation of embryonic development, cell proliferation, cell migration, survival and chemotaxis. It also plays an important role in wound healing. - it induces macrophage recruitment, increased interstitial pressure, and blood vessel

maturation during angiogenesis. It can initiate events that lead to a mesangial proliferative glomerulonephritis, including influx of monocytes and macrophages and production of extracellular matrix.

Dysregulation of paracrine PDGF signalling can cause extracellular matrix remodelling in a tumour-promoting way to facilitate migration, invasion and angiogenesis (Ehnman & Östman, 2014),(Andrae, Gallini, & Betsholtz, 2008).

PDGF also plays a major role in initiating the desmoplastic response of breast cancers (Walker, 2001) (Shao, Nguyen, & Barsky, 2000). Patients with recurrent disease have elevated circulating PDGF levels, suggesting that it may serve as a recurrence marker (Pasanisi et al., 2008).

At the stage of *in situ* carcinoma, growth factors secreted by the malignant epithelial cells, either PDGF (Shao et al., 2000) or TGF-β_1 (Walker & Dearing, 1992) or both, with or without other factors, stimulate myofibroblasts within the adjacent stroma. These synthesise a variety of stromal proteins (such as fibronectin, tenascin and collagens 1 and 3), metalloproteinases (Rønnov-Jessen, Petersen, & Bissell, 1996),(Jones, Glynn, & Walker, 1999) and growth factors with angiogenic effects (de Jong, van Diest, van der Valk, & Baak, 1998) which aid invasion, aid the subsequent growth of cancer cells and promote metastasis.

4.3.4 CA11

Carbonic anhydrases (CAs) are a large family of zinc metalloenzymes that catalyse the reversible hydration of carbon dioxide. They participate in a variety of biological processes, including respiration, calcification and acid-base balance. They show extensive diversity in tissue distribution and in their subcellular localisation (Dodgson, Tashian, Gross, & Carter, 1991).

Shiozaki et al., investigated the role of CA11 in gastric carcinogenesis. Northern blot analysis showed that expression of CA11 gene in cancer tissue was down-regulated compared with normal tissue, semi-quantitative RT-PCR also demonstrated that CA11 gene expression was decreased in 41 out of 50 (82%) of gastric cancer tissues, when compared with normal stomach tissues. These findings suggest that the loss of CA11 expression in gastric tissues may play an important role in gastric carcinogenesis (Shiozaki et al., 2001). There are no reported studies for a role in DCIS or breast cancer biology.

4.3.5 CERK

CERK converts ceramide to ceramide-1-phosphate (C1P), a sphingolipid metabolite. Both CERK and C-1-P is involved in various cellular processes, including proliferation, apoptosis, phagocytosis, and inflammation (T. J. Kim, Mitsutake, & Igarashi, 2006). C-1-P also prevents apoptosis by inhibiting the caspase-9/caspase-3 pathway. This is thought to occur via C-1-P interacting with and blocking functionality of acid sphingomyelinase. This results in diminished ceramide production, which precludes apoptosis. Phosphorylation of ceramide via CERK has been shown to stimulate myoblast proliferation. CERK has demonstrated an ability to activate phosphatidylinositol 3-kinase/Akt (PI3K/Akt), ERK1/2, and mTOR (Gangoiti et al., 2012). CERKs ability to activate signalling molecules that facilitate the cell proliferation as well as its interaction with PI3K/Akt, and mTOR indicate that dysregulated CERK expression may contribute to cancer progression.

Elevated CERK expression is associated with an increased risk of recurrence in women with breast cancer. It is suggested that CERK inhibition might be a potential target for tumour recurrence (Pastukhov et al., 2014). In addition, although CERK expression is associated with aggressive subtypes of breast cancer, including those that are oestrogen receptor-negative, HER2(+), basal-like, or high grade, its association with poor clinical outcome is independent of these clinicopathologic variables (A. W. Payne, Pant, Pan, & Chodosh, 2014).

4.3.6 SYT16 (Synaptotagmin 16)

SYT16 (Synaptotagmin 16) is a Protein Coding gene. Gene Ontology (GO) annotations related to this gene include calcium ion binding and protein heterodimerization activity, which may be involved in the trafficking and exocytosis of secretory vesicles in non-neuronal tissues. There have been no previous roles identified in breast pathology.

4.3.7 SYT11 (Synaptotagmin 11)

This gene is a member of the synaptotagmin gene family and encodes a protein similar to other family members that are known calcium sensors and mediate calcium-dependent regulation of membrane trafficking in synaptic transmission ("https://www.ncbi.nlm.nih.gov/gene/23208
"). The protein expression of SYT11 is mainly cytoplasmic in the central nervous system and peripheral nervous system. SYT11 has an association with Parkinsons disease. There are low levels of protein expression in breast tissue.

4.3.8 LGR5 (Leucine Rich Repeat Containing G Protein-Coupled Receptor 5)

LGR5 encoded protein is a receptor involved in the Wnt signalling pathway. This protein plays a role in the formation and maintenance of adult intestinal stem cells during postembryonic development (Hou, Chen, & Chu, 2018). LGR5 Is involved not only in early events, but also in late events in colorectal tumorigenesis. Zheng et al demonstrated that LGR5 expression in colorectal cancer is higher at the invasive front than at the tumour centre. Colorectal cancer cells expressing LGR5 are reported to have a higher potential for invasion and metastasis (Zheng et al., 2018).

The cancer stem cell hypothesis suggests that a subset of cancer cells retain stem cell properties. LGR5 is a marker of adult stem cells. Yang et al showed

LGR5 overexpression was detected in breast cancer and significantly associated with breast cancer recurrence and poor outcome. LGR5 promoted cell motility, tumour formation, and epithelial-mesenchymal transition in breast cancer cells by activating Wnt/β-catenin signalling (L. Yang et al., 2015).

4.3.9 RASGRP1

This gene is from a family of genes characterized by the presence of a Ras superfamily guanine nucleotide exchange factor (GEF) domain. It functions as a diacylglycerol (DAG)-regulated nucleotide exchange factor specifically activating Ras through the exchange of bound GDP for GTP. It activates the Erk/MAP kinase cascade and regulates T-cell and B-cell development, homeostasis and differentiation ("https://www.ncbi.nlm.nih.gov/sites/entrez?Db=gene&Cmd=ShowDetailView&TermToSearch=10125," 2008). Wang et al have evaluated gene expression in total RNA isolated from formalin-fixed paraffin-embedded tumour samples using the NanoString Counter assay for 469 triple negative breast cancer cases from the Shanghai Breast Cancer Survival Study. A twofold higher expression of *RASGRP1* (HR 0.89, 95% CI 0.82–0.97), was associated with better overall survival and was also associated with better disease-free survival (Wang et al., 2018).

Overexpression of RasGRP1 had a profound effect on keratinocyte morphology and cell biology as it increases apoptosis (Rambaratsingh, Stone, Blumberg, & Lorenzo, 2003). The reason that RasGRP1's differential effect on JNK-1 and -2 is interesting is that phospho-JNK2 has been reported to have pro-tumorigenic effects in mouse keratinocytes, whereas pJNK1 has the opposite effect raising the possibility that dysregulated levels of RasGRP1 could have oncogenic properties through specific activation of JNK2 (Sharma, Luke, Dower, Stone, & Lorenzo, 2010).

4.3.10 CHN1 Chimerin 1

This gene encodes GTPase-activating protein for ras-related p21-rac and a phorbol ester receptor. It is predominantly expressed in neurons and plays an important role in neuronal signal-transduction mechanisms. Mutations in this gene are associated with Duane's retraction syndrome 2 (DURS2) ("https://www.ncbi.nlm.nih.gov/gene/1123
 ").

4.4 Up-regulated genes in Galectin-7 knockdown cells

4.4.1 LOX

LOXL2 is highly expressed in the basal/myoepithelial mammary cell lines this was shown in a study by Erler et al., which studied 3 main breast cancer cell lines (Barker et al., 2011) like many other genes that are up-regulated in basal-like breast cancers. LOXL2 catalyses the cross-linking of collagens and elastin (Csiszar, 2001), (Y. M. Kim, Kim, & Kim, 2011).

Weaver et al have shown how modulating the activity of LOX can directly modify tumour progression by regulating collagen crosslinking and stiffness. The results are consistent with data indicating that LOX enzymes are elevated in many cancers (Erler & Weaver, 2009) and that LOX is induced by hypoxia inducible factor (HIF-1) and TGFβ; two key regulators of tumour behaviour (Postovit et al., 2008). Indeed, cellular LOX promotes breast cell migration and invasion and enhances tumour proliferation and survival (Kirschmann et al., 2002).

There are also contradictory reports that LOX may act as a tumour suppressor (S. L. Payne, Hendrix, & Kirschmann, 2007) possibly by directly inhibiting ECM adhesions and integrin signaling (Zhao et al., 2009). LOX-mediated ECM stiffening could also impede cell invasion in the absence of MMP activity (Zaman et al., 2006) reminiscent of highly crosslinked, stiff fibrotic tissues and scars that often never progress to malignancy.

4.4.2 NT5E (also known as CD73)

High CD73 expression has been significantly associated with lymph node metastases in different types of cancers (Jiang et al., 2018). Targeting CD73 results in favourable antitumor effects in preclinical studies and combination of CD73 blockade with other immune checkpoint inhibitors, such as anti-cytotoxic T-lymphocyte antigen (CTLA)-4 antibody or anti-programmed cell death protein (PD)-1/PD-1 ligand (PDL1) antibody, is particularly promising (Antonioli, Yegutkin, Pacher, Blandizzi, & Haskó, 2016)) . Increasing evidence suggests that

CD73 is highly expressed in a wide range of cancer types, including breast cancer, colorectal cancer, glioblastoma, melanoma, prostate cancer, ovarian cancer, and non-small-cell lung cancer (NSCLC). High CD73 expression is frequently reported to be associated with poor prognosis in different cancer types, however, several studies found high CD73 expression was not correlated with the prognosis of patients with breast cancer (Supernat et al., 2012). It has been shown recently that CD73 expression negatively correlates with oestrogen receptor (ER) signalling and is associated with poor prognosis and chemoresistance in the triple-negative breast cancer (Loi et al., 2013)

4.4.3 Cadherin 11 (CDH11)

Cadherins are calcium-dependent cell adhesion proteins, which play an essential role in tissue morphogenesis and homeostasis. The cadherin 11 gene encodes a type II classical cadherin from the cadherin superfamily. Mature cadherin proteins are composed of a large N-terminal extracellular domain, a single membrane-spanning domain, and a small, highly conserved C-terminal cytoplasmic domain. Type II (atypical) cadherins are defined based on their lack of a HAV cell adhesion recognition sequence specific to type I cadherins. Cadherins are thought to play an important role in development and maintenance of tissues through selective cell-cell adhesion activity and may be involved also in the invasion and metastasis of malignant tumours (Tanihara, Sano, Heimark, St John, & Suzuki, 1994).

CDH11 is overexpressed in 15% of breast cancers. CDH11 expressing basal-like breast carcinomas and other CDH11 expressing malignancies exhibit poor prognosis. CDH11 is increased in early breast cancer and ductal carcinoma in situ (Assefnia et al., 2014). The overexpression in a subset of DCIS suggests it is an early event in breast cancer development. Not all DCIS lesions are CDH11 positive and high expression occurs when comedo necrosis is present: this type DCIS is a subtype thought to have a greater invasive potential (Burstein et al., 2004)

4.4.4 TMCO1 (Transmembrane and Coiled-Coil Domains 1)

This locus encodes a transmembrane protein. TMCO1 transcript was downregulated in the progression of urinary bladder urothelial carcinoma (UBUC). Shiue et al investigated this further showing that TMCO1 dysregulates cell cycle progression via suppression of the AKT pathway and S60 of the TMCO1 protein is crucial for its tumour suppressor roles. Stable overexpression of the TMCO1 gene suppressed tumour growth in xenograft mice (C. F. Li et al., 2017).

4.4.5 TNFSF18

The protein encoded by this gene is a cytokine that belongs to the tumour necrosis factor (TNF) ligand family. This cytokine is a ligand for receptor TNFRSF18/AITR/GITR. It has been shown to modulate T lymphocyte survival in peripheral tissues. This cytokine is also found to be expressed in endothelial cells and is thought to be important for interaction between T lymphocytes and endothelial cells ("https://www.ncbi.nlm.nih.gov/gene/8995,").

4.4.6 CDC42EP5- Cell division control protein 42 Effector Protein 5

Cell division control protein 42 (CDC42), a small Rho GTPase, regulates the formation of F-actin-containing structures through its interaction with the downstream effector proteins. The protein encoded by this gene is a member of the Borg (binder of Rho GTPases) family of CDC42 effector proteins. Borg family proteins contain a CRIB (Cdc42/Rac interactive-binding) domain. They bind to CDC42 and regulate its function negatively. The encoded protein may inhibit c-Jun N-terminal kinase (JNK) independently of CDC42 binding. The protein may also play a role in septin organization and inducing pseudopodia formation in fibroblasts ("https://www.ncbi.nlm.nih.gov/gene/148170,").

In most human cancers CDC42 is abnormally expressed and promoting neoplastic growth and metastasis. Regarding possible new treatments for cancer, miRNA and small molecules targeting CDC42 and related pathways have been recently found to be effective on cancer (Xiao et al., 2018).

The gene expression of CDC42 is different in several types of cancer (Xiao et al., 2018), as is the case with Galectin-7. Research has shown CdcC42 induces invasiveness and metastatic activity by breast cancer cells (S. Lee, Craig, Romain, Qiao, & Chung, 2014).

4.5 Discussion

The hypothesis was that loss of myoepithelial cell Galectin-7 in DCIS alters myoepithelial cell function and contributes to disease progression. RNA sequencing comparing myoepithelial cells treated with non-targeting control siRNA and Galectin-7 siRNA knockdown was performed to assess the global effect of Galectin-7 knockdown on myoepithelial cell function, to better understand the biology of Galectin-7 and how this might contribute to the development of a DCIS risk stratification tool.

RNA sequencing was performed to identify potential direction for future work. The sequencing data has identified a number of interesting genes of potential relevance. Genes which had particular relevance to breast pathology these were further studied; genes down regulated in the Galectin-7 knockdown cells were GPER1, PDGFR, MAP3K12 and genes which were upregulated in the Galectin-7 knockdown cells were LOX, CDH11 and NT5E.

Following the bioinformatics sequence analysis, validation for selected genes was performed using qPCR and immunohistochemistry. Empirically, three genes that were up-regulated and three genes that were down-regulated in the in the Galectin-7 knockdown that appeared relevant to breast cell biology were selected. Ideally all the genes would have been validated however it was not possible due time limitations. qPCR is an established technique for validating RNA sequencing data("https://www.phalanxbiotech.com/validating-rna-seq-results-with-qpcr/," 2017). Samples from the same 4 patients used in RNA sequencing were used. In one of the patients, labelled as 2585, there was a lot of variation in the results including for the housekeeping genes, possibly as a result of RNA degradation, and therefore these results were excluded. Ideally, more samples would have been used for validation, but time restraints precluded this.

There was variation in the qPCR results, however, NTSE showed consistent up-regulation, concordant with the RNA sequencing results. There was increased

expression of CDH11 in 2 of the 3 samples on qPCR, but apparent reduced expression of LOX in 2 of 3 samples. For the genes found to be down-regulated on RNA sequencing, two of the three genes showed reduced expression on qPCR in 2 of 3 samples. It is clear that further validation is required. In our experience qPCR generates considerable variation in results (Dr M Allen, personal communication). Orthogonal testing, using Western blotting and immunohistochemistry, would be important.

Where antibodies were available, further validation was attempted using immunohistochemistry. LOX is of particular interest causing cross-linking of collagen leading to increased stiffness and promoting tumorigenesis of pre-malignant cells (Levental et al., 2009). A study has shown up regulation of LOX in the periductal stroma in DCIS with associated invasion when compared to pure DCIS (Castro et al., 2008).

The DCIS cohort that has been used throughout the thesis was stained for LOX. Disappointingly the results were inconclusive: the first batch of staining showed a lot of background and was hard to interpret therefore the staining was repeated and this showed very different staining patterns, making it difficult to be confident about these results. Increased ECM stiffness can promote cancer cell invasion (Levental et al., 2009) there was up regulation of LOX when Galectin-7 was knocked down in the myoepithelial cells. This is an exciting and interesting finding, the hypothesis that lower levels of myoepithelial Galectin-7 promotes the transition of DCIS to invasive cancer would fit with this hypothesis that increased levels of LOX would promote a more fibrotic stroma. Further work is needed to further validate the up regulation of LOX following Galectin-7 knockdown. Because of the potential relevance to DCIS progression, this should be pursued. An alternative technique, such as RNA scope may be more appropriate, or sourcing alternative antibodies.

Knockdown of Galectin-7 showed a down-regulation of GPER1 in the RNA sequencing. GPER may be included among the factors facilitating oestrogen-

activated cross-talk within the tumour microenvironment contributing towards breast tumour progression. GPER triggers the expression of various genes involved in the growth and migration of diverse oestrogen-responsive tumours (De Francesco et al., 2014; Lappano, Rosano, et al., 2012; Lappano, Santolla, et al., 2012; D. P. Pandey et al., 2009). Tamoxifen is an agonist of the G protein-coupled oestrogen receptor (GPER). Cortes et al., have investigated the role of tamoxifen in modulating the stroma of pancreatic adenocarcinoma and shown that tamoxifen can inhibit myofibroblastic differentiation of pancreatic stellate cells (PSCs) in the tumour microenvironment of pancreatic cancer in a GPER-dependent manner (Cortes et al., 2019). This again implicates myoepithelial cell control of the periductal stromal microenvironment. Unfortunately, the quality of immunohistochemical staining for GPER again made interpretation difficult and further work is needed to verify the RNA sequencing results.

In conclusion, RNA sequencing of primary myoepithelial cells has indicated as series of genes up- or down-regulated by altered Galectin-7 expression. Further validation is needed, but there are a number of genes of potential relevance to DCIS progression that should be pursued.

5 Final discussion and future work

This study aimed to investigate the hypothesis that changes in MEC in DCIS contribute to progression to invasion by altering the tumour microenvironment. Specifically, the study focussed on altered Galectin-7 in MEC, its effect on MEC function and its relationship with another DCIS marker αvβ6.

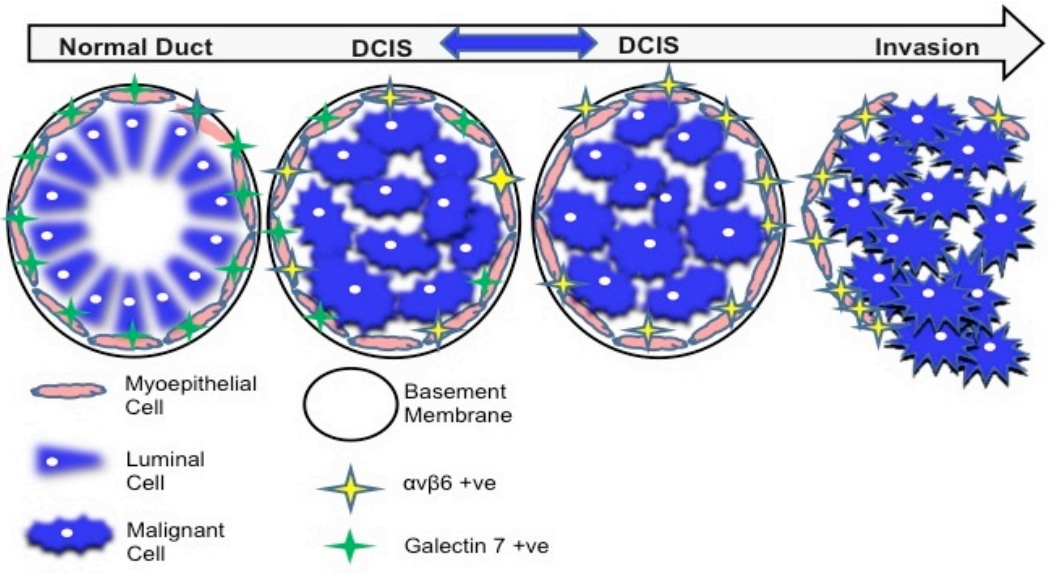

Figure 5-1 Hypothetical DCIS progression

This schematic illustrates a normal breast duct with luminal cells organised and polarised with myoepithelial cells strongly positive for Galectin-7 and negative for αvβ6. There is then transition to DCIS with neoplastic proliferation of epithelial cells within the ductal-lobular structures of the breast that does not penetrate the myoepithelial basement membrane interface. The myoepithelial cells have an altered phenotype with loss of Galectin-7 and up-regulation of αvβ6. In the DCIS ducts that progress to invasive disease there is loss of the myoepithelial basement membrane interface, possibly through TRAIL-induced apoptosis.

Up-regulation of αvβ6 by MEC in DCIS has previously been reported and shown to be associated with disease progression Expression of αvβ6 is almost universal (95%) in DCIS with an established invasive component. This study

identified loss of Galectin-7 in DCIS-MEC in a subset of cases, with significantly less Galectin-7 positive ducts in DCIS with associated invasion compared to pure DCIS. Any DCIS risk score will be improved by the integration of multiple markers, thus each duct was assigned a αvβ6- Galectin-7 score. These indicated that scores of Galectin-7 positive/ αvβ6 heterogeneous, Galectin-7 positive/αvβ6 negative, Galectin-7 heterogeneous/ αvβ6 negative were significantly more frequent in DCIS ducts in the pure DCIS cohort compared to the DCIS with associated invasion cohort. Conversely, the combinations of Galectin-7 heterogeneous /αvβ6 positive, Galectin-7 negative /αvβ6 positive and Galectin-7 negative /αvβ6 heterogeneous were seen in a significantly higher number of DCIS ducts in the DCIS with associated invasion cohort. These findings suggest an inverse relationship between Galectin-7 and αvβ6 integrin in DCIS-myoepithelial cells.

These results tentatively support the hypothesis in figure 5.1 where combined loss of Galectin-7 and upregulation of αvβ6 represents 'late stage' DCIS, with an increased likelihood to progress to invasion. To further validate this, it would be useful to test the predictive power of αvβ6 and Galectin-7 in a series of pure DCIS with long term follow up, where a subset of patients will have developed ipsilateral invasive recurrence.

It could be argued that to develop a robust and clinically useful progression tool, it is important to establish the functional relevance of individual markers. This study therefore sought to establish the functional impact of loss of Galectin-7 in MECs. Experiments were performed with a combination of established cell lines and primary cells. There are advantages and disadvantages to the use of cell lines versus primary cells. Cell lines do not have the heterogeneity that is evident in patient samples and in clinical practice, and do not always fully replicate the in-vivo situation. In contrast, primary cells are likely to be more physiologically relevant, but they are a finite resource and more challenging to work with. It is extremely important to consider these factors when interpreting data from

experiments both with primary cells and cell lines. Cell lines are prone to genotypic and phenotypic drift during their continual culture. In the current study, marked differences were seen between the cell lines and the primary MECs, and the results seen with the primary cells are considered more relevant, since the primary MECs exhibited a phenotype more representative of MECs in vivo.

Galectin-7 is implicated in apoptosis, and therefore the impact of loss of Galectin-7 on MEC apoptosis was investigated. This demonstrated that knockdown of Galectin-7 in primary MECs there was an increase in apoptosis, with or without exposure to TRAIL. This could feasibly contribute to the pathognomonic loss of MECs seen as DCIS progresses, and be one mechanism y which loss of Galectin-7 contributes to DCIS progression. Another important role of MEC is to maintain the myoepithelial-basement membrane (BM) barrier, with strong adhesion to BM, to adjacent MECs and to luminal cells. This study has shown decreased adhesion to BM associated laminin, increased adhesion to collagen I, decreased migration to collagen I, and increased migration to laminin in Galectin-7 knockdown primary MECs. This suggests Galectin-7 negative MECs are less adhesive to BM extracellular matrix proteins and more adhesive to interstitial collagen, which may reflect the altered interactions in DCIS progression to invasion.

Another key element of tumour invasion is the release of proteolytic enzymes that can breakdown BM and modify interstitial matrix. (Kessenbrock, Plaks, & Werb, 2010) Conditioned media from primary MEC treated either with Galectin-7 siRNA or non-targeting control siRNA was applied to protease proteome profiles. This demonstrated down-regulation of a range of proteolytic enzymes when Galectin-7 was knocked down. This seems counterintuitive since loss of Galectin-7 appears to be associated with more advanced disease. Interestingly, in invasion assays with MDA MD 231 breast cancer cells, conditioned media from Galectin-7 knockdown MEC resulted in reduced invasion compared to conditioned media from non-targeting control cells, which would be consistent with down-regulation of proteolytic enzymes. We previously have shown that MEC up-regulate $\alpha v\beta 6$ and this leads to up-regulation of MMP-9, which promotes tumour invasion. It is

feasible that both loss of Galectin-7 and gain of αvβ6 is required to develop the full pro-tumourigenic effect of MEC.

Galectins are complex and implicated in multiple functions therefore RNA sequencing of primary MEC with Galectin-7 knockdown versus non-target control cells was carried out to gain a global view of its role in MEC. A number of genes showed altered expression but of particular interest were LOX and GPER1. Both LOX and GPER1 have been shown to have influence changes in the tumour microenvironment (Levental et al., 2009), (Cortes et al., 2019) and would be predicted to contribute to a pro-invasive environment. qPCR and immunohistochemistry was carried out with the aim of validating the RNA seq, however, results were not conclusive and further work is required.

In conclusion, loss of Galectin-7 in DCIS-associated MEC is more frequent in more advanced disease and is inversely related to up-regulation of αvβ6. Functional assays suggest that loss of Galectin-7 alters DCIS behaviour and could contribute to the destabilisation of the MEC-BM interface thus promoting progression of DCIS to invasive disease. RNA seq analysis has identified a series of genes modulated by Galectin-7 which also could contribute to disease progression, though this requires further validation. Given loss of Galectin-7 is such a consistent change and of functional relevance in DCIS, it could be incorporated into a risk algorithm to help stratify management of patients with DCIS and so reduce issues of overtreatment in this disease.

5.1 Future work

The immunohistochemistry analysis of the 2 DCIS cohorts used in this study has shown very promising results, however further validation is required. Ideally this validation set of tissues would have long term follow up data, this could potentially assess if Galectin-7 expression is able to predict recurrence. The SLOANE study would potentially offer an ideal validation set.

In DCIS progression the myoepithelial maybe lost through apoptosis, data in this study shows that Galectin-7 in primary myoepithelial cells has anti apoptotic role. A wider range of primary myoepithelial cells and apoptotic markers could be used to further validate this.

Organotypic models were used as an alternative model further optimisation of the organotypic model is required potentially using primary fibroblasts , ideally the primary fibroblasts and the primary myoepithelial would be from the same patient.

RNA sequencing provided interesting results however this requires much more extensive validation. In particular validation of the changes in LOX expression is important, an alternative LOX antibodies would be beneficial to assess if the results were more consistent. RNA scope is an alternative method that could potentially be used to assess LOX expression in the DCIS cohorts used in this study.

6 Supplementary

6.1 A comparison of heterogeneity between pure DCIS and DCIS with associated invasion using ER, PR and HER-2 immunohistochemical markers

Another method to compare the pure DCIS and DCIS with associated invasion cohorts was to compare diversification of the scores between the 2 groups for ER, PR and HER 2. These markers were scored at strongly (3) positive, moderately (2) positive and weakly (1) positive, strongly (3) heterogeneous, moderately(2) heterogeneous and weakly (1) heterogeneous and negative. Having seven categories enabled further assessment of the diversification of results. Heterogeneity is a challenge in DCIS diagnostics. This has shown there is a slight increased diversification in the pure DCIS (41.1%) compared to 37.4% in the DCIS with associated invasion in the ER staining. There is decreased diversification for PR in the pure DCIS (36.6%) compared to 47.7% in the DCIS with associated invasion. There is increased diversification for HER-2 in the pure DCIS (47.4%) compared to 34.5% in the DCIS with associated invasion

ER Pure DCIS Diversification							
	Positive 3	Positive 2	Positive 1	Hetero 3	Hetero 2	Hetero 1	Negative
Sum^2	36864	3721	729	25	324	1600	126736
sum(x^2)	488601						
sum(x)^2	169999						
Diversification	41.1%						

Table 6-1 ER diversification for Pure DCIS

Represents the diversification of 41.1% for ER in pure DCIS.

ER DCIS with associated invasion Diversification							
	Positive 3	Positive 2	Positive 1	Hetero 3	Hetero 2	Hetero 1	Negative
Sum^2	39204	1024	100	0	64	729	70225
sum(x^2)	291600						
sum(x)^2	111346						
Diversification	37.4%						

Table 6-2 ER diversification for DCIS with associated invasion

Represents the diversification of 37.4% for ER in DCIS with associated invasion.

PR Pure DCIS Diversification							
	Positive 3	Positive 2	Positive 1	Hetero 3	Hetero 2	Hetero 1	Negative
Sum^2	529	1849	8649	4	1156	8281	176400
sum(x^2)	498436						
sum(x)^2	196868						
Diversification	36.2%						

Table 6-3 PR diversification in Pure DCIS

Represents the diversification of 36.2% for PR in pure DCIS.

PR DCIS with associated invasion Diversification							
	Positive 3	Positive 2	Positive 1	Hetero 3	Hetero 2	Hetero 1	Negative
Sum^2	15876	1681	4356	9	256	1296	64516
sum(x^2)	293764						
sum(x)^2	87990						
Diversification	47.7%						

Table 6-4 PR diversification in DCIS with associated invasion

Represents the diversification of 47.7% of PR in DCIS with associated invasion.

HER 2 Pure DCIS Diversification							
	Positive 3	Positive 2	Positive 1	Hetero 3	Hetero 2	Hetero 1	Negative
Sum^2	89401	2025	2209	225	1444	1296	72900
sum(x^2)	562500						
sum(x)^2	169500						
Diversification	47.4%						

Table 6-5 HER-2 diversification in Pure DCIS

Represents the diversification of 47.4% of HER-2 in pure DCIS.

HER-2 DCIS with associated invasion Diversification							
	Positive 3	Positive 2	Positive 1	Hetero 3	Hetero 2	Hetero 1	Negative
Sum^2	7921	4900	289	25	576	49	105625
sum(x^2)	288369						
sum(x)^2	119385						
Diversification	34.5%						

Table 6-6 HER-2 diversification in DCIS with associated invasion

Represents the diversification of 34.5% for HER-2 in DCIS with associated invasion.

6.2 Immunofluorescence- Dual staining P-Cadherin and ZO-1

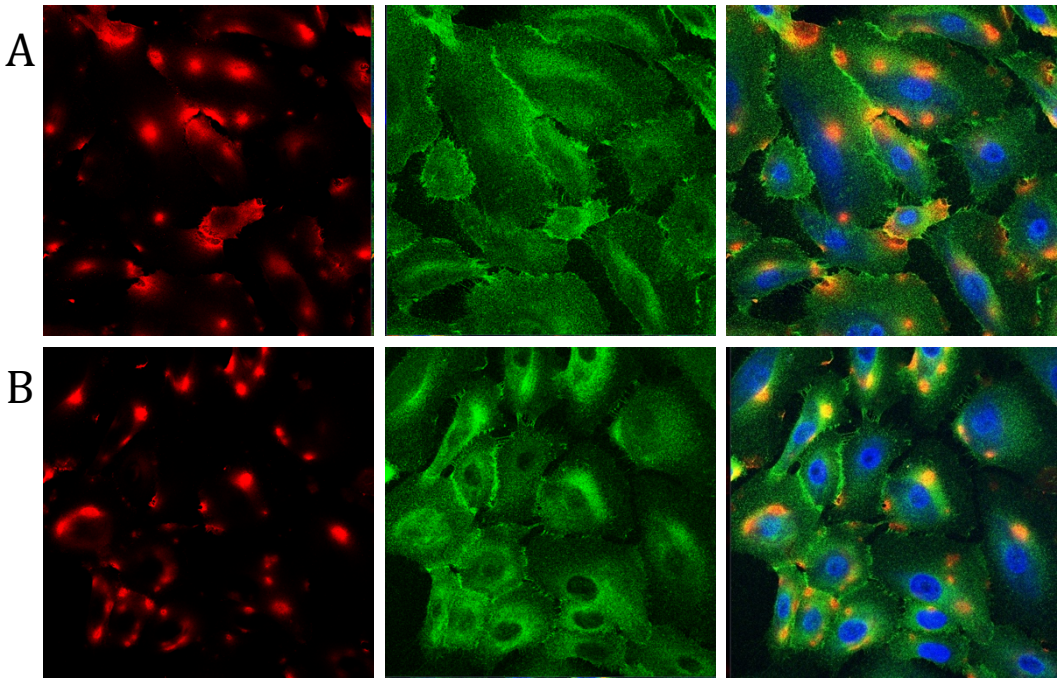

Figure 6-1 Immunofluorescence duel staining P-Cadherin and zo-1

P-Cadherin (green) and zo-1 (red) A) control myoepithelial cells and B) Galectin-7 knockdown myoepithelial cells (staining is non specific)

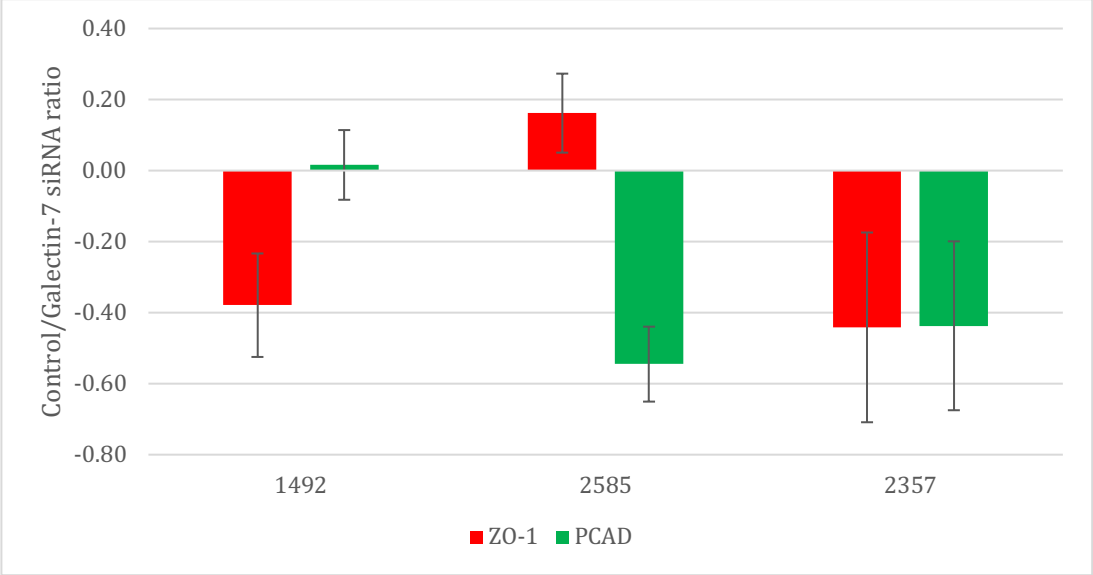

Figure 6-2 Dual immunofluorescence analysis P-Cadherin and ZO-1

Ratio of expression of zo-1 and PCAD control versus Galectin-7 knock down myoepithelial cells. This shows that 2 patients have a reduction in in zo-1 expression. 2585 has a slight increase in zo-1 expression in the control cell versus Galectin-7 knockdown cells however staining is non specific.

6.3 Differential gene expression across patient groups

Patient 1 Patient 4	Patient 1-Patient 3	Patient 1, Patient 2, Patient 4	Patient 2-Patient 4
LGALS7B	ANKRD1	GNRHR	MMP13
LGALS7	LUCAT1	EXTL1	NOV
DNAH10OS	MPZL3	PDE4B	PDGFD
CNNM1	SHISA9	ASB13	ANGPTL7
LOX	SPRR1A	SOSTDC1	COMP
CERK	IFIT3	SLC7A8	DIO2
SCG5	CCDC188	PEG10	NT5E
TMCO1	MRGPRX3	CXCL5	NEGR1
LGR5	FGF1	FREM2	STON1
LIMS2	LHFPL6	ENOX1	TCHH
MICB	RSAD2	IGFBP7	CA11
GPER1	MAP3K12	LINC00702	P2RX5
SYT11	UHRF1BP1	DIRAS3	LINC01704
CDH11	NACAD		STRADB
RASGRP1	SLCO2A1		SYT16
LINC01564			MEX3A
			TAS1R3
			WNT10A
			CHN1
			PRR9
			CSF3
			MST1
			CSGALNACT1
			CDC42EP5
			GAB3
			FZD4
			LINC02407
			LINC01291
			LINC02154
			ACADSB
			MALL
			SERPINB4
			NREP

Table 6-7 Differential gene expression across patient groups between control and Galectin-7 knock down

References

Adams, M., Jones, J. L., Walker, R. A., Pringle, J. H., & Bell, S. C. (2002). Changes in tenascin-C isoform expression in invasive and preinvasive breast disease. *Cancer Res, 62*(11), 3289-3297.

Adriance, M. C., Inman, J. L., Petersen, O. W., & Bissell, M. J. (2005). Myoepithelial cells: good fences make good neighbors. *Breast Cancer Res, 7*(5), 190-197. doi:10.1186/bcr1286

Ahmed, A. (1974). The myoepithelium in human breast carcinoma. *J Pathol, 113*(2), 129-135. doi:10.1002/path.1711130208

Alberts, B., Johnson, A., Lewis, J., Morgan, D., Raff, M. C., Roberts, K., . . . Hunt, T. *Molecular biology of the cell* (Sixth edition. ed.).

Alkasalias, T., Moyano-Galceran, L., Arsenian-Henriksson, M., & Lehti, K. (2018). Fibroblasts in the Tumor Microenvironment: Shield or Spear? *Int J Mol Sci, 19*(5). doi:10.3390/ijms19051532

Allen, M., & Louise Jones, J. (2011). Jekyll and Hyde: the role of the microenvironment on the progression of cancer. *J Pathol, 223*(2), 162-176. doi:10.1002/path.2803

Allen, M. D., Marshall, J. F., & Jones, J. L. (2014). αvβ6 Expression in myoepithelial cells: a novel marker for predicting DCIS progression with therapeutic potential. *Cancer Res, 74*(21), 5942-5947. doi:10.1158/0008-5472.CAN-14-1841

Allen, M. D., Thomas, G. J., Clark, S., Dawoud, M. M., Vallath, S., Payne, S. J., . . . Jones, J. L. (2014). Altered microenvironment promotes progression of preinvasive breast cancer: myoepithelial expression of αvβ6 integrin in DCIS identifies high-risk patients and predicts recurrence. *Clin Cancer Res, 20*(2), 344-357. doi:10.1158/1078-0432.CCR-13-1504

Allinen, M., Beroukhim, R., Cai, L., Brennan, C., Lahti-Domenici, J., Huang, H., . . . Polyak, K. (2004). Molecular characterization of the tumor microenvironment in breast cancer. *Cancer Cell, 6*(1), 17-32. doi:10.1016/j.ccr.2004.06.010

Allred, D. C. (2010). Ductal carcinoma in situ: terminology, classification, and natural history. *J Natl Cancer Inst Monogr, 2010*(41), 134-138. doi:10.1093/jncimonographs/lgq035

Alvarado, M., Carter, D. L., Guenther, J. M., Hagans, J., Lei, R. Y., Leonard, C. E., . . . Schultz, M. J. (2015). The impact of genomic testing on the recommendation for radiation therapy in patients with ductal carcinoma in situ: A prospective clinical utility assessment of the 12-gene DCIS score™ result. *J Surg Oncol, 111*(8), 935-940. doi:10.1002/jso.23933

Andrae, J., Gallini, R., & Betsholtz, C. (2008). Role of platelet-derived growth factors in physiology and medicine. *Genes Dev, 22*(10), 1276-1312. doi:10.1101/gad.1653708

Antonioli, L., Yegutkin, G. G., Pacher, P., Blandizzi, C., & Haskó, G. (2016). Anti-CD73 in cancer immunotherapy: awakening new opportunities. *Trends Cancer, 2*(2), 95-109. doi:10.1016/j.trecan.2016.01.003

Assefnia, S., Dakshanamurthy, S., Guidry Auvil, J. M., Hampel, C., Anastasiadis, P. Z., Kallakury, B., . . . Byers, S. W. (2014). Cadherin-11 in poor prognosis malignancies

and rheumatoid arthritis: common target, common therapies. *Oncotarget, 5*(6), 1458-1474. doi:10.18632/oncotarget.1538

Bandyopadhyay, A., & Raghavan, S. (2009). Defining the role of integrin alphavbeta6 in cancer. *Curr Drug Targets, 10*(7), 645-652. doi:10.2174/138945009788680374

Barker, H. E., Chang, J., Cox, T. R., Lang, G., Bird, D., Nicolau, M., . . . Erler, J. T. (2011). LOXL2-mediated matrix remodeling in metastasis and mammary gland involution. *Cancer Res, 71*(5), 1561-1572. doi:10.1158/0008-5472.CAN-10-2868

Barsky, S. H., & Karlin, N. J. (2006). Mechanisms of disease: breast tumor pathogenesis and the role of the myoepithelial cell. *Nat Clin Pract Oncol, 3*(3), 138-151. doi:10.1038/ncponc0450

Beau, A. B., Lynge, E., Njor, S. H., Vejborg, I., & Lophaven, S. N. (2017). Benefit-to-harm ratio of the Danish breast cancer screening programme. *Int J Cancer, 141*(3), 512-518. doi:10.1002/ijc.30758

Beral, V., Alexander, M., Duffy, S., Ellis, I. O., Given-Wilson, R., Holmberg, L., . . . Young, K. C. (2011). The number of women who would need to be screened regularly by mammography to prevent one death from breast cancer. *J Med Screen, 18*(4), 210-212. doi:10.1258/jms.2011.011134

Berg, J. W., & Hutter, R. V. (1995). Breast cancer. *Cancer, 75*(1 Suppl), 257-269.

Bergstraesser, L. M., Srinivasan, G., Jones, J. C., Stahl, S., & Weitzman, S. A. (1995). Expression of hemidesmosomes and component proteins is lost by invasive breast cancer cells. *Am J Pathol, 147*(6), 1823-1839.

Bhathal, P. S., Brown, R. W., Lesueur, G. C., & Russell, I. S. (1985). Frequency of benign and malignant breast lesions in 207 consecutive autopsies in Australian women. *Br J Cancer, 51*(2), 271-278.

Biron-Pain, K., Grosset, A. A., Poirier, F., Gaboury, L., & St-Pierre, Y. (2013). Expression and functions of galectin-7 in human and murine melanomas. *PLoS One, 8*(5), e63307. doi:10.1371/journal.pone.0063307

Bissell, M. J., & Bilder, D. (2003). Polarity determination in breast tissue: desmosomal adhesion, myoepithelial cells, and laminin 1. *Breast Cancer Res, 5*(2), 117-119.

Bombonati, A., & Sgroi, D. C. (2011). The molecular pathology of breast cancer progression. *J Pathol, 223*(2), 307-317. doi:10.1002/path.2808

Boyd, N. F., Rommens, J. M., Vogt, K., Lee, V., Hopper, J. L., Yaffe, M. J., & Paterson, A. D. (2005). Mammographic breast density as an intermediate phenotype for breast cancer. *Lancet Oncol, 6*(10), 798-808. doi:10.1016/S1470-2045(05)70390-9

Brewer, H. R., Jones, M. E., Schoemaker, M. J., Ashworth, A., & Swerdlow, A. J. (2017). Family history and risk of breast cancer: an analysis accounting for family structure. *Breast Cancer Res Treat, 165*(1), 193-200. doi:10.1007/s10549-017-4325-2

Burdall, S. E., Hanby, A. M., Lansdown, M. R., & Speirs, V. (2003). Breast cancer cell lines: friend or foe? *Breast Cancer Res, 5*(2), 89-95.

Burstein, H. J., Polyak, K., Wong, J. S., Lester, S. C., & Kaelin, C. M. (2004). Ductal carcinoma in situ of the breast. *N Engl J Med, 350*(14), 1430-1441. doi:10.1056/NEJMra031301

Bussolati, G., Cassoni, P., Ghisolfi, G., Negro, F., & Sapino, A. (1996). Immunolocalization and gene expression of oxytocin receptors in carcinomas and non-neoplastic tissues of the breast. *Am J Pathol, 148*(6), 1895-1903.

Campbell, H. K., Maiers, J. L., & DeMali, K. A. (2017). Interplay between tight junctions & adherens junctions. *Exp Cell Res, 358*(1), 39-44. doi:10.1016/j.yexcr.2017.03.061

Campbell, M. J., Baehner, F., O'Meara, T., Ojukwu, E., Han, B., Mukhtar, R., . . . Esserman, L. (2017). Characterizing the immune microenvironment in high-risk ductal carcinoma in situ of the breast. *Breast Cancer Res Treat, 161*(1), 17-28. doi:10.1007/s10549-016-4036-0

Carey, L. A., Perou, C. M., Livasy, C. A., Dressler, L. G., Cowan, D., Conway, K., . . . Millikan, R. C. (2006). Race, breast cancer subtypes, and survival in the Carolina Breast Cancer Study. *JAMA, 295*(21), 2492-2502. doi:10.1001/jama.295.21.2492

Carney, P. A., Abraham, L. A., Miglioretti, D. L., Yabroff, K. R., Sickles, E. A., Buist, D. S., . . . Consortium, B. C. S. (2007). Factors associated with imaging and procedural events used to detect breast cancer after screening mammography. *AJR Am J Roentgenol, 188*(2), 385-392. doi:10.2214/AJR.05.1718

Casasent, A. K., Schalck, A., Gao, R., Sei, E., Long, A., Pangburn, W., . . . Navin, N. E. (2018). Multiclonal Invasion in Breast Tumors Identified by Topographic Single Cell Sequencing. *Cell, 172*(1-2), 205-217.e212. doi:10.1016/j.cell.2017.12.007

Castro, N. P., Osório, C. A., Torres, C., Bastos, E. P., Mourão-Neto, M., Soares, F. A., . . . Carraro, D. M. (2008). Evidence that molecular changes in cells occur before morphological alterations during the progression of breast ductal carcinoma. *Breast Cancer Res, 10*(5), R87. doi:10.1186/bcr2157

Chapman, J. A., Miller, N. A., Lickley, H. L., Qian, J., Christens-Barry, W. A., Fu, Y., . . . Axelrod, D. E. (2007). Ductal carcinoma in situ of the breast (DCIS) with heterogeneity of nuclear grade: prognostic effects of quantitative nuclear assessment. *BMC Cancer, 7*, 174. doi:10.1186/1471-2407-7-174

Chen, J., Miller, E. M., & Gallo, K. A. (2010). MLK3 is critical for breast cancer cell migration and promotes a malignant phenotype in mammary epithelial cells. *Oncogene, 29*(31), 4399-4411. doi:10.1038/onc.2010.198

Clark, S. E., Warwick, J., Carpenter, R., Bowen, R. L., Duffy, S. W., & Jones, J. L. (2011). Molecular subtyping of DCIS: heterogeneity of breast cancer reflected in pre-invasive disease. *Br J Cancer, 104*(1), 120-127. doi:10.1038/sj.bjc.6606021

Colpaert, C. G., Vermeulen, P. B., Fox, S. B., Harris, A. L., Dirix, L. Y., & Van Marck, E. A. (2003). The presence of a fibrotic focus in invasive breast carcinoma correlates with the expression of carbonic anhydrase IX and is a marker of hypoxia and poor prognosis. *Breast Cancer Res Treat, 81*(2), 137-147. doi:10.1023/A:1025702330207

Cortes, E., Sarper, M., Robinson, B., Lachowski, D., Chronopoulos, A., Thorpe, S. D., . . . Del Río Hernández, A. E. (2019). GPER is a mechanoregulator of pancreatic stellate cells and the tumor microenvironment. *EMBO Rep, 20*(1). doi:10.15252/embr.201846556

Cox, T. R., Rumney, R. M. H., Schoof, E. M., Perryman, L., Høye, A. M., Agrawal, A., . . . Erler, J. T. (2015). The hypoxic cancer secretome induces pre-metastatic bone

lesions through lysyl oxidase. *Nature, 522*(7554), 106-110. doi:10.1038/nature14492

Csiszar, K. (2001). Lysyl oxidases: a novel multifunctional amine oxidase family. *Prog Nucleic Acid Res Mol Biol, 70*, 1-32.

Cuzick, J., Sestak, I., Forbes, J. F., Dowsett, M., Knox, J., Cawthorn, S., . . . investigators, I.-I. (2014). Anastrozole for prevention of breast cancer in high-risk postmenopausal women (IBIS-II): an international, double-blind, randomised placebo-controlled trial. *Lancet, 383*(9922), 1041-1048. doi:10.1016/S0140-6736(13)62292-8

Cuzick, J., Warwick, J., Pinney, E., Duffy, S. W., Cawthorn, S., Howell, A., . . . Warren, R. M. (2011). Tamoxifen-induced reduction in mammographic density and breast cancer risk reduction: a nested case-control study. *J Natl Cancer Inst, 103*(9), 744-752. doi:10.1093/jnci/djr079

Dall, G. V., & Britt, K. L. (2017). Estrogen Effects on the Mammary Gland in Early and Late Life and Breast Cancer Risk. *Front Oncol, 7*, 110. doi:10.3389/fonc.2017.00110

De Francesco, E. M., Pellegrino, M., Santolla, M. F., Lappano, R., Ricchio, E., Abonante, S., & Maggiolini, M. (2014). GPER mediates activation of HIF1α/VEGF signaling by estrogens. *Cancer Res, 74*(15), 4053-4064. doi:10.1158/0008-5472.CAN-13-3590

de Jong, J. S., van Diest, P. J., van der Valk, P., & Baak, J. P. (1998). Expression of growth factors, growth-inhibiting factors, and their receptors in invasive breast cancer. II: Correlations with proliferation and angiogenesis. *J Pathol, 184*(1), 53-57. doi:10.1002/(SICI)1096-9896(199801)184:1<53::AID-PATH6>3.0.CO;2-7

Delva, E., Tucker, D. K., & Kowalczyk, A. P. (2009). The desmosome. *Cold Spring Harb Perspect Biol, 1*(2), a002543. doi:10.1101/cshperspect.a002543

Demers, M., Biron-Pain, K., Hébert, J., Lamarre, A., Magnaldo, T., & St-Pierre, Y. (2007). Galectin-7 in lymphoma: elevated expression in human lymphoid malignancies and decreased lymphoma dissemination by antisense strategies in experimental model. *Cancer Res, 67*(6), 2824-2829. doi:10.1158/0008-5472.CAN-06-3891

Demers, M., Magnaldo, T., & St-Pierre, Y. (2005). A novel function for galectin-7: promoting tumorigenesis by up-regulating MMP-9 gene expression. *Cancer Res, 65*(12), 5205-5210. doi:10.1158/0008-5472.CAN-05-0134

Demers, M., Rose, A. A., Grosset, A. A., Biron-Pain, K., Gaboury, L., Siegel, P. M., & St-Pierre, Y. (2010). Overexpression of galectin-7, a myoepithelial cell marker, enhances spontaneous metastasis of breast cancer cells. *Am J Pathol, 176*(6), 3023-3031. doi:10.2353/ajpath.2010.090876

Dodgson, S. J., Tashian, R., Gross, G., & Carter, N. D. (1991). *The Carbonic Anhydrases: Cellular Physiology and Molecular Genetics.* (Vol. 1): Springer US.

Duffy, S. W., Tabar, L., Olsen, A. H., Vitak, B., Allgood, P. C., Chen, T. H., . . . Smith, R. A. (2010). Absolute numbers of lives saved and overdiagnosis in breast cancer screening, from a randomized trial and from the Breast Screening Programme in England. *J Med Screen, 17*(1), 25-30. doi:10.1258/jms.2009.009094

Ehnman, M., & Östman, A. (2014). Therapeutic targeting of platelet-derived growth factor receptors in solid tumors. *Expert Opin Investig Drugs, 23*(2), 211-226. doi:10.1517/13543784.2014.847086

Ellis, I. O., Coleman, D., Wells, C., Kodikara, S., Paish, E. M., Moss, S., . . . Winder, R. (2006). Impact of a national external quality assessment scheme for breast pathology in the UK. *J Clin Pathol, 59*(2), 138-145. doi:10.1136/jcp.2004.025551

Elshof, L. E., Schmidt, M. K., Rutgers, E. J. T., van Leeuwen, F. E., Wesseling, J., & Schaapveld, M. (2018). Cause-specific Mortality in a Population-based Cohort of 9799 Women Treated for Ductal Carcinoma In Situ. *Ann Surg, 267*(5), 952-958. doi:10.1097/SLA.0000000000002239

Engels, K., Fox, S. B., Whitehouse, R. M., Gatter, K. C., & Harris, A. L. (1997). Distinct angiogenic patterns are associated with high-grade in situ ductal carcinomas of the breast. *J Pathol, 181*(2), 207-212. doi:10.1002/(SICI)1096-9896(199702)181:2<207::AID-PATH758>3.0.CO;2-4

Erler, J. T., Bennewith, K. L., Nicolau, M., Dornhöfer, N., Kong, C., Le, Q. T., . . . Giaccia, A. J. (2006). Lysyl oxidase is essential for hypoxia-induced metastasis. *Nature, 440*(7088), 1222-1226. doi:10.1038/nature04695

Erler, J. T., & Weaver, V. M. (2009). Three-dimensional context regulation of metastasis. *Clin Exp Metastasis, 26*(1), 35-49. doi:10.1007/s10585-008-9209-8

Esserman, L. J., Kumar, A. S., Herrera, A. F., Leung, J., Au, A., Chen, Y. Y., . . . Hylton, N. M. (2006). Magnetic resonance imaging captures the biology of ductal carcinoma in situ. *J Clin Oncol, 24*(28), 4603-4610. doi:10.1200/JCO.2005.04.5518

Eusebi, V., Feudale, E., Foschini, M. P., Micheli, A., Conti, A., Riva, C., . . . Rilke, F. (1994). Long-term follow-up of in situ carcinoma of the breast. *Semin Diagn Pathol, 11*(3), 223-235.

Farrow, J. H. (1970). Current concepts in the detection and treatment of the earliest of the early breast cancers. *Cancer, 25*(2), 468-477.

Gangoiti, P., Bernacchioni, C., Donati, C., Cencetti, F., Ouro, A., Gómez-Muñoz, A., & Bruni, P. (2012). Ceramide 1-phosphate stimulates proliferation of C2C12 myoblasts. *Biochimie, 94*(3), 597-607. doi:10.1016/j.biochi.2011.09.009

Gendronneau, G., Sidhu, S. S., Delacour, D., Dang, T., Calonne, C., Houzelstein, D., . . . Poirier, F. (2008). Galectin-7 in the control of epidermal homeostasis after injury. *Mol Biol Cell, 19*(12), 5541-5549. doi:10.1091/mbc.E08-02-0166

Gil Del Alcazar, C. R., Huh, S. J., Ekram, M. B., Trinh, A., Liu, L. L., Beca, F., . . . Polyak, K. (2017). Immune Escape in Breast Cancer During. *Cancer Discov, 7*(10), 1098-1115. doi:10.1158/2159-8290.CD-17-0222

Girgert, R., Emons, G., & Gründker, C. (2012). Inactivation of GPR30 reduces growth of triple-negative breast cancer cells: possible application in targeted therapy. *Breast Cancer Res Treat, 134*(1), 199-205. doi:10.1007/s10549-012-1968-x

Gomm, J. J., Browne, P. J., Coope, R. C., Liu, Q. Y., Buluwela, L., & Coombes, R. C. (1995). Isolation of pure populations of epithelial and myoepithelial cells from the normal human mammary gland using immunomagnetic separation with Dynabeads. *Anal Biochem, 226*(1), 91-99. doi:10.1006/abio.1995.1196

Grosset, A. A., Labrie, M., Gagné, D., Vladoiu, M. C., Gaboury, L., Doucet, N., & St-Pierre, Y. (2014). Cytosolic galectin-7 impairs p53 functions and induces chemoresistance in breast cancer cells. *BMC Cancer, 14*, 801. doi:10.1186/1471-2407-14-801

Guidi, A. J., Schnitt, S. J., Fischer, L., Tognazzi, K., Harris, J. R., Dvorak, H. F., & Brown, L. F. (1997). Vascular permeability factor (vascular endothelial growth factor)

expression and angiogenesis in patients with ductal carcinoma in situ of the breast. *Cancer, 80*(10), 1945-1953.

Gøtzsche, P. C., & Jørgensen, K. J. (2013). Screening for breast cancer with mammography. *Cochrane Database Syst Rev*(6), CD001877. doi:10.1002/14651858.CD001877.pub5

Haagensen, C. D., Lane, N., & Lattes, R. (1972). Neoplastic proliferation of the epithelium of the mammary lobules: adenosis, lobular neoplasia, and small cell carcinoma. *Surg Clin North Am, 52*(2), 497-524.

Hanahan, D., & Coussens, L. M. (2012). Accessories to the crime: functions of cells recruited to the tumor microenvironment. *Cancer Cell, 21*(3), 309-322. doi:10.1016/j.ccr.2012.02.022

Hanley, J. A., McGregor, M., Liu, Z., Strumpf, E. C., & Dendukuri, N. (2013). Measuring the mortality impact of breast cancer screening. *Can J Public Health, 104*(7), e437-442.

Harvie, M., Howell, A., Vierkant, R. A., Kumar, N., Cerhan, J. R., Kelemen, L. E., . . . Sellers, T. A. (2005). Association of gain and loss of weight before and after menopause with risk of postmenopausal breast cancer in the Iowa women's health study. *Cancer Epidemiol Biomarkers Prev, 14*(3), 656-661. doi:10.1158/1055-9965.EPI-04-0001

Holmes, P., Lloyd, J., Chervoneva, I., Pequinot, E., Cornfield, D. B., Schwartz, G. F., . . . Palazzo, J. P. (2011). Prognostic markers and long-term outcomes in ductal carcinoma in situ of the breast treated with excision alone. *Cancer, 117*(16), 3650-3657. doi:10.1002/cncr.25942

Hopkins, P. C., & Whisstock, J. (1994). Function of maspin. *Science, 265*(5180), 1893-1894.

Hou, M. F., Chen, P. M., & Chu, P. Y. (2018). LGR5 overexpression confers poor relapse-free survival in breast cancer patients. *BMC Cancer, 18*(1), 219. doi:10.1186/s12885-018-4018-1

http://www.cancerresearchuk.org/health-professional/cancer-statistics/statistics-by-cancer-type/breast-cancer/incidence-in-situ.

https://deepmind.com/blog/applying-machine-learning-mammography/. (2017).

https://www.dcisprecision.org/clinical-trials/comet/.

https://www.dcisprecision.org/clinical-trials/lord/.

https://www.dcisprecision.org/clinical-trials/loris/.

https://www.ncbi.nlm.nih.gov/gene/1123

https://www.ncbi.nlm.nih.gov/gene/2852.

https://www.ncbi.nlm.nih.gov/gene/8995.

https://www.ncbi.nlm.nih.gov/gene/23208

https://www.ncbi.nlm.nih.gov/gene/148170.

https://www.ncbi.nlm.nih.gov/sites/entrez?Db=gene&Cmd=ShowDetailView&TermToSearch=10125. (2008).

https://www.phalanxbiotech.com/validating-rna-seq-results-with-qpcr/. (2017).

Hu, M., Peluffo, G., Chen, H., Gelman, R., Schnitt, S., & Polyak, K. (2009). Role of COX-2 in epithelial-stromal cell interactions and progression of ductal carcinoma in situ of

the breast. *Proc Natl Acad Sci U S A, 106*(9), 3372-3377. doi:10.1073/pnas.0813306106

Hu, M., Yao, J., Cai, L., Bachman, K. E., van den Brûle, F., Velculescu, V., & Polyak, K. (2005). Distinct epigenetic changes in the stromal cells of breast cancers. *Nat Genet, 37*(8), 899-905. doi:10.1038/ng1596

Inman, J. L., Robertson, C., Mott, J. D., & Bissell, M. J. (2015). Mammary gland development: cell fate specification, stem cells and the microenvironment. *Development, 142*(6), 1028-1042. doi:10.1242/dev.087643

Jiang, T., Xu, X., Qiao, M., Li, X., Zhao, C., Zhou, F., . . . Zhou, C. (2018). Comprehensive evaluation of NT5E/CD73 expression and its prognostic significance in distinct types of cancers. *BMC Cancer, 18*(1), 267. doi:10.1186/s12885-018-4073-7

Johnson, G. L., & Lapadat, R. (2002). Mitogen-activated protein kinase pathways mediated by ERK, JNK, and p38 protein kinases. *Science, 298*(5600), 1911-1912. doi:10.1126/science.1072682

Jones, J. L., Glynn, P., & Walker, R. A. (1999). Expression of MMP-2 and MMP-9, their inhibitors, and the activator MT1-MMP in primary breast carcinomas. *J Pathol, 189*(2), 161-168. doi:10.1002/(SICI)1096-9896(199910)189:2<161::AID-PATH406>3.0.CO;2-2

Jones, J. L., Shaw, J. A., Pringle, J. H., & Walker, R. A. (2003). Primary breast myoepithelial cells exert an invasion-suppressor effect on breast cancer cells via paracrine down-regulation of MMP expression in fibroblasts and tumour cells. *J Pathol, 201*(4), 562-572. doi:10.1002/path.1483

Joshi, K., Smith, J. A., Perusinghe, N., & Monoghan, P. (1986). Cell proliferation in the human mammary epithelium. Differential contribution by epithelial and myoepithelial cells. *Am J Pathol, 124*(2), 199-206.

Kagan, H. M., & Li, W. (2003). Lysyl oxidase: properties, specificity, and biological roles inside and outside of the cell. *J Cell Biochem, 88*(4), 660-672. doi:10.1002/jcb.10413

Kamińska, M., Ciszewski, T., Łopacka-Szatan, K., Miotła, P., & Starosławska, E. (2015). Breast cancer risk factors. *Prz Menopauzalny, 14*(3), 196-202. doi:10.5114/pm.2015.54346

Kessenbrock, K., Plaks, V., & Werb, Z. (2010). Matrix metalloproteinases: regulators of the tumor microenvironment. *Cell, 141*(1), 52-67. doi:10.1016/j.cell.2010.03.015

Kim, H. J., Jeon, H. K., Lee, J. K., Sung, C. O., Do, I. G., Choi, C. H., . . . Lee, J. W. (2013). Clinical significance of galectin-7 in epithelial ovarian cancer. *Anticancer Res, 33*(4), 1555-1561.

Kim, S. J., Hwang, J. A., Ro, J. Y., Lee, Y. S., & Chun, K. H. (2013). Galectin-7 is epigenetically-regulated tumor suppressor in gastric cancer. *Oncotarget, 4*(9), 1461-1471. doi:10.18632/oncotarget.1219

Kim, T. J., Mitsutake, S., & Igarashi, Y. (2006). The interaction between the pleckstrin homology domain of ceramide kinase and phosphatidylinositol 4,5-bisphosphate regulates the plasma membrane targeting and ceramide 1-phosphate levels. *Biochem Biophys Res Commun, 342*(2), 611-617. doi:10.1016/j.bbrc.2006.01.170

Kim, Y. M., Kim, E. C., & Kim, Y. (2011). The human lysyl oxidase-like 2 protein functions as an amine oxidase toward collagen and elastin. *Mol Biol Rep, 38*(1), 145-149. doi:10.1007/s11033-010-0088-0

Kirschmann, D. A., Seftor, E. A., Fong, S. F., Nieva, D. R., Sullivan, C. M., Edwards, E. M., . . . Hendrix, M. J. (2002). A molecular role for lysyl oxidase in breast cancer invasion. *Cancer Res, 62*(15), 4478-4483.

Klyosov, A. A., & Traber, P. G. (2012). *Galectins and Disease Implications for Targeted Therapeutics*.

Koh, V. C. Y., Lim, J. C. T., Thike, A. A., Cheok, P. Y., Thu, M. M. M., Li, H., . . . Tan, P. H. (2019). Behaviour and characteristics of low-grade ductal carcinoma in situ of the breast: literature review and single centre retrospective series. *Histopathology*. doi:10.1111/his.13837

Koukoulis, G. K., Virtanen, I., Korhonen, M., Laitinen, L., Quaranta, V., & Gould, V. E. (1991). Immunohistochemical localization of integrins in the normal, hyperplastic, and neoplastic breast. Correlations with their functions as receptors and cell adhesion molecules. *Am J Pathol, 139*(4), 787-799.

KRAUS, F. T., & NEUBECKER, R. D. (1962). The differential diagnosis of papillary tumors of the breast. *Cancer, 15*, 444-455.

Labrie, M., Vladoiu, M., Leclerc, B. G., Grosset, A. A., Gaboury, L., Stagg, J., & St-Pierre, Y. (2015). A Mutation in the Carbohydrate Recognition Domain Drives a Phenotypic Switch in the Role of Galectin-7 in Prostate Cancer. *PLoS One, 10*(7), e0131307. doi:10.1371/journal.pone.0131307

Labrie, M., Vladoiu, M. C., Grosset, A. A., Gaboury, L., & St-Pierre, Y. (2014). Expression and functions of galectin-7 in ovarian cancer. *Oncotarget, 5*(17), 7705-7721. doi:10.18632/oncotarget.2299

Lappano, R., Pisano, A., & Maggiolini, M. (2014). GPER Function in Breast Cancer: An Overview. *Front Endocrinol (Lausanne), 5*, 66. doi:10.3389/fendo.2014.00066

Lappano, R., Rosano, C., Santolla, M. F., Pupo, M., De Francesco, E. M., De Marco, P., . . . Maggiolini, M. (2012). Two novel GPER agonists induce gene expression changes and growth effects in cancer cells. *Curr Cancer Drug Targets, 12*(5), 531-542.

Lappano, R., Santolla, M. F., Pupo, M., Sinicropi, M. S., Caruso, A., Rosano, C., & Maggiolini, M. (2012). MIBE acts as antagonist ligand of both estrogen receptor α and GPER in breast cancer cells. *Breast Cancer Res, 14*(1), R12. doi:10.1186/bcr3096

Lee, A. H., Happerfield, L. C., Bobrow, L. G., & Millis, R. R. (1997a). Angiogenesis and inflammation in ductal carcinoma in situ of the breast. *J Pathol, 181*(2), 200-206. doi:10.1002/(SICI)1096-9896(199702)181:2<200::AID-PATH726>3.0.CO;2-K

Lee, A. H., Happerfield, L. C., Bobrow, L. G., & Millis, R. R. (1997b). Angiogenesis and inflammation in invasive carcinoma of the breast. *J Clin Pathol, 50*(8), 669-673.

Lee, S., Craig, B. T., Romain, C. V., Qiao, J., & Chung, D. H. (2014). Silencing of CDC42 inhibits neuroblastoma cell proliferation and transformation. *Cancer Lett, 355*(2), 210-216. doi:10.1016/j.canlet.2014.08.033

Leonard, G. D., & Swain, S. M. (2004). Ductal carcinoma in situ, complexities and challenges. *J Natl Cancer Inst, 96*(12), 906-920.

Lester, S. C., Bose, S., Chen, Y. Y., Connolly, J. L., de Baca, M. E., Fitzgibbons, P. L., . . . Members of the Cancer Committee, C. l. o. A. P. (2009). Protocol for the

examination of specimens from patients with ductal carcinoma in situ of the breast. *Arch Pathol Lab Med, 133*(1), 15-25. doi:10.1043/1543-2165-133.1.15

Levental, K. R., Yu, H., Kass, L., Lakins, J. N., Egeblad, M., Erler, J. T., . . . Weaver, V. M. (2009). Matrix crosslinking forces tumor progression by enhancing integrin signaling. *Cell, 139*(5), 891-906. doi:10.1016/j.cell.2009.10.027

Li, C. F., Wu, W. R., Chan, T. C., Wang, Y. H., Chen, L. R., Wu, W. J., . . . Shiue, Y. L. (2017). Transmembrane and Coiled-Coil Domain 1 Impairs the AKT Signaling Pathway in Urinary Bladder Urothelial Carcinoma: A Characterization of a Tumor Suppressor. *Clin Cancer Res, 23*(24), 7650-7663. doi:10.1158/1078-0432.CCR-17-0002

Li, C. I., Anderson, B. O., Daling, J. R., & Moe, R. E. (2003). Trends in incidence rates of invasive lobular and ductal breast carcinoma. *JAMA, 289*(11), 1421-1424.

Loi, S., Pommey, S., Haibe-Kains, B., Beavis, P. A., Darcy, P. K., Smyth, M. J., & Stagg, J. (2013). CD73 promotes anthracycline resistance and poor prognosis in triple negative breast cancer. *Proc Natl Acad Sci U S A, 110*(27), 11091-11096. doi:10.1073/pnas.1222251110

Lopez-Garcia, M. A., Geyer, F. C., Lacroix-Triki, M., Marchió, C., & Reis-Filho, J. S. (2010). Breast cancer precursors revisited: molecular features and progression pathways. *Histopathology, 57*(2), 171-192. doi:10.1111/j.1365-2559.2010.03568.x

Lu, J., Pei, H., Kaeck, M., & Thompson, H. J. (1997). Gene expression changes associated with chemically induced rat mammary carcinogenesis. *Mol Carcinog, 20*(2), 204-215.

Lyons, T. R., O'Brien, J., Borges, V. F., Conklin, M. W., Keely, P. J., Eliceiri, K. W., . . . Schedin, P. (2011). Postpartum mammary gland involution drives progression of ductal carcinoma in situ through collagen and COX-2. *Nat Med, 17*(9), 1109-1115. doi:10.1038/nm.2416

Man, Y. G. (2007). Focal degeneration of aged or injured myoepithelial cells and the resultant auto-immunoreactions are trigger factors for breast tumor invasion. *Med Hypotheses, 69*(6), 1340-1357. doi:10.1016/j.mehy.2007.02.031

Man, Y. G., & Sang, Q. X. (2004). The significance of focal myoepithelial cell layer disruptions in human breast tumor invasion: a paradigm shift from the "protease-centered" hypothesis. *Exp Cell Res, 301*(2), 103-118. doi:10.1016/j.yexcr.2004.08.037

Manders, J. B., Kuerer, H. M., Smith, B. D., McCluskey, C., Farrar, W. B., Frazier, T. G., . . . participants, S. i. a. s. (2017). Clinical Utility of the 12-Gene DCIS Score Assay: Impact on Radiotherapy Recommendations for Patients with Ductal Carcinoma In Situ. *Ann Surg Oncol, 24*(3), 660-668. doi:10.1245/s10434-016-5583-7

Martelotto, L. G., Baslan, T., Kendall, J., Geyer, F. C., Burke, K. A., Spraggon, L., . . . Reis-Filho, J. S. (2017). Whole-genome single-cell copy number profiling from formalin-fixed paraffin-embedded samples. *Nat Med, 23*(3), 376-385. doi:10.1038/nm.4279

Massat, N. J., Dibden, A., Parmar, D., Cuzick, J., Sasieni, P. D., & Duffy, S. W. (2016). Impact of Screening on Breast Cancer Mortality: The UK Program 20 Years On. *Cancer Epidemiol Biomarkers Prev, 25*(3), 455-462. doi:10.1158/1055-9965.EPI-15-0803

Millis, R. R., & Thynne, G. S. (1975). In situ intraduct carcinoma of the breast: a long term follow-up study. *Br J Surg, 62*(12), 957-962.

Murrell, T. G. (1995). The potential for oxytocin (OT) to prevent breast cancer: a hypothesis. *Breast Cancer Res Treat, 35*(2), 225-229.

Navin, N., Kendall, J., Troge, J., Andrews, P., Rodgers, L., McIndoo, J., . . . Wigler, M. (2011). Tumour evolution inferred by single-cell sequencing. *Nature, 472*(7341), 90-94. doi:10.1038/nature09807

Nelson, H. D., Tyne, K., Naik, A., Bougatsos, C., Chan, B., Nygren, P., & Humphrey, L. (2009). Screening for Breast Cancer: Systematic Evidence Review Update for the US Preventive Services Task Force. In.

Niu, J., & Li, Z. (2017). The roles of integrin αvβ6 in cancer. *Cancer Lett, 403*, 128-137. doi:10.1016/j.canlet.2017.06.012

O'Hare, M. J., Bond, J., Clarke, C., Takeuchi, Y., Atherton, A. J., Berry, C., . . . Jat, P. S. (2001). Conditional immortalization of freshly isolated human mammary fibroblasts and endothelial cells. *Proc Natl Acad Sci U S A, 98*(2), 646-651. doi:10.1073/pnas.98.2.646

Orimo, A., Gupta, P. B., Sgroi, D. C., Arenzana-Seisdedos, F., Delaunay, T., Naeem, R., . . . Weinberg, R. A. (2005). Stromal fibroblasts present in invasive human breast carcinomas promote tumor growth and angiogenesis through elevated SDF-1/CXCL12 secretion. *Cell, 121*(3), 335-348. doi:10.1016/j.cell.2005.02.034

Osborne, C. K., Hobbs, K., & Trent, J. M. (1987). Biological differences among MCF-7 human breast cancer cell lines from different laboratories. *Breast Cancer Res Treat, 9*(2), 111-121.

Ozanne, E. M., Shieh, Y., Barnes, J., Bouzan, C., Hwang, E. S., & Esserman, L. J. (2011). Characterizing the impact of 25 years of DCIS treatment. *Breast Cancer Res Treat, 129*(1), 165-173. doi:10.1007/s10549-011-1430-5

Ozawa, T., Tsuruta, D., Jones, J. C., Ishii, M., Ikeda, K., Harada, T., . . . Kobayashi, H. (2010). Dynamic relationship of focal contacts and hemidesmosome protein complexes in live cells. *J Invest Dermatol, 130*(6), 1624-1635. doi:10.1038/jid.2009.439

Page, D. L., Dupont, W. D., Rogers, L. W., Jensen, R. A., & Schuyler, P. A. (1995). Continued local recurrence of carcinoma 15-25 years after a diagnosis of low grade ductal carcinoma in situ of the breast treated only by biopsy. *Cancer, 76*(7), 1197-1200.

Page, D. L., Dupont, W. D., Rogers, L. W., & Landenberger, M. (1982). Intraductal carcinoma of the breast: follow-up after biopsy only. *Cancer, 49*(4), 751-758.

Paget, S. (1989). The distribution of secondary growths in cancer of the breast. 1889. *Cancer Metastasis Rev, 8*(2), 98-101.

Pandey, D. P., Lappano, R., Albanito, L., Madeo, A., Maggiolini, M., & Picard, D. (2009). Estrogenic GPR30 signalling induces proliferation and migration of breast cancer cells through CTGF. *EMBO J, 28*(5), 523-532. doi:10.1038/emboj.2008.304

Pandey, P. R., Saidou, J., & Watabe, K. (2010). Role of myoepithelial cells in breast tumor progression. *Front Biosci (Landmark Ed), 15*, 226-236.

Paredes, J., Milanezi, F., Viegas, L., Amendoeira, I., & Schmitt, F. (2002). P-cadherin expression is associated with high-grade ductal carcinoma in situ of the breast. *Virchows Arch, 440*(1), 16-21.

Park, K., Han, S., Kim, H. J., Kim, J., & Shin, E. (2006). HER2 status in pure ductal carcinoma in situ and in the intraductal and invasive components of invasive ductal carcinoma determined by fluorescence in situ hybridization and

immunohistochemistry. *Histopathology, 48*(6), 702-707. doi:10.1111/j.1365-2559.2006.02403.x

Pasanisi, P., Venturelli, E., Morelli, D., Fontana, L., Secreto, G., & Berrino, F. (2008). Serum insulin-like growth factor-I and platelet-derived growth factor as biomarkers of breast cancer prognosis. *Cancer Epidemiol Biomarkers Prev, 17*(7), 1719-1722. doi:10.1158/1055-9965.EPI-07-0654

Pastukhov, O., Schwalm, S., Römer, I., Zangemeister-Wittke, U., Pfeilschifter, J., & Huwiler, A. (2014). Ceramide kinase contributes to proliferation but not to prostaglandin E2 formation in renal mesangial cells and fibroblasts. *Cell Physiol Biochem, 34*(1), 119-133. doi:10.1159/000362989

Paszek, M. J., Zahir, N., Johnson, K. R., Lakins, J. N., Rozenberg, G. I., Gefen, A., . . . Weaver, V. M. (2005). Tensional homeostasis and the malignant phenotype. *Cancer Cell, 8*(3), 241-254. doi:10.1016/j.ccr.2005.08.010

Payne, A. W., Pant, D. K., Pan, T. C., & Chodosh, L. A. (2014). Ceramide kinase promotes tumor cell survival and mammary tumor recurrence. *Cancer Res, 74*(21), 6352-6363. doi:10.1158/0008-5472.CAN-14-1292

Payne, S. L., Hendrix, M. J., & Kirschmann, D. A. (2007). Paradoxical roles for lysyl oxidases in cancer--a prospect. *J Cell Biochem, 101*(6), 1338-1354. doi:10.1002/jcb.21371

Pemberton, P. A., Wong, D. T., Gibson, H. L., Kiefer, M. C., Fitzpatrick, P. A., Sager, R., & Barr, P. J. (1995). The tumor suppressor maspin does not undergo the stressed to relaxed transition or inhibit trypsin-like serine proteases. Evidence that maspin is not a protease inhibitory serpin. *J Biol Chem, 270*(26), 15832-15837.

Perou, C. M., Sørlie, T., Eisen, M. B., van de Rijn, M., Jeffrey, S. S., Rees, C. A., . . . Botstein, D. (2000). Molecular portraits of human breast tumours. *Nature, 406*(6797), 747-752. doi:10.1038/35021093

Pilewskie, M., Stempel, M., Rosenfeld, H., Eaton, A., Van Zee, K. J., & Morrow, M. (2016). Do LORIS Trial Eligibility Criteria Identify a Ductal Carcinoma In Situ Patient Population at Low Risk of Upgrade to Invasive Carcinoma? *Ann Surg Oncol, 23*(11), 3487-3493. doi:10.1245/s10434-016-5268-2

Pinder, S. E. (2010). Ductal carcinoma in situ (DCIS): pathological features, differential diagnosis, prognostic factors and specimen evaluation. *Mod Pathol, 23 Suppl 2*, S8-13. doi:10.1038/modpathol.2010.40

Pitelka, D. R., Hamamoto, S. T., Duafala, J. G., & Nemanic, M. K. (2009). Cell contacts in the mouse mammary gland: i. Normal gland in postnatal development and the secretory cycle. 1973. *J Mammary Gland Biol Neoplasia, 14*(3), 295-316. doi:10.1007/s10911-009-9131-y

Polyak, K. (2010). Molecular markers for the diagnosis and management of ductal carcinoma in situ. *J Natl Cancer Inst Monogr, 2010*(41), 210-213. doi:10.1093/jncimonographs/lgq019

Postovit, L. M., Abbott, D. E., Payne, S. L., Wheaton, W. W., Margaryan, N. V., Sullivan, R., . . . Kirschmann, D. A. (2008). Hypoxia/reoxygenation: a dynamic regulator of lysyl oxidase-facilitated breast cancer migration. *J Cell Biochem, 103*(5), 1369-1378. doi:10.1002/jcb.21517

Provenzano, E., Hopper, J. L., Giles, G. G., Marr, G., Venter, D. J., & Armes, J. E. (2003). Biological markers that predict clinical recurrence in ductal carcinoma in situ of the breast. *Eur J Cancer, 39*(5), 622-630.

Provenzano, P. P., Eliceiri, K. W., Campbell, J. M., Inman, D. R., White, J. G., & Keely, P. J. (2006). Collagen reorganization at the tumor-stromal interface facilitates local invasion. *BMC Med, 4*(1), 38. doi:10.1186/1741-7015-4-38

Provenzano, P. P., Inman, D. R., Eliceiri, K. W., Knittel, J. G., Yan, L., Rueden, C. T., . . . Keely, P. J. (2008). Collagen density promotes mammary tumor initiation and progression. *BMC Med, 6*, 11. doi:10.1186/1741-7015-6-11

Rakha, E. A., El-Sayed, M. E., Green, A. R., Paish, E. C., Lee, A. H., & Ellis, I. O. (2007). Breast carcinoma with basal differentiation: a proposal for pathology definition based on basal cytokeratin expression. *Histopathology, 50*(4), 434-438. doi:10.1111/j.1365-2559.2007.02638.x

Ramachandra, S., Machin, L., Ashley, S., Monaghan, P., & Gusterson, B. A. (1990). Immunohistochemical distribution of c-erbB-2 in in situ breast carcinoma--a detailed morphological analysis. *J Pathol, 161*(1), 7-14. doi:10.1002/path.1711610104

Rambaratsingh, R. A., Stone, J. C., Blumberg, P. M., & Lorenzo, P. S. (2003). RasGRP1 represents a novel non-protein kinase C phorbol ester signaling pathway in mouse epidermal keratinocytes. *J Biol Chem, 278*(52), 52792-52801. doi:10.1074/jbc.M308240200

Rattanasinchai, C., & Gallo, K. A. (2016). MLK3 Signaling in Cancer Invasion. *Cancers (Basel), 8*(5). doi:10.3390/cancers8050051

Roka, S., Rudas, M., Taucher, S., Dubsky, P., Bachleitner-Hofmann, T., Kandioler, D., . . . Jakesz, R. (2004). High nuclear grade and negative estrogen receptor are significant risk factors for recurrence in DCIS. *Eur J Surg Oncol, 30*(3), 243-247. doi:10.1016/j.ejso.2003.11.004

Runswick, S. K., O'Hare, M. J., Jones, L., Streuli, C. H., & Garrod, D. R. (2001). Desmosomal adhesion regulates epithelial morphogenesis and cell positioning. *Nat Cell Biol, 3*(9), 823-830. doi:10.1038/ncb0901-823

Rønnov-Jessen, L., Petersen, O. W., & Bissell, M. J. (1996). Cellular changes involved in conversion of normal to malignant breast: importance of the stromal reaction. *Physiol Rev, 76*(1), 69-125. doi:10.1152/physrev.1996.76.1.69

Salehi, E., Vodjgani, M., Massoud, A., Keyhani, A., Rajab, A., Shafaghi, B., . . . Aboufazeli, T. (2007). Increased expression of TRAIL and its receptors on peripheral T-cells in type 1 diabetic patients. *Iran J Immunol, 4*(4), 197-205. doi:IJIv4i4A2

Sanders, M. E., Schuyler, P. A., Dupont, W. D., & Page, D. L. (2005). The natural history of low-grade ductal carcinoma in situ of the breast in women treated by biopsy only revealed over 30 years of long-term follow-up. *Cancer, 103*(12), 2481-2484. doi:10.1002/cncr.21069

Sato, K., Niessner, A., Kopecky, S. L., Frye, R. L., Goronzy, J. J., & Weyand, C. M. (2006). TRAIL-expressing T cells induce apoptosis of vascular smooth muscle cells in the atherosclerotic plaque. *J Exp Med, 203*(1), 239-250. doi:10.1084/jem.20051062

Screening, I. U. P. o. B. C. (2012). The benefits and harms of breast cancer screening: an independent review. *Lancet, 380*(9855), 1778-1786. doi:10.1016/S0140-6736(12)61611-0

Sgroi, D. C. (2010). Preinvasive breast cancer. *Annu Rev Pathol, 5*, 193-221. doi:10.1146/annurev.pathol.4.110807.092306

Shao, Z. M., Nguyen, M., & Barsky, S. H. (2000). Human breast carcinoma desmoplasia is PDGF initiated. *Oncogene, 19*(38), 4337-4345. doi:10.1038/sj.onc.1203785

Sharma, A., Luke, C. T., Dower, N. A., Stone, J. C., & Lorenzo, P. S. (2010). RasGRP1 is essential for ras activation by the tumor promoter 12-O-tetradecanoylphorbol-13-acetate in epidermal keratinocytes. *J Biol Chem, 285*(21), 15724-15730. doi:10.1074/jbc.M109.100016

Shiozaki, K., Nakamori, S., Tsujie, M., Okami, J., Yamamoto, H., Nagano, H., . . . Monden, M. (2001). Human stomach-specific gene, CA11, is down-regulated in gastric cancer. *Int J Oncol, 19*(4), 701-707.

Siegel, R. L., Miller, K. D., & Jemal, A. (2017). Cancer Statistics, 2017. *CA Cancer J Clin, 67*(1), 7-30. doi:10.3322/caac.21387

Silverstein, M. J. (2003). The University of Southern California/Van Nuys prognostic index for ductal carcinoma in situ of the breast. *Am J Surg, 186*(4), 337-343.

Solin, L. J., Gray, R., Baehner, F. L., Butler, S. M., Hughes, L. L., Yoshizawa, C., . . . Badve, S. (2013). A multigene expression assay to predict local recurrence risk for ductal carcinoma in situ of the breast. *J Natl Cancer Inst, 105*(10), 701-710. doi:10.1093/jnci/djt067

Steiman, J., Peralta, E. A., Louis, S., & Kamel, O. (2013). Biology of the estrogen receptor, GPR30, in triple negative breast cancer. *Am J Surg, 206*(5), 698-703. doi:10.1016/j.amjsurg.2013.07.014

Sun, Y. S., Zhao, Z., Yang, Z. N., Xu, F., Lu, H. J., Zhu, Z. Y., . . . Zhu, H. P. (2017). Risk Factors and Preventions of Breast Cancer. *Int J Biol Sci, 13*(11), 1387-1397. doi:10.7150/ijbs.21635

Supernat, A., Markiewicz, A., Welnicka-Jaskiewicz, M., Seroczynska, B., Skokowski, J., Sejda, A., . . . Zaczek, A. (2012). CD73 expression as a potential marker of good prognosis in breast carcinoma. *Appl Immunohistochem Mol Morphol, 20*(2), 103-107.

Tanihara, H., Sano, K., Heimark, R. L., St John, T., & Suzuki, S. (1994). Cloning of five human cadherins clarifies characteristic features of cadherin extracellular domain and provides further evidence for two structurally different types of cadherin. *Cell Adhes Commun, 2*(1), 15-26.

Teo, N. B., Shoker, B. S., Jarvis, C., Martin, L., Sloane, J. P., & Holcombe, C. (2003). Angiogenesis and invasive recurrence in ductal carcinoma in situ of the breast. *Eur J Cancer, 39*(1), 38-44.

Thomas, E. T., Del Mar, C., Glasziou, P., Wright, G., Barratt, A., & Bell, K. J. L. (2017). Prevalence of incidental breast cancer and precursor lesions in autopsy studies: a systematic review and meta-analysis. *BMC Cancer, 17*(1), 808. doi:10.1186/s12885-017-3808-1

Thomas, G. J., Nyström, M. L., & Marshall, J. F. (2006). Alphavbeta6 integrin in wound healing and cancer of the oral cavity. *J Oral Pathol Med, 35*(1), 1-10. doi:10.1111/j.1600-0714.2005.00374.x

Tonelli, M., Connor Gorber, S., Joffres, M., Dickinson, J., Singh, H., Lewin, G., . . . Care, C. T. F. o. P. H. (2011). Recommendations on screening for breast cancer in average-risk women aged 40-74 years. *CMAJ, 183*(17), 1991-2001. doi:10.1503/cmaj.110334

Tsai, C. J., Sulman, E. P., Eifel, P. J., Jhingran, A., Allen, P. K., Deavers, M. T., & Klopp, A. H. (2013). Galectin-7 levels predict radiation response in squamous cell carcinoma of the cervix. *Gynecol Oncol, 131*(3), 645-649. doi:10.1016/j.ygyno.2013.04.056

Ueda, S., Kuwabara, I., & Liu, F. T. (2004). Suppression of tumor growth by galectin-7 gene transfer. *Cancer Res, 64*(16), 5672-5676. doi:10.1158/0008-5472.CAN-04-0985

van der Slot, A. J., van Dura, E. A., de Wit, E. C., De Groot, J., Huizinga, T. W., Bank, R. A., & Zuurmond, A. M. (2005). Elevated formation of pyridinoline cross-links by profibrotic cytokines is associated with enhanced lysyl hydroxylase 2b levels. *Biochim Biophys Acta, 1741*(1-2), 95-102. doi:10.1016/j.bbadis.2004.09.009

van Seijen, M., Lips, E. H., Thompson, A. M., Nik-Zainal, S., Futreal, A., Hwang, E. S., . . . team, P. (2019). Ductal carcinoma in situ: to treat or not to treat, that is the question. *Br J Cancer, 121*(4), 285-292. doi:10.1038/s41416-019-0478-6

Vladoiu, M. C., Labrie, M., & St-Pierre, Y. (2014). Intracellular galectins in cancer cells: potential new targets for therapy (Review). *Int J Oncol, 44*(4), 1001-1014. doi:10.3892/ijo.2014.2267

Walker, R. A. (2001). The complexities of breast cancer desmoplasia. *Breast Cancer Res, 3*(3), 143-145.

Walker, R. A., & Dearing, S. J. (1992). Transforming growth factor beta 1 in ductal carcinoma in situ and invasive carcinomas of the breast. *Eur J Cancer, 28*(2-3), 641-644.

Walko, G., Castañón, M. J., & Wiche, G. (2015). Molecular architecture and function of the hemidesmosome. *Cell Tissue Res, 360*(3), 529-544. doi:10.1007/s00441-015-2216-6

Wang, S., Beeghly-Fadiel, A., Cai, Q., Cai, H., Guo, X., Shi, L., . . . Shu, X. O. (2018). Gene expression in triple-negative breast cancer in relation to survival. *Breast Cancer Res Treat, 171*(1), 199-207. doi:10.1007/s10549-018-4816-9

Watson, M., & screening and immunisation team, N. d. (2019). *Breast Screening Programme*

England, 2017-18. NHS digital

Welch, H. G., & Black, W. C. (1997). Using autopsy series to estimate the disease "reservoir" for ductal carcinoma in situ of the breast: how much more breast cancer can we find? *Ann Intern Med, 127*(11), 1023-1028.

Wellings, S. R., & Jensen, H. M. (1973). On the origin and progression of ductal carcinoma in the human breast. *J Natl Cancer Inst, 50*(5), 1111-1118.

Xiao, X. H., Lv, L. C., Duan, J., Wu, Y. M., He, S. J., Hu, Z. Z., & Xiong, L. X. (2018). Regulating Cdc42 and Its Signaling Pathways in Cancer: Small Molecules and MicroRNA as New Treatment Candidates. *Molecules, 23*(4). doi:10.3390/molecules23040787

Xu, X., Hou, Y., Yin, X., Bao, L., Tang, A., Song, L., . . . Li, Y. (2012). Single-cell exome sequencing reveals single-nucleotide mutation characteristics of a kidney tumor. *Cell, 148*(5), 886-895. doi:10.1016/j.cell.2012.02.025

Yang, L., Tang, H., Kong, Y., Xie, X., Chen, J., Song, C., . . . Wang, N. (2015). LGR5 Promotes Breast Cancer Progression and Maintains Stem-Like Cells Through Activation of Wnt/β-Catenin Signaling. *Stem Cells, 33*(10), 2913-2924. doi:10.1002/stem.2083

Yang, R. Y., Rabinovich, G. A., & Liu, F. T. (2008). Galectins: structure, function and therapeutic potential. *Expert Rev Mol Med, 10*, e17. doi:10.1017/S1462399408000719

Zaman, M. H., Trapani, L. M., Sieminski, A. L., Siemeski, A., Mackellar, D., Gong, H., . . . Matsudaira, P. (2006). Migration of tumor cells in 3D matrices is governed by matrix stiffness along with cell-matrix adhesion and proteolysis. *Proc Natl Acad Sci U S A, 103*(29), 10889-10894. doi:10.1073/pnas.0604460103

Zhao, Y., Min, C., Vora, S. R., Trackman, P. C., Sonenshein, G. E., & Kirsch, K. H. (2009). The lysyl oxidase pro-peptide attenuates fibronectin-mediated activation of focal adhesion kinase and p130Cas in breast cancer cells. *J Biol Chem, 284*(3), 1385-1393. doi:10.1074/jbc.M802612200

Zheng, Z., Yu, H., Huang, Q., Wu, H., Fu, Y., Shi, J., . . . Fan, X. (2018). Heterogeneous expression of Lgr5 as a risk factor for focal invasion and distant metastasis of colorectal carcinoma. *Oncotarget, 9*(53), 30025-30033. doi:10.18632/oncotarget.23144

Zhu, H., Wu, T. C., Chen, W. Q., Zhou, L. J., Wu, Y., Zeng, L., & Pei, H. P. (2013). Roles of galectin-7 and S100A9 in cervical squamous carcinoma: Clinicopathological and in vitro evidence. *Int J Cancer, 132*(5), 1051-1059. doi:10.1002/ijc.27764

Zhu, X., Ding, M., Yu, M. L., Feng, M. X., Tan, L. J., & Zhao, F. K. (2010). Identification of galectin-7 as a potential biomarker for esophageal squamous cell carcinoma by proteomic analysis. *BMC Cancer, 10*, 290. doi:10.1186/1471-2407-10-290

Zong, C., Lu, S., Chapman, A. R., & Xie, X. S. (2012). Genome-wide detection of single-nucleotide and copy-number variations of a single human cell. *Science, 338*(6114), 1622-1626. doi:10.1126/science.1229164